

AD \_\_\_\_\_

Award Number: DAMD17-99-1-9291

TITLE: A Novel Signaling Perturbation and Ribozyme Gene Therapy  
Procedures to Block Rho-Kinase (ROK) Activations and  
Breast Tumor Metastasis

PRINCIPAL INVESTIGATOR: Lily Y. W. Bourguignon, Ph.D.

CONTRACTING ORGANIZATION: Northern California Institute for  
Research and Education, Incorporated  
San Francisco, California 94121-1545

REPORT DATE: September 2002

TYPE OF REPORT: Annual

PREPARED FOR: U.S. Army Medical Research and Materiel Command  
Fort Detrick, Maryland 21702-5012

DISTRIBUTION STATEMENT: Approved for Public Release;  
Distribution Unlimited

The views, opinions and/or findings contained in this report are  
those of the author(s) and should not be construed as an official  
Department of the Army position, policy or decision unless so  
designated by other documentation.

20030211 212

**REPORT DOCUMENTATION PAGE**Form Approved  
OMB No. 074-0188

Public reporting burden for this collection of information is estimated to average 1 hour per response, including the time for reviewing instructions, searching existing data sources, gathering and maintaining the data needed, and completing and reviewing this collection of information. Send comments regarding this burden estimate or any other aspect of this collection of information, including suggestions for reducing this burden to Washington Headquarters Services, Directorate for Information Operations and Reports, 1215 Jefferson Davis Highway, Suite 1204, Arlington, VA 22202-4302, and to the Office of Management and Budget, Paperwork Reduction Project (0704-0188), Washington, DC 20503

**1. AGENCY USE ONLY (Leave blank)****2. REPORT DATE**

September 2002

**3. REPORT TYPE AND DATES COVERED**

Annual (1 Sep 01 - 31 Aug 02)

**4. TITLE AND SUBTITLE**

A Novel Signaling Perturbation and Ribozyme Gene Therapy Procedures to Block Rho-Kinase (ROK) Activations and Breast Tumor Metastasis

**5. FUNDING NUMBERS**

DAMD17-99-1-9291

**6. AUTHOR(S):**

Lily Y. W. Bourguignon, Ph.D.

**7. PERFORMING ORGANIZATION NAME(S) AND ADDRESS(ES)**Northern California Institute for Research  
and Education, Incorporated  
San Francisco, California 94121-1545

Email:lillyb@itsa.ucsf.edu

**8. PERFORMING ORGANIZATION  
REPORT NUMBER****9. SPONSORING / MONITORING AGENCY NAME(S) AND ADDRESS(ES)**U.S. Army Medical Research and Materiel Command  
Fort Detrick, Maryland 21702-5012**10. SPONSORING / MONITORING  
AGENCY REPORT NUMBER****11. SUPPLEMENTARY NOTES**

report contains color

**12a. DISTRIBUTION / AVAILABILITY STATEMENT**

Approved for Public Release; Distribution Unlimited

**12b. DISTRIBUTION CODE**

**13. Abstract (Maximum 200 Words)** *(abstract should contain no proprietary or confidential information)* In breast tumor cells (e.g. Met-1 and SP-1 cell lines), the Rho-Kinase (ROK) is detected as a 160kDa protein. We have demonstrated that ROK phosphorylates the cytoplasmic domain of CD44 [a hyaluronan (HA) receptor] and up-regulates the interaction between CD44 and the cytoskeletal protein, ankyrin during HA/CD44-regulated breast tumor cell migration. Most recently, we have found that CD44 and Rho-Kinase (ROK) are also physically associated as a complex in breast tumor cells. Biochemical analyses show that the C-terminal pleckstrin homology (PH) domain is the primary ROK binding region for CD44. Most importantly, HA binding to cells promotes RhoA-mediated ROK activity which, in turn, increases phosphorylation of three different inositol 1, 4, 5-trisphosphate receptors (IP<sub>3</sub>Rs) [in particular, subtype 1 (IP<sub>3</sub>R1), and to a lesser extent subtype 2 (IP<sub>3</sub>R2) and subtype 3 (IP<sub>3</sub>R3)] all known as IP<sub>3</sub>-gated Ca<sup>2+</sup> channels. The phosphorylated IP<sub>3</sub>R1 (but not IP<sub>3</sub>R2 or IP<sub>3</sub>R3) is enhanced in its binding to IP<sub>3</sub> which subsequently stimulates IP<sub>3</sub>-mediated Ca<sup>2+</sup> flux and breast tumor cell migration. We have also constructed two dominant-negative ROK cDNA constructs which encode for the Rho-binding (RB) domain and the pleckstrin homology (PH) domain. Our data indicate that transfection of breast tumor cells with ROK's RB or PHcDNA significantly blocks HA and CD44-induced Ca<sup>2+</sup> signaling and breast tumor cell migration. Taken together, we believe that ROK plays a pivotal role in CD44-cytoskeleton interaction and IP<sub>3</sub>R-mediated Ca<sup>2+</sup> signaling during HA-mediated breast tumor progression.

**14. SUBJECT TERMS**

breast cancer metastasis, oncogenic signaling, RhoGTPases, ROK

**15. NUMBER OF PAGES**

77

**16. PRICE CODE****17. SECURITY CLASSIFICATION  
OF REPORT**

Unclassified

**18. SECURITY CLASSIFICATION  
OF THIS PAGE**

Unclassified

**19. SECURITY CLASSIFICATION  
OF ABSTRACT**

Unclassified

**20. LIMITATION OF ABSTRACT**

Unlimited

## Table of Contents

Cover.....	1
SF 298.....	2
Table of Contents.....	3
Introduction.....	4
Body.....	4
Key Research Accomplishments.....	5
Reportable Outcomes.....	6
Conclusions.....	7
References.....	8-10
Paper Publications & Abstracts.....	10-12
Appendices .....	(see attached)

## (5) INTRODUCTION

Members of the Rho subclass of the Ras superfamily [small molecular weight GTPases, (e.g. RhoA, Rac1 and Cdc42)] are known to transduce signals regulating many cellular processes including  $\text{Ca}^{2+}$  mobilization [Ahgkatchai and Finkel, 1999; Hong-Geller and Cerione, 2000] and cell migration [Henke et al., 1996; Trochon et al., 1996; Bourguignon et al., 1999]. HA-mediated CD44 signaling has been shown to be closely associated with the activation of RhoGTPases (e.g. RhoA and Rac1) in tumor cells [Bourguignon et al., 1999, 2000a & b, 2001a & b]. Several enzymes have been identified as possible downstream targets for RhoGTPase signaling such as RhoA. One such enzyme is Rho-Kinase (ROK-also called RhoA-associated kinase) which is a serine-threonine kinase known to interact with Rho in a GTP-dependent manner [Matsui et al., 1996; Amano et al., 1999]. ROK is composed of four functional domains including a kinase domain (catalytic site), a coiled-coil domain, a Rho-binding (RB) domain and a pleckstrin-homology (PH) domain [Amano et al., 1996, 1997]. This enzyme has been shown to regulate cytoskeleton function by phosphorylating several important cytoskeletal regulators including myosin light chain Amano et al., 1996], the myosin-binding subunit (MBS) of myosin phosphatase [Kimura et al., 1996], adducin [Fukata et al., 1999] and LIM kinase [Amano et al., 2001]. ROK is also involved in the "cross-talk" between Ras and Rho signaling leading to cellular transformation [Sahai et al., 2001]. ROK expression has been detected in numerous cell lines, including breast tumor cells [Bourguignon et al., 1999]. However, the question whether ROK activation contributes to invasive properties of breast tumor cells is addressed in this study.

## (6) BODY

### **(A) RHO-KINASE (ROK) PROMOTES CD44<sub>v3,8-10</sub>-ANKYRIN INTERACTION AND TUMOR CELL MIGRATION IN METASTATIC BREAST CANCER CELLS**

Metastatic breast tumor Met-1 cells express CD44<sub>v3,8-10</sub>, a major adhesion receptor which binds extracellular matrix components at its extracellular domain and interacts with the cytoskeletal protein, ankyrin, at its cytoplasmic domain. In this study we have determined that CD44<sub>v3,8-10</sub> and RhoA GTPases are physically associated *in vivo*, and that CD44<sub>v3,8-10</sub>-bound RhoA displays GTPase activity which can be inhibited by botulinum toxin C3-mediated ADP-ribosylation. In addition, we have identified a 160kDa Rho-Kinase (ROK) as one of the downstream targets for CD44<sub>v3,8-10</sub>-bound RhoA GTPase. Specifically, RhoA (complexed with CD44<sub>v3,8-10</sub>) stimulates ROK-mediated phosphorylation of certain cellular proteins including the cytoplasmic domain of CD44<sub>v3,8-10</sub>. Most importantly, phosphorylation of CD44<sub>v3,8-10</sub> by ROK enhances its interaction with the cytoskeletal protein, ankyrin.

We have also constructed two ROK cDNA constructs which encode for proteins consisting of 537 amino acids [designated as the constitutively active form of ROK containing the catalytic domain (CAT, also the kinase domain)], and 173 amino acids [designated as the dominant-negative form of ROK containing the Rho-binding domain (RB)]. Microinjection of the ROK's CAT domain into Met-1 cells promotes CD44-ankyrin associated membrane ruffling and projections. This membrane motility can be blocked by CD44 antibodies and cytochalasin D (a microfilament inhibitor). Furthermore, overexpression of a dominant-negative form of ROK by transfection of Met-1 cells with ROK's Rho-binding (RB) domain cDNA effectively inhibits

CD44-ankyrin-mediated metastatic behavior (e.g. membrane motility and tumor cell migration). These findings support the hypothesis that ROK plays a pivotal role in CD44<sup>v3,8-10</sup>-ankyrin interaction and RhoA-mediated oncogenic signaling required for membrane-cytoskeleton function and metastatic tumor cell migration.

#### **(B) CD44 INTERACTION WITH RHO-KINASE (ROK) ACTIVATES INOSITOL 1,4,5-TRIPHOSPHATE (IP<sub>3</sub>) RECEPTOR-MEDIATED Ca<sup>2+</sup> SIGNALING DURING HYALURONAN (HA)-INDUCED BREAST TUMOR CELL MIGRATION**

In this study we have determined that CD44 and Rho-Kinase (ROK) are physically associated as a complex in breast tumor cells (SP-1). Using a recombinant fragment of ROK [in particular, the pleckstrin homology (PH) domain] and *in vitro* binding assays, we have detected a specific binding interaction between the PH domain of ROK and the cytoplasmic domain of CD44. Scatchard plot analysis indicates that there is a single high affinity CD44 binding site in the PH domain of ROK with an apparent dissociation constant (K<sub>d</sub>) of 1.76nM which is comparable to CD44 binding (K<sub>d</sub> ~1.56nM) to intact ROK. These findings suggest that the PH domain is the primary ROK binding region for CD44.

Furthermore, HA binding to SP-1 cells promotes RhoA-mediated ROK activity which, in turn, increases phosphorylation of three different inositol 1, 4, 5-trisphosphate receptors (IP<sub>3</sub>Rs) [in particular, subtype 1 (IP<sub>3</sub>R1), and to a lesser extent subtype 2 (IP<sub>3</sub>R2) and subtype 3 (IP<sub>3</sub>R3)] all known as IP<sub>3</sub>-gated Ca<sup>2+</sup> channels. The phosphorylated IP<sub>3</sub>R1 (but not IP<sub>3</sub>R2 and IP<sub>3</sub>R3) is enhanced in its binding to IP<sub>3</sub> which subsequently stimulates IP<sub>3</sub>-mediated Ca<sup>2+</sup> flux. Transfection of SP-1 cells with ROK's PH cDNA significantly reduces ROK association with CD44<sup>v10</sup>, and effectively inhibits ROK-mediated phosphorylation of IP<sub>3</sub>Rs and IP<sub>3</sub>R-mediated Ca<sup>2+</sup> flux *in vitro*. The PH domain of ROK also functions as a dominant-negative mutant *in vivo* to block HA-dependent, CD44<sup>v10</sup>-specific intracellular Ca<sup>2+</sup> mobilization and breast tumor cell migration. Taken together, we believe that CD44 interaction with ROK plays a pivotal role in IP<sub>3</sub>R-mediated Ca<sup>2+</sup> signaling during HA-mediated breast tumor cell migration.

#### **(7) KEY RESEARCH ACCOMPLISHMENTS:**

##### **(A) Rho-Kinase (ROK) Interaction With CD44 and the Cytoskeletal Protein, Ankyrin in Breast Tumor Cells:**

- We have found that Rho-Kinase (ROK) is one of the known RhoA-activated enzymes and is expressed in breast tumor cells (e.g. Met-1 and SP-1 cell lines).
- Our data indicate that the interaction between the metastasis-specific molecule, CD44 [a hyaluronan (HA) receptor] and ROK occurs in metastatic breast tumor cells (SP1 cell line).
- Scatchard plot analysis indicates that there is a single high affinity CD44 binding site in ROK's PH domain. These findings suggest that the PH domain is the primary ROK binding region for CD44.

- The binding of HA to CD44 of breast tumor cells (Met-1 cells) stimulates RhoA signaling and ROK activation which, in turn, increases phosphorylation of CD44. Most importantly, phosphorylation of CD44 by ROK enhances its interaction with the cytoskeletal protein, ankyrin. Most importantly, CD44 phosphorylation by ROK enhances its interaction with the cytoskeletal protein, ankyrin in breast tumor cells.

**(B) Rho-Kinase (ROK)-CD44 interaction Promotes Inositol 1,4,5-Triphosphate (IP<sub>3</sub>) Receptor-Mediated Ca<sup>2+</sup> Signaling and Breast Tumor Cell Migration:**

- We have found that CD44-associated Rho-Kinase (ROK) is capable of phosphorylating three different inositol 1, 4, 5-trisphosphate receptors (IP<sub>3</sub>Rs) [in particular, subtype 1 (IP<sub>3</sub>R1), and to a lesser extent subtype 2 (IP<sub>3</sub>R2) and subtype 3 (IP<sub>3</sub>R3)] all known as IP<sub>3</sub>-gated Ca<sup>2+</sup> channels.
- Phosphorylation of IP<sub>3</sub>R1 (but not IP<sub>3</sub>R2 and IP<sub>3</sub>R3) by ROK enhances in its binding to IP<sub>3</sub> which subsequently stimulates IP<sub>3</sub>-mediated Ca<sup>2+</sup> flux in breast tumor cells.
- Transfection of SP-1 cells with ROK's RB or PH cDNA significantly reduces ROK/CD44 interaction with the cytoskeleton, and effectively inhibits ROK phosphorylation of IP<sub>3</sub>Rs and IP<sub>3</sub>R-mediated Ca<sup>2+</sup> flux *in vitro*. Both PH and RB domains of ROK also function as potent dominant-negative mutants *in vivo* to block HA-dependent, CD44-specific intracellular Ca<sup>2+</sup> mobilization, cytoskeleton function and breast tumor cell migration.
- These observations clearly suggest that ROK contains multiple functional domains [e.g. membrane localization site(s) and Rho-binding regulatory domains] required for the regulation of CD44-cytoskeleton interaction and IP<sub>3</sub> receptor-mediated Ca<sup>2+</sup> signaling leading to metastatic breast tumor cell progression.

**(8) REPORTABLE OUTCOMES:**

- Manuscripts and abstracts: see section #13 (final report section).
- Funding applied for based on work supported by this award:

Funded Active Grants:

NCI Grant (2000-2005) "CD44/Variant-Cytoskeleton In Breast Cancer Progression".

NCI Grant (1999-2008) "CD44-p185<sup>HER2</sup> Interaction In Ovarian Cancer Progression".

NCI Grant (2001-2003) "CD44 Interaction With Cytokine Receptors in Breast Cancer Bone Metastasis".

US Army Breast Cancer Grant (DOD) (1999-2002) "A Novel Signaling Perturbation and Ribozyme Gene Therapy Procedures to Block Rho-Kinase (ROK) Activation and Breast Tumor Metastasis".

## (9) CONCLUSIONS:

Rho GTPases such as RhoA-activated Rho-Kinase (ROK) participate in CD44-cytoskeleton interaction and  $\text{Ca}^{2+}$  signaling in many different cells including breast tumor cells [Bourguignon, et al., 1999; Singleton and Bourguignon, 2002]. When complexed with CD44, RhoA stimulates Rho-kinase (ROK) to phosphorylate several cellular proteins including CD44<sub>v3,8-10</sub>. Most importantly, phosphorylation of CD44<sub>v3,8-10</sub> by ROK promotes the binding of CD44<sub>v3,8-10</sub> to ankyrin. Overexpression of the ROK's Rho-binding (RB) domain can act as a dominant-negative inhibitor of ROK and reverse tumor cell-specific phenotypes [Bourguignon, et al., 1999]. Therefore, it has been proposed that RhoA-activated ROK signaling is necessary for membrane-cytoskeleton interaction and tumor cell migration during the progression of breast cancers [Bourguignon, et al., 1999].

The binding of hyaluronan (HA) to some CD44 expressing cells also activates  $\text{Ca}^{2+}$  signaling, a pathway known to regulate cell motility, survival and death signals [Berridge, et al., 1998]. There is compelling evidence that RhoGTPases are involved in the regulation of  $\text{Ca}^{2+}$  mobilization [Hong-Geller and Cerione, 2000; Singleton and Bourguignon, et al., 2002]. Our recent work indicates that HA-CD44 interaction promotes RhoA-activated ROK signaling and  $\text{Ca}^{2+}$  mobilization in breast tumor cells. Specifically, we have found that CD44 and RhoA-activated Rho-Kinase (ROK) are physically associated as a complex *in vivo*. Most importantly, HA binding to cells promotes RhoA-mediated ROK activity which, in turn, increases phosphorylation of three different inositol 1, 4, 5-trisphosphate receptors (IP<sub>3</sub>Rs) [in particular, subtype 1 (IP<sub>3</sub>R1), and to a lesser extent subtype 2 (IP<sub>3</sub>R2) and subtype 3 (IP<sub>3</sub>R3)] all known as IP<sub>3</sub>-gated  $\text{Ca}^{2+}$  channels. The phosphorylated IP<sub>3</sub>R1 (but not IP<sub>3</sub>R2 or IP<sub>3</sub>R3) is enhanced in its binding to IP<sub>3</sub> which subsequently stimulates IP<sub>3</sub>-mediated  $\text{Ca}^{2+}$  flux. These findings suggest that CD44 interaction with RhoA-activated ROK plays a pivotal role in IP<sub>3</sub>R-mediated  $\text{Ca}^{2+}$  signaling during HA-mediated cellular functions such as cell migration [Singleton and Bourguignon, 2002].

One of the mechanisms by which  $\text{Ca}^{2+}$  may trigger early signal transducing events during HA and CD44-mediated cell migration involves its interaction with calmodulin, an ubiquitous  $\text{Ca}^{2+}$  binding protein [Bourguignon et al., 1993; Chin and Means, 2000].  $\text{Ca}^{2+}$ -dependent calmodulin activity is known to be responsible for the activation of a number of important cellular enzymes, including myosin light chain kinase (MLCK) [Tran et al., 2000; Kamm and Stull, 2001; Stull, 2001].  $\text{Ca}^{2+}$ /calmodulin-dependent phosphorylation of myosin light chain has been shown to be important for cell migration [Birukov et al., 2001]. In summary, we would like to propose that the transmembrane interaction between CD44 and ROK not only stimulates CD44-cytoskeleton interaction but also promotes IP<sub>3</sub> receptor phosphorylation and subsequent IP<sub>3</sub> receptor-mediated  $\text{Ca}^{2+}$  signaling that is required for HA-mediated breast cell migration.

## (10) REFERENCES:

- Amano M., Ito M., Kimura K., Fukata Y., Chihara K., Nakano T., Matsuura Y., Kaibuchi K. 1996. Phosphorylation and activation of myosin by Rho-associated kinase (Rho-kinase). *J. Biol. Chem* 271:20246-20249.
- Amano M., Chihara K., Kimura K., Fukata Y., Nakamura N., Matsuura Y., Kaibuchi K. 1997. Formation of actin stress fibers and focal adhesions enhanced by Rho-kinase. *Science* 275:1308-1311.
- Amano M., Chihara K., Nakamura N., Kaneko T., Matsuura Y., Kaibuchi K. 1999. The COOH terminus of Rho-kinase negatively regulates rho-kinase activity. *J. Biol. Chem* 274:32418-32424.
- Amano T., Tanabe K., Eto T., Narumiya S., Mizuno K. 2001. LIM-kinase 2 induces formation of stress fibres, focal adhesions and membrane blebs, dependent on its activation by Rho-associated kinase-catalysed phosphorylation at threonine-505. *Biochem J* 354:149-159.
- Angkachatchai V., Finkel T.H. 1999. ADP-ribosylation of rho by C3 ribosyltransferase inhibits IL-2 production and sustained calcium influx in activated T cells. *J. Immunol* 163:3819-3825.
- Berridge MJ., Bootman MD., Lipp P. 1998. Calcium--a life and death signal. *Nature* 395:645-648.
- Birukov KG., Csontos C., Marzilli L., Dudek S., Ma SF., Bresnick AR., Verin AD., Cotter RJ., Garcia J.G. 2001. Differential regulation of alternatively spliced endothelial cell myosin light chain kinase isoforms by p60(Src). *J Biol Chem* 276:8567-8573.
- Bourguignon LY., Lokeshwar VB., Chen X., Kerrick WG. 1993. Hyaluronic acid-induced lymphocyte signal transduction and HA receptor (GP85/CD44)-cytoskeleton interaction. *J Immunol* 151:6634-6644.
- Bourguignon LY., Zhu H., Shao L., Zhu D., Chen YW. 1999. Rho-kinase (ROK) promotes CD44v<sub>3,8-10</sub>-ankyrin interaction and tumor cell migration in metastatic breast cancer cells. *Cell Motil Cytoskel* 43:269-287.
- Bourguignon LY., Zhu H., Shao L., Chen YW. 2000a. CD44 interaction with tiam1 promotes Rac1 signaling and hyaluronic acid-mediated breast tumor cell migration. *J Biol Chem* 275:1829-1838.
- Bourguignon LY., Zhu H., Shao L., Chen YW. 2000b. Ankyrin-Tiam1 interaction promotes Rac1 signaling and metastatic breast tumor cell invasion and migration. *J Cell Biol* 150:177-191.

- Bourguignon LY. 2001a. CD44-mediated oncogenic signaling and cytoskeleton activation during mammary tumor progression. *J Mamm Gland Biol & Neo* 6:287-297.
- Bourguignon LY., Zhu H., Zhou B., Diedrich F., Singleton PA., Hung MC. 2001b. Hyaluronan promotes CD44v3-Vav2 interaction with Grb2-p185<sup>HER2</sup> and induces Rac1 and Ras signaling during ovarian tumor cell migration and growth. *J Biol Chem* 276:48679-48692.
- Chin D., Means AR. 2000. Calmodulin: a prototypical calcium sensor. *Trend Cell Biol* 10:322-328.
- Fukata Y., Oshiro N., Kinoshita N., Kawano Y., Matsuoka Y., Bennett V., Matsuura Y., Kaibuchi K. 1999. Phosphorylation of adducin by Rho-kinase plays a crucial role in cell motility. *J Cell Biol* 145:347-361.
- Henke CA., Roongta U., Mickelson DJ., Knutson JR., McCarthy JB. 1996. CD44-related chondroitin sulfate proteoglycan, a cell surface receptor implicated with tumor cell invasion, mediates endothelial cell migration on fibrinogen and invasion into a fibrin matrix. *J Clin Invest* 97:2541-2552.
- Hong-Geller E., Cerione RA. 2000. Cdc42 and Rac stimulate exocytosis of secretory granules by activating the IP<sub>3</sub>/calcium pathway in RBL-2H3 mast cells. *J Cell Biol* 148:481-494.
- Kamm KE., Stull JT. 2001. Dedicated myosin light chain kinases with diverse cellular functions. *J Biol Chem* 276:4527-4530.
- Kimura K., Ito M., Amano M., Chihara K., Fukata Y., Nakafuku M., Yamamori B., Feng J., Nakano T., Okawa K., Iwamatsu A., Kaibuchi K. 1996. Regulation of myosin phosphatase by Rho and Rho-associated kinase (Rho-kinase). *Science*. 273:245-248.
- Matsui T., Amano M., Yamamoto T., Chihara K., Nakafuku M., Ito M., Nakano T., Okawa K., Iwamatsu A., Kaibuchi K. 1996. Rho-associated kinase, a novel serine/threonine kinase, as a putative target for small GTP binding protein Rho. *EMBO J* 15:2208-2216.
- Sahai E., Olson MF., Marshall CJ. 2001. Cross-talk between Ras and Rho signalling pathways in transformation favours proliferation and increased motility. *EMBO J* 20:755-766.
- Singleton, PA., Bourguignon, LYW. 2002. CD44v10 interaction with Rho-kinase (ROK) activates inositol 1,4,5-triphosphate (IP<sub>3</sub>) receptor-mediated Ca<sup>2+</sup> signaling during hyaluronan (HA)-mediated endothelial cell migration. *Cell Motility and the Cytoskeleton* Vol. 54 (in press).
- Stull JT. 2001. Ca<sup>2+</sup>-dependent cell signaling through calmodulin-activated protein phosphatase and protein kinases minireview series. *J Biol Chem* 276:2311-2312.
- Tran QK., Ohashi K., Watanabe H. 2000. Calcium signalling in endothelial cells. *Cardiovas Res* 48:13-22.

Trochon V., Mabilat C., Bertrand P., Legrand Y., Smadja-Joffe F., Soria C., Delpech B., Lu H. 1996. Evidence of involvement of CD44 in endothelial cell proliferation, migration and angiogenesis in vitro. *Int J Cancer* 66:664-668.

**(11) APPENDICES:** (see attached reprints).

**(12) BINDING:** We have prepared the report according to the instruction provided by DOD.

**(13) FINAL REPORTS:**

**Paper Publications:**

1. Kalish, E., N. Iida, F.L. Moffat and Lilly Y. W. Bourguignon. A New CD44v3-Containing Isoform Is Involved in Tumor Cell Migration and Human Breast Cancer Progression. *Front Biosci.* 4:1-8 (1999).
2. Ameen, N.A., B. Martensson, Lilly Y. W. Bourguignon, C. Marino, J. Isenberg and G.E. McLaughlin. CFTR Channel Insertion to The Apical Surface In Rat Duodenal Villus Epithelial Cell Is Upregulated By VIP In Vivo. *J. Cell Sci.* 112:887-894 (1999).
3. Bourguignon, Lilly Y.W., H.Zhu, L. Shao, D. Zhu and Y.W.Chen, Rho-Kinase (ROK) Promotes CD44v<sub>3,8-10</sub>-Ankyrin Interaction And Tumor Cell Migration In Metastatic Breast Cancer Cells. *Cell Motility & The Cytoskeleton*, 43:269-287 (1999).
4. Bourguignon, Lilly Y.W., H.Zhu, L. Shao and Y.W.Chen, CD44 Interaction with Tiam1 Promotes Rac1 Signaling and Hyaluronic Acid (HA)-Mediated Breast Tumor Cell Migration. *J. Biol. Chem.* 275:1829-1838 (2000).
5. Zhu, D. and Lilly Y.W. Bourguignon. Interaction Between CD44 and The Repeat Domain of Ankyrin Promotes Hyaluronic Acid (HA)-Mediated Ovarian Tumor Cell Migration. *J. Cell Physiol.* 183:182-195 (2000).
6. Diaz, F. and Lilly Y.W. Bourguignon. Selective Down-Regulation of IP3 Receptor Subtypes By Caspases and Calpain During TNF-Induced Apoptosis of Human T-Lymphoblasts. *Cell Calcium*, 27:315-328 (2000).
7. Bourguignon, Lilly Y.W., H.Zhu, L. Shao and Y.W.Chen, Ankyrin-Tiam1 Interaction Promotes Rac1 Signaling and Metastatic Breast Tumor Cell Invasion and Migration. *J. Cell Biol.* 150:177-191 (2000).
8. Bourguignon, Lilly Y.W., H. Zhu, L. Shao, and Y.W. Chen. CD44 Interaction With c-Src Kinase Promotes Cortactin-Mediated Cytoskeleton Function and Hyaluronic acid (HA)-Dependent Ovarian Tumor Cell Migration. *J. Biol. Chem.* 276:7327-7336 (2001).

9. Franzmann, E.J., D.T. Weed, F.J. Civantos, W.J. Goodwin, and Lilly Y.W. Bourguignon. A Novel CD44v3 Isoform Is Involved in Head and Neck Squamous Cell Carcinomous Progression. *Otolaryngol Head Neck Surg* 124:426-432 (2001).
10. Bourguignon, Lilly Y.W. CD44-Mediated Oncogenic Signaling and Cytoskeleton Activation During Mammary Tumor Progression. *Journal of Mammary Gland Biology and Neoplasia* (Invited Review Article) 6:287-297 (2001).
11. Lin, S.Y., A., K. Makino, W. Xia, A. Martin, Y. Wen, K.Yin, Lilly Y.W. Bourguignon and M.C. Hung. Nuclear Localization of EGF Receptor and Its Potential New Role As A Transcription Factor. *Nature Cell Biol.* 3:802-808 (2001).
12. Chang, W., S. Pratt, T.H. Chen, Lilly Y. W.Bourguignon, and D. Shoback. Amino Acids In the Cytoplasmic Carboxyl-Terminus of the Parathyroid  $\text{Ca}^{2+}$ -Sensing Receptor Mediate Efficient Cell-Surface Expression and Phospholipase C Activation. *J. Biol. Chem.* 276:44129-44136 (2001).
13. Bourguignon, Lilly Y., Hongbo Zhu, Bo Zhou, Falko Diedrich, Patrick, A Singleton and Mien-Chie Hung. Hyaluronan (HA) Promotes CD44v3-Vav2 Interaction With Grb2-p185<sup>HER2</sup> and Induces Rac1 & Ras Signaling During Ovarian Tumor Cell Migration and Growth. *J. Biol. Chem.* 276:48679-48692 (2001).
14. Bourguignon, Lilly, Keng-hsueh Lan, Patrick Singleton, Shiaw-Yih Lin, Dihua Yu and Mien-Chie Hung. Localizing the EGF Receptor. *Nature Cell Biol.* 4:E22-23 (2002).
15. Turley, E. A., P. W. Nobel and Lilly Y. W. Bourguignon. Signaling Properties of Hyaluronan Receptors.[Mini-Review] *J. Biol. Chem.* 277:4589-4592 (2002).
16. Singleton, P.A. and Lilly Y.W. Bourguignon. CD44v10 Interaction With Rho-Kinase (ROK) Activates Inositol 1,4,5-Triphosphate (IP3) Receptor-Mediated  $\text{Ca}^{2+}$  Signaling During Hyaluronan (HA)-Induced Endothelial Cell Migration. *Cell Motility & The Cytoskeleton* (in Press, 2002).
17. Bourguignon, Lilly Y.W., Patrick Singleton, Hongbo Zhu, and Bo. Zhou. Hyaluronan (HA) Promotes Signaling Interaction Between CD44 and The  $\text{TGF}\beta$ -RI receptor in Metastatic Breast Tumor Cells. *J. Biol. Chem.* (In Press, 2002).

#### **Abstracts:**

1. Bourguignon, Lilly Y.W., H.Zhu, L. Shao, and Y.W.Chen, Identification Of An Ankyrin-Binding Domain In TIAM1 And Its Role In Regulating CD44v<sub>3,8-10</sub>-Associated Metastatic Breast Tumor Cell Invasion And Migration. *Proceeding of the American Association for Cancer Res.* 40:196 (1999).

2. Bourguignon, Lilly Y.W., H.Zhu, L. Shao, D. Zhu and Y.W.Chen, Rho-Kinase (ROK) Promotes CD44<sup>v3,8-10</sup>-Ankyrin Interaction And Tumor Cell Migration In Metastatic Breast Cancer Cells. Proceeding of the American Association for Cancer Res. 40:105 (1999).
3. Zhu, D. and Lilly Y.W. Bourguignon. Interaction Between CD44 and The Repeat Domain of Ankyrin Promotes Hyaluronic Acid (HA)-Mediated Ovarian Tumor Cell Migration. Proceeding of the American Association for Cancer Res. (2000).
4. Bourguignon, Lilly Y.W., H.Zhu, L. Shao and Y.W.Chen, CD44 Interaction with Tiam1 Promotes Rac1 Signaling and Hyaluronic Acid (HA)-Mediated Breast Tumor Cell Migration. Proceeding of the American Association for Cancer Res. (2000).
5. Bourguignon, Lilly Y.W., H.Zhu, L. Shao and Y.W.Chen, Ankyrin-Tiam1 Interaction Promotes Rac1 Signaling and Metastatic Breast Tumor Cell Invasion and Migration. Mol. Biol. Cell (2000).
6. Singleton, P.A. and Bourguignon, Lilly Y.W. CD44<sup>v10</sup> Interaction with Rho-Kinase (ROK) Promotes Cytoskeleton Function and HA-Mediated Endothelial Cell migration. Mol. Biol. Cell (2000).
7. Bourguignon, Lilly Y.W., P.A. Singleton, Chia-Ling Tu, Wenhan Chang and Dan Bikle. CD44 Interactions With  $Ca^{2+}$  Signaling Molecules Are Required for Keratinocyte Differentiation. The Society for Investigative Dermatology (2001).
8. Bourguignon, Lilly Y., Hongbo Zhu, Bo Zhou, Falko Diedrich, Patrick, A Singleton and Mien-Chie Hung. Hyaluronan (HA) Promotes CD44<sup>v3</sup>-Vav2 Interaction With Grb2-p185<sup>HER2</sup> and Induces Rac1 & Ras Signaling During Ovarian Tumor Cell Migration and Growth. American Association for Cancer Research meeting (2002).
9. Singleton, P.A. and Lilly Y.W. Bourguignon. CD44<sup>v10</sup> Interaction With Rho-Kinase (ROK) Activates Inositol 1,4,5-Triphosphate (IP3) Receptor-Mediated  $Ca^{2+}$  Signaling During Hyaluronan (HA)-Induced Endothelial Cell Migration. Mol. Biol. Cell (2002).
10. Bourguignon, Lilly Y.W. and P.A. Singleton. Hyaluronan and CD44-Induced  $Ca^{2+}$  Signaling In Keratinocytes. Mol. Biol. Cell (2002).

#### **A list of personnel:**

Lilly Y.W. Bourguignon, Ph.D., Principal Investigator.  
 F. Diaz, Ph.D. Postdoctoral fellow.  
 D. Zhu, Ph.D. Research Associate.  
 H.B. Zhu, Technician.  
 L.J. Shao, Technician.  
 Bo Zhou, Research Associate  
 P.A. Singleton, Research Associate

## Rho-Kinase (ROK) Promotes CD44<sub>v3,8–10</sub>-Ankyrin Interaction and Tumor Cell Migration in Metastatic Breast Cancer Cells

Lilly Y.W. Bourguignon,\* Hongbo Zhu, Lijun Shao, Dan Zhu, and You-Wei Chen

*Department of Cell Biology and Anatomy, University of Miami Medical School, Miami, Florida*

Metastatic breast tumor Met-1 cells express CD44<sub>v3,8–10</sub>, a major adhesion receptor that binds extracellular matrix components at its extracellular domain and interacts with the cytoskeletal protein, ankyrin, at its cytoplasmic domain. In this study, we have determined that CD44<sub>v3,8–10</sub> and RhoA GTPases are physically associated *in vivo*, and that CD44<sub>v3,8–10</sub>-bound RhoA displays GTPase activity, which can be inhibited by botulinum toxin C3-mediated ADP-ribosylation. In addition, we have identified a 160 kDa Rho-Kinase (ROK) as one of the downstream targets for CD44<sub>v3,8–10</sub>-bound RhoA GTPase. Specifically, RhoA (complexed with CD44<sub>v3,8–10</sub>) stimulates ROK-mediated phosphorylation of certain cellular proteins including the cytoplasmic domain of CD44<sub>v3,8–10</sub>. Most importantly, phosphorylation of CD44<sub>v3,8–10</sub> by ROK enhances its interaction with the cytoskeletal protein, ankyrin. We have also constructed two ROK cDNA constructs that encode for proteins consisting of 537 amino acids [designated as the constitutively active form of ROK containing the catalytic domain (CAT, also the kinase domain)], and 173 amino acids [designated as the dominant-negative form of ROK containing the Rho-binding domain (RB)]. Microinjection of the ROK's CAT domain into Met-1 cells promotes CD44-ankyrin associated membrane ruffling and projections. This membrane motility can be blocked by CD44 antibodies and cytochalasin D (a microfilament inhibitor). Furthermore, overexpression of a dominant-negative form of ROK by transfection of Met-1 cells with ROK's Rho-binding (RB) domain cDNA effectively inhibits CD44-ankyrin-mediated metastatic behavior (e.g., membrane motility and tumor cell migration). These findings support the hypothesis that ROK plays a pivotal role in CD44<sub>v3,8–10</sub>-ankyrin interaction and RhoA-mediated oncogenic signaling required for membrane-cytoskeleton function and metastatic tumor cell migration. *Cell Motil. Cytoskeleton* 43:269–287, 1999. © 1999 Wiley-Liss, Inc.

**Key words:** CD44<sub>v3</sub>; ankyrin; Rho kinase (ROK); breast tumor

### INTRODUCTION

A number of studies have been aimed at identifying molecules expressed by breast tumor cells that correlate with metastatic behavior. One such candidate is CD44, which belongs to a family of transmembrane glycoproteins. Specifically, CD44s (the standard form, molecular mass of 85–95 kDa) is widely expressed on hematopoietic cells, fibroblasts, and certain transformed epithelial

Contract grant sponsor: United States Public Health; Contract grant numbers: CA66163, CA78633; Contract grant sponsor: DOD; Contract grant numbers: DAMD 17-94-J-4121, DAMD 17-97-1-7014, DAMD 17-99-1-9291.

\*Correspondence to: Dr. Lilly Y.W. Bourguignon, Department of Cell Biology and Anatomy, University of Miami Medical School, 1600 N.W. 10th Avenue, Miami, FL 33136.

E-mail: lbourgui@mednet.med.miami.edu

Received 22 December 1998; accepted 24 May 1999

cells [Bourguignon et al., 1986, 1997; Green et al., 1988; Iida and Bourguignon, 1995; Iida and Bourguignon, 1997; Kalomiris and Bourguignon, 1988; Lesley et al., 1985; Letarte et al., 1985; Stamenkovic et al., 1991; Zhu and Bourguignon, 1996]. A larger protein, CD44E (the epithelial form, molecular mass of 125–150 kDa), results from the alternative splicing of three additional exons [exons 12–14 (v8–10)] into the membrane proximal region of the CD44 molecule and is preferentially expressed on epithelial cells [Screaton et al., 1992; Stamenkovic et al., 1991]. Higher molecular weight “variant” isoforms of CD44 (CD44v) are derived from the alternative splicing of up to ten additional exons in various combinations of the extracellular domain of the molecule [Screaton et al., 1992]. Cell surface expression of certain CD44v isoforms (e.g., CD44v3-containing isoforms) appears to change profoundly during tumor metastasis—particularly during the progression of various carcinomas including breast carcinomas [Arch et al., 1992; Bennet et al., 1995; Droll et al., 1995; Gunthert et al., 1991; Herrlich et al., 1993; Hofmann et al., 1991; Iida and Bourguignon, 1995; Welsh et al., 1995]. Furthermore, CD44v isoforms have been detected on highly metastatic cell lines and transfection of these molecules confers metastatic properties on otherwise non-metastatic cells [Hofmann et al., 1991; Iida and Bourguignon, 1997].

All CD44 isoforms (e.g., CD44s, CD44E, and CD44v) contain several hyaluronic acid (HA)-binding sites in their extracellular domain [Bourguignon et al., 1992, 1993a, 1995b; Lesley et al., 1985; Lokeshwar et al., 1991]. The binding of CD44 isoforms to HA causes cell adhesion to the extracellular matrix (ECM) components [Bourguignon et al., 1992, 1993a, 1995b; Lesley et al., 1993; Lokeshwar and Bourguignon, 1991] and has also been implicated in the stimulation of cell proliferation, cell migration, and angiogenesis [Lokeshwar et al., 1996; Rooney et al., 1995; Turley et al., 1991; West and Kumar, 1989]. The intracellular domain of CD44 binds to certain cytoskeletal proteins such as ankyrin [Bourguignon et al., 1991, 1992, 1993a, 1994, 1995b, 1998a,b; Kalomiris and Bourguignon, 1988, 1989; Lokeshwar and Bourguignon, 1991, 1992; Lokeshwar et al., 1994, 1996; Zhu and Bourguignon, 1996, 1998] and ERM proteins (exrin, radixin and moesin) [Tsukita et al., 1994]. Post-translational modification of CD44's cytoplasmic domain by either acylation [Bourguignon et al., 1991], protein kinase C-mediated phosphorylation [Lokeshwar and Bourguignon, 1992; Kalomiris and Bourguignon, 1989], or GTP binding [Iida and Bourguignon, 1995; Kalomiris and Bourguignon, 1988] enhances the binding between CD44 and cytoskeletal proteins. The transmembrane interaction between CD44 isoforms and ankyrin/ERM provides a direct link between the ECM and the cytoskeleton. A recent study has shown that CD44v isoforms,

such as CD44v<sub>3,8–10</sub>, are involved in cytoskeleton-mediated breast tumor cell migration and invasion [Bourguignon et al., 1998a,b]. However, very little is presently known concerning the CD44v3-associated oncogenic signaling cascade that results in the metastatic phenotype of breast tumor cells.

Members of the Rho subclass of the ras superfamily [small molecular weight GTPases (e.g., RhoA, Rac1, and Cdc42)] are known to be associated with changes in the membrane-linked cytoskeleton [Hall, 1998; Narumiya, 1996]. For example, activation of RhoA, Rac1, and Cdc42 have been shown to produce specific structural changes in the plasma membrane-cytoskeleton associated with membrane ruffling, lamellipodia, filopodia, and stress fiber formation [Hall, 1998; Narumiya, 1996]. The coordinated activation of these GTPases is considered to be a possible mechanism underlying cell motility, an obvious prerequisite for metastasis [Jiang et al., 1994; Lauffenburger and Horwitz, 1996]. Hirao and his co-workers have reported that Rho-like proteins participate in the interaction between the CD44 and the ERM cytoskeletal proteins [Hirao et al., 1996]. The question whether Rho-like proteins play a direct role in regulating CD44v<sub>3</sub>-specific metastatic behaviors in breast tumor cells is addressed in this study.

Several enzymes have been identified as possible downstream targets for Rho GTPases in regulating cytoskeleton-mediated cell motility. One such enzyme is Rho-Kinase (ROK—also called Rho-binding kinase), which is a serine-threonine kinase known to interact with Rho in a GTP-dependent manner [Hall, 1998; Matsui et al., 1996]. Structurally, ROK is composed of catalytic (CAT), coiled-coil, Rho-binding (RB), and pleckstrin-homology (PH) domains [Hall, 1998; Matsui et al., 1996]. Expression of the catalytic domain alone by deleting the regulatory domain [e.g., Rho-binding (RB) domain] causes ROK constitutively active [Amano et al., 1997]. Therefore, the catalytic fragments may act as dominant active forms and the Rho-binding fragments can function as dominant negative form of the ROK molecule [Amano et al., 1997]. Currently, two substrates, myosin light chain and myosin light chain phosphatase, have been shown to be phosphorylated by ROK [Amano et al., 1996; Kimura et al., 1996]. Importantly, ROK-mediated phosphorylation of these two proteins activates myosin adenosine triphosphatase (ATPase) leading to actomyosin-mediated membrane motility and cell movement [Amano et al., 1996, 1997; Kimura et al., 1996]. This information has prompted us to examine whether ROK plays a role in regulating CD44v<sub>3,8–10</sub>-mediated cytoskeleton function in metastatic tumor cells.

In this paper, using a variety of biochemical and molecular biological techniques, we have found that the

cell adhesion receptor, CD44<sub>v3,8-10</sub>, is preferentially expressed in Met-1 breast tumor cells (derived from a high metastatic potential tumor in transgenic mice expressing polyomavirus middle T oncogene). In addition, CD44<sub>v3,8-10</sub> is found to be physically linked to RhoA GTPase in Met-1 cells. We have also demonstrated that RhoA (complexed with CD44<sub>v3,8-10</sub>) stimulates Rho-Kinase (ROK) (a known downstream target for RhoA) to phosphorylate several cellular proteins including CD44<sub>v3,8-10</sub>. Most importantly, the phosphorylation of CD44<sub>v3,8-10</sub> by ROK promotes the binding of CD44<sub>v3,8-10</sub> to ankyrin. Overexpression of the Rho-binding (RB) domain (a dominant-negative form) of ROK by transfecting Met-1 cells with RB cDNA induces reversal of tumor cell-specific phenotypes. Therefore, we believe that CD44<sub>v3,8-10</sub> and RhoA-mediated signaling is involved in the up-regulation of ROK needed for membrane-cytoskeleton interaction and tumor cell migration during the progression of metastatic breast tumor cells.

## MATERIALS AND METHODS

### Cell Culture

Mammary tumor cells containing the polyoma virus middle T (PyV-MT) transgene under the transcriptional control of the MMTV LTR promoter were used to initiate a transplantable line in nude mice. The PyV-MT transgenic mammary tumor cells were obtained from mammary tumors which arose in the transgenic colony at the Institute for Molecular Biology and Biotechnology, McMaster University, Hamilton, Ontario, Canada (Dr. William J. Muller) [Guy et al., 1992]. Mammary tumors were collagenase/dispase (Worthington, Freehold, NJ) treated, and  $5 \times 10^5$  cells per 100  $\mu$ l were transplanted subcutaneously as a bolus via syringe and a 25 gauge needle into the thoracic region of nude mice. The resulting high potential metastatic PyV-MT transgenic mammary tumor line, Met-1, was maintained by serial transplantation of 1 mm<sup>3</sup> tumor segments into either subcutaneous tissue (ectopic) or intact mammary fat pads (orthotopic).

The Met-1 tumor line was dissociated after transplant generation one and plated onto T-75 flasks to develop a tissue culture line [Cheung et al., 1997]. The Met-1 cell line was cultured in high glucose DMEM supplemented by 10% fetal bovine serum, 2 mM glutamine, and antibiotics (Sigma, St Louis, MO).

### Antibodies and Reagents

Monoclonal rat anti-human CD44 antibody (Clone: 020; Isotype: IgG<sub>2b</sub>; obtained from CMB-TECH, Inc., Miami, FL) used in this study recognizes a common determinant of the CD44 class of glycoproteins including CD44s and other variant isoforms [Iida and Bourguignon,

1995] and is capable of precipitating all CD44 variants. For the preparation of polyclonal rabbit anti-CD44v3 or rabbit anti-Rho-Kinase (ROK) antibody, specific synthetic peptides ( $\approx 15$ –17 amino acids unique for either CD44v3 or N-terminus ROK) were prepared, respectively, by the Peptide Laboratories of Department of Biochemistry and Molecular Biology at the University of Miami Medical School using an Advanced Chemtech automatic synthesizer (model ACT350). Conjugated CD44v3 or ROK peptides (to polylysine) were injected into rabbits to raise the antibodies. All antibodies (e.g., anti-CD44v3 or anti-ROK sera) were collected from each bleed and stored at 4°C containing 0.1% azide. All antibodies (e.g., rabbit anti-CD44v3 IgG or rabbit anti-ROK IgGs) were prepared using conventional DEAE-cellulose chromatography and were tested to be monospecific (by immunoblot assays). Mouse monoclonal ankyrin (Ank1) antibody was prepared as described previously [Bourguignon et al., 1993a]. Rabbit anti-Ank3 antibody was kindly provided by Dr. L. L. Peters (Jackson Laboratory, Bar Harbor, ME) [Peters et al., 1995]. Mouse monoclonal anti-green fluorescent protein (GFP) and anti-glutathione S-transferase (GST) were purchased from PharMingen and Pharmacia, respectively. Rhodamine-labeled phalloidin was purchased from Molecular Probes, Inc. *Clostridium botulinum* C3 toxin was obtained from List Biological Laboratories, Inc. *Escherichia coli*-derived GST-tagged RhoA was a gift from Dr. Martin Schwartz (Scripps Research Institute, La Jolla, CA).

### Cloning, Expression, and Purification of CD44 Cytoplasmic Domain (CD44cyt) from *E. coli*

The cytoplasmic domain of human CD44 (CD44cyt) was cloned into pFLAG-AST using the PCR-based cloning strategy. Using human CD44 cDNA as template, one PCR primer pair (left, FLAG-EcoRI; right, FLAG-XbaI) was designed to amplify the complete the CD44 cytoplasmic domain. The amplified DNA fragments were one-step cloned into a pCR2.1 vector and sequenced. Then, the DNA fragments were cut out by double digestion with EcoRI and XbaI and subcloned into EcoRI/XbaI double-digested pFLAG-AST (Eastman Kodak Co.-IBI, Rochester, NY) to generate FLAG-pCD44cyt construct. The nucleotide sequence of FLAG/CD44cyt junction was confirmed by sequencing. The recombinant plasmids were transformed to BL21-DE3 to produce FLAG-CD44cyt fusion protein. The FLAG-CD44cyt fusion protein was purified by anti-FLAG M2 affinity gel column (Eastman Kodak Co.-IBI). The nucleotide sequence of primers used in this cloning protocol are: FLAG-EcoRI: 5'-GAGAATTCTGAACAGTCGAAGAAG-GTGTCTCTTAAGC-3'; FLAG-XbaI: 5'-AGCTCTAG-ATTACACCCCAATCTTCAT-3'.

### Preparations of Constitutively Active Form and Dominant-Negative Form of Rho-Kinase (ROK)

**Method for preparing GST-tagged constitutively active form [containing catalytic domain (CAT)] of Rho-Kinase (ROK).** The cDNA fragment encoding the constitutively active form of ROK [1–1,611 bp, containing the catalytic domain (CAT)] was generated by reverse transcription-polymerase chain reaction (RT-PCR) using CAT-specific primers, 5'-GACGACGACAAGATGTC-GACTGGGGACAGTTTTGAGAC-3' and 5'-CAGGACAGAGCATCAATTAGCAAGCTGTGAATTCTGACT-3'. These cDNA fragments were then cloned into pESP-2 vector using ESP LIC Cloning Kit (Stratagene) to produce GST-CAT construct. The inserted CAT sequence was verified by nucleotide sequencing analyses. Subsequently, this GST-CAT cDNA was introduced to an eukaryotic expression system such as yeast *Schizosaccharomyces pombe* [Kohli, 1987] to express GST-CAT fusion protein (M.W. 80 kDa). The fusion protein was purified by a glutathione-Sepharose column, analyzed by SDS-PAGE, immunoblot and ROK activity as described below.

**Method for preparing GFP (green fluorescent protein)-tagged dominant-negative form [containing Rho-binding domain (RB)] of Rho-Kinase (ROK).** The cDNA fragment encoding the dominant-negative form of ROK (2,719–3,237 bp, containing the Rho-binding sequence (RB)) was amplified by RT-PCR using RB-specific primers linked with enzyme (Xho I and Hind III) digestion site, 5'-CGATCTCGAGGGCCTTCTGGAG-GAGAGTA-3' and 5'-CGATAAGCTTCTG CATCT-GAAGCTCATTCC-3'. PCR product digested with Xho I and Hind III was purified with QIAquick PCR purification Kit (Qiagen, Valencia, CA). The RB cDNA fragments were cloned into pEGFPC1 vector (Clontech, Palo Alto, CA) digested with Xho I and Hind III. The inserted RB sequence was confirmed by nucleotide sequencing analyses. This GFP-RB cDNA was then used for a transient expression in Met-1 cells. The GFP-RB (M.W.  $\approx$ 50 kDa) expressed in Met-1 cells was analyzed by SDS-PAGE, immunoblot and ROK activity assays as described below.

### Cell Transfection

To establish a transient expression system, Met-1 cells were transfected with various plasmid DNAs (e.g., GFP-tagged RB cDNA or pEGFPC1 vector alone) using electroporation methods according to those procedures described previously [Chu et al., 1987]. Briefly, Met-1 cells were plated at a density of  $2 \times 10^6$  cells per 100 mm dish and transfected with 25  $\mu$ g/dish plasmid cDNA using electroporation at 230 v and 960  $\mu$ FD with a Gene Pulser (Bio-Rad, Hercules, CA). Transfected cells were grown in the culture medium for at least 24–48 h. Various

transfectants were then analyzed for their protein expression (e.g., ROK-related proteins) by immunoblot, ROK activity and cell migration assays as described below.

### Microinjection Procedures

Met-1 cells or COS-7 cells (a CD44-negative cell line) [Lokeshwar et al., 1994] were plated onto glass coverslips and cultured in high-glucose DMEM supplemented by 10% fetal bovine serum and 2 mM glutamine. Both CAT and RB domains (50  $\mu$ g/ml) [in a microinjection buffer containing 50 mM Hepes (pH 7.2), 100 mM KCl, 5 mM NaHPO<sub>4</sub> (pH 7.0)] or buffer alone (as a control) was microinjected into cytosol of Met-1 cells or COS-7 using Micromanipulator 5171 and Transjector 5246 (Eppendorf, Germany). Six hours after injection, cells were fixed with 2% formaldehyde in phosphate-buffered saline for 1 h and processed for immunocytochemical staining as described below.

### Immunoprecipitation and Immunoblotting Techniques

Met-1 cells ( $5 \times 10^5$  cells) were washed in 0.1M phosphate buffered saline (PBS; pH 7.2) and incubated with a solution containing 5 mM HEPES (pH 7.5), 150 mM KCl, 1 mM MgCl<sub>2</sub> and 100  $\mu$ M GTP $\gamma$ S. Cells were then solubilized in 50 mM Tris-HCl (pH 7.4), 150 mM NaCl, and 1% Nonidet P-40 (NP-40) buffer followed by immunoprecipitation by rabbit anti-CD44v3 (or mouse anti-RhoA antibody) plus goat anti-rabbit IgG (or goat anti-mouse IgG), respectively. The immunoprecipitated material was solubilized in SDS sample buffer and analyzed by SDS-PAGE (with 7.5% gel). Separated polypeptides were then transferred onto nitrocellulose filters. After blocking non-specific sites with 3% bovine serum albumin, the nitrocellulose filters were incubated with rabbit anti-CD44v3 antibody (5  $\mu$ g/ml) or mouse anti-RhoA antibody (5  $\mu$ g/ml) plus peroxidase-conjugated goat anti-mouse IgG (1:10,000 dilution). The blots were developed using ECL chemiluminescence reagent (Amersham Life Science, Piscataway, NJ) according to the manufacturer's instructions.

In some cases, NP-40 solubilized plasma membranes were incubated with sulfosuccinimidobiotin (Pierce Co., Rockford, IL) (0.1 mg/ml) in labeling buffer (150  $\mu$ M NaCl, 0.1M HEPES, pH 8.0) for 30 min at room temperature followed by extensive dialysis against PBS buffer [0.1M phosphate buffer (pH 7.5) and 150 mM NaCl]. This biotinylated material was analyzed by SDS-PAGE followed by transferring to the nitrocellulose filters and incubated with ExtrAvidin-peroxidase (Sigma Co.). After an addition of peroxidase substrate (Pierce Co.), the blots were developed using Renaissance chemiluminescence reagent (Amersham Life Science) according to the manufacturer's instructions.

To analyze GTP binding to RhoA, the anti-RhoA-immunoprecipitated materials were transferred to nitrocellulose membrane and probed with 0.25  $\mu\text{M}$  [ $^{35}\text{S}$ ] GTP $\gamma\text{S}$  (1,250 Ci/mmol) in the presence or in the absence of 100  $\mu\text{M}$  unlabeled GTP $\gamma\text{S}$ . To test the binding of RhoA to various ROK proteins, Met-1 ROK (isolated by anti-ROK-conjugated beads) (1  $\mu\text{g}$ ) or GST-CAT (1  $\mu\text{g}$ ) or GFP-RB (1  $\mu\text{g}$ ) were separated on an SDS-PAGE (5–12% gradient gel), transferred to nitrocellulose membrane, and probed with [ $^{35}\text{S}$ ]GTP $\gamma\text{S}$ -GST-RhoA as described previously [Amano et al., 1997]. The radioactively labeled bands were detected by fluorography.

In some cases, GST-tagged CAT fusion protein or cell lysate of Met-1 cells (transiently transfected with either GFP-tagged RB ROK cDNA or pEGFPC1 vector alone) were immunoblotted with mouse anti-GST (5  $\mu\text{g}/\text{ml}$ ) or mouse anti-GFP antibody (5  $\mu\text{g}/\text{ml}$ ) for 1 h at room temperature followed by incubation with horseradish peroxidase-conjugated goat anti-mouse IgG (1:10,000 dilution) at room temperature for 1 h. The blots were developed using ECL chemiluminescence reagent (Amersham Life Science) according to the manufacturer's instructions.

The procedures for [ $^{32}\text{P}$ ]ADP-ribosylation with botulinum toxin C3 were the same as described previously [Aktories et al., 1987; Ohashi and Narumiya, 1987]. Radioactively labeled proteins were immunoprecipitated by anti-CD44v3 antibody followed by SDS-PAGE and autoradiographic analyses.

### GTPase Activity Assay

The GTPase activity was performed as described previously with the following modification [Kabcenell et al., 1990; O'Neil et al., 1990]. The CD44<sub>v3,8-10</sub>-bound RhoA complex (20 pmol) (with or without C3-mediated ADP-ribosylation reaction) were incubated in the GTPase assay buffer [20 mM Tris-HCl (pH 7.4), 5 mM MgCl<sub>2</sub>, 0.1% cholate, and 1 mM dithiothreitol (DTT)] in the presence of 1  $\mu\text{M}$  [ $\gamma$ - $^{32}\text{P}$ ]GTP ( $4 \times 10^4$  cpm/pmol) and 0.1 mM ATP in a reaction volume of 50  $\mu\text{l}$  at 4°C for 30 min. The samples were then incubated at 37°C for various time intervals. Following incubation, 100  $\mu\text{l}$  of 1% BSA, 0.1% dextran sulfate made in 20 mM phosphate buffer (pH 8.0) was added to the reaction mixtures followed by the addition of 750  $\mu\text{l}$  of activated charcoal suspension containing 20 mM phosphate buffer (pH 8.0). Following incubation at 4°C for 30 min, the reaction mixtures were centrifuged, and  $^{32}\text{P}_i$  released in the supernatant was determined by liquid scintillation counting. The results are expressed as pmol of  $\text{P}_i$  released per  $\mu\text{g}$  of protein. In control samples, the non-specific release of  $\text{P}_i$  caused by the background level of GTPase activity (associated with preimmune rabbit IgG-bead associated materials) was determined. The non-specific release of  $\text{P}_i$  in control

samples was less than 10% of that released by CD44v3-bound RhoA complex samples and has been subtracted. Each assay was set up in triplicate and repeated at least 3 times. All data were analyzed statistically by Student's *t*-test and statistical significance was set at  $P < 0.01$ .

**Double immunofluorescence staining.** Met-1 cells (microinjected with CAT or RB) grown in the absence or presence of certain agents [e.g., rabbit anti-CD44v3 antibody (50  $\mu\text{g}/\text{ml}$ ) or preimmune rabbit serum (50  $\mu\text{g}/\text{ml}$ ) or cytochalasin D (20  $\mu\text{g}/\text{ml}$ )] were first washed with PBS [0.1M phosphate buffer (pH 7.5) and 150 mM NaCl] buffer and fixed by 2% paraformaldehyde. Subsequently, cells were surface stained with FITC-labeled rat anti-CD44 antibody. These FITC-labeled cells were then rendered permeable by ethanol treatment followed by incubating with rhodamine (Rh)-conjugated mouse anti-Ank1 or rabbit anti-Ank3 IgG. To detect non-specific antibody binding, FITC-CD44 labeled cells were incubated with Rh-conjugated normal mouse IgG. No labeling was observed in such control samples. The fluorescein- and rhodamine-labeled samples were examined with a confocal laser scanning microscope (MultiProbe 2001 Inverted CLSM system, Molecular Dynamics, Sunnyvale, CA).

**Protein phosphorylation assay.** The kinase reaction was carried out in 50  $\mu\text{l}$  of the reaction mixture containing 40 mM Tris-HCl (pH 7.5), 2 mM EDTA, 1 mM DTT, 7 mM MgCl<sub>2</sub>, 0.1% CHAPS, 0.1  $\mu\text{M}$  calyculin A, 100  $\mu\text{M}$  [ $\gamma$ - $^{32}\text{P}$ ]ATP (15–600 mCi/mmol), purified enzymes (e.g., 100 ng Met-1 ROK, or 20 ng GST-CAT) and 1  $\mu\text{g}$  cellular proteins (e.g., smooth muscle myosin light chain, CD44<sub>v3,8-10</sub> and FLAG-tagged CD44 cytoplasmic domain (FLAG-CD44cyt)) in the presence or absence of GTP $\gamma\text{S}$ -GST-RhoA (complexed with CD44<sub>v3,8-10</sub>) (1  $\mu\text{M}$ ) or GTP $\gamma\text{S}$ -RhoA (dissociated from CD44<sub>v3,8-10</sub>-RhoA complex by 0.6 M NaCl) (1  $\mu\text{M}$ ) or GTP $\gamma\text{S}$ -GST-RhoA fusion protein (1  $\mu\text{M}$ ) (or GST-RhoA alone) or inhibitors such as GFP-RB (1  $\mu\text{M}$ ) or staurosporine (1  $\mu\text{M}$ ). After an incubation for various time intervals (e.g., 0, 10, 20, 30, 60, and 120 min) at 30°C, the reaction mixtures were boiled in SDS-sample buffer and subjected to SDS-PAGE. The protein bands were revealed by silver stain and the radiolabeled bands were visualized by fluorography or analyzed by liquid scintillation counting as described previously [Matsui et al., 1998].

**Binding of  $^{125}\text{I}$ -labeled ankyrin to CD44<sub>v3,8-10</sub> and FLAG-tagged CD44 cytoplasmic domain (FLAG-CD44cyt).** Purified  $^{125}\text{I}$ -labeled ankyrin ( $\approx 0.32$  nM protein,  $1.5 \times 10^4$  cpm/ng) was incubated with purified CD44<sub>v3,8-10</sub> (bound to anti-CD44v3-conjugated beads) or FLAG-tagged CD44 cytoplasmic domain (FLAG-CD44cyt) (bound to anti-FLAG-conjugated beads) ( $\approx 0.75$   $\mu\text{g}$  protein in phosphorylated or unphosphorylated form) in 0.5 ml of the binding buffer [20 mM Tris-HCl (pH 7.4),

150 mM NaCl, 0.1% (w/v) BSA and 0.05% Triton X-100]. Binding was carried out at 4°C for 5 h under equilibrium conditions. Equilibrium conditions were determined by performing a time course (e.g., 1–10 h) of the binding reaction. Following binding, the beads were washed in the binding buffer and the bead bound radioactivity was determined. Non-specific binding was determined in the presence of either a 100-fold excess of unlabeled ankyrin or using bovine serum albumin conjugated Sepharose beads. Non-specific binding was approximately 20–30% of the total binding, and was subtracted from the total binding.

**Tumor cell migration assays.** Twenty-four transwell units were used for monitoring in vitro cell migration as described previously [Merzak et al., 1994]. Specifically, the 8  $\mu$ m porosity polycarbonate filters were used for the cell migration assay [Merzak et al., 1994]. Met-1 cells [ $\approx 1 \times 10^4$  cells/well in phosphate buffered saline (PBS), pH 7.2] [in the presence or absence of rabbit anti-CD44v3 antibody (50  $\mu$ g/ml) or cytochalasin D (20  $\mu$ g/ml)] were placed in the upper chamber of the transwell unit. In some cases, Met-1 cells were transfected with either GFP-tagged RB cDNA or pEGFPC1 vector alone. The growth medium containing high-glucose DMEM supplemented by 10% fetal bovine serum was placed in the lower chamber of the transwell unit. After 18 h incubation at 37°C in a humidified 95% air/5% CO<sub>2</sub> atmosphere, cells on the upper side of the filter were removed by wiping with a cotton swap. Cell migration processes were determined by measuring the cells that migrate to the lower side of the polycarbonate filters by standard cell number counting methods as described previously [Merzak et al., 1994]. Each assay was set up in triplicate and repeated at least 3 times. All data were analyzed statistically using the Student's *t*-test and statistical significance was set at  $P < 0.01$ .

## RESULTS

### Characterization of CD44 Variant Isoform(s) in Met-1 Cells

Breast tumor cells (Met-1 cell line) were derived from a high metastatic potential tumor in transgenic mice expressing polyoma virus middle T oncogene [Cheung et al., 1997; Guy et al., 1992]. They are capable of inducing a high level of intratumoral microvessel formation [Cheung et al., 1997]. Our recent results indicate that Met-1 cells express a CD44 variant isoform, CD44v<sub>3,8-10</sub>, which contains v3 and v8-10 exon insertions [Bourguignon et al., 1998a,b]. This CD44v<sub>3,8-10</sub> variant exon structure was previously identified in human breast carcinoma samples [Bourguignon et al., 1998a,b; Iida and Bourguignon, 1995]. In this study, we have used biotinylation labeling of NP-40 solubilized plasma membranes

and SDS-PAGE analyses to resolve a number of cellular proteins (ranging from  $\approx 300$  kDa to  $\approx 25$  kDa) (Fig. 1, lane 1) in the membrane-cytoskeleton fraction of Met-1 cells. Immunoblotting with anti-CD44v3 antibody indicates that a single polypeptide (M. W.  $\approx 260$  kDa) expressed in Met-1 cells belongs to the CD44v<sub>3,8-10</sub> isoform (Fig. 1, lane 3). No CD44v<sub>3</sub>-containing material is observed in control samples when preimmune rabbit serum is used (Fig. 1, lane 2). These results are consistent with a previous report that determined the molecular mass of this CD44v<sub>3,8-10</sub> isoform to be  $\approx 260$  kDa [Bennet et al., 1995].

Recently, the 260 kDa CD44v<sub>3,8-10</sub> molecule has been found to be closely associated with a matrix metalloproteinase (MMP-9) and also interacts with the cytoskeleton during "invadopodia" formation and tumor cell migration [Bourguignon et al., 1998a,b]. These findings suggest that CD44v<sub>3,8-10</sub> and the associated cytoskeleton play an important role in metastatic tumor cell behavior [Bourguignon et al., 1998a,b]. The question regarding which transmembrane signaling pathways are involved in regulating these CD44v<sub>3,8-10</sub>-mediated cytoskeletal activities in metastatic breast tumor cells is the focus of this study.

### Physical Linkage Between CD44v<sub>3,8-10</sub> and RhoA GTPase

Certain cytoskeleton functions are regulated by activation of Rho GTPases such as RhoA, Rac1, and Cdc42 [Hall, 1998; Narumiya, 1996]. Specifically, RhoA is required for actin filament bundling to regulate stress fiber formation and acto-myosin-based contractility [Hall, 1998; Narumiya, 1996]. The rationale for our focusing on the interaction between small molecular weight GTPases and CD44v<sub>3,8-10</sub>-cytoskeleton-linked invasive phenotypes is based on a previous report by Hirao and co-workers suggesting the involvement of CD44-associated cytoskeletal proteins (ERM) in Rho-induced cytoskeletal effects [Hirao et al., 1996]. In this study, we have detected that the 260 kDa CD44v<sub>3,8-10</sub> band and a 25 kDa RhoA-like protein are physically associated as a complex (Fig. 1, lanes 4 and 5). Specifically, we have used Met-1 cells and anti-RhoA-mediated or anti-CD44v3-immunoprecipitation followed by anti-CD44v3 immunoblot (Fig. 1, lane 4) or anti-RhoA immunoblot (Fig. 1, lane 5), respectively. Together, our results clearly indicate that the CD44v<sub>3,8-10</sub> band is revealed in anti-RhoA-immunoprecipitated materials (Fig. 1, lane 4). The RhoA band is also detected in the anti-CD44v3-immunoprecipitated materials (Fig. 1, lane 5). Control results confirm the specificity of these immunological techniques. For example, very little RhoA is detected in anti-CD44v3-immunoprecipitated materials blotted by an anti-RhoA-free serum (anti-RhoA antibody pre-absorbed by an excess amount

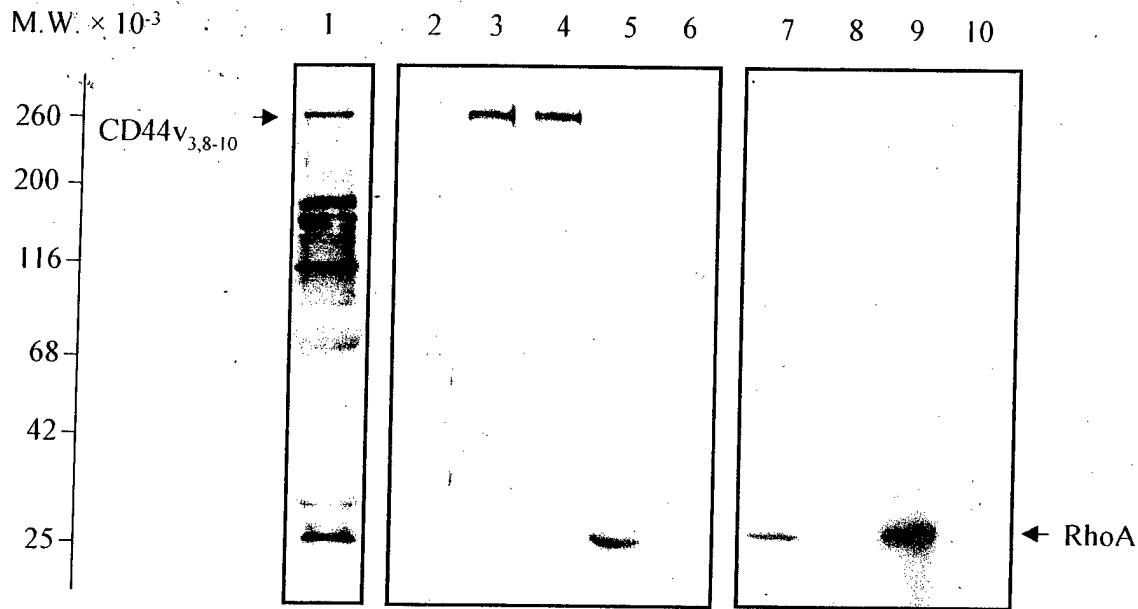


Fig. 1. Analysis of CD44<sub>v3,8-10</sub> expression and CD44<sub>v3,8-10</sub>-RhoA complex in mouse breast tumor cell (Met-1 cells). Met-1 cells ( $5 \times 10^5$  cells) were washed in 0.1M phosphate buffered saline (PBS; pH 7.2) and incubated with a solution containing 5 mM HEPES (pH 7.5), 150 mM KCl, 1 mM MgCl<sub>2</sub>, and 100  $\mu$ M GTP $\gamma$ S. Cells were then solubilized in 50 mM Tris-HCl (pH 7.4), 150 mM NaCl, and 1% Nonidet P-40 (NP-40) buffer followed by immunoblot and/or immunoprecipitation by rabbit anti-CD44v3 or mouse anti-RhoA. The immunoprecipitated material was solubilized in SDS sample buffer and analyzed by SDS-PAGE (with 7.5% gel). The procedures for identifying RhoA by [<sup>35</sup>S]GTP $\gamma$ S binding or botulinum toxin C3-mediated [<sup>32</sup>P]ADP-ribosylation are described in Materials and Methods. **Lane 1:** Biotinylated total NP-40 solubilized plasma membrane-associated proteins. **Lane 2:** Immunoblot of Met-1 cells with preimmune rabbit serum. **Lane 3:** Identification of CD44<sub>v3,8-10</sub> by immunoblotting Met-1 cells with rabbit anti-CD44v3-specific antibody. **Lane 4:** Detection of CD44<sub>v3,8-10</sub> in the complex by anti-RhoA-mediated immunoprecipita-

tion followed by immunoblotting with anti-CD44v3-specific antibody. **Lane 5:** Detection of RhoA in the complex by anti-CD44v3-mediated immunoprecipitation followed by immunoblotting with anti-RhoA-specific antibody. **Lane 6:** Control experiments to detect RhoA in the complex by anti-CD44v3-mediated immunoprecipitation followed by immunoblotting with anti-RhoA-free serum (anti-RhoA antibody pre-absorbed by an excess amount of RhoA). **Lane 7:** Autoradiogram of [<sup>35</sup>S]GTP $\gamma$ S binding (in the absence of unlabeled GTP $\gamma$ S) to RhoA obtained from anti-RhoA-mediated immunoprecipitated materials. **Lane 8:** Autoradiogram of [<sup>35</sup>S]GTP $\gamma$ S binding (in the presence of unlabeled GTP $\gamma$ S) to RhoA obtained from anti-RhoA-mediated immunoprecipitated materials. **Lane 9:** Autoradiogram of [<sup>32</sup>P]ADP-ribosylation of RhoA obtained from anti-RhoA-mediated immunoprecipitated materials in the presence of botulinum toxin C3. **Lane 10:** Autoradiogram of [<sup>32</sup>P]ADP-ribosylation of RhoA obtained from anti-RhoA-mediated immunoprecipitated materials in the absence of botulinum toxin C3.

of RhoA) (Fig. 1, lane 6). Similarly, no CD44<sub>v3,8-10</sub> is observed in anti-RhoA- immunoprecipitated materials blotted by an anti-CD44v3-free serum (anti-CD44v3 antibody pre-absorbed by an excess amount of CD44<sub>v3,8-10</sub>) (data not shown). Preliminary data indicate that approximately 50% of CD44 is associated with RhoA in the plasma membrane fraction of Met-1 cells. These findings establish the fact that CD44<sub>v3,8-10</sub> and RhoA are closely associated with each other as a complex in vivo.

Using an in vitro [<sup>35</sup>S]GTP $\gamma$ S binding assay, we have determined that the 25 kDa RhoA-like protein displays guanine nucleotide binding activity (Fig. 1, lane 7). In the presence of excess amounts of unlabeled GTP $\gamma$ S, no radioactive labeling was observed (Fig. 1, lane 8). Since RhoA has been shown to possess an intrinsic GTPase activity [Hall, 1998], we decided to test whether there is GTPase activity associated with this CD44<sub>v3,8-10</sub>-RhoA complex. As shown in Figure 2, the CD44<sub>v3,8-10</sub>-RhoA complex clearly displays GTPase ac-

tivity, which hydrolyzes [ $\gamma$ -<sup>32</sup>P]GTP in a linear time-dependent manner (Fig. 2A).

However, it is also possible that other small GTP-binding proteins, such as Rac or Cdc42, are also complexed with CD44<sub>v3,8-10</sub> and contribute some of the GTPase activity measured in these experiments. One way to address this issue is to utilize specific Rho inhibitors. For example, RhoA (but not Rac and Cdc42) is a substrate for certain bacterial toxins such as *Clostridium botulinum* C3 toxin [Aktories et al., 1987; Ohashi and Narumiya, 1987]. C3 toxin ADP-ribosylates RhoA (but not Rac and Cdc42) and inactivates RhoA GTPase [Aktories et al., 1987; Ohashi and Narumiya, 1987]. Here, we have found that the 25 kDa protein complexed with CD44<sub>v3,8-10</sub> can be [<sup>32</sup>P]ADP-ribosylated by C3 toxin (Fig. 1, lane 9). In a control sample, when [<sup>32</sup>P]ADP-ribosylation of CD44<sub>v3,8-10</sub> bound RhoA was carried out in the absence of C3 toxin, no labeling of RhoA was observed (Fig. 1, lane 10). Most importantly, C3-mediated ADP-ribosyla-

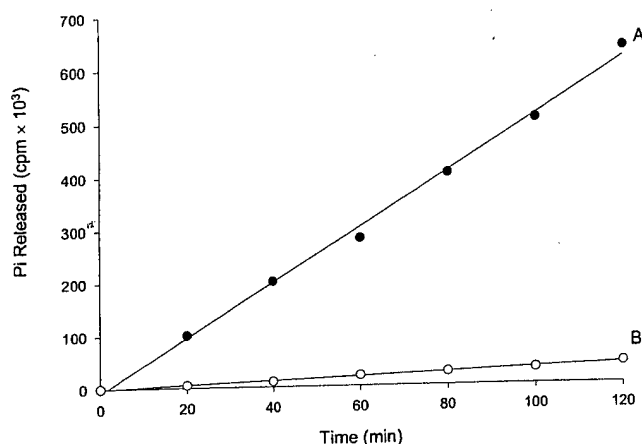


Fig. 2. GTPase activity assay of RhoA complexed with CD44v<sub>3,8-10</sub>. Aliquots of RhoA complexed with CD44v<sub>3,8-10</sub> (as described in Fig. 1) (20 pmol) were incubated with 1  $\mu$ M [ $\gamma$ -<sup>32</sup>P]GTP ( $4 \times 10^4$  cpm/pmol) for various time periods. The amount of <sup>32</sup>P<sub>i</sub> liberated was determined as described in Materials and Methods. Data represent an average of triplicates. The standard deviation was less than 5%. A: In the absence of C3-mediated ADP-ribosylation; B: in the presence of C3-mediated ADP-ribosylation.

tion of RhoA complexed with CD44v<sub>3,8-10</sub> eliminates more than 90% of the GTPase activity (Fig. 2B). These data suggest that CD44v<sub>3,8-10</sub>-bound RhoA displays GTPase activity and also contains a site for ADP-ribosylation mediated by the RhoA inhibitor.

### Rho-Kinase (ROK) as a Downstream Effector for RhoA (Complexed With CD44v<sub>3,8-10</sub>) in Met-1 Cells

**Characterization of rho-kinase (ROK) in Met-1 cells.** In order to identify the downstream target(s) for RhoA GTPase complexed with CD44v<sub>3,8-10</sub> (Fig. 1), we have initially focused on Rho-Kinase (ROK), one of the known effectors for Rho GTPases [Leung et al., 1996; Matsui et al., 1996]. ROK is composed of four functional domains: a kinase domain (catalytic site or CAT), a coiled-coil domain, a Rho-binding (RB) domain, and a pleckstrin-homology (PH) domain [Leung et al., 1996; Matsui et al., 1996] (Fig. 3A-a). Both the kinase (CAT) and Rho-binding (RB) domains share a great deal of sequence homology with a family of related kinases known to bind Rho GTPase and participate in cell motility and cytoskeleton functions [Amano et al., 1997]. To analyze the expression of ROK in Met-1 cells, we have prepared a ROK-specific antibody that is raised against the N-terminal sequence of ROK. Using the ROK-specific antibody and immunoblot of cellular proteins from Met-1 cells, we have identified a 160 kDa polypeptide (Fig. 3B, lane 1). We believe that this antibody is specific since no protein is detected in these cells in the presence of preimmune rabbit IgG

(Fig. 3B, lane 4). Furthermore, we have incubated [<sup>35</sup>S]GTP $\gamma$ S-GST-RhoA with nitrocellulose papers containing ROK (prepared by anti-ROK-mediated immunoprecipitation followed by transfer to nitrocellulose papers). Our results indicate that the 160 kDa polypeptide is capable of binding to GST-RhoA directly (Fig. 3B, lane 2), (but not GST alone) (Fig. 3B, lane 3), and therefore, it is a RhoA-binding protein.

In addition, we have constructed two ROK cDNAs (e.g., CAT cDNA and RB cDNA). These two constructs encode for proteins consisting of 537 amino acids [1-1,611 bp (or aa1-aa537), designated as the constitutively active form of ROK containing the catalytic domain (CAT, also the kinase domain)] (Fig. 3A-b) and 173 amino acids [2,719-3,237bp (or aa907-aa1070), designated as the dominant-negative form of ROK containing the Rho-binding domain (RB)] (Fig. 3A-c), respectively [Amano et al., 1997]. The CAT cDNA was cloned into a GST-tagged expression vector (pESP-2 vector) and then introduced to an eukaryotic expression system such as yeast (*S. pombe*) to produce GST-CAT fusion protein. The RB cDNA was cloned into a green fluorescent protein (GFP)-tagged expression vector (pEFGPC1 vector) followed by a transient transfection of GFP-RB cDNA into Met-1 cells.

Using mouse anti-GST (Fig. 3C, lane 1) and rabbit anti-ROK immunoblot (Fig. 3C, lane 2) analyses, we have detected the GST-CAT fusion protein as a single polypeptide with a molecular mass of 80 kDa. We have also identified the presence of GFP-RB (M.W.  $\approx$ 50kDa) in Met-1 cells (Fig. 3D, lane 1) by anti-GFP immunoblot. No immuno-labeling was observed if normal mouse IgG was used in these samples (Fig. 3C, lane 4 and Fig. 3D, lane 4). To test the ability of these ROK-related proteins to bind RhoA, we have incubated nitrocellulose papers containing ROK-related proteins (e.g. GST-CAT or GFP-RB) with [<sup>35</sup>S]GTP $\gamma$ S-GST-RhoA. Our results indicate that GST-CAT fails to bind RhoA (Fig. 3C, lane 3); whereas GFP-RB binds specifically to [<sup>35</sup>S]GTP $\gamma$ S-GST-RhoA (Fig. 3D, lane 2) (but not GST alone) (Fig. 3D, lane 3). These findings strongly suggest that the Rho-binding site reside in the RB domain but not in the CAT domain.

To determine whether there is kinase(s) activity associated with the 160 kDa protein and/or the two ROK-related proteins (e.g., GST-CAT or GFP-RB), we have carried out the kinase reaction using smooth muscle myosin light chain as a substrate [Amano et al., 1997; Leung et al., 1996] in the presence of various ROK-related proteins including 160 kDa (isolated from Met-1 cells by anti-ROK immuno-beads), GST-CAT and GFP-RB and [ $\gamma$ -<sup>32</sup>P]ATP. As shown in Figure 4A, a significant amount of 160 kDa protein-mediated myosin light chain (MLC) phosphorylation occurs in the presence

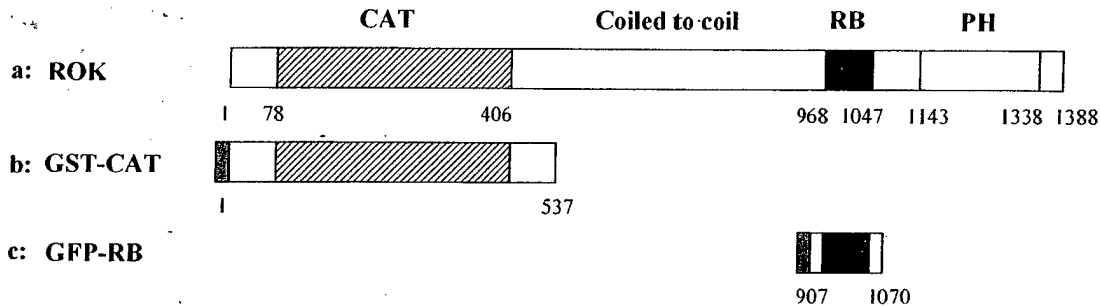
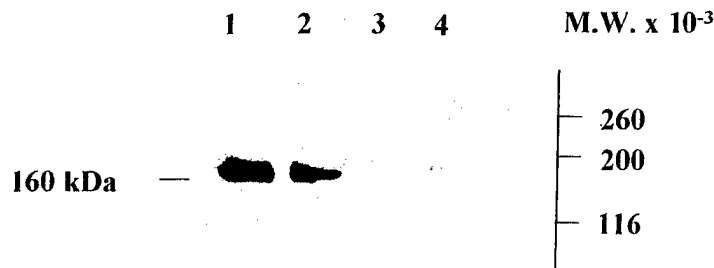
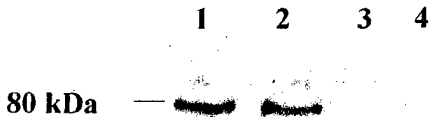
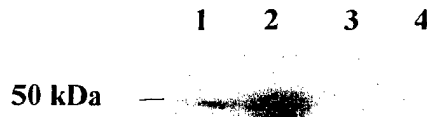
**A: ROK-RELATED PROTEINS****B: ROK****C: GST-CAT****D: GFP-RB**

Fig. 3. Characterization of three ROK-related proteins (e.g., 160 kDa protein, GFP-CAT, and GFP-RB). Three ROK-related proteins (e.g., 160 kDa protein, GFP-CAT, and GFP-RB) were analyzed by immunoblot analyses and [<sup>35</sup>S]GTPγS-GST-RhoA binding as described in Materials and Methods. **A:** Illustration of ROK-related mutant cDNA constructs. **a:** The full-length ROK contains a kinase domain (catalytic domain or CAT), a coiled-coil domain, a rho-binding (RB) domain, and a pleckstrin-homology (PH) domain. **b:** GST-CAT fusion protein represents the catalytic (CAT) domain of ROK (aa1-aa537). **c:** GFP-RB fusion protein represents the rho-binding (RB) domain (aa907-aa1070). **B:** ROK expression in Met-1 cells. **Lane 1:** Identification of ROK by immunoblotting Met-1 cells with rabbit anti-ROK-specific antibody. **Lane 2:** Autoradiogram of [<sup>35</sup>S]GTPγS-GST-RhoA binding to ROK (obtained from anti-ROK-mediated immunoprecipitated materials). **Lane 3:** Autoradiogram of [<sup>35</sup>S]GTPγS binding [in the presence of GST alone (without RhoA)] to ROK (obtained from anti-ROK-

mediated immunoprecipitated materials). **Lane 4:** Immunoblot of Met-1 cells with preimmune rabbit serum. **C:** Characterization of GST-CAT fusion protein. **Lane 1:** Immunoblot of GST-CAT with mouse anti-GST antibody. **Lane 2:** Immunoblot of GST-CAT with rabbit anti-ROK antibody. **Lane 3:** Autoradiogram of [<sup>35</sup>S]GTPγS-GST-RhoA binding to GST-CAT. **Lane 4:** Immunoblot of GST-CAT with normal mouse IgG. **D:** GFP-RB expression in Met-1 cells transfected with GFP-RB cDNA. **Lane 1:** Immunoblot of Met-1 transfectants with mouse anti-GFP antibody. **Lane 2:** Autoradiogram of [<sup>35</sup>S]GTPγS-GST-RhoA binding to GFP-RB (obtained from Met-1 transfectants using anti-GFP-mediated immunoprecipitation). **Lane 3:** Autoradiogram of [<sup>35</sup>S]GTPγS binding [in the presence of GST alone (without RhoA)] to GFP-RB (obtained from Met-1 transfectants using anti-GFP-mediated immunoprecipitated materials). **Lane 4:** Immunoblot of Met-1 transfectants with normal mouse IgG.

of GTPγS-GST-RhoA (Fig. 4A, lane 1). GST-CAT is also found to phosphorylate myosin light chain in the absence of GTPγS-GST-RhoA (Fig. 4A, lane 2). A minimal amount of myosin light chain phosphorylation is detected in the presence of GFP-RB plus GTPγS-GST-RhoA (Fig. 4A, lane 3) or staurosporine (a serine-threo-

nine kinase inhibitor)-treated 160 kDa ROK in the presence of GTPγS-GST-RhoA (Fig. 4A, lane 4). These results are consistent with previous findings [Amano et al., 1996, 1997] suggesting this 160 kDa polypeptide expressed in Met-1 cells belongs to a family of kinases known to bind RhoA GTPase [also called Rho-Kinase

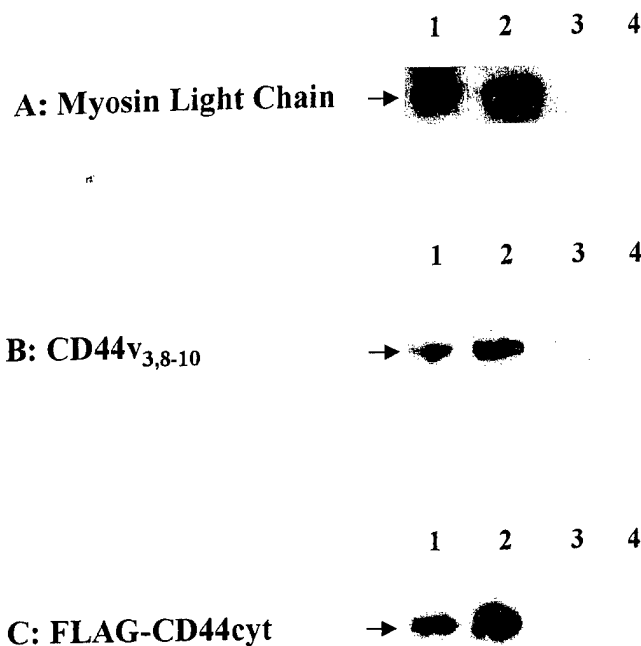


Fig. 4. Effects of ROK and ROK mutant proteins on protein phosphorylation. The kinase reaction was carried out in the reaction mixture containing 100  $\mu$ M [ $\gamma$ - $^{32}$ P]ATP (15–600 mCi/mmol), purified enzymes [e.g., 100 ng Met-1 ROK (isolated from anti-ROK-conjugated beads) or 20 ng GST-CAT] and 1  $\mu$ g cellular proteins [e.g., smooth muscle myosin light chain, CD44<sub>v3,8-10</sub> and FLAG-tagged CD44 cytoplasmic domain (FLAG-CD44cyt)] with or without GTP $\gamma$ S-RhoA (isolated from CD44<sub>v3,8-10</sub>-RhoA complex) (1  $\mu$ M) or GTP $\gamma$ S-GST-RhoA (1  $\mu$ M) or GST-RhoA (1  $\mu$ M) or certain inhibitor (e.g., GFP-RB) as described in Materials and Methods. **A:** Myosin light chain phosphorylation. **Lane 1:** Autoradiogram of myosin light chain phosphorylation by 160 kDa ROK (isolated from Met-1 cells) activated by GTP $\gamma$ S-GST-RhoA. **Lane 2:** Autoradiogram of myosin light chain phosphorylation by GST-CAT in the absence of GTP $\gamma$ S-GST-RhoA. **Lane 3:** Autoradiogram of myosin light chain phosphorylation by GFP-RB (isolated from Met-1 transfectants) in the presence of GTP $\gamma$ S-GST-RhoA. **Lane 4:** Autoradiogram of myosin light chain phosphorylation by 160 kDa ROK in the presence of unactivated GST-RhoA. **B:** CD44<sub>v3,8-10</sub> phosphorylation. **Lane 1:** Autoradiogram of CD44<sub>v3,8-10</sub> phosphorylation by 160 kDa ROK (isolated from Met-1 cells) in the presence of GTP $\gamma$ S-RhoA (isolated from CD44<sub>v3,8-10</sub>-RhoA complex). **Lane 2:** Autoradiogram of CD44<sub>v3,8-10</sub> phosphorylation by GST-CAT in the absence of GTP $\gamma$ S-RhoA. **Lane 3:** Autoradiogram of CD44<sub>v3,8-10</sub> phosphorylation by 160 kDa ROK in the presence of GTP $\gamma$ S-RhoA (isolated from CD44<sub>v3,8-10</sub>-RhoA complex) and GFP-RB. **Lane 4:** Autoradiogram of CD44<sub>v3,8-10</sub> phosphorylation by 160 kDa ROK in the presence of unactivated GST-RhoA. **C:** FLAG-tagged CD44cyt phosphorylation. **Lane 1:** Autoradiogram of FLAG-CD44cyt phosphorylation by GTP $\gamma$ S-GST-RhoA-activated ROK. **Lane 2:** Autoradiogram of FLAG-CD44cyt phosphorylation by GST-CAT in the absence of GTP $\gamma$ S-GST-RhoA. **Lane 3:** Autoradiogram of FLAG-CD44cyt phosphorylation by 160 kDa ROK in the presence of GTP $\gamma$ S-RhoA (isolated from CD44<sub>v3,8-10</sub>-RhoA complex) and GFP-RB. **Lane 4:** Autoradiogram of FLAG-CD44cyt phosphorylation by 160 kDa ROK in the presence of unactivated GST-RhoA.

(ROK)] and to phosphorylate MLC. The CAT (but not RB) of ROK acts as a constitutively active form of kinase.

**Effects of ROK-mediated CD44<sub>v3,8-10</sub> phosphorylation on membrane-cytoskeleton interaction and tumor cell migration.** To identify other possible cellular substrate(s) of ROK in Met-1 cells, we have examined the ability of various ROK-related proteins (e.g., ROK, GST-CAT, and GFP-RB) to CD44 [e.g., CD44<sub>v3,8-10</sub> and/or *E. coli*-derived FLAG tagged-CD44 cytoplasmic domain fusion protein (designated as FLAG-CD44cyt)]. Specifically, we have found that GTP $\gamma$ S-RhoA stimulates 160 kDa ROK to phosphorylate CD44<sub>v3,8-10</sub> (Fig. 4B, lane 1). In the presence of unactivated RhoA (e.g., GST-RhoA), ROK-mediated CD44<sub>v3,8-10</sub> phosphorylation is significantly blocked (Fig. 4B, lane 4). The constitutively active form of ROK (GST-CAT) also causes phosphorylation of CD44<sub>v3,8-10</sub> (Fig. 4B, lane 2); whereas the dominant-negative form (GFP-RB) of ROK inhibits ROK-mediated CD44<sub>v3,8-10</sub> phosphorylation in the presence of GTP $\gamma$ S-RhoA (Fig. 4B, lane 3).

Similarly, our data show that the 160 kDa protein isolated from Met-1 cells is capable of phosphorylating the cytoplasmic domain of CD44 (FLAG-CD44cyt) (Fig. 4C). Specifically, there is a significant increase of 160 kDa protein-mediated phosphorylation of FLAG-CD44cyt in the presence of activated GTP $\gamma$ S-GST-RhoA (Fig. 4C, lane 1). The level of ROK-mediated FLAG-CD44cyt phosphorylation becomes very low if unactivated GST-RhoA is used (Fig. 4C, lane 4). Furthermore, GST-CAT (Fig. 4C, lane 2) causes a significant stimulation of FLAG-CD44cyt phosphorylation (with no addition of GTP $\gamma$ S-GST-RhoA). In the presence of GFP-RB, phosphorylation of FLAG-CD44cyt by GTP $\gamma$ S-GST-RhoA-activated ROK is inhibited (Fig. 4C, lane 3). These findings support the notion that GST-CAT acts as a constitutively active form of ROK and GFP-RB functions as a dominant-negative form of ROK. Together, we conclude that the cytoplasmic domain of CD44 serves as one of the cellular substrates for the 160 kDa Rho-binding-dependent kinase, such as ROK.

In addition, we have analyzed the stoichiometry of CD44 phosphorylation by Rho-Kinase (ROK), along with a time course, and myosin light chain phosphorylation as a positive control. As shown in Figure 5,  $\approx 1.25$  mol of phosphate is maximally incorporated into 1 mol of FLAG-CD44cyt (the cytoplasmic domain of CD44 fusion protein tagged with FLAG) by ROK in the presence of activated GTP $\gamma$ S-GST-RhoA in a time-dependent manner (Fig. 5A-a). Phosphorylation of CD44cyt appears to be minimal (at most  $\approx 0.1$  mol of phosphate incorporated into per mol of FLAG-CD44cyt) using ROK treated with unactivated GST-RhoA (Fig. 5A-b). In addition, we have found that approximately 1 mol of phosphate becomes

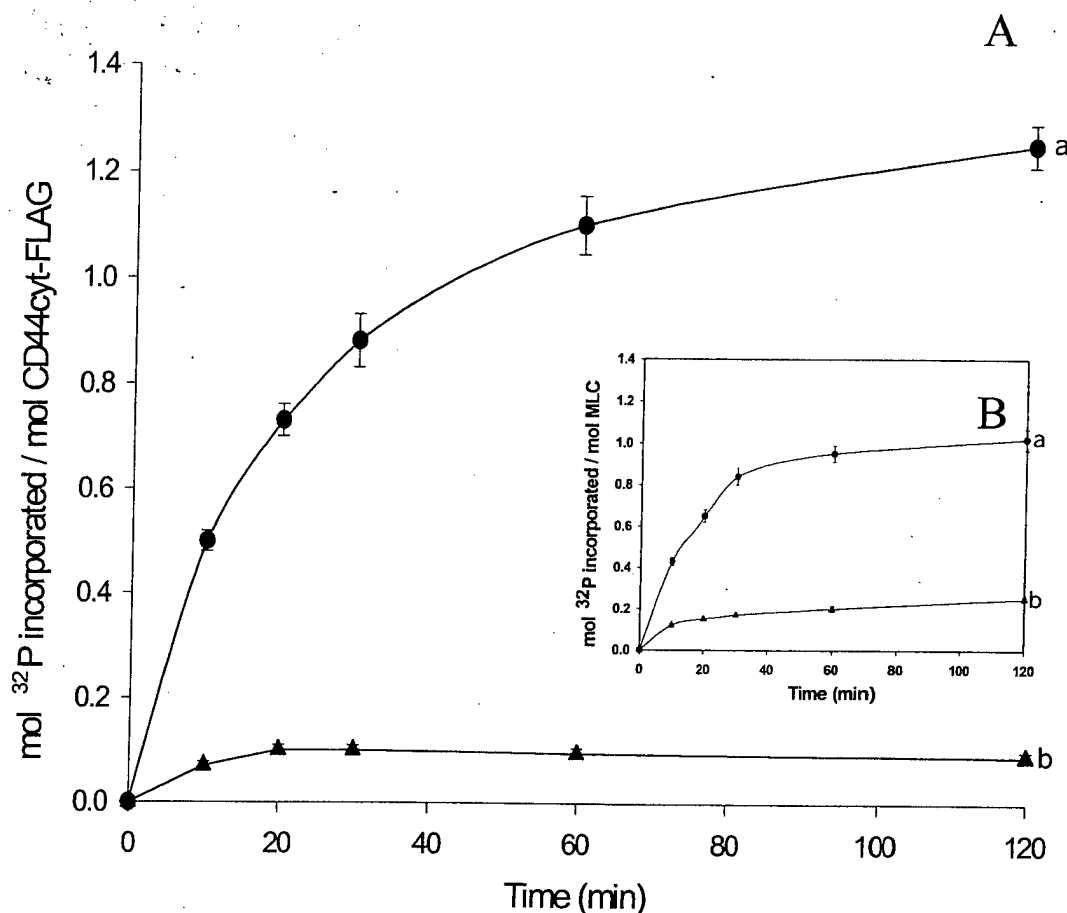


Fig. 5. Measurement of FLAG-CD44cyt phosphorylation by ROK-related proteins. The kinase reaction used in these experiments was the same as described in the legend of Figure 4. The amount of [ $\gamma$ - $^{32}$ P]ATP incorporated into FLAG-CD44cyt by 160 kDa ROK (in the presence of activated GTP $\gamma$ S-GST-RhoA or unactivated GST-RhoA) was measured at various time intervals (e.g., 0, 10, 20, 30, 60, and 120 min) as described in Materials and Methods. Data are means  $\pm$  SEM of

triplicate determinations from 3–5 different experiments. **A-a**: ROK-mediated FLAG-CD44cyt phosphorylation in the presence of activated GTP $\gamma$ S-GST-RhoA. **A-b**: ROK-mediated FLAG-CD44cyt phosphorylation in the presence of unactivated GST-RhoA. **B-a**: ROK-mediated myosin light chain (MLC) phosphorylation in the presence of activated GTP $\gamma$ S-GST-RhoA. **B-b**: ROK-mediated myosin light chain (MLC) phosphorylation in the presence of unactivated GST-RhoA.

maximally incorporated into 1 mol of myosin light chain (MLC) by GTP $\gamma$ S-GST-RhoA-activated ROK (Fig. 5B-a). In contrast, the level of ROK-mediated MLC phosphorylation is greatly reduced [only  $\approx 0.28$  mol of phosphate incorporated into 1 mol of myosin light chain (MLC)] in the presence of unactivated GST-RhoA (Fig. 5B-b). Since the stoichiometry of CD44 phosphorylation by activated ROK is comparable to that of MLC phosphorylation (by activated ROK), we conclude that CD44 is a good cellular substrate for ROK.

Phosphorylation of CD44's cytoplasmic domain has been shown to be important for its interaction with the cytoskeletal proteins such as ankyrin [Bourguignon et al., 1992; Kalomiris and Bourguignon, 1989]. In this study, we decided to examine the effect of ROK-mediated CD44 phosphorylation on ankyrin binding. Specifically, the

highly phosphorylated form of FLAG-CD44cyt (by GTP $\gamma$ S-GST-RhoA-activated ROK; as shown in Fig. 4, lane 1) or the minimally phosphorylated form of FLAG-CD44cyt (using ROK treated with unactivated GST-RhoA; as shown in Fig. 4, lane 4) was incubated with various concentrations of  $^{125}$ I-labeled ankyrin under equilibrium binding conditions. Our results indicate that the total amount of  $^{125}$ I- ankyrin binding to the highly phosphorylated form of FLAG-CD44cyt is significantly higher (Fig. 6C-a) than that detected in the minimally phosphorylated form of FLAG-CD44cyt (Fig. 6C-b). Further Scatchard plot analyses indicate that ankyrin binds to either highly phosphorylated FLAG-CD44cyt or minimally phosphorylated CD44cyt at a single site (Fig. 6A and B). Importantly, the highly phosphorylated FLAG-CD44cyt displays at least 40-fold higher ankyrin binding

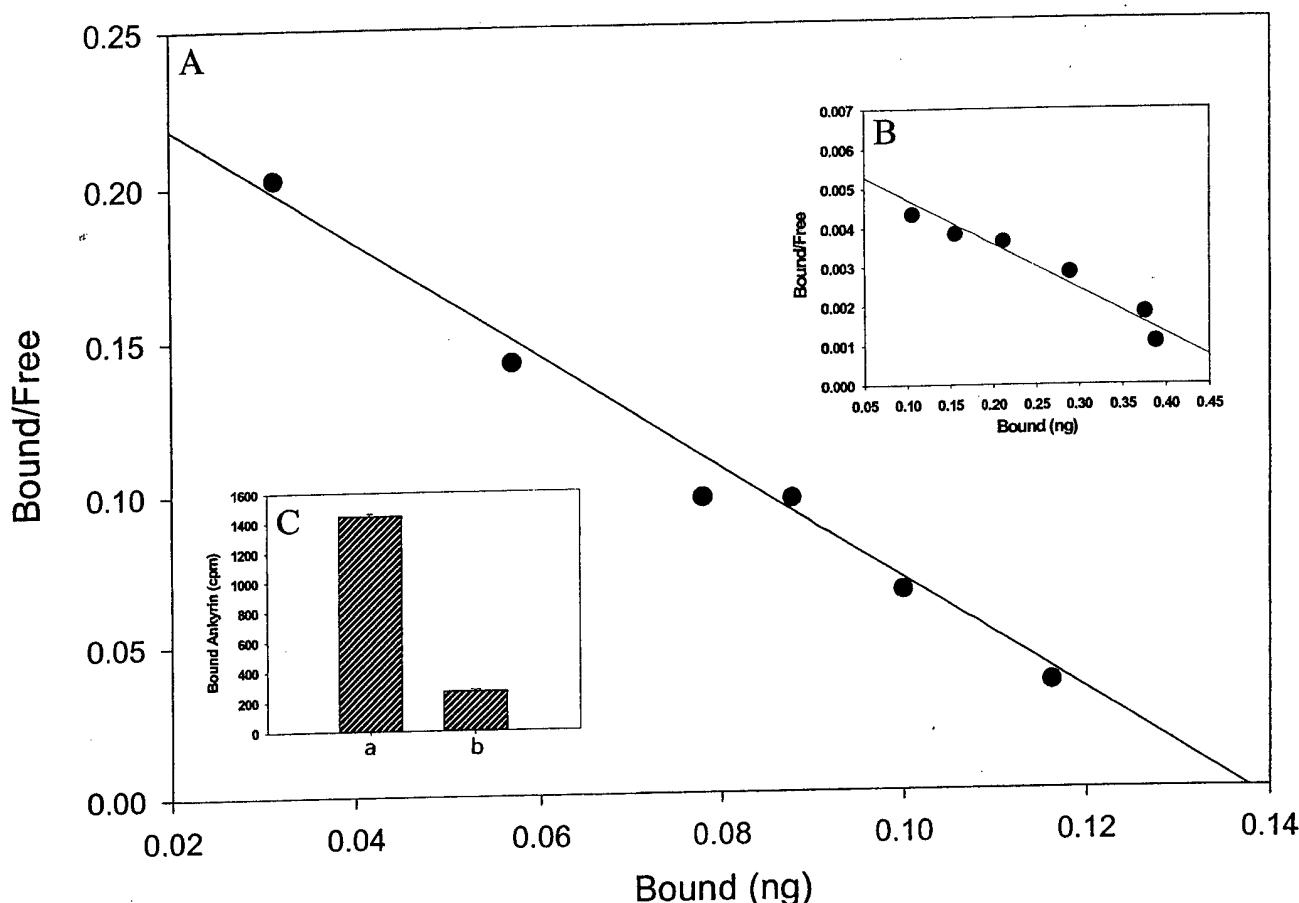


Fig. 6.  $^{125}\text{I}$ -Ankyrin binding to ROK-phosphorylated FLAG-CD44cyt by Scatchard plot analyses. Purified  $^{125}\text{I}$ -labeled ankyrin ( $\approx 0.32$  nM protein,  $1.5 \times 10^4$  cpm/ng) was incubated with FLAG-tagged CD44 cytoplasmic tail (FLAG-CD44cyt) [bound to anti-FLAG-conjugated beads] ( $\approx 0.75$   $\mu\text{g}$  protein in ROK- phosphorylated or unphosphorylated form) in 0.5 ml of the binding buffer [20 mM Tris-HCl (pH 7.4), 150 mM NaCl, 0.1% (w/v) BSA, and 0.05% Triton X-100] as described in Materials and Methods. Following binding, the beads were washed in the binding buffer and the bead bound radioactivity was determined. Non-specific binding was determined in the presence of a 100-fold

excess of unlabeled ankyrin. A: Scatchard plot analysis of the  $^{125}\text{I}$ -Ankyrin binding to highly phosphorylated FLAG-CD44cyt (by GTP $\gamma$ S-GST-RhoA-activated ROK). B: Scatchard plot analysis of the  $^{125}\text{I}$ -Ankyrin binding to minimally phosphorylated FLAG-CD44cyt (by GTP $\gamma$ S-GST-RhoA-treated ROK in the presence of staurosporine). C: The total amount of  $^{125}\text{I}$ -Ankyrin binding to highly phosphorylated FLAG-CD44cyt (by GTP $\gamma$ S-GST-RhoA-activated ROK) (a) or minimally phosphorylated FLAG-CD44cyt (by GTP $\gamma$ S-GST-RhoA-treated ROK in the presence of staurosporine) (b).

affinity (with an apparent  $K_d \approx 0.05$  nM) (Fig. 6A) than the minimally phosphorylated FLAG-CD44cyt (with an apparent  $K_d \approx 2.1$  nM) (Fig. 6B). These results clearly support the notion that phosphorylation of the cytoplasmic domain of CD44 by ROK enhances its binding interaction with ankyrin, which may be required for cytoskeleton-mediated function.

Previous studies indicate that CD44 $v_{3,8-10}$ -mediated invasive phenotype of breast tumor cells (e.g. Met-1 cells) characterized by an "invadopodia" structure (or membranous projections) and tumor cell migration is closely associated with ankyrin-linked cytoskeleton function [Bourguignon et al., 1998b]. Ankyrin is a family of membrane-associated cytoskeletal proteins expressed in a variety of biological systems including epithelial cells

and tissues [Peters and Lux, 1993]. Presently, at least three ankyrin genes have been identified: ankyrin 1 (Ank 1 or ankyrin R), ankyrin 2 (Ank 2 or ankyrin B), and ankyrin 3 (Ank 3 or ankyrin G) [Lux et al., 1990; Otto, et al., 1991; Kordeli, et al., 1995; Peters, et al., 1995]. These molecules belong to a family of related genes that probably arose by duplication and divergence of a common ancestral gene. Using specific anti-Ank1 and anti-Ank3 antibody, we have identified the presence of at least two ankyrin species (e.g., Ank1 and Ank3) in breast tumor cells such as Met-1 (Fig. 7). In particular, we have found that microinjection of CAT domain (Fig. 7A-D) promotes CD44 (e.g., CD44 $v_{3,8-10}$ ) (Fig. 7A and C) co-localization with ankyrin [e.g., Ank1 (Fig. 7B) and Ank3 (Fig. 7D)] in the plasma membranes and mem-

brane projections (Fig. 7A–D). In contrast, treatment of Met-1 cells (microinjected with CAT domain) with rabbit anti-CD44v3 antibody (specific for v3 sequence) (Fig. 7a and b) or cytochalasin D, the microfilament inhibitor (Fig. 7c and d) blocks CD44 (Fig. 7a and c) and ankyrin (Fig. 7b and d)-associated membrane projections. Cells that are not injected (Fig. 7e and f) and COS cells that do not express CD44 but were injected with CAT or ROK (Fig. 7g and h) fail to display active membrane motility (e.g., membrane projections). Moreover, our data show that CD44-ankyrin-associated membrane projections is significantly inhibited in Met-1 cells microinjected with RB domain (Fig. 7E and F). Together, these findings suggest that ROK (in particular CAT domain but not RB domain)-activation and ankyrin-CD44v3 signaling are closely coupled in Met-1 cell membrane motility.

Furthermore, using *in vitro* migration assays, we have found that CD44<sub>v3,8-10</sub>-containing Met-1 cells undergo active cell migration (Table I). Treatments of Met-1 cells with various agents such as anti-CD44v3 antibody and cytochalasin D, cause a significant inhibition of tumor cell migration (Table I). Importantly, transfection of Met-1 cells with the dominant-negative form of ROK cDNA (e.g., GFP-RB cDNA) but not vector alone (pEGFPC1 vector) also effectively blocks CD44<sub>v3,8-10</sub>-cytoskeleton-dependent Met-1 tumor cell motility (Table I). Together, these findings suggest that CD44<sub>v3,8-10</sub>, cytoskeleton and ROK must be functionally linked during metastatic breast tumor progression.

## DISCUSSION

CD44 [CD44 standard form (CD44s) and variant isoforms (CD44v)] belong to a family of transmembrane glycoproteins known to bind extracellular matrix components [e.g., hyaluronic acid (HA)] in its extracellular domain and interact with the cytoskeletal protein, ankyrin, at its cytoplasmic domain [Bourguignon, 1996; Lesley et al., 1993]. Cells expressing a high level of CD44 isoforms often display enhanced hyaluronic acid binding, which is directly related to tumor cell growth and migration [Zhang et al., 1995]. HA binding to CD44s has been shown to stimulate the p185<sup>HER2</sup>-associated tyrosine kinase, which is linked to CD44s via a disulfide linkage [Bourguignon et al., 1997], and results in direct “cross-talk” between two different signaling pathways (e.g., proliferation vs. motility/invasion) [Bourguignon et al., 1998a,b]. Most importantly, certain angiogenic factors and matrix degrading enzymes (MMPs) are also tightly associated with CD44v isoforms [Bourguignon et al., 1998b], and are believed to play synergistic roles in the generation of oncogenic signals leading to tumor-specific behaviors (e.g., invasion and motility/migration)

in a cytoskeleton-dependent manner [Bourguignon et al., 1998b].

As the histologic grade of each tumor progresses, the percentage of lesions expressing CD44 variant isoforms increases. In particular, the CD44v3-containing isoforms (e.g., CD44<sub>v3,8-10</sub>) are expressed preferentially on highly malignant breast carcinoma tissue samples [Bourguignon et al., 1995b; Bourguignon, 1996; Iida and Bourguignon, 1997] and metastatic breast tumor cells (Fig. 1) [Bourguignon et al., 1998a,b]. In fact, there is a direct correlation between CD44v3 isoform expression and increased histologic grade of the malignancy [Bourguignon et al., 1995b; Iida and Bourguignon, 1997; Sinn et al., 1995]. One study indicates that expression of the CD44v3 isoform in breast tumors may be used as an accurate predictor of overall survival [Kaufmann et al., 1995]. Previously, CD44<sub>v3,8-10</sub> has been shown to contain sulfated oligosaccharides [Bennet et al., 1995; Jackson et al., 1995]. Our recent results indicate that <sup>35</sup>SO<sub>4</sub><sup>2-</sup> is incorporated into the glycosaminoglycan (GAG) chains of CD44<sub>v3,8-10</sub> isolated from Met-1 cells [Bourguignon et al., 1998a,b]. The GAG chains of CD44v3-containing isoforms appear to be important in the linkage of heparin binding growth factors [Bennet et al., 1995; Bourguignon et al., 1998a,b; Jackson et al., 1995]. For example, CD44<sub>v3,8-10</sub> of Met-1 cells binds preferentially to vascular endothelial growth factor (VEGF), but not basic fibroblast growth factor (bFGF) [Bourguignon et al., 1998a,b]. VEGF is a specific mitogen for endothelial cells and a potent microvascular permeability factor [Dvorak et al., 1995; Folkman, 1985]. It plays an integral role in angiogenesis and thus in potentiation of solid tumor growth [Dvorak et al., 1995; Folkman, 1985]. Therefore, the attachment of VEGF to the heparin sulfate sites on CD44<sub>v3,8-10</sub> may be responsible for the onset of breast tumor-associated angiogenesis. It is also speculated that some of these CD44v3 isoforms on epithelial cells may act as surface modulators to facilitate unwanted growth factor receptor-growth factor interactions [Bennet et al., 1995; Bourguignon et al., 1998a,b; Jackson et al., 1995] and subsequent tumor metastasis. Recently, we have found that the CD44<sub>v3,8-10</sub> isoform expressed on Met-1 cell surface is closely associated with the matrix metalloproteinase, MMP-9, and interacts with the cytoskeleton to promote tumor cell-specific phenotypes including “invasion” formation and tumor cell migration [Bourguignon et al., 1998a,b]. These findings suggest that CD44<sub>v3,8-10</sub> and its associated cytoskeleton play an important role in metastatic tumor cell behavior.

Cytoskeletal reorganization has been linked to the activation of Rho-like proteins including RhoA, Rac1, and Cdc42 [Hall, 1998; Narumiya, 1996]. Specifically, RhoA is required for actin filament bundling, stress fiber formation, and acto-myosin-based contractility [Hall,

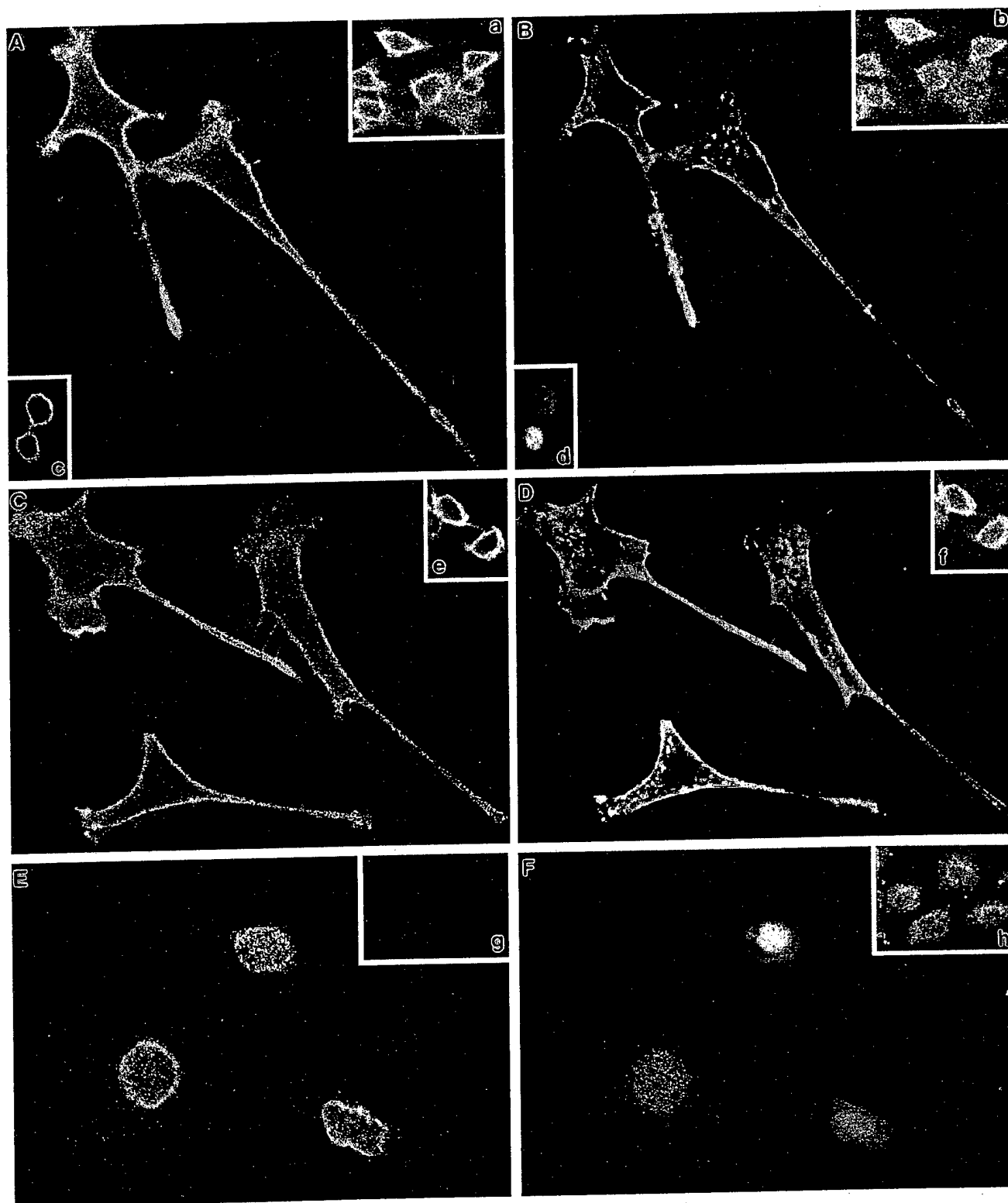


Figure 7

TABLE I. Measurement of Tumor Cell Migration\*

Cells	Cell migration (% of control)		
	No treatment	Anti-CD44v3-treated	Cytochalasin D treated
Untransfected cells (control)	100	27	24
Vector-transfected cells	98	25	22
GFP-RB cDNA-transfected cells	21	≤5	≤5

\*Met-1 cells [ $\approx 1 \times 10^4$  cells/well in phosphate buffered saline (PBS), pH 7.2] [in the presence or absence of rabbit anti-CD44v3 antibody (50  $\mu$ g/ml) or cytochalasin D (20  $\mu$ g/ml)] were placed in the upper chamber of the transwell unit. In some cases, Met-1 cells were transfected with either GFP-tagged RB cDNA or GFP-vector alone. After 18 h incubation at 37°C in a humidified 95% air/5% CO<sub>2</sub> atmosphere, cells on the upper side of the filter were removed by wiping with a cotton swab. Cell migration processes were determined by measuring the cells that migrate to the lower side of the polycarbonate filters by standard cell number counting methods as described previously (58). Each assay was set up in triplicate and repeated at least 3 times. All data were analyzed statistically by Student's *t*-test and statistical significance was set at  $P < 0.01$ . In these experiments  $\approx 30$  to 40% of input cells ( $\approx 1 \times 10^4$  cells/well) undergo in vitro migration in the control samples. The values expressed represent an average of triplicate determinations of 3–5 experiments with a standard deviation less than  $\pm 5\%$ .

1998; Narumiya, 1996]. In this study we have demonstrated that RhoA is closely associated with CD44<sub>v3,8-10</sub> as a complex (Fig. 1). RhoA complexed with CD44<sub>v3,8-10</sub> binds GTP and displays GTPase activity which can be inhibited by C3 toxin-mediated ADP-ribosylation (Fig. 2). In order to establish the functional involvement of this CD44<sub>v3,8-10</sub>-RhoA complex in regulating the metastatic phenotype, we have searched for the downstream effector(s) for this transmembrane complex. Rho-Kinase (ROK) (also called Rho-binding Kinase) is known to bind Rho GTPase and participate in cytoskeleton functions and membrane motility [Amano et al., 1997; Leung et al., 1996; Matsui et al., 1996]. ROK also phosphorylates

myosin light chain phosphatase and myosin light chain [Amano et al., 1996; Kimura et al., 1996], thereby activating myosin adenosine triphosphatase (ATPase) and generating actomyosin-mediated membrane motility [Amano et al., 1996; Kimura et al., 1996]. ROK is also responsible for the phosphorylation of CD44-associated cytoskeletal proteins [e.g., Ezrin/Radixin/Moesin (ERM)] during actin filament and plasma membrane interaction [Matsui et al., 1998]. When ROK is overexpressed or constitutively activated, changes in actin cytoskeleton organization occur that are similar to those observed during Rho-activated conditions [Kimura et al., 1996; Leung et al., 1996]. This evidence prompted us to investigate ROK as a possible downstream effector for RhoA (complexed with CD44<sub>v3,8-10</sub>). In Met-1 cells, we have identified a 160 kDa protein as a ROK-like protein containing RhoA-binding properties (Fig. 3B). This 160 kDa ROK activity can be activated by binding to activated RhoA but not unactivated RhoA (Figs. 4 and 5). Both 160 kDa ROK and the catalytic domain (GST-CAT) (but not the Rho-binding domain, GFP-RB) of ROK appear to be essential for activating ROK-mediated phosphorylation of cellular proteins including myosin light chain (Fig. 4A), CD44<sub>v3,8-10</sub> (Fig. 4B), and the cytoplasmic domain of CD44 (Figs. 4C and 5). These results clearly indicate that ROK acts as one of the downstream effectors of RhoA (complexed with CD44<sub>v3,8-10</sub>).

Ankyrin (e.g., Ank1, Ank2, or Ank3) is known to bind to a number of plasma membrane-associated proteins including band 3, two other members of the anion exchange gene family [Bennet, 1992], Na<sup>+</sup>/K<sup>+</sup>-ATPase [Zhang et al., 1998], the amiloride-sensitive Na<sup>+</sup> channel [Smith et al., 1991], the voltage-dependent Na<sup>+</sup> channel [Kordeli et al., 1995], Ca<sup>2+</sup> channels [Bourguignon et al., 1993b, 1995a; Bourguignon and Jin, 1995], and the adhesion molecule, CD44 [Bourguignon et al., 1995b, 1997; Bourguignon, 1996]. It has been suggested that the binding of ankyrin to certain membrane-associated mol-

Fig. 7. Double immunofluorescence staining of CD44 and ankyrin in Met-1 cells microinjected with CAT or RB domain. Met-1 cells (microinjected with CAT or RB domain) grown in the presence and absence of certain agents [e.g., rabbit anti-CD44v3 antibody (50  $\mu$ g/ml) or cytochalasin D (20  $\mu$ g/ml)] were fixed by 2% paraformaldehyde. Subsequently, cells were surface labeled with FITC-labeled rat anti-CD44 antibody. These cells were then rendered permeable by ethanol treatment and stained with rhodamine (Rh)-labeled mouse anti-Ank1 IgG or Rh-labeled rabbit anti-Ank3 IgG. To detect non-specific antibody binding, FITC-CD44-labeled cells were incubated with Rh-conjugated normal mouse IgG or Rh-conjugated rabbit preimmune serum. No labeling was observed in such control samples. A–D: Staining of surface CD44 with FITC-conjugated rat anti-CD44 antibody (A and C); and intracellular ankyrin (Ank1) with Rh-conjugated mouse anti-Ank1 antibody (B) and Ank3 antibody (D) in Met-1 cells microinjected with CAT domain. E,F: Staining of surface CD44 with FITC-conjugated rat

anti-CD44 antibody (E); and intracellular ankyrin with Rh-conjugated mouse anti-Ank1 antibody (F) in Met-1 cells microinjected with RB domain. a,b: Staining of surface CD44 with FITC-conjugated rat anti-CD44 antibody (a), and intracellular ankyrin with Rh-conjugated mouse anti-Ank1 antibody (b) in Met-1 cells microinjected with CAT domain and incubated with rabbit anti-CD44v3 antibody. c,d: Staining of surface CD44 with FITC-conjugated rat anti-CD44 antibody (c), and intracellular ankyrin with Rh-conjugated mouse anti-Ank1 antibody (d) in Met-1 cells microinjected with CAT domain and incubated with cytochalasin D. e,f: Staining of surface CD44 with FITC-conjugated rat anti-CD44 antibody (e), and intracellular Ank1 with Rh-conjugated mouse anti-Ank1 antibody (f) in Met-1 cells without any injection treatment. g, h: Staining of surface CD44 with FITC-conjugated rat anti-CD44 antibody (g), and intracellular ankyrin with Rh-conjugated mouse anti-Ank1 antibody (h) in COS-7 cells (a CD44-negative cell line) microinjected with CAT domain.

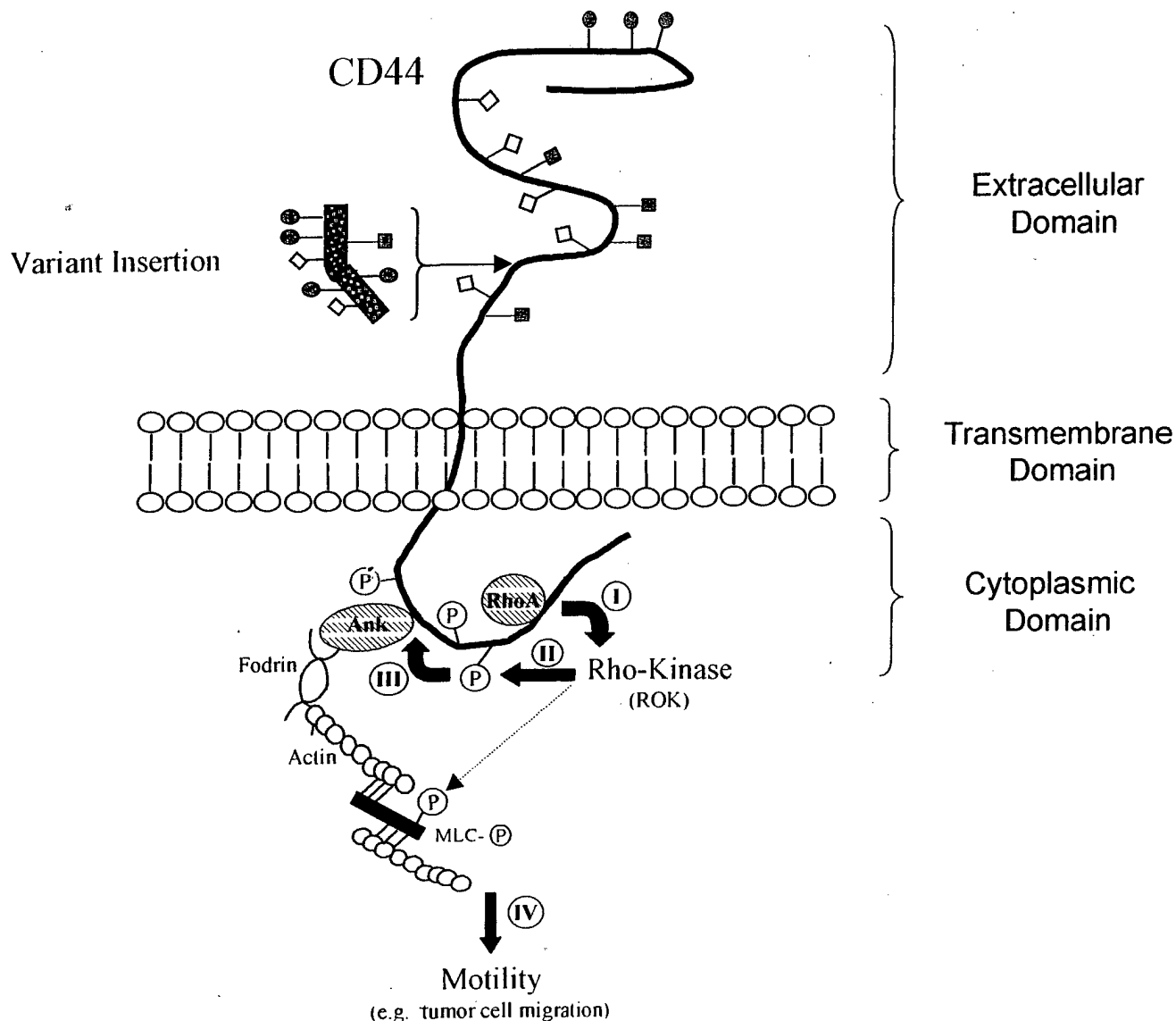


Fig. 8. A proposed model for the regulation of membrane-cytoskeleton interaction and cell motility in metastatic breast tumor cells by CD44<sub>v3,8-10</sub>-RhoA signaling and ROK activation. Step I: CD44<sub>v3,8-10</sub> (containing oncogenic signaling-related v3 exon-encoded structure) is tightly coupled with RhoA in a complex which can up-regulate Rho-Kinase (ROK) activity. Step II: Activated ROK phosphorylates cellular proteins including the cytoplasmic domain of CD44<sub>v3,8-10</sub> and

possibly myosin light chain (MLC-P-shown by a thin dotted line). Step III: Phosphorylation of CD44<sub>v3,8-10</sub>'s cytoplasmic domain by ROK promotes the binding of CD44<sub>v3,8-10</sub> to the cytoskeletal protein, ankyrin (Ank), which in turn interacts with fodrin and actin-myosin-based microfilamentous contractile elements. Step IV: This membrane-cytoskeleton interaction is required for cell motility including tumor cell migration during breast cancer progression.

ecules may be needed for signal transduction, cell adhesion, cell migration, and tumor metastasis [Bourguignon et al., 1993a,b, 1995a,b]. The cytoplasmic domain of CD44s (approximately 70 a. a. long) is highly conserved ( $\approx 90\%$ ) in most of the CD44 isoforms, and is clearly involved in specific ankyrin binding [Lokeshwar et al., 1994; Zhu and Bourguignon, 1998]. The ankyrin-binding domain of CD44 has also been mapped using deletion mutation analyses and mammalian expression systems [Lokeshwar et al., 1994; Zhu and Bourguignon, 1998].

The results of these experiments indicate that at least two subregions within the CD44 cytoplasmic domain constitute the ankyrin binding-region I (i.e., the high-affinity ankyrin-binding region) and region II (i.e., the regulatory region). In particular, the region I ankyrin-binding domain (e.g., "NGGNGTVEDRKPSSEL" between aa 306 and aa 320 in the mouse CD44 and "NSGNQAVEDRKPSGL" aa 304 and aa 318 in human CD44) is required for cell adhesion, Src kinase recruitment, and tumor cell transformation [Lokeshwar et al., 1994; Zhu and Bourguignon,

1998]. Recent data indicate that the amino acid sequence-“NGNGTVEDRKPSSEL” (located between aa 480 and aa 494 of CD44<sub>v3,8-10</sub>) in Met-1 cells binds specifically to the cytoskeletal protein, ankyrin (but not fodrin or spectrin), and belongs to the ankyrin-binding domain of CD44<sub>v3,8-10</sub> [Bourguignon et al., 1998a,b].

Previously, it has been shown that the binding interaction between CD44 and ankyrin is up-regulated by several factors including protein kinase C-mediated phosphorylation [Bourguignon et al., 1992; Kalomiris and Bourguignon, 1989], palmitoylation [Bourguignon et al., 1991] and GTP-binding [Hirao et al., 1996; Lokeshwar and Bourguignon, 1992]. In this study, we have provided new evidence that phosphorylation of CD44 by RhoA-activated ROK also stimulates its binding to ankyrin (Fig. 6). Further analyses using double immunofluorescence staining show that Met-1 cells express both Ank1 (Fig. 7B) and Ank3 (Fig. 7D). In particular, the catalytic domain (CAT) but not the Rho-binding domain (RB) of ROK is responsible for promoting CD44 phosphorylation (Figs. 4 and 5), which up-regulates CD44-ankyrin (e.g., Ank1 and/or Ank3)-mediated membrane motility (Fig. 7A-D). Moreover, Met-1 tumor cell migration is inhibited by cytochalasin D (Table I), suggesting that some actin polymerization or microfilamentous cytoskeleton might be required. Our findings are consistent with a previous study indicating CD44 and its associated cytoskeletal proteins [e.g., ERM (ezrin, radixin, and moesin)-F-actin complex] appear to be an essential prerequisite for the Rho GTPase-induced cytoskeletal changes [Hirao et al., 1996; Tsukita et al., 1994]. This membrane-cytoskeleton interaction could also lead to abnormal tumor cell motility (e.g., membrane projections and cell migration) (Fig. 7A-D; and Table I) in Met-1 cells. In addition, we have found that treatment of Met-1 cells with anti-CD44v3 antibody/cytochalasin D (Fig. 7a-d) or overexpression of the Rho-binding (RB) domain of ROK (by transfecting Met-1 cells with RBcDNA) (Fig. 7E and F) induces reversal of tumor cell-specific phenotypes such as membrane motility and tumor cell migration (Table I). Together, these findings strongly suggest that oncogenic signaling (derived from the v3-coded structure of CD44<sub>v3,8-10</sub>) and ROK activation are closely coupled during the onset of cytoskeleton function and tumor-specific behavior in metastatic breast tumor cells. As summarized in Figure 8, we propose that CD44<sub>v3,8-10</sub> (containing oncogenic signaling-related v3 exon-encoded structure) is tightly coupled with RhoA in a complex that can up-regulate Rho-Kinase (ROK) activity (Step I). Activated ROK then phosphorylates certain cellular proteins including the cytoplasmic domain of CD44<sub>v3,8-10</sub> and possibly myosin light chain (Step II). Most importantly, phosphorylation of CD44<sub>v3,8-10</sub>'s cytoplasmic domain by ROK promotes the binding of CD44<sub>v3,8-10</sub> to the

cytoskeletal protein, ankyrin (e.g., Ank1 and/or Ank3) (Step III), which in turn interacts with fodrin and actin-myosin based microfilaments. We proposed that this membrane-cytoskeleton interaction is required for stimulating membrane motility and tumor cell migration (Step IV) during breast cancer progression.

## ACKNOWLEDGMENTS

We gratefully acknowledge Dr. Gerard J. Bourguignon's assistance in the preparation of this paper. We also thank Dr. F. Diaz for her help in preparing photographs and illustrations as well as reviewing the manuscript.

## REFERENCES

- Aktories K, Weller U, Chhatwal GS. 1987. Botulinum ADP-ribosyltransferase C3 but not botulinum neurotoxins C1 and D ADP-ribosylates low molecular mass GTP-binding proteins. *FEBS Lett* 212:109-113.
- Amano M, Ito M, Kimura K, Fukata Y, Chihara K, Nakano T, Matsuura Y, Kaibuchi K. 1996. Phosphorylation and activation of myosin by Rho-associated kinase (Rho-kinase). *J Biol Chem* 271:20246-20249.
- Amano M, Chihara K, Kimura K, Fukata Y, Nakamura N, Matsuura Y, Kaibuchi K. 1997. Formation of actin stress fibers and focal adhesions enhanced by Rho-kinase. *Science* 275:1308-1311.
- Arch R, Wirth K, Hofmann M, Ponta H, Matzku S, Herrlich P, Zoller M. 1992. Participation in normal immune responses of a metastasis-inducing splice variant of CD44. *Science* 257:682-685.
- Bennet V. 1992. Ankyrins: adaptors between diverse plasmamembrane proteins and cytoplasm. *J Biol Chem* 267:8703-8706.
- Bennet K, Jackson DG, Simon JC, Tanczos E, Peach R, Modrell B, Stamenkovic I, Plowman G, Aruffo A. 1995. CD44 isoforms containing exon v3 are responsible for the presentation of heparin-binding growth factor. *J Cell Biol* 128:687-698.
- Bourguignon LYW. 1996. Interactions between the membrane-cytoskeleton and CD44 during lymphocyte signal transduction and cell adhesion. *Curr Topics Membr* 43:293-312.
- Bourguignon LYW, Jin H. 1995. Identification of the ankyrin-binding domain of the mouse T-lymphoma cell inositol 1,4,5-trisphosphate (IP<sub>3</sub>) receptor and its role in the regulation of IP<sub>3</sub>-mediated internal Ca<sup>2+</sup> release. *J Biol Chem* 270:7257-7260.
- Bourguignon LYW, Walker G, Suchard S, Balazovich K. 1986. A lymphoma plasma membrane-associated protein with ankyrin-like properties. *J Cell Biol* 102:2115-2124.
- Bourguignon LYW, Kalomiris E, Lokeshwar VB. 1991. Acylation of the lymphoma transmembrane glycoprotein, GP85 may be required for GP85-ankyrin interaction. *J Biol Chem* 266:11761-11765.
- Bourguignon LYW, Lokeshwar B, He J, Chen X, Bourguignon GJ. 1992. A CD44-like endothelial cell transmembrane glycoprotein (GP116) interacts with extracellular matrix and ankyrin. *Mol Cell Biol* 12:4464-4471.
- Bourguignon LYW, Lokeshwar VB, Chen X, Kerrick WG. 1993a. Hyaluronic acid-induced lymphocyte signal transduction and HA receptor (GP85/CD44)-cytoskeleton interaction. *J Immunol* 151:6634-6644.

- Bourguignon LYW, Jin H, Iida N, Brandt NR, Zhang S. 1993b. The involvement of ankyrin in the regulation of inositol 1,4,5-trisphosphate receptor-mediated internal  $\text{Ca}^{2+}$  from storage vesicles in mouse T-lymphoma cells. *J Biol Chem* 268:7290-7297.
- Bourguignon LYW, Chu A, Jin H, Brandt NR. 1995a. Ryanodine receptor-ankyrin interaction regulates internal  $\text{Ca}^{2+}$  release in T-lymphoma cells. *J Biol Chem* 270:17917-17922.
- Bourguignon LYW, Iida N, Welsh CF, Zhu D, Krongrad A, Pasquale D. 1995b. Involvement of CD44 and its variant isoforms in membrane-cytoskeleton interaction, cell adhesion and tumor metastasis. *J Neuro-Oncol* 26:201-208.
- Bourguignon LYW, Zhu H, Chu A, Iida N, Zhang L, Hung MC. 1997. Interaction between the adhesion receptor, CD44, and the oncogene product, p185<sup>HER2</sup>, promotes human ovarian tumor cell activation. *J Biol Chem* 272:27913-27918.
- Bourguignon LYW, Zhu H, Zhu D. 1998a. CD44 isoform-cytoskeleton interaction in oncogenic signaling and tumor progression. *Frontiers Biosci* 3:637-649.
- Bourguignon LYW, Gunja-Smith S, Iida N, Zhu HB, Young LJ, Muller WJ, Cardiff RD. 1998b. CD44<sup>v(3,8-10)</sup> is involved in cytoskeleton-mediated tumor cell migration and matrix metalloproteinase (MMP-9) association in metastatic breast cancer cells. *J Cell Physiol* 176:206-215.
- Cheung ATW, Young LJ, Chen PCY, Chao CY, Ndoye A, Barry PA, Muller WJ, Cardiff RD. 1997. Microcirculation and Metastasis in a new mammary tumor model system. *Int J Oncol* 11:69-77.
- Chu G, Hayakawa H, Berg P. 1987. Electroporation for the efficient transfection of mammalian cells with DNA. *Nucleic Acid Res* 15:1311-1326.
- Droll A, Dougherty ST, Chiu RK, Dirks JF, McBride WH, Cooper DL, Dougherty GJ. 1995. Adhesive interactions between alternatively spliced CD44 isoforms. *J Biol Chem* 270:11567-11573.
- Dvorak HF, Brown LF, Detmar M, Dvorak AM. 1995. Vascular permeability factor/vascular endothelial growth factor, microvascular hyperpermeability, and angiogenesis. *Am J Pathol* 146:1029-1039.
- Folkman J. 1985. Tumor angiogenesis. *Adv Cancer Res* 43:175-203.
- Green S J, Tarone G, Underhill CB. 1988. Aggregation of macrophages and fibroblasts is inhibited by a monoclonal antibody to the hyaluronate receptor. *Exp Cell Res* 178:224-232.
- Gunthert U, Hoffman M, Rudy W, Reber S, Zoller M, Haubmann I, Matzku S, Wenzel A, Ponta H, Herrlich P. 1991. A new variant of glycoprotein CD44 confers metastatic potential to rat carcinoma cells. *Cell* 65:13-24.
- Guy CT, Cardiff RD, Muller WJ. 1992. Induction of mammary tumors by expression of polyomavirus middle T oncogene: a transgenic mouse model for metastatic disease. *Mol Cell Biol* 12:954-961.
- Hall A. 1998. G proteins and small GTPases: distant relatives keep in touch. *Science* 279:509-514.
- Haynes BF, Telen MJ, Hale LP, Denning SM. 1989. CD44-a molecule involved in leukocyte adherence and T-cell activation. *Immunol Today* 10:423-428.
- Herrlich P, Zoller M, Pals ST, Ponta H. 1993. CD44 splice variants: metastases meet lymphocytes. *Immunol Today* 14:395-399.
- Hirao M, Sato N, Kondo T, Yonemura S, Monden M, Sasaki T, Takai Y, Tsukita S, Tsukita S. 1996. Regulation mechanism of ERM (ezrin/radixin/moesin) protein/plasma membrane association: possible involvement of phosphatidylinositol turnover and rho-dependent signaling pathway. *J Cell Biol* 135:36-51.
- Hofmann M, Rudy W, Zoller M, Tol C, Ponta H, Herrlich P, Gunthert U. 1991. CD44 splice variants confer metastatic behavior in rats: homologous sequences are expressed in human tumor cell lines. *Cancer Res* 51:5292-5297.
- Iida N, Bourguignon LYW. 1995. New CD44 splice variants associated with human breast cancer. *J Cell Physiol* 162:127-133.
- Iida N, Bourguignon LYW. 1997. Coexpression of CD44 variant (v10/ex14) and CD44s in human mammary epithelial cells promotes tumorigenesis. *J Cell Physiol* 171:152-160.
- Jackson DG, Bell JI, Dickinson R, Timans J, Shields J, Whittle N. 1995. Proteoglycan forms of the lymphocyte homing receptor CD44 are alternatively spliced variants containing the v3 exon. *J Cell Biol* 128:673-685.
- Jiang W G, Puntis MCA, Hallett MB. 1994. Inhibition of neutrophil respiratory burst and cytokine priming by gamma-linolenic acid. *Br J Surg* 81:1576-1590.
- Kabcenell AK, Goud B, Northup JK, Novick PJ. 1990. Binding and hydrolysis of guanine nucleotides by Sec4p, a yeast protein involved in the regulation of vesicular traffic. *J Biol Chem* 265:9366-9372.
- Kalomiris EL, Bourguignon LYW. 1988. Mouse T lymphoma cells contain a transmembrane glycoprotein (GP85) that binds ankyrin. *J Cell Biol* 106:319-327.
- Kalomiris E L, Bourguignon LYW. 1989. Lymphoma protein kinase C is associated with the transmembrane glycoprotein, GP85 and may function in GP85-ankyrin binding. *J Biol Chem* 264:8113-8119.
- Kaufmann M, Heider KH, Sinn HP, von Minckwitz G, Ponta H, Herrlich P. 1995. CD44 variant exon epitopes in primary breast cancer and length of survival. *Lancet* 345:615-619.
- Kimura N, Ito M, Amano M, Chihara K, Fukata Y, Nakafuku M, Yamamori B, J Feng, Nakano T, Okawa K, Iwamatsu K, Kaibuchi K. 1996. Regulation of myosin phosphatase by Rho and Rho-associated kinase (Rho-kinase). *Science* 273:245-248.
- Kohli J. 1987. Genetic nomenclature and gene list of the fission yeast *Schizosaccharomyces pombe*. *Curr Genet* 11:575-589.
- Kordeli E, Lambert S, Bennet V. 1995. Ankyrin G: a new ankyrin gene with neural-specific isoforms localized to the axonal initial segment and node of Ranvier. *J Biol Chem* 270:2352-2359.
- Lauffenburger DA, Horwitz AF. 1996. Cell migration: a physically integrated molecular process. *Cell* 84:359-369.
- Lesley J, Trotter J, Hyman R. 1985. The Pgp-1 antigen is expressed on early fetal thymocytes. *Immunogenetics* 22:149-157.
- Lesley J, Hyman R, Kincade P. 1993. CD44 and its interaction with extracellular matrix. *Adv Immunol* 54:271-235.
- Letarte M, Iturbe S, Quackenbush EJ. 1985. A glycoprotein of molecular weight 85,000 on human cells of B-lineage: detection with a family of monoclonal antibodies. *Mol Immunol* 22:113-124.
- Leung T, Chen XQ, Manser E, Lim L. 1996. The p160 RhoA-binding kinase ROK alpha is a member of a kinase family and is involved in the reorganization of the cytoskeleton. *Mol Cell Biol* 16:5313-5327.
- Lokeshwar VB, Bourguignon LYW. 1991. Post-translational protein modification and expression of ankyrin-binding site(s) in GP85 (Pgp-1/CD44) and its biosynthetic precursors during T-lymphoma membrane biosynthesis. *J Biol Chem* 266:17983-17989.
- Lokeshwar VB, Bourguignon LYW. 1992. The lymphoma transmembrane glycoprotein CD44 GP85 is a novel guanine nucleotide-binding protein which regulates GP85.(CD44)-ankyrin interaction. *J Biol Chem* 267:22073-22078.
- Lokeshwar VB, Fregien N, Bourguignon LYW. 1994. Ankyrin binding domain of CD44 (GP85) is required for the expression of hyaluronic acid-mediated adhesion function. *J Cell Biol* 126:1099-1109.

- Lokeshwar VB, Iida N, Bourguignon LYW. 1996. The cell adhesion molecule, GP116, is a new CD44 variant (ex14/v10) involved in hyaluronic acid binding and endothelial cell proliferation. *J Biol Chem* 271:23853-23864.
- Lux SE, John KM, Bennett V. 1990. Analysis of cDNA for human erythrocyte ankyrin indicates a repeated structure with homology to tissue-differentiation and cell cycle control proteins. *Nature* 344:36-43.
- Matsui T, Amano M, Yamamoto T, Chihara K, Nakafuku M, Ito M, Nakano T, Okawa K, Iwamatsu A, Kaibuchi K. 1996. Rho-associated kinase, a novel serine/threonine kinase, as a putative target for small GTP binding protein Rho. *EMBO J* 15:2208-2216.
- Matsui T, Maeda M, Doi Y, Yonemura S, Amano M, Kaibuchi K, Tsukita S, Tsukita S. 1998. Rho-Kinase phosphorylates COOH-terminal threonines of Ezrin/Radixin/Moesin (ERM) proteins and regulates their head-to-tail association. *J Cell Biol* 140:647-657.
- Merzak A, Koochekpour S, Pilkington GJ. 1994. CD44 mediates human glioma cell adhesion and invasion in vitro. *Cancer Res* 54:3988-3992.
- Narumiya S. 1996. The small GTPase Rho: cellular functions and signal transduction. *J Biochem* 120:215-228.
- Ohashi Y, Narumiya S. 1987. ADP-ribosylation of a Mr 21,000 membrane protein by type D botulinum toxin. *J Biol Chem* 262:1430-1433.
- O'Neil LA J, Bird TA, Gearing AJH, Saklatvala J. 1990. Interleukin-1 signal transduction. Increased GTP binding and hydrolysis in membranes of a murine thymoma line (EL4). *J Biol Chem* 265:3146-3152.
- Otto E, kunimoto M, McLaughlin T, Bennett V. 1991. Isolation and characterization of cDNA encoding human brain ankyrins reveal a family of alternatively spliced genes. *J Cell Biol* 114:241-253.
- Peters LL, Lux SE. 1993. Ankyrins: structure and function in normal cells and hereditary spherocytes. *Semin Hematol* 30:85-118.
- Peters LL, John KM, Lu FM, Eicher EM, Higgins A, Yialamas M, Turtzo L C, Otsuka AJ, Lux SE. 1995. Ank3 (epithelial ankyrin), a widely distributed new member of the ankyrin gene family and the major ankyrin in kidney, is expressed in alternatively spliced forms, including forms that lack the repeat domain. *J Cell Biol* 130:313-330.
- Rooney P, Kumar S, Wang M. 1995. The role of hyaluronan in tumor neovascularization. *Int J Cancer* 60:632-636.
- Screaton GR, Bell MV, Jackson DG, Cornelis FB, Gerth U, Bell JI. 1992. Genomic structure of DNA coding the lymphocyte homing receptor CD44 reveals at least 12 alternatively spliced exons. *Proc Natl Acad Sci USA* 89:12160-12164.
- Sinn HP, Heider KH, Skroch-Angel P, von Minckwitz G, Kaufmann M, Herrlich P, and Ponta H. 1995. Human mammary carcinomas express homologues of rat metastasis-associated variants of CD44. *Breast Cancer Res Treat* 36:307-313.
- Smith PR, Saccomani GM, Joe EH, Angelides KJ, Benos DJ. 1991. Amiloride-sensitive sodium channel is linked to the cytoskeleton in renal epithelial cells. *Proc Natl Acad Sci USA* 88:6971-6975.
- Stamenkovic I, Amiot M, Pesando JM, Seed B. 1991. The hematopoietic and epithelial forms of CD44 are distinct polypeptides with different adhesion potentials for hyaluronate-bearing cells. *EMBO J* 10:343-347.
- Takahashi K, Sasaki T, Mammoto A, Takaishi K, Kameyama T, Tsukita S, Tsukita S, Takai Y. 1997. Direct interaction of the Rho GDP dissociation inhibitor with ezrin/radixin/moesin initiates the activation of the Rho small G protein. *J Biol Chem* 272:23371-23375.
- Tsukita S, Oishi K, Sato N, Sagara I, Kawai A, Tsukita S. 1994. ERM family members as molecular linkers between the cell surface glycoprotein CD44 and actin based cytoskeletons. *J Cell Biol* 126:391-401.
- Turley EA, Austen L, Vandeligt K, Clary C. 1991. Hyaluronan and a cell-associated hyaluronan binding protein regulate the locomotion of ras-transformed cells. *J Cell Biol* 112:1041-1047.
- Welsh CF, Zhu D, Bourguignon LYW. 1995. Interaction of CD44 variant isoforms with hyaluronic acid and the cytoskeleton in human prostate cancer cells. *J Cell Physiol* 164:605-612.
- West D C, Kumar S. 1989. The effects of hyaluronate and its oligosaccharides on endothelial cell proliferation and monolayer integrity. *Exp Cell Res* 183:179-196.
- Zhang L, Underhill CB, Chen LP. 1995. Hyaluronan on the surface of tumor cells is correlated with metastatic behavior. *Cancer Res* 55:428-433.
- Zhang Z, Devarajan P, Dorfman AL, Morrow JS. 1998. Structure of the ankyrin-binding domain of alpha-Na,K-ATPase. *J Biol Chem* 273:18681-18684.
- Zhu D, Bourguignon LYW. 1996. Overexpression of CD44 in p185<sup>neu</sup>-transfected NIH3T3 cells promotes an up-regulation of hyaluronic acid-mediated membrane-cytoskeleton interaction and cell adhesion. *Oncogene* 12:2309-2314.
- Zhu D, Bourguignon LYW. 1998. The ankyrin-binding domain of CD44s is involved in regulating hyaluronic acid-mediated functions and prostate tumor cell transformation. *Cell Motil Cytoskeleton* 39:209-222.

# Ankyrin-Tiam1 Interaction Promotes Rac1 Signaling and Metastatic Breast Tumor Cell Invasion and Migration

Lilly Y.W. Bourguignon, Hongbo Zhu, Lijun Shao, and Yue Wei Chen

Department of Cell Biology and Anatomy, School of Medicine, University of Miami, Miami, Florida 33136

**Abstract.** Tiam1 (T-lymphoma invasion and metastasis 1) is one of the known guanine nucleotide (GDP/GTP) exchange factors (GEFs) for Rho GTPases (e.g., Rac1) and is expressed in breast tumor cells (e.g., SP-1 cell line). Immunoprecipitation and immunoblot analyses indicate that Tiam1 and the cytoskeletal protein, ankyrin, are physically associated as a complex in vivo. In particular, the ankyrin repeat domain (ARD) of ankyrin is responsible for Tiam1 binding. Biochemical studies and deletion mutation analyses indicate that the 11-amino acid sequence between amino acids 717 and 727 of Tiam1 (<sup>717</sup>GEGTDAVKRS<sup>727</sup>L) is the ankyrin-binding domain. Most importantly, ankyrin binding to Tiam1 activates GDP/GTP exchange on Rho GTPases (e.g., Rac1).

Using an *Escherichia coli*-derived calmodulin-binding peptide (CBP)-tagged recombinant Tiam1 (amino acids 393–728) fragment that contains the ankyrin-binding domain, we have detected a specific binding interaction between the Tiam1 (amino acids 393–738)

fragment and ankyrin in vitro. This Tiam1 fragment also acts as a potent competitive inhibitor for Tiam1 binding to ankyrin. Transfection of SP-1 cell with Tiam1 cDNAs stimulates all of the following: (1) Tiam1–ankyrin association in the membrane projection; (2) Rac1 activation; and (3) breast tumor cell invasion and migration. Cotransfection of SP1 cells with green fluorescent protein (GFP)-tagged Tiam1 fragment cDNA and Tiam1 cDNA effectively blocks Tiam1–ankyrin colocalization in the cell membrane, and inhibits GDP/GTP exchange on Rac1 by ankyrin-associated Tiam1 and tumor-specific phenotypes. These findings suggest that ankyrin–Tiam1 interaction plays a pivotal role in regulating Rac1 signaling and cytoskeleton function required for oncogenic signaling and metastatic breast tumor cell progression.

**Key words:** Tiam1 • ankyrin • Rac1 signaling • invasion/migration • metastatic breast tumor cells

## Introduction

Members of the Rho subclass of the ras superfamily (small molecular masses GTPases, e.g., Rac1, RhoA, and Cdc42) are known to be associated with changes in the membrane-linked cytoskeleton (Ridley and Hall, 1992; Hall, 1998). For example, activation of Rac1, RhoA, and Cdc42 has been shown to produce specific structural changes in the plasma membrane cytoskeleton associated with membrane ruffling, lamellipodia, filopodia, and stress fiber formation (Ridley and Hall, 1992; Hall, 1998). The coordinated activation of these GTPases is thought to be a possible mechanism underlying cell motility, an obvious prerequisite for metastasis (Jiang et al., 1994; Dickson and Lippman, 1995; Lauffenburger and Horwitz, 1996).

Several guanine nucleotide exchange factors (GEFs,<sup>1</sup> the dbl or DH family) have been identified as oncogenes because of their ability to upregulate Rho GTPase activity during malignant transformation (Van Aelst and D'Souza-Schorey, 1997). One of these GEFs is Tiam1 (T-lymphoma invasion and metastasis 1), which was identified by retroviral insertional mutagenesis and selected for its invasive cell behavior in vitro (Habets et al., 1994, 1995). This molecule is largely hydrophilic and contains several functional domains found in signal transduction proteins. For example, the COOH-terminal region of the Tiam1 molecule has a Dbl homology (DH) domain (Hart et al., 1991, 1994; Habets et al., 1994) and an adjacent pleckstrin homology

Address correspondence to Dr. Lilly Y.W. Bourguignon, Department of Cell Biology and Anatomy, University of Miami Medical School, 1600 N.W. 10th Avenue, Miami, FL 33101. Tel.: (305) 547-6691. Fax: (305) 545-7166. E-mail: Lbourgui@med.miami.edu

<sup>1</sup>Abbreviations used in this paper: ARD, ankyrin repeat domain; CBP, calmodulin-binding peptide; DH, Dbl homology; GFP, green fluorescent protein; GFP-SBD, GFP-tagged spectrin binding domain; GEF, guanine nucleotide exchange factor; HA, hemagglutinin; PH, pleckstrin homology; PHn, NH<sub>2</sub>-terminal PH; Rh, rhodamine; S1P, sphingosine-1-phosphate; SBD, spectrin binding domain; Tiam1, T lymphoma invasion and metastasis 1.

(PH) domain, which exists in most GEFs (Hart et al., 1991, 1994; Habets et al., 1994; Lemmon et al., 1996). In particular, the DH domain of these proteins exhibits GDP/GTP exchange activity for specific members of the Ras superfamily of GTP-binding proteins (Hart et al., 1991, 1994). Tiam1 also contains an additional PH domain, a Disc-large homology region (DHR; Habets et al., 1994; Pontings and Phillips, 1995), and a potential myristoylation site in the NH<sub>2</sub>-terminal part of the protein (Habets et al., 1994).

Overexpression of both NH<sub>2</sub> and COOH terminally truncated as well as full-length Tiam1 proteins induces the invasive phenotype in otherwise noninvasive lymphoma cell lines (Michiels et al., 1995). It is also well established that Tiam1 is capable of activating Rac1 in vitro as a GEF, and induces membrane cytoskeleton-mediated cell shape changes, cell adhesion, and cell motility (Woods and Bryant 1991; Michiels et al., 1995; Nobes and Hall, 1995; Van Leeuwen et al., 1995). These findings have prompted investigations into the mechanisms involved in the regulation of Tiam1. In fact, it has been found that addition of certain serum-derived lipids (e.g., sphingosine-1-phosphate [S1P] and LPA) to T-lymphoma cells promotes Tiam1-mediated Rac1 signaling and T-lymphoma cell invasion (Stam et al., 1998). A Tiam1 transcript has been detected in breast cancer cells (Habets et al., 1995). Tiam1 is shown to function as a GEF in activating Rac1 signaling in breast tumor cells (Bourguignon et al., 2000). The question of how this molecule is regulated in invasive and metastatic processes of breast cancer cells is addressed in the present study.

Ankyrin belongs to a family of cytoskeletal proteins that mediate linkage of integral membrane proteins with the spectrin-based skeleton in regulating a variety of biological activities (Bennett, 1992; Bennett and Gilligan, 1993; De Matteis and Morrow, 1998). Presently, at least three ankyrin genes have been identified: *ankyrin 1* (ANK1 or *ankyrin R*), *ankyrin 2* (ANK2 or *ankyrin B*), and *ankyrin 3* (ANK3 or *ankyrin G*) (Lambert et al., 1990; Lux et al., 1990; Tse et al., 1991; Otto et al., 1991; Peters and Lux 1993; Kordeli et al., 1995; Peters et al., 1995). All ankyrin species (e.g., ANK1, ANK2, and ANK3) are monomers comprised of two highly conserved domains and a variable domain. Both conserved domains are located in the NH<sub>2</sub>-terminal region and include a membrane-binding site (~89–95 kD, also called the ankyrin repeat domain [ARD]; Davis and Bennet, 1990; Lux et al., 1990), and a spectrin binding domain (SBD, ~62 kD; Platt et al., 1993). The striking feature shared by all three forms of ankyrins is the repeated 33-amino acid motif present in 24 contiguous copies within the ARD. The ARD of ANK1, ANK2, and ANK3 is highly conserved. A number of tumor cells express ankyrin such as ANK1 and ANK3 (Bourguignon et al., 1998a,b; Zhu and Bourguignon, 2000). Most recently, we have found that ankyrin's ARD interacts with the adhesion molecule, CD44, and promotes tumor cell migration (Zhu and Bourguignon, 2000). In addition, the ARD domain (also referred to as cdc 10 repeats, cdc10/SW16 repeats, and SW16/ANK repeats) has been detected in a number of functionally distinct proteins participating in protein-protein binding and protein-DNA interactions (Davis and Bennett, 1990; Lux et al., 1990).

In this study, we have focused on the regulatory aspect of Tiam1-Rac1 signaling in metastatic breast tumor cells (SP-1 cell line). Our results indicate that Tiam1 interacts with ankyrin in vivo and in vitro. In particular, the ankyrin repeat domain (ARD) is directly involved in Tiam1 binding. Biochemical analyses show that the Tiam1 fragment (amino acids 393–738) contains an ankyrin-binding site and competes for Tiam1 binding to ankyrin. Most importantly, the binding of ankyrin, in particular, the ankyrin repeat domain (ARD), to Tiam1 activates Rho-like GTPases such as Rac1. Overexpression of Tiam1 in SP-1 cells by transfecting Tiam1 cDNA induces Tiam1-ankyrin association in the cell membrane, Rac1 signaling, and metastatic phenotypes. Both Tiam1-ankyrin interaction and tumor-specific behaviors are significantly inhibited by cotransfecting SP-1 cells with the Tiam1 (amino acids 393–738) fragment cDNA and Tiam1 cDNA. Our observations suggest that Tiam1 interaction with ankyrin promotes Rho GTPase activation and cytoskeletal changes required for metastatic breast tumor cell invasion and migration.

## Materials and Methods

### Cell Culture

Mouse breast tumor cells (e.g., SP1 cell line; provided by Dr. Bruce Elliott, Department of Pathology and Biochemistry, Queen's University, Kingston, Ontario, Canada) were used in this study. Specifically, the SP1 cell line was derived from a spontaneous intraductal mammary adenocarcinoma that arose in a retired female CBA/J breeder in the Queen's University animal colony. These cells were capable of inducing lung metastases by sequential passage of SP1 cells into mammary gland (Elliott et al., 1988). These cells were cultured in RPMI 1640 medium supplemented with either 5 or 20% FCS, folic acid (290 mg/l), and sodium pyruvate (100 mg/l). COS-7 cells were obtained from American Type Culture Collection and grown routinely in DME containing 10% FBS, 1% glutamine, 1% penicillin, and 1% streptomycin.

### Antibodies and Reagents

For the preparation of polyclonal rabbit anti-Tiam1 antibody, specific synthetic peptides (~15–17 amino acids unique for the COOH-terminal sequence of Tiam1) were prepared by the Peptide Laboratories of the Department of Biochemistry and Molecular Biology using an automatic synthesizer (model ACT350; Advanced Chemtech). These Tiam1-related polypeptides were conjugated to polylysine and subsequently injected into rabbits to raise the antibodies. The anti-Tiam1-specific antibody was collected from each bleed and stored at 4°C containing 0.1% azide. The anti-Tiam1 IgG fraction was prepared by conventional DEAE-cellulose chromatography. Mouse monoclonal anti-hemagglutinin (HA epitope) antibody (clone 12 CA5) and mouse monoclonal anti-green fluorescent protein (GFP) antibody were purchased from Boehringer Mannheim and PharMingen, respectively. *Escherichia coli* (*E. coli*)-derived GST-tagged Rac1/Cdc42 and GST-tagged RhoA was provided by Dr. Richard A. Cerione (Cornell University, Ithaca, NY) and Dr. Martin Schwartz (Scripps Research Institute, La Jolla, CA), respectively. Mouse monoclonal erythrocyte ankyrin (ANK1) and ANK3 antibodies were prepared as described previously (Bourguignon et al., 1993a). Rabbit anti-ANK3 antibody was provided by Dr. L.L. Peters (Jackson Laboratory, Bar Harbor, ME; Peters et al., 1995).

### Cloning, Expression, and Purification of GST-tagged Ankyrin Repeat Domain (GST-ARD) and GFP-tagged Spectrin Binding Domain (GFP-SBD) of Ankyrin

pGEX-2TK recombinant plasmid expressing GST-ARD (NH<sub>2</sub>-terminal portion of ankyrin, residues 1–834) was constructed as follows. Two pGEX-2TK recombinant plasmids pA3-79 (expressing epithelial Ank3 NH<sub>2</sub>-terminal 1–455 amino acids) and pA3-88 (expressing epithelial Ank3

NH<sub>2</sub>-terminal 317–834 amino acids; Peters et al., 1995) were provided by Dr. L.L. Peters from the Jackson Laboratory. The two plasmids were digested by EcoRI (one of pGEX-2TK vector cloning sites) and NheI (in ankyrin cDNA 1,176 bp) sequentially. The digested products were run in 1% agarose gel and purified with a purification kit (QIAGEN). The larger cDNA fragment in pA3-79-digested products (containing the pGEX-2TK vector and ankyrin cDNA 1–1,176 bp) and the smaller one in pA3-88-digested products (containing ankyrin cDNA 1,176–2,556 bp) were cut and purified. These two cDNA fragments were ligated and transformed to INVaF<sup>+</sup>-competent cells. The obtained clones were sequenced to verify the correct generation of the full-length ARD.

Spectrin binding domain (SBD) cDNA of human erythrocyte ankyrin was cloned into the eukaryotic expression vector, GFPN1 (CLONTECH Laboratories, Inc.) using the PCR-based cloning strategy. Ankyrin's SBD cDNA was amplified by PCR with two specific primers (left, 5'-CGCTC-GAGATGAAGGCTGAGAGGCGGGATTCC-3' and right, 5'-ATAAGCTTCAGGGGCGTCGGGGTCTTCT-3') linked with specific enzyme digestion site (XhoI and HindIII). The PCR product, which was digested with XhoI and HindIII, was purified with QIAquick PCR purification kit (QIAGEN). Ankyrin's SBD cDNA fragment was cloned into GFPN1 vector digested with XhoI and HindIII. The cDNA sequence was confirmed by nucleotide sequencing analysis. The GFP-tagged spectrin binding domain (GFP-SBD) of ankyrin is expressed as an 89-kD polypeptide in SP1 or COS-7 cells by SDS-PAGE and immunoblot analyses. The 89-kD GFP-SBD (but not ARD) displays specific spectrin binding property as described previously (Platt et al., 1993). Subsequently, GFP-SBD was isolated from anti-GFP-conjugated affinity columns and used in various in vitro binding experiments as described below.

## Expression Constructs

Both the full-length mouse Tiam1 cDNA (FL1591) and the NH<sub>2</sub> terminally truncated Tiam1 cDNA (C1199) were provided by Dr. John G. Colard (The Netherlands Cancer Institute, The Netherlands). Specifically, the full-length Tiam1 (FL1591) cDNA was cloned into the eukaryotic expression vector, pMT2SM. The truncated C1199 Tiam1 cDNA (carrying a hemagglutinin epitope [HA] tag at the 3' end) was cloned in the eukaryotic expression vector, pUTSV1 (Eurogentec, Belgium).

The deletion construct, HA-tagged C1199 Tiam1Δ717-727 (deleting the sequence between amino acids 717 and 727 of Tiam1) was derived from C1199 Tiam1 using QuickChange™ site-directed mutagenesis kit (Stratagene). In brief, two complementary mutagenic oligonucleotide primers containing the desired deletion (5'-CCCAACCATCAACCAGGTGTTTGAGGGAATATTTGATG-3') was designed and synthesized. First, the cycling reaction, using 30-ng double-stranded DNA template of C1199 Tiam1 plasmid and two complementary primers, was performed to produce mutated cDNA according to the manufacturer's instruction. Subsequently, 1 μl of the DpnI restriction enzyme (10 U/μl) was added directly to the cycling reaction products to digest the parental supercoiled double-stranded DNA. This DpnI-treated cDNA was used to transform supercompetent cells (e.g., *Epicurian coli* XL 1-blue). Finally, the deletion construct was confirmed by DNA sequencing.

The Tiam1 (amino acids 393–728) fragment was cloned into calmodulin-binding peptide (CBP)-tagged vector (pCAL-n; Stratagene) using the PCR-based cloning strategy. Using human Tiam1 cDNA as a template, the Tiam1 fragment was amplified by PCR with two specific primers (left, 5'-AACTCGAGATGAGTACCACCAACAGTGAG-3' and right, 5'-AAAAAGCTTTCAGCCATCTGGAACAGTGTATC-3') linked with a specific enzyme digestion site (XhoI or HindIII). The PCR product, which was digested with XhoI and HindIII, was purified with QIAquick PCR purification kit (QIAGEN). The Tiam1 fragment cDNA was cloned into pCAL-n vector digested with XhoI and HindIII. The inserted Tiam1 fragment sequence was confirmed by nucleotide sequencing analyses. The recombinant plasmids were transformed to BL21-DE3 to produce CBP-tagged Tiam1 fragment fusion protein. This fusion protein was purified from bacteria lysate by calmodulin affinity resin column (Sigma Chemical Co.).

The Tiam1 fragment cDNA was also cloned into pEGFPN1 vector (CLONTECH Laboratories, Inc.) digested with XhoI and HindIII to create GFP-tagged Tiam1 fragment cDNA. The inserted Tiam1 fragment sequence was confirmed by nucleotide sequencing analyses. This GFP-tagged Tiam1 fragment cDNA was used for transient expression in SP1 cells as described below. The GFP-tagged Tiam1 fragment is expressed as a 68-kD polypeptide in SP1 or COS-7 cells by SDS-PAGE and immunoblot analyses.

## Cell Transfection

To establish a transient expression system, cells (e.g., SP-1 or COS-7 cells) were transfected with various plasmid DNAs including Tiam1 cDNAs (e.g., the full-length mouse Tiam1 cDNA [FL1591], or HA-tagged C1199 Tiam1 cDNA, or HA-tagged C1199 Tiam1Δ717-727 cDNA, or GFP-tagged Tiam1 fragment cDNA, or HA-tagged C1199 Tiam1 cDNA plus GFP-tagged Tiam1 fragment cDNA (cotransfection), or vector control constructs) using electroporation methods. In brief, cells (e.g., SP-1 or COS-7 cells) were plated at a density of 10<sup>6</sup> cells per 100-mm dish, and were transfected with 25 μg/dish plasmid DNA using electroporation at 230 V and 960 μFD with a gene pulser (Bio-Rad). Transfected cells were grown in 5 or 20% FCS-containing culture medium for at least 24–48 h. Various transfectants were analyzed for the expression of Tiam1 or HA-tagged (or GFP-tagged) Tiam1 mutant proteins by immunoblot, immunoprecipitation, and functional assays as described below.

## Immunoprecipitation and Immunoblotting Techniques

SP-1 cells or COS cells (e.g., untransfected or transfected by various Tiam1 cDNAs including the full-length mouse Tiam1 cDNA [FL1591] or HA-tagged C1199 Tiam1 cDNA) were first extracted with a solution containing 50 mM Tris-HCl, pH 7.4, 150 mM NaCl, and 1% NP-40 buffer, followed by solubilizing in SDS sample buffer, and analyzed by SDS-PAGE (with 7.5% gel). Separated polypeptides were transferred onto nitrocellulose filters. After blocking nonspecific sites with 3% BSA, the nitrocellulose filters were incubated with 5 μg/ml either of rabbit anti-Tiam1 or mouse anti-HA (or preimmune serum) plus peroxidase-conjugated goat anti-rabbit IgG or goat anti-mouse IgG (1:10,000 dilution), respectively. In controls, peroxidase-conjugated normal mouse IgG or preimmune rabbit IgG was also incubated with anti-Tiam1-mediated immunocomplex. The blots were developed using ECL chemiluminescence reagent (Amersham Life Science) according to the manufacturer's instructions.

In some cases, SP-1 cells (transfected with HA-tagged C1199 Tiam1 cDNA, or HA-tagged C1199 Tiam1Δ717-727 cDNA, or GFP-tagged Tiam1 fragment cDNA, or cotransfected with HA-tagged C1199 Tiam1 cDNA and GFP-tagged Tiam1 fragment cDNA) were immunoblotted with anti-HA antibody (5 μg/ml) or anti-GFP antibody (5 μg/ml), respectively, followed by incubation with HRP-conjugated goat anti-mouse IgG (1:10,000 dilution) at room temperature for 1 h.

SP-1 cells were also immunoprecipitated with rabbit anti-Tiam1 (5 μg/ml) or mouse anti-ankyrin antibodies (e.g., 5 μg/ml of either mouse anti-ANK3 antibody or mouse anti-ANK1 antibody), followed by immunoblotting/reblotting with ankyrin antibodies (e.g., 1 μg/ml mouse anti-ANK3 antibody, or 5 μg/ml mouse anti-ANK1 antibody, or 1 μg/ml rabbit anti-Tiam1), respectively, followed by incubation with HRP-conjugated goat anti-mouse IgG or goat anti-rabbit IgG (1:10,000 dilution) at room temperature for 1 h. In reblotting controls, both peroxidase-conjugated normal mouse IgG or rabbit preimmune IgG was also used. The blots were developed using ECL chemiluminescence reagent (Amersham Life Science) according to the manufacturer's instructions.

## Effects of Synthetic Peptides on Ankyrin-Tiam1 Interaction

Nitrocellulose discs (1-cm diam) were coated with ~1 μg of a panel of synthetic peptides including the ankyrin-binding region peptide (<sup>717</sup>GEGTDAVKRS<sup>727</sup>L), a scrambled peptide (GRATLEGSDKV) and another Tiam1-related peptide (<sup>399</sup>GTIKRAPFLG<sup>409</sup>P; synthesized by Dr. Eric Smith, University of Miami). After coating, the unoccupied sites on the discs were blocked by incubation with a solution containing 20 mM Tris-HCl, pH 7.4, and 0.3% BSA at 4°C for 2 h. The discs were incubated with various concentration of <sup>125</sup>I-labeled cytoskeletal proteins (erythrocyte ankyrin/ARD/ankyrin's SBD/spectrin; ~3000 cpm/ng) at 4°C for 2 h in 1 ml binding buffer (20 mM Tris-HCl, pH 7.4, 150 mM NaCl, 0.2% BSA).

In some experiments, <sup>125</sup>I-labeled Tiam1 (~3,000 cpm/ng) was incubated with ankyrin-coated beads in the presence of various concentrations (10<sup>-10</sup>–10<sup>-6</sup> M) of unlabeled synthetic peptide (e.g., <sup>717</sup>GEGTDAVKRS<sup>727</sup>L or the scrambled sequence, GRATLEGSDKV, or another Tiam1-related peptide, <sup>399</sup>GTIKRAPFLG<sup>409</sup>P) at 4°C for 2 h in 1 ml binding buffer (20 mM Tris-HCl, pH 7.4, 150 mM NaCl, 0.2% BSA). <sup>125</sup>I-labeled Tiam1 fragment (~3,000 cpm/ng) was also incubated with beads containing 1.0 μg of each of the following four proteins: intact ankyrin, ARD, or spectrin binding domain of ankyrin (GFP-SBD), or GFP alone.

After binding, the peptide-coated discs (or cytoskeletal protein-conjugated beads) were washed three times in the binding buffer, and the radioactivity associated with the peptide-coated discs (or cytoskeletal protein-conjugated beads) was estimated. As a control, the ligands were also incubated with uncoated nitrocellulose discs (or beads) to determine the binding observed because of the stickiness of various ligands. Nonspecific binding was observed in these controls. In the peptide competition assay, the specific binding observed in the absence of any of the competing peptides is designated as 100%. The results represent an average of duplicate determinations for each concentration of the competing peptide used.

### Binding of Ankyrin or ARD to Tiam1 In Vitro

Aliquots (0.5–1.0  $\mu$ g of protein) of purified Tiam1 (e.g., intact Tiam1, or C1199 Tiam1, or Tiam1 fragment)-conjugated beads were incubated in 0.5 ml of binding buffer (20 mM Tris-HCl, pH 7.4, 150 mM NaCl, 0.1% BSA, and 0.05% Triton X-100) containing various concentrations (10–800 ng/ml) of  $^{125}$ I-labeled intact ankyrin (purified from human erythrocytes; 5,000 cpm/ng protein) or  $^{125}$ I-labeled recombinant ARD fragment at 4°C for 4 h. Specifically, equilibrium binding conditions were determined by performing a time course (1–10 h) of  $^{125}$ I-labeled ankyrin (or ARD) binding to Tiam1 at 4°C. The binding equilibrium was found to be established when the in vitro ankyrin (or ARD)-Tiam1 binding assay was conducted at 4°C after 4 h. After binding, beads were washed extensively in binding buffer, and the bead-bound radioactivity was counted.

As a control,  $^{125}$ I-labeled ankyrin or  $^{125}$ I-labeled ARD was also incubated with uncoated beads to determine the binding observed because of the nonspecific binding of various ligands. Nonspecific binding, which represented ~20% of the total binding, was always subtracted from the total binding. Our binding data are highly reproducible. The values expressed in the Results represent an average of triplicate determinations of three to five experiments with an SD less than  $\pm 5\%$ . In some cases,  $^{125}$ I-ankyrin (1–10 ng) was incubated with a polyacrylamide gel containing purified Tiam1 (obtained from anti-Tiam1 affinity column chromatography) in the absence or the presence of 100-fold excess amount of unlabeled ankyrin/spectrin (in the same binding buffer as described above) for 1 h at room temperature. After incubation, the gel was washed five times with the same binding solution and analyzed by autoradiographic analyses.

An in vitro binding assay designed to measure the stoichiometry of GST-ARD fusion protein and C1199 Tiam1 was also carried out. Specifically, in each reaction, 15–60  $\mu$ l of glutathione-Sepharose bead slurry containing GST-ARD or GST alone was suspended in 0.5 ml of binding buffer (20 mM Tris-HCl, pH 7.4, 150 mM NaCl, 0.1% BSA, and 0.05% Triton X-100). Purified C1199 Tiam1 (0.5–1.0  $\mu$ g) was added to the bead suspension in the absence or the presence of an excess amount of CBP-tagged Tiam1 fragment (100  $\mu$ g) at 4°C for 4 h. After binding, the GST fusion protein was eluted with its associated C1199 Tiam1 using 150  $\mu$ l of 50 mM Tris-HCl, pH 8.0, buffer containing 30 mM glutathione. The amount of eluted GST fusion protein and C1199 Tiam1 was determined by SDS-PAGE and Coomassie blue staining followed by densitometric scanning using a software NIH Image V1.54. The amount of ARD (mol) per C1199 Tiam1 (mol) was calculated. Values represent relative binding abilities averaged from three experiments  $\pm$  SEM.

### Binding of $^{125}$ I-Labeled Ankyrin to C1199 Tiam1 and the Mutant Protein

SP1 cells were transfected with HA-tagged C1199 Tiam1 cDNA, or HA-tagged C1199 Tiam1 $\Delta$ 717-727 cDNA, or vector alone. These transfectants were extracted with a solution containing 50 mM Tris-HCl, pH 7.4, 150 mM NaCl, and 1% NP-40, and immunoprecipitated with anti-HA immunoaffinity beads. Subsequently, aliquots (50 ng proteins) of these beads were incubated with 0.5 ml of a binding buffer (20 mM Tris-HCl, pH 7.4, 150 mM NaCl, 0.1% BSA, and 0.05% Triton X-100) in presence of various concentrations (10–400 ng/ml) of  $^{125}$ I-labeled ankyrin (5,000 cpm/ng protein) at 4°C for 5 h. After binding, beads were washed extensively in binding buffer and the bead-bound radioactivity was counted.

As a control,  $^{125}$ I-labeled ankyrin was also incubated with uncoated beads to determine the binding observed because of the nonspecific binding of the ligand. Nonspecific binding, which represented ~15–20% of the total binding, was always subtracted from the total binding. The values expressed in the Results represent an average of triplicate determinations of three to five experiments with an SD less than  $\pm 5\%$ .

### Tiam1-mediated GDP/GTP Exchange for Rho GTPases

Purified *E. coli*-derived GST-tagged GTPases (e.g., Rac1, Cdc42, or RhoA; 20 pmol) were preloaded with GDP (30  $\mu$ M) in 10  $\mu$ l buffer containing 25 mM Tris-HCl, pH 8.0, 1 mM DTT, 4.7 mM EDTA, 0.16 mM  $\text{MgCl}_2$ , and 200  $\mu$ g/ml BSA at 37°C for 7 min. To terminate preloading procedures, additional  $\text{MgCl}_2$  was added to the solution (reaching a final concentration of 9.16 mM) as described previously (Zhang et al., 1995). Tiam1 was isolated from COS-7 cells (transfected with either the full-length Tiam1 cDNA or HA-tagged C1199 Tiam1 cDNA) or SP1 cells (transfected with various plasmid DNAs such as HA-tagged C1199 Tiam1 cDNA, GFP-tagged Tiam1 fragment cDNA, or HA-tagged C1199 Tiam1 cDNA plus GFP-tagged Tiam1 fragment cDNA [as cotransfection] or vector alone) using anti-Tiam1 (or anti-HA or anti-GFP)-conjugated beads. In some cases, ankyrin-associated Tiam1 was isolated from SP1 cells (transfected with HA-tagged C1199 Tiam1 cDNA, GFP-tagged Tiam1 fragment cDNA, or HA-tagged C1199 Tiam1 cDNA plus GFP-tagged Tiam1 fragment cDNA [as a cotransfection], or vector alone) using anti-ankyrin-conjugated beads.

Subsequently, 2 pmol of Tiam1, isolated from untransfected or transfected cells according to the procedures described above, was preincubated with no ankyrin or ankyrin (e.g., 1  $\mu$ g/ml of either intact ankyrin or ARD), followed by adding to the reaction buffer containing 20 mM Tris-HCl, pH 8.0, 100 mM NaCl, 10 mM  $\text{MgCl}_2$ , 100  $\mu$ M AMP-PNP, 0.5 mg/ml BSA, and 2.5  $\mu$ M GTP- $\gamma$ - $^{35}$ S (~1,250 Ci/mmol). Subsequently, 2.5 pmol GDP-loaded GST-tagged Rho GTPases (e.g., Rac1, RhoA, or Cdc42) or GDP-treated GST were mixed with the reaction buffer containing Tiam1 and GTP- $\gamma$ - $^{35}$ S to initiate the exchange reaction at room temperature. At various time points, the reaction of each sample was terminated by adding ice-cold termination buffer containing 20 mM Tris-HCl, pH 8.0, 100 mM NaCl, and 10 mM  $\text{MgCl}_2$  as described previously (Michiels et al., 1995; Zhang et al., 1995). The termination reactions were filtered immediately through nitrocellulose filters, followed by one wash with the termination buffer. The filters were dissolved completely in scintillation fluid, and the radioactivity associated with the filters were measured by scintillation fluid. The amount of GTP- $\gamma$ - $^{35}$ S bound to Tiam1 or control sample (pre-immune serum-conjugated Sepharose beads) in the absence of Rho GTPases (e.g., Rac1, Cdc42, or RhoA) was subtracted from the original values. Data represent an average of triplicates from three to five experiments. SD < 5%.

### Double Immunofluorescence Staining

SP1 cells (untransfected or transfected with various plasmid DNAs such as HA-tagged C1199 Tiam1 cDNA, GFP-tagged Tiam1 fragment cDNA, or HA-tagged C1199 Tiam1 cDNA plus GFP-tagged Tiam1 fragment cDNA [as a cotransfection], or vector alone) were first washed with PBS (0.1 M phosphate buffer, pH 7.5, and 150 mM NaCl) buffer and fixed by 2% paraformaldehyde. Subsequently, cells were rendered permeable by ethanol treatment followed by staining with different immunoreagents. Specifically, untransfected cells were incubated with rhodamine (Rh)-conjugated mouse anti-ANK3 (50  $\mu$ g/ml) and fluorescein (FITC)-conjugated rabbit anti-Tiam1 (50  $\mu$ g/ml), respectively. HA-tagged C1199 cDNA-transfected cells were stained with Rh-conjugated mouse anti-ANK3 antibody (50  $\mu$ g/ml) and FITC-conjugated mouse anti-HA IgG (50  $\mu$ g/ml), respectively. GFP-tagged Tiam1 fragment cDNA-transfected cells were labeled with Rh-conjugated anti-ANK3 (50  $\mu$ g/ml). Some SP1 transfectants (cotransfected with Tiam1 fragment cDNA and HA-tagged C1199 Tiam1 cDNA) were stained with Rh-conjugated anti-HA (50  $\mu$ g/ml) or Rh-conjugated anti-ANK3 (50  $\mu$ g/ml), respectively. To detect nonspecific antibody binding, vector-transfected cells were labeled with Rh-conjugated anti-ANK3 (50  $\mu$ g/ml) followed by incubating with FITC-conjugated anti-HA (50  $\mu$ g/ml). No anti-HA labeling was observed in such control samples. In some experiments, GFP-tagged Tiam1 fragment cDNA-transfected cells were also incubated with Rh-labeled rabbit pre-immune IgG (50  $\mu$ g/ml). No nonspecific rhodamine staining was detected in these samples. The FITC- and Rh-labeled samples were examined with a confocal laser scanning microscope (MultiProbe 2001 inverted CLSM system; Molecular Dynamics).

### Tumor Cell Migration and Invasion Assays

24 transwell units were used for monitoring in vitro cell migration and invasion as described previously (Merzak et al., 1994; Bourguignon et al., 1998b, 2000). Specifically, the 5- $\mu$ m porosity polycarbonate filters coated with the reconstituted basement membrane substance Matrigel (Collabo-

rative Research) were used for the cell invasion assay (Merzak et al., 1994; Bourguignon et al., 1998b). The 5- $\mu$ m porosity polycarbonate filters (without Matrigel coating) were used for the cell migration assay (Merzak et al., 1994; Bourguignon et al., 1998b, 2000). SP-1 cells transfected with various Tiam1-related cDNAs (e.g., full-length Tiam1 cDNA, HA-tagged C1199 Tiam1 cDNA, or GFP-tagged Tiam1 fragment cDNA, or HA-tagged C1199 Tiam1 cDNA plus GFP-tagged Tiam1 fragment cDNA [cotransfection], or vector alone) ( $\sim 10^4$  cells/well in PBS, pH 7.2, untreated or treated with cytochalasin D [20  $\mu$ g/ml] or DMSO alone) were placed in the upper chamber of the transwell unit. The growth medium containing high glucose DME supplemented by 10% FBS was placed in the lower chamber of the transwell unit. After an 18-h incubation at 37°C in a humidified 95% air/5% CO<sub>2</sub> atmosphere, cells on the upper side of the filter were removed by wiping with a cotton swap. Cell migration and invasion processes were determined by measuring the cells that migrate to the lower side of the polycarbonate filters by standard cell number counting methods as described previously (Merzak et al., 1994; Zhu and Bourguignon, 2000). Each assay was set up in triplicate and repeated at least five times. All data were analyzed statistically by *t* test and statistical significance was set at *P* < 0.01.

## Results

### Identification of the GEF, Tiam1 in Breast Tumor Cells (SP-1 Cells)

Rho GTPases such as Rac1 become activated when bound GDP is exchanged for GTP by a process catalyzed by GEFs such as Tiam1 (Habets et al., 1994). A Tiam1 transcript has been detected previously in breast cancer cells (Habets et al., 1995). In this study, we have analyzed Tiam1 expression (at the protein level) in SP-1 breast tumor cells. Immunoblot analysis, using anti-Tiam1 antibody designed to recognize the specific epitope located at the COOH terminus of Tiam1 molecule, reveals a single polypeptide ( $\sim 200$  kD; Fig. 1, lane 1). This 200-kD Tiam1-like molecule, expressed in SP-1 cells, is very similar to the Tiam1 detected in COS-7 cells that were transiently transfected with the full-length Tiam1 cDNA (Fig. 1, lane 2) or NH<sub>2</sub> terminally truncated C1199 Tiam1 cDNA (Fig. 1, lane 3 revealing primarily C1199 Tiam1 [160 kD] and a low level of endogenous Tiam1 [200 kD]). We believe that the Tiam1 detected in SP-1 cells or COS-7 transfectants, revealed by anti-Tiam1-mediated immunoblot, is specific

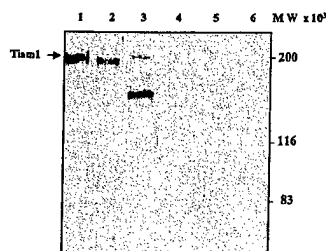


**Figure 1.** Detection of Tiam1 expression in SP-1 cells or COS-7 transfectants. SP-1 and COS-7 cells, which were transfected with the full-length Tiam1 cDNA (FL1591) or NH<sub>2</sub> terminally truncated C1199 Tiam1 cDNA or vector alone, were solubilized in SDS sample

buffer and analyzed by SDS-PAGE and immunoblot as described in Materials and Methods. (lane 1) Anti-Tiam1-mediated immunoblot of SP-1 cells. (lane 2) Anti-Tiam1-mediated immunoblot of COS-7 cells transfected with the full-length Tiam1 cDNA (FL1591). (lane 3) Anti-Tiam1-mediated immunoblot of COS-7 cells transfected with the NH<sub>2</sub> terminally truncated C1199 Tiam1 cDNA. (lane 4) Immunoblot of SP-1 cells with preimmune rabbit serum. (lane 5) Immunoblot of COS-7 cells, which were transfected with Tiam1 cDNA [FL1591], with preimmune rabbit serum. (lane 6) Immunoblot of COS-7 cells, which were transfected with the NH<sub>2</sub> terminally truncated C1199 Tiam1 cDNA, with preimmune rabbit serum.

since no protein is detected in these cells using preimmune rabbit IgG (Fig. 1, lanes 4–6).

To confirm that the Tiam1-like molecule functions as a GDP/GTP exchange factor (or a GDP-dissociation stimulator protein) for Rac1, we have isolated Tiam1 from SP-1 cells using anti-Tiam1-conjugated Sepharose beads. Our results indicate that SP1's Tiam1 activates GDP/GTP exchange on GST-Rac1 (Fig. 2 A, a) and, to a lesser extent, on GST-Cdc42 (Fig. 2 A, b) and GST-RhoA (Fig. 2 A, c). The initial onset of the exchange reaction on GST-Rac1

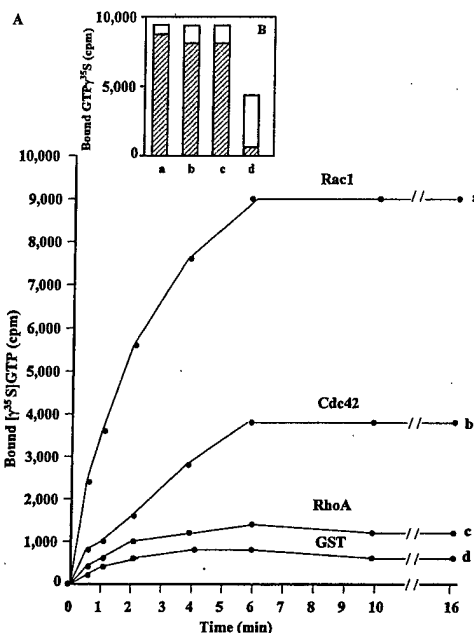


**Figure 2.** Tiam1-mediated GDP/GTP exchange for Rho GTPases. Purified *E. coli*-derived GST-tagged GTPases (e.g., Rac1, Cdc42, or RhoA) were preloaded with GDP. First, 2 pmol Tiam1 that was isolated from SP1 cells or COS-7 transfectants was added to the reaction buffer containing 20 mM Tris-HCl, pH 8.0, 100 mM NaCl, 10 mM MgCl<sub>2</sub>, 100  $\mu$ M AMP-PNP, 0.5 mg/ml BSA, and 2.5  $\mu$ M GTP- $\gamma$ -<sup>35</sup>S ( $\sim 1,250$  Ci/mmol). Subsequently, 2.5 pmol GDP-loaded GST-tagged Rho GTPases (e.g., Rac1, RhoA, Cdc42, or GST alone) were mixed with the reaction buffer containing Tiam1 and GTP- $\gamma$ -<sup>35</sup>S to initiate the exchange reaction at room temperature. At various time points, the reaction of each sample was terminated by adding ice-cold termination buffer as described in Materials and Methods. The termination reactions were filtered immediately through nitrocellulose filters, and the radioactivity associated with the filters were measured by scintillation fluid. The amount of GTP- $\gamma$ -<sup>35</sup>S bound to Tiam1 or control sample (preimmune serum-conjugated Sepharose beads) in the absence of Rho GTPases (e.g., Rac1, Cdc42, or RhoA) was subtracted from the original values. Data represent an average of triplicates from three to five experiments. SD < 5%. (A) Kinetics of GTP- $\gamma$ -<sup>35</sup>S bound to GDP-loaded GST-Rac1 (a), GST-Cdc42 (b), or GST-RhoA (c), or GST alone (d) in the presence of Tiam1 (isolated from SP-1 cells). (B) The maximal level of GTP- $\gamma$ -<sup>35</sup>S bound to GST-Rac1 in the presence of Tiam1 isolated from SP1 grown in 5% FCS (a, shaded bar) or 20% FCS (a, blank bar); or the full-length Tiam1 (1,591) isolated from COS-7 transfectants grown in 5% FCS (b, shaded bar) or 20% FCS (b, blank bar); or the C1199 Tiam1 isolated from COS-7 transfectants grown in 5% FCS (c, shaded bar), or 20% FCS (c, blank bar); or Tiam1 isolated from vector-transfected COS-7 cells grown in 5% FCS (d, shaded bar) or 20% FCS (d, blank bar).

occurs within 0.5–1 min after the addition of Tiam1, and the reaction reaches its maximal level ~16 min after Tiam1 addition (Fig. 2 A, a). In contrast, the initial rate of Tiam1-catalyzed GDP/GTP exchange on Cdc42 (Fig. 2 A, b) and RhoA (Fig. 2 A, c) appears to be significantly lower than that detected on Rac1 (Fig. 2 A, a). In the control samples, the amount of [<sup>35</sup>S]GTP-γ-S associated with GST alone is found to be significantly decreased (Fig. 2 A, d). Further analysis indicates that the ability of Tiam1 isolated from SP-1 cells to promote GDP/GTP exchange on Rac1 (Fig. 2 B, a) is identical to that carried out by the Tiam1 isolated from COS-7 transfected with the full-length Tiam1 cDNA (Fig. 2 B, b) or NH<sub>2</sub> terminally truncated C1199 Tiam1 cDNA (Fig. 2 B, c). Therefore, we believe that the Tiam1 in SP-1 cells clearly functions as a GDP/GTP exchange factor for Rho-like GTPases such as Rac1 GTPase.

We have also noticed that Tiam1 isolated from nontransfected COS-7 cells grown in the presence of 20% FCS is capable of catalyzing GDP/GTP exchange on Rac1 at a much higher level (Fig. 2 B, d, blank bar) than Tiam1 isolated from nontransfected COS-7 cells grown in the presence of 5% FCS (Fig. 2 B, d, shaded bar). This observation is consistent with the previous findings that some serum components play an important role in upregulating the ability of Tiam1 to promote GDP/GTP exchange on Rac1 (Stam et al., 1998). In SP1 cells (Fig. 2 B, a, blank and shaded bars) or Tiam1 cDNA-transfected COS-7 cells (Fig. 2 B, b and c, blank and shaded bars), neither high nor low serum causes significant changes in the ability of Tiam1 to catalyze GDP/GTP exchange on Rac1. These differential serum effects on the activity of Tiam1 isolated from low or high Tiam1-expressing cells await future investigation.

### Interaction between Tiam1 and the Cytoskeletal Proteins, Ankyrin

Certain cytoskeleton proteins, such as ankyrin, are known to be involved in regulating a variety of cellular activities (Bennett, 1992; Bennett and Gilligan, 1993; Bourguignon, 1996; Bourguignon et al., 1998a; De Matteis and Morrow, 1998). Both ankyrin1 (ANK1) and ankyrin 3 (ANK3) have been shown to be expressed in breast tumor cells (Bourguignon et al., 1998b, 1999). In this study, we have carried out anti-ANK1 or anti-ANK3-mediated immunoprecipitation of SP-1 cellular proteins, followed by anti-Tiam1 immunoblot (Fig. 3, A and B, lane 2) and anti-ANK1 (Fig. 3 A, lane 3)/ANK3 (Fig. 3 B, lane 3) immunoblot, respectively. Our results indicate that the Tiam1 band is revealed in anti-ankyrin (e.g., ANK1 or ANK3)-mediated immunoprecipitated materials (Fig. 3, A and B, lane 2). Apparently, Tiam1 is coprecipitated with ANK1 and/or ANK3 (revealed by reblotting with anti-ANK1/ANK3 antibody; Fig. 3, A and B). In control samples, immunoblotting of anti-ANK1 or anti-ANK3-immunoprecipitated material using rabbit preimmune serum (Fig. 3, A and B, lane 1) does not reveal any protein associated with this material. Anti-Tiam1-mediated immunoprecipitation of SP-1 cellular proteins, followed by anti-ANK1 (Fig. 3 A, lane 4) or anti-ANK3 (Fig. 3 B, lane 4)-mediated immunoblot also shows that both ANK1 (Fig. 3 A, lane 4) and ANK3 (Fig.

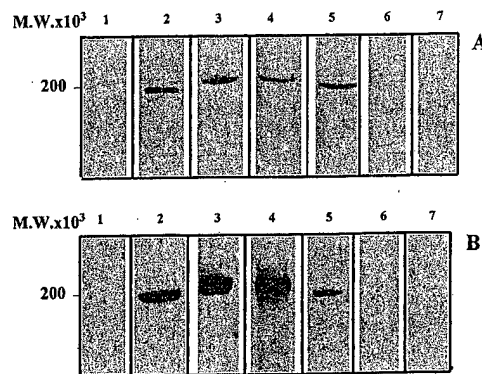


**Figure 3.** Detection of Tiam1-ankyrin complex in SP1 cells. SP1 cells ( $5 \times 10^5$  cells) were solubilized by 1% NP-40 buffer and processed for anti-ankyrin or anti-Tiam1-mediated immunoprecipitation, followed by immunoblotting with anti-Tiam1 or anti-ANK1 (or anti-ANK3) antibody, respectively, as described in Materials and Methods. (A) Analysis of Tiam1-ANK1 complex (lane 1). Anti-ANK1-mediated immunoprecipitation followed by immunoblotting with rabbit preimmune serum. (lanes 2 and 3) Detection of Tiam1 in the complex by mouse anti-ANK1-mediated immunoprecipitation, followed by immunoblotting with rabbit anti-Tiam1 antibody (lane 2) or reblotting with mouse anti-ANK1 antibody (lane 3). (lanes 4–7) Detection of ANK1 in the complex by rabbit anti-Tiam1-mediated immunoprecipitation, followed by immunoblotting with mouse anti-ANK1 antibody (lane 4) or reblotting with rabbit anti-Tiam1 antibody (lane 5), or peroxidase-conjugated normal mouse IgG (lane 6) or peroxidase-conjugated rabbit preimmune IgG (lane 7). (B) Analysis of Tiam1-ANK3 complex: (lane 1) anti-ANK3-mediated immunoprecipitation followed by immunoblotting with rabbit preimmune serum. (lanes 2 and 3) Detection of Tiam1 in the complex by mouse anti-ANK3-mediated immunoprecipitation, followed by immunoblotting with rabbit anti-Tiam1 antibody (lane 2) or reblotting with mouse anti-ANK3 antibody (lane 3). (lanes 4–7) Detection of ANK3 in the complex by rabbit anti-Tiam1-mediated immunoprecipitation, followed by immunoblotting with mouse anti-ANK3 antibody (lane 4) or reblotting with rabbit anti-Tiam1 antibody (lane 5), or peroxidase-conjugated normal mouse IgG (lane 6), or peroxidase-conjugated rabbit preimmune IgG (lane 7).

3 B, lane 4) can be coprecipitated with Tiam1 (revealed by reblotting with anti-Tiam1 antibody; Fig. 3, A and B, lane 5). In controls, very little material is detected in this anti-Tiam1-mediated immunocomplex using either normal mouse IgG (Fig. 3, A and B, lane 6) or rabbit preimmune serum-mediated immunoblot (Fig. 3 A, lane 7). These findings clearly establish the fact that Tiam1 and ankyrin (e.g., ANK1 and ANK3) are closely associated with each other as an *in vivo* complex in breast tumor cells.

Further analyses using an *in vitro* binding assay show that <sup>125</sup>I-labeled ankyrin (i.e., erythrocyte ankyrin [ANK1]) binds Tiam1, which was isolated from SP1 cells, specifically (Fig. 4 A, a). In addition, we have used <sup>125</sup>I-labeled ankyrin to bind purified Tiam1 (isolated from SP-1 cells) on a gel (Fig. 4 B, a). Our data indicate that Tiam1 binds to ankyrin (ANK1; Fig. 4 B, a) directly. In the presence of an excess amount of unlabeled ankyrin, the binding between ankyrin and Tiam1 is greatly reduced (Fig. 4, A and B, b). Other cytoskeletal proteins, such as spectrin,

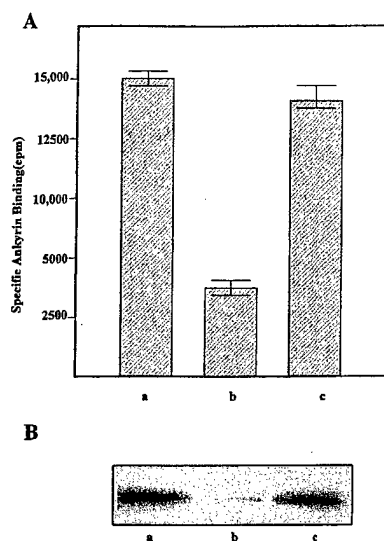


**Figure 4.** Binding interaction between Tiam1 and the cytoskeletal protein ankyrin. (A) Tiam1 (isolated from SP-1 cells) bound to the anti-Tiam1 immunobeads were incubated with  $^{125}\text{I}$ -labeled ankyrin (5,000 cpm/ng protein) in the absence (a) or the presence of 100-fold excess of unlabeled ankyrin (b) or spectrin (c). After binding, the immunobeads were washed extensively in binding buffer and the bead-bound radioactivity was estimated. (B) Autoradiogram of  $^{125}\text{I}$ -labeled ankyrin binding to a polyacrylamide gel containing purified Tiam1 (isolated from SP-1 cells) in the absence (a) or the presence of 100-fold excess of unlabeled ankyrin (b) or spectrin (c).

do not interfere with ankyrin binding to Tiam1 (Fig. 4, A and B, c). However, the precise functional domain of ankyrin involved in Tiam1 binding remains to be determined.

The  $\text{NH}_2$ -terminal region of ankyrin's membrane binding domain (Fig. 5 A, a) is comprised of a tandem array of 24 ankyrin repeats (so-called ankyrin repeat domain, ARD; Fig. 5 A, b). The question of whether the membrane-binding domain of ankyrin (in particular, ARD) is involved in Tiam1 binding is now addressed in this study. First, the pGEX-2TK recombinant plasmid encoding ARD ( $\text{NH}_2$ -terminal portion of ankyrin, from amino acids 1 to 834) was constructed with a GST tag and expressed in *E. coli* (Zhu and Bourguignon, 2000). The purified GST-tagged ARD fusion protein is expressed as a 116-kD protein (Fig. 5 B, lane 1). After the removal of GST tag by thrombin digestion, the ARD itself is found to be an 89-kD polypeptide (Fig. 5 B, lane 2), which is similar to the 89-kD ARD obtained by enzymatic digestion of erythrocyte ankyrin (Davis and Bennett, 1990).

Next, we have used the ARD fragment of ANK3 (GST-ARD) and purified Tiam1 to identify the exact Tiam1 binding site(s) on the ankyrin molecule. Specifically, we have tested the binding of Tiam1 to  $^{125}\text{I}$ -labeled intact erythrocyte ankyrin (ANK1), or  $^{125}\text{I}$ -labeled GST-ARD fragment of ANK3, under equilibrium binding conditions. Scatchard plot analyses indicate that intact erythrocyte ankyrin (ANK1) binds to Tiam1 at a single site (Fig. 5 C) with high affinity (an apparent dissociation constant [ $K_d$ ] of  $\sim 0.72$  nM). This ankyrin-Tiam1 binding interaction is

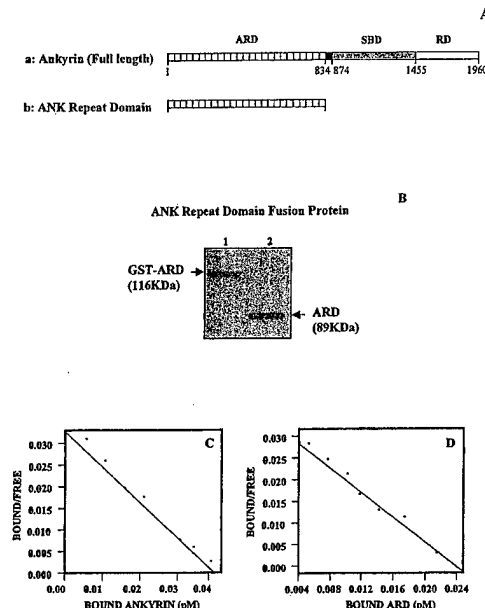


**Figure 5.** Ankyrin structure and ankyrin repeat domain (ARD) fusion protein. (A, a) Schematic illustration of functional domains in full-length ankyrin: ankyrin repeat domain (ARD), spectrin binding domain (SBD), and regulatory domain (RD). (A, b) ARD cDNA was constructed according to the strategy described in Materials and Methods. This ARD cDNA construct encodes for the  $\text{NH}_2$ -terminal region of the ankyrin membrane binding domain with a tandem array of 24 ankyrin repeats. (B) A Coomassie blue stain of the 116-kD GST-ARD fusion protein purified by affinity column chromatography (lane 1), and the 89-kD ARD (lane 2) after the removal of GST by thrombin digestion. (C and D) Scatchard plot analyses of the equilibrium binding between  $^{125}\text{I}$ -labeled ankyrin and Tiam1. Various concentrations of  $^{125}\text{I}$ -labeled ankyrin (e.g., intact erythrocyte ankyrin [ANK1] or ARD) were incubated with purified Tiam1-coupled beads at  $4^\circ\text{C}$  for 4 h. After binding, beads were washed extensively in binding buffer and the bead-bound radioactivity was counted. As a control,  $^{125}\text{I}$ -labeled ankyrin or  $^{125}\text{I}$ -labeled ARD was also incubated with uncoated beads to determine the binding observed because of the nonspecific binding of various ligands. Nonspecific binding, which represented  $\sim 20\%$  of the total binding, was always subtracted from the total binding. Our binding data are highly reproducible. Scatchard plot analysis of the equilibrium binding data between  $^{125}\text{I}$ -labeled intact erythrocyte ankyrin (ANK1) and Tiam1 (C); and Scatchard plot analysis of the equilibrium binding data between  $^{125}\text{I}$ -labeled ARD and Tiam1 (D).

comparable in affinity to Tiam1 binding ( $K_d \sim 1.42$  nM) to ANK3's ARD fragment (Fig. 5 D). These findings strongly support the notion that ankyrin (in particular, the ARD) is involved in the Tiam1 binding site.

#### Determination of Tiam1's Ankyrin-binding Domain

Previous studies indicate that Tiam1's  $\text{NH}_2$ -terminal pleckstrin homology (PHn) domain and an adjacent protein interaction domain (i.e., a sequence between amino acids 393 and 738 of Tiam1; Fig. 6 A, a-c) is required for the activation of Rac1 signaling pathways leading to membrane ruffling and c-Jun  $\text{NH}_2$ -terminal kinase activation (Michiels

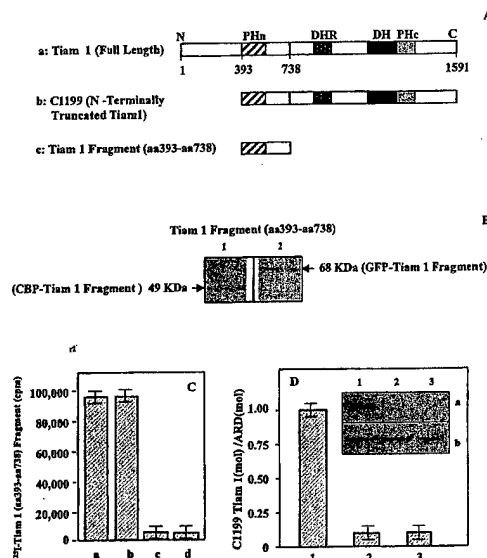


**Figure 6.** Properties of Tiam1 and Tiam1 mutant proteins. (A, a) The full-length Tiam1 contains DH, *dbl* homology domain; DHR, *discs-large* homology domain; two pleckstrin homology (PH) domains (including the NH<sub>2</sub>-terminal PH [PHn] and the COOH-terminal PH [PHc]). (A, b) The NH<sub>2</sub> terminally truncated C1199 Tiam1 encodes the COOH-terminal 1,199 amino acids. (A, c) The Tiam1 fragment encodes the sequence between amino acids 393 and 738. (B) Characterization of Tiam1 fragment (amino acids 393–738) fusion proteins. Coomassie blue staining of *E. coli*-derived CBP-Tiam1 fragment fusion protein purified by calmodulin affinity column chromatography (lane 1); and GFP-tagged Tiam1 fragment fusion purified by anti-GFP-conjugated affinity column chromatography (lane 2). (C, a) Binding of <sup>125</sup>I-Tiam1 fragment to ankyrin. (C, b) Binding of <sup>125</sup>I-Tiam1 fragment to ARD. (C, c) Binding of <sup>125</sup>I-Tiam1 fragment to the spectrin binding domain of ankyrin. (C, d) Binding of <sup>125</sup>I-Tiam1 fragment to spectrin. (D and E) Binding analysis between GST-ARD and the recombinant C1199 Tiam1 in vitro. In each reaction, glutathione-Sepharose bead slurry containing GST-ARD or GST alone was suspended in the binding buffer (20 mM Tris-HCl, pH 7.4, 150 mM NaCl, 0.1% BSA, and 0.05% Triton X-100). Purified C1199 Tiam1 (0.5–1.0 μg) was added to the bead suspension in the absence or the presence of an excess amount of CBP-tagged Tiam1 fragment (100 μg) at 4°C for 4 h. After binding, the GST fusion protein was eluted with its associated C1199 Tiam1 using 150 μl of 50 mM Tris-HCl, pH 8.0, buffer containing glutathione. The amount of eluted GST fusion protein and C1199 Tiam1 was determined by SDS-PAGE and Coomassie blue staining, followed by densitometric scanning using a software NIH Image V1.54. The amount of ARD (mol) per C1199 Tiam1 (mol) was calculated. Values represent relative binding abilities averaged from three experiments ± SEM. (D) The amount of C1199 Tiam1 (mol) associated with GST-ARD (mol) was measured in the absence (lane 1) or the presence of the recombinant Tiam1 fragment (lane 2) or C1199 Tiam1 associated with GST-coated beads (lane 3) using SDS-PAGE and Coomassie blue staining followed by densitometric analyses. (E) Coomassie blue staining of C1199 Tiam1 associated with GST-ARD in the absence (lane 1) or the presence of recombinant Tiam1 fragment (lane 2) or C1199 Tiam1 associated with GST-coated beads (lane 3).

et al., 1997; Stam et al., 1997). Using a 49-kD *E. coli*-derived CBP-tagged Tiam1 fragment (i.e., amino acids 393–738 of Tiam1; Fig. 6 B, lane 1) and an in vitro binding assay (Fig. 6 C), we have detected a specific binding inter-

action between the Tiam1 fragment and ankyrin (Fig. 6 C, a) and ARD (Fig. 6 C, b) but not the spectrin binding domain of ankyrin (Fig. 6 C, c) or spectrin (Fig. 6 C, d).

Furthermore, we have evaluated the binding interaction between GST-ARD fusion protein and the recombinant C1199 Tiam1 (NH<sub>2</sub> terminally truncated Tiam1; Fig. 6 D). First, glutathione-Sepharose beads containing GST-ARD were incubated with C1199 Tiam1 in the absence (Fig. 6, D and E, lane 1) or the presence of an excess amount of Tiam1 fragment (Fig. 6, D and E, lane 2). In controls, C1199 Tiam1 was also added to Sepharose beads containing GST alone (Fig. 6, D and E, lane 3). After binding, the GST fusion protein was eluted with its associated C1199 Tiam1 using a buffer containing glutathione. The amount of eluted GST fusion protein and C1199 Tiam1 was determined by SDS-PAGE and Coomassie blue staining (Fig. 6 E) followed by densitometric scanning analyses (Fig. 6 D). Our results indicate that the stoichiometry of ARD–C1199 Tiam1 interaction is ~1:1 (Fig. 6 D, lane 1, and Fig. 6 E, lane 1, a and b). In the presence of an excess amount (~100-fold) of recombinant Tiam1 fragment, the binding between ankyrin ARD and C1199 Tiam1 is significantly reduced (Fig. 6, D and E, lane 2, a and b). The control beads containing GST alone fail to bind C1199 Tiam1 (Fig. 6 D, lane 3, and Fig. 6 E, lane 3, a and b). These observations suggest that ankyrin ARD directly interacts with Tiam1, and that the ankyrin-binding domain (ARD)-containing Tiam1 fragment act as a potent competitive inhibitor of Tiam1 binding to ankyrin in vitro.

Protein sequence analyses show that Tiam1 contains the sequence <sup>717</sup>GEGTDAVKRS<sup>727</sup>L (in mouse), or <sup>717</sup>GEGTEAVKRS<sup>727</sup>L (in human) that shares a great deal of sequence homology with the ankyrin-binding domain of the cell adhesion receptor, CD44 family (Lokeshwar et al., 1994; Zhu and Bourguignon, 1998). To test whether the sequence GEGTDAVKRS<sup>727</sup>L of Tiam1 protein is in fact involved in ankyrin binding, we have examined the ability of an 11-amino acid synthetic peptide, identical to GEGTDAVKRS<sup>727</sup>L, to bind various cytoskeletal proteins. As shown in Table I, this synthetic peptide binds specifically to intact ankyrin and the ARD, but not the SBD of ankyrin or other cytoskeletal proteins such as spectrin. Control peptides, containing the scrambled sequence (GRATLEGSDKV) with the same amino acid composition as that of the synthetic peptide or another peptide (GTIKRAPFLGP) from a different region (i.e., the sequence between amino acids 399 and 409) of Tiam1, fail to bind any cytoskeletal proteins tested (Table I).

We have also used the synthetic peptide corresponding to Tiam1's amino acid 717–727 sequence to compete for the binding of purified Tiam1 to ankyrin. As shown in Fig. 7 A (c), the synthetic peptide competes effectively with Tiam1 to bind ankyrin with an apparent inhibition constant (*K<sub>i</sub>*) ~0.5 nM. However, control peptides such as GRATLEGSDKV (Fig. 7 A, a) or GTIKRAPFLGP (Fig. 7 A, b) do not compete at all with Tiam1 in ankyrin binding. These results suggest that the amino acid 717–727 sequence of Tiam1 is a critical part of the ankyrin-binding domain of Tiam1. Finally, we have constructed an HA-tagged C1199 Tiam1 deletion mutant lacking the ankyrin binding sequence, amino acids 717–727 (designated as C1199 Tiam1Δ717-727; Fig. 7 B, b). The truncated C1199

Table 1. Binding of  $^{125}$ I-Labeled Cytoskeletal Proteins to Synthetic Peptides

	nM $\times$ CPM Bound
Binding to GEGTDAVKRSL (the sequence between amino acids 717 and 727 of Tiam1)	
$^{125}$ I-Labeled ankyrin	15,260 $\pm$ 120
$^{125}$ I-Labeled ARD	14,560 $\pm$ 105
$^{125}$ I-Labeled ankyrin's spectrin binding domain	770 $\pm$ 22
$^{125}$ I-Labeled spectrin	850 $\pm$ 34
Binding to GRATLEGSDKV (the scrambled sequence)	
$^{125}$ I-Labeled ankyrin	1,020 $\pm$ 36
$^{125}$ I-Labeled ARD	920 $\pm$ 29
$^{125}$ I-Labeled ankyrin's spectrin binding domain	901 $\pm$ 24
$^{125}$ I-Labeled spectrin	996 $\pm$ 27
Binding to GTIKRAPFLGP (the sequence between amino acids 399 and 409 of Tiam1)	
$^{125}$ I-Labeled ankyrin	899 $\pm$ 23
$^{125}$ I-Labeled ARD	854 $\pm$ 17
$^{125}$ I-Labeled ankyrin's spectrin binding domain	842 $\pm$ 19
$^{125}$ I-Labeled spectrin	863 $\pm$ 20

$^{125}$ I-labeled cytoskeletal proteins (e.g., intact ankyrin [100 ng] or ARD [100 ng] or spectrin binding domain of ankyrin [100 ng] or spectrin [100 ng] were incubated with nitrocellulose discs coated with either the synthetic peptide GEGTDAVKRSL (corresponding to the sequence between amino acids 717 and 727 of Tiam1), or the scrambled peptide GRATLEGSDKV, or another Tiam1-related peptide, GTIKRAPFLGP (corresponding to the sequence between amino acids 399 and 409 of Tiam1) at 4°C for 4 h as described in Materials and Methods. As a control, the radiolabeled ligands including  $^{125}$ I-labeled ankyrin,  $^{125}$ I-labeled ARD, and  $^{125}$ I-labeled spectrin were also incubated with uncoated beads to determine the binding observed because of the nonspecific binding of various ligands. Nonspecific binding, which represented ~20% of the total binding, was always subtracted from the total binding.

Tiam1 717-727 cDNA (Fig. 7 B, b) and the wild-type C1199 Tiam1 (Fig. 7 B, a) were transiently transfected into SP-1 cells. Our results indicate that both the C1199 Tiam1 $\Delta$ 717-727 mutant (Fig. 7 C, lane 3) and the wild-type C1199 Tiam1 (Fig. 7 C, lane 2) are expressed as a 160-kD polypeptide in SP-1 transfectants using anti-HA-mediated immunoblotting. No protein band was detected in vector-transfected SP-1 cells (Fig. 7 C, lane 1). In vitro binding data reveal that there is a strong binding interaction between ankyrin and HA-tagged C1199 (Fig. 7 D, b). In contrast, the HA-tagged C1199 Tiam1 $\Delta$ 717-727 mutant protein isolated from SP-1 transfectants displays a drastic reduction (~90–95% inhibition) in ankyrin-binding ability (Fig. 7 D, c) compared with the HA-tagged wild-type C1199 Tiam1 (Fig. 7 D, b). No ankyrin binding is observed in materials associated with anti-HA beads using cell lysate isolated from vector-transfected cells (Fig. 7 D, a). These findings suggest that the amino acid 717–727 region is critical for the interaction of Tiam1 with ankyrin.

Most importantly, we have found that the binding of ankyrin (e.g., erythrocyte ankyrin [ANK1], Fig. 8 A, or ANK3's ARD, Fig. 8 B) to Tiam1 significantly increases the GDP/GTP exchange activity of Rac1 GTPase as compared with untreated Tiam1-mediated Rac1 activation (Fig. 8 C). The SBD of ankyrin or other cytoskeletal proteins, such as spectrin, fails to stimulate Tiam1-mediated

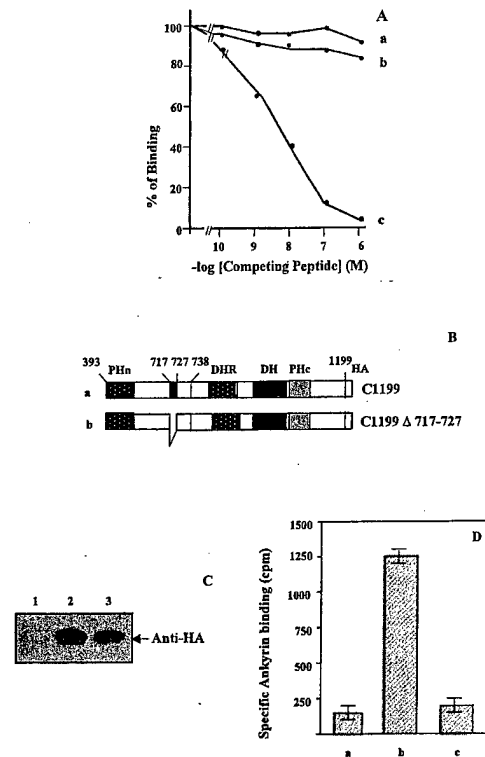
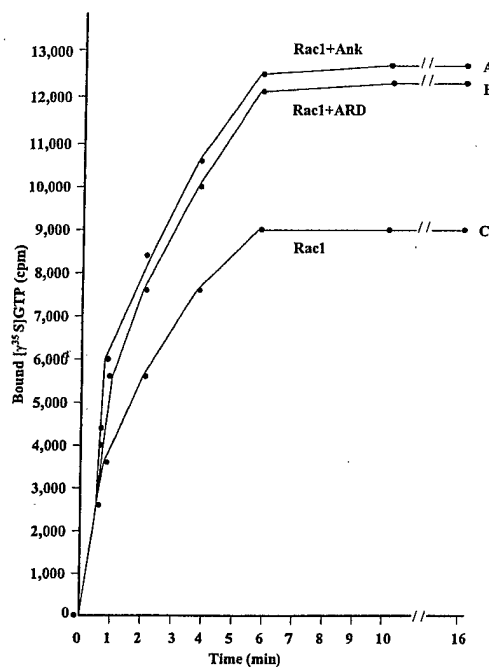


Figure 7. Identification of the ankyrin binding domain of Tiam1. (A)  $^{125}$ I-labeled Tiam1 was incubated with ankyrin-coated beads in the presence of various concentrations of unlabeled synthetic peptide (GEGTDAVKRSL, corresponding to the sequence between amino acids 17 and 727 of Tiam1) (c), or the scrambled sequence (GRATLEGSDKV; a), or another Tiam1-related peptide (GTIKRAPFLGP, corresponding to the sequence between amino acids 399 and 409 of Tiam1; b) as described in Materials and Methods. The specific binding observed in the absence of any of the competing peptides is designated as 100%. The results represent an average of duplicate determinations for each concentration of the competing peptide used. (B) Schematic illustration of the in vitro mutagenesis approach used in this study. Both C1199 Tiam1 (a) and C1199 Tiam1 717-727 (lacking the sequence between amino acids 17 and 727; b) were constructed according to the strategy described in Materials and Methods. (C) Anti-HA-mediated immunoblot of SP-1 cells transiently transfected with vector alone (lane 1), or HA-tagged C1199 Tiam1 cDNA (lane 2), or HA-tagged C1199 Tiam1 717-727 cDNA (lane 3). (D) The amount of  $^{125}$ I-ankyrin binding to anti-HA-mediated immunoprecipitates isolated from SP-1 cells transfected with vector alone (a), or HA-tagged C1199 Tiam1 cDNA (b), or HA-tagged C1199 Tiam1 717-727 cDNA (c).

GDP/GTP exchange on Rac1 GTPase (data not shown). Therefore, we believe that ankyrin binding to Tiam 1 plays a pivotal role in the upregulation of Tiam 1-mediated GDP/GTP exchange activity of Rho-like GTPases (e.g., Rac1).

#### Effect of Tiam1 or the Tiam1 Fragment on Rac1 Activation, Tumor Cell Invasion, and Migration

Previous studies have indicated that both ankyrin and Tiam1 are closely associated with certain tumor-specific behaviors, characterized by an invadopodia structure (or membranous projections) during epithelial tumor cell mi-



**Figure 8.** Stimulation of Tiam1-catalyzed GDP/GTP exchange activity by ankyrin. Purified *E. coli*-derived GST-tagged GTPases (e.g., Rac1, Cdc42, or RhoA) was preloaded with GDP. Subsequently, 2 pmol of Tiam1 (isolated from untransfected or transfected cells according to the procedures described above) was preincubated with no ankyrin or ankyrin (e.g., intact ankyrin or ARD; 1  $\mu$ g/ml), followed by adding to the reaction buffer containing 20 mM Tris-HCl, pH 8.0, 100 mM NaCl, 10 mM MgCl<sub>2</sub>, 100  $\mu$ M AMP-PNP, 0.5 mg/ml BSA, and 2.5  $\mu$ M GTP- $\gamma$ -<sup>35</sup>S (~1,250 Ci/mmol). Subsequently, 2.5 pmol of GDP-loaded GST-tagged Rho GTPases (e.g., Rac1, Rac1, or Cdc42) was mixed with the reaction buffer containing Tiam1 and GTP- $\gamma$ -<sup>35</sup>S to initiate the exchange reaction at room temperature. At various time points, the reaction of each sample was terminated by adding ice-cold termination buffer containing 20 mM Tris-HCl, pH 8.0, 100 mM NaCl, and 10 mM MgCl<sub>2</sub> as described in Materials and Methods. The termination reactions were filtered immediately through nitrocellulose filters, and the radioactivity associated with the filters was measured by scintillation fluid. The amount of GTP- $\gamma$ -<sup>35</sup>S bound to Tiam1 or control sample (preimmune serum-conjugated Sepharose beads) in the absence of Rho GTPases (e.g., Rac1, Cdc42, or RhoA) was subtracted from the original values. Data represent an average of triplicates from three to five experiments. SD < 5%. (A–C) Kinetics of GTP- $\gamma$ -<sup>35</sup>S bound to GDP-loaded GST-Rac1 by Tiam1 (isolated from SP-1 cells) in the absence (C) or in the presence of ankyrin, e.g., intact erythrocyte ankyrin (ANK1; A) or ARD fragment (B).

gration (Bourguignon et al., 1998a,b, 2000; Zhu and Bourguignon, 2000). In this study, using double immunolabeling staining, we have observed that both ankyrin (Fig. 10 A) and Tiam1 (Fig. 10 B) are colocalized in the plasma membrane and long projections of SP1 cells (Fig. 10 C). Furthermore, we have transiently transfected breast tumor cells (e.g., SP-1 cells) with HA-tagged NH<sub>2</sub> terminally truncated C1199 Tiam1 cDNA. Our results show that the C1199 Tiam1 is expressed as a 160-kD protein (Fig. 9 B, a) detected by anti-HA-mediated immunoblot in SP1 cells. No protein band was detected in vector-transfected SP1 cells by anti-HA-mediated immunoblotting (Fig. 9 A, a).

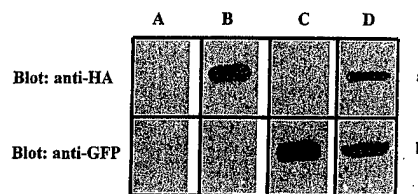


**Figure 9.** Transfection of SP1 cells with HA-tagged C1199 Tiam1 cDNA (A) or GFP-tagged Tiam1 fragment cDNA (B) or cotransfection of HA-tagged C1199 Tiam1 cDNA and GFP-tagged Tiam1 fragment cDNA (C). Detection of C1199 Tiam1 expression by anti-HA-mediated immunoblot in HA-tagged C1199 Tiam1 cDNA-transfected cells (B, a) or in vector-transfected cells (A, a). Detection of Tiam1 fragment expression by anti-GFP-mediated immunoblot in GFP-tagged Tiam1 fragment cDNA-transfected cells (C, b) or vector-transfected cells (A, b). Detection of coexpression of C1199 Tiam1 and Tiam1 fragment by immunoblotting of cells (cotransfected with HA-tagged C1199 Tiam1 cDNA and GFP-tagged Tiam1 fragment cDNA) with anti-HA antibody (D, a) and anti-GFP antibody (D, b), respectively. In controls, no signal was detected in HA-tagged C1199 Tiam1 cDNA-transfected cells or GFP-tagged Tiam1 fragment cDNA-transfected cells using anti-GFP (B, b) or anti-HA (C, a)-mediated immunoblotting, respectively.

Double immunofluorescence staining data show that ankyrin (Fig. 10 D) and C1199 Tiam1 (Fig. 10 E) are also colocalized on the plasma membrane-related long projections of these C1199 Tiam1 cDNA-transfected cells (Fig. 10 F). Furthermore, we have demonstrated that transfection of SP1 cells with C1199 Tiam1 cDNA stimulates ankyrin-associated Tiam1-catalyzed GDP/GTP exchange on Rac1 (Fig. 11 a), and induces a significant amount of increase in breast tumor cell invasion (Table II, A) and migration (Table II, B) as compared with vector-transfected SP1 transfectants (Fig. 11 b and Table II, A and B). These results are consistent with previous findings indicating that transfection of NIH3T3 cells with the NH<sub>2</sub> terminally truncated C1199 Tiam1 cDNA confers potent oncogenic properties (Van Leeuwen et al., 1995).

Treatment of SP1 cells (e.g., untransfected or transfected cells) with certain agents (e.g., cytochalasin D, a microfilament inhibitor) causes a remarkable inhibition of tumor cell invasion (Table II A) and migration (Table II B). Tiam1-Rac1 signaling initiates oncogenic cascades including c-Jun kinase (JNK) activation, which triggers gene transcription through c-jun and promotes cell transformation (Michiels et al., 1995, 1997). In addition, Tiam1-activated Rac1 stimulates the novel family of serine/threonine kinases, p-21 activated kinases (Manser et al., 1994; Knaus et al., 1995; Bagrodia and Cerione, 1999), which mediates actin assembly and induce the formation of membrane ruffling and lamellipodia (membrane projections). In fact, cytoskeleton-associated membrane projections are often tightly linked to matrix degrading enzymes during breast tumor cell invasion and migration (Bourguignon et al., 1998b). These findings suggest that Tiam1-Rac1 signaling and selective effector(s) play an important role in promoting certain gene expression required for cellular transformation and the upregulation of cytoskeletal changes needed for tumor cell invasion and migration. Identifica-

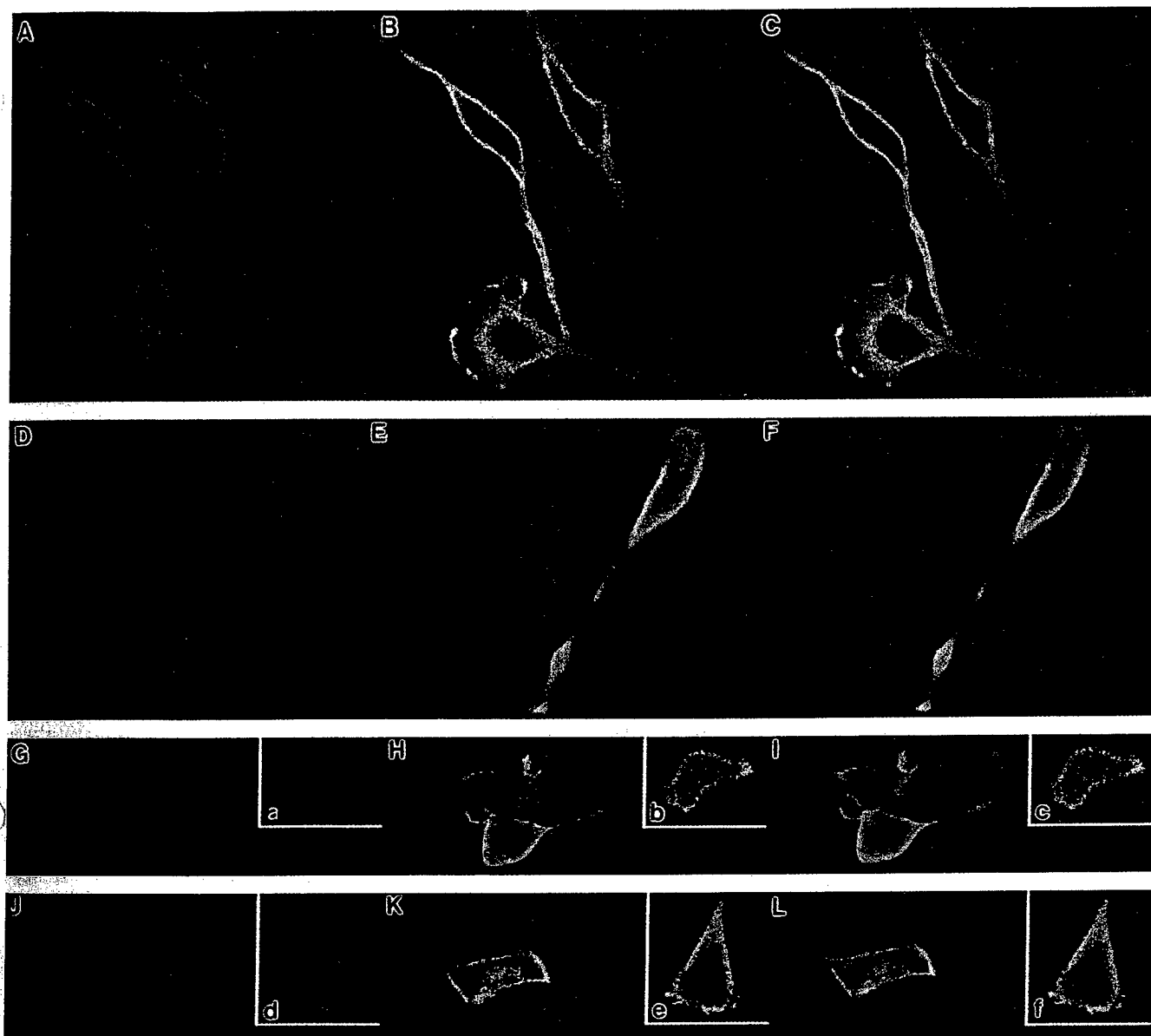


**Figure 10.** Double immunofluorescence staining of ankyrin and Tiam1 in untransfected SP1 cells or SP1 transfectants. SP1 cells (untransfected or transfected with HA-tagged C1199 Tiam1 cDNA or GFP-tagged Tiam1 fragment cDNA or cotransfected with HA-tagged C1199 Tiam1 cDNA plus GFP-tagged Tiam1 fragment cDNA) were fixed by 2% paraformaldehyde. Subsequently, cells were rendered permeable by ethanol treatment and stained with various immunoreagents as described in Materials and Methods. (A–C) Rh-labeled anti-ANK3 staining (A) FITC-anti-Tiam1 staining (B) and colocalization of ankyrin and Tiam1 (C) in untransfected SP1 cells. (D–F) Rh-labeled anti-ANK3 staining (D) FITC-anti-HA-labeled C1199 Tiam1 staining (E), and colocalization of ankyrin and C1199 Tiam1 (F) in HA-tagged C1199 Tiam1 cDNA-transfected SP1 cells. (G–I) Rh-labeled anti-ANK3 staining (G), GFP-tagged Tiam1 fragment (H), and colocalization of ankyrin and Tiam1 fragment (I) in GFP-tagged Tiam1 fragment cDNA-transfected SP1 cells. (a–c) Rh-labeled normal mouse IgG staining (a), GFP-tagged Tiam1 fragment (b), and colocalization of normal mouse IgG and Tiam1 fragment (c) in GFP-tagged Tiam1 fragment cDNA-transfected SP1 cells. (J–L) Rh-labeled anti-HA staining of C1199 Tiam1 (J), GFP-tagged Tiam1 fragment (K), and colocalization of C1199 and Tiam1 fragment (L) in SP1 cells cotransfected with HA-tagged C1199 cDNA and GFP-tagged Tiam1 fragment cDNA. (d–f) Rh-labeled anti-ANK3 staining (d), GFP-tagged Tiam1 fragment (e), and colocalization of ankyrin and Tiam1 fragment (f) in SP1 cells cotransfected with HA-tagged C1199 cDNA and GFP-tagged Tiam1 fragment cDNA.

tion of immediate downstream targets for ankyrin-mediated Tiam1-Rac1 signaling is currently under investigation in our laboratory.

We have also found that SP1 cells transfected with GFP-tagged Tiam1 fragment cDNA express a 68-kD protein as detected by anti-GFP antibody (Fig. 6 B, lane 2; Fig. 9 C, b). In vector-transfected SP1 cells, we are not able to de-

tect any protein band by anti-GFP-mediated immunoblotting (Fig. 9 A, b). Double immunofluorescence staining shows that both ankyrin (Fig. 10 G) and the GFP-tagged Tiam1 fragment (Fig. 10 H) are colocalized in the cell membranes in SP1 transfectants (Fig. 10 I). We believe that the ankyrin staining detected in these SP1 transfectants, revealed by antiankyrin-mediated immunostaining,

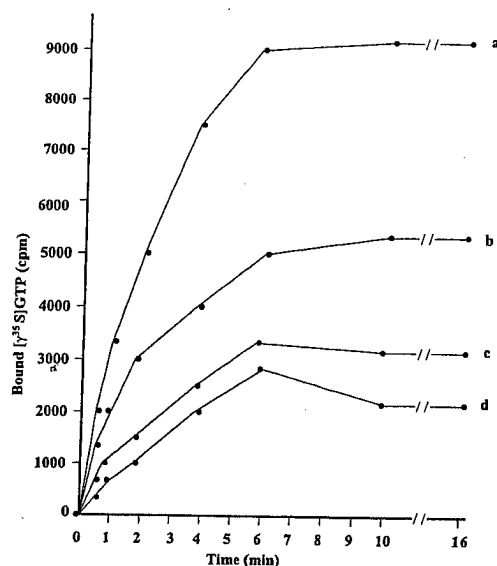


**Figure 11.** Kinetics of GTP- $\gamma$ - $^{35}$ S bound to GDP-loaded GST-Rac1 in the presence of ankyrin-associated Tiam1 isolated from SP-1 cells: transfected with HA-tagged C1199 Tiam1 cDNA (a) or GFP-tagged Tiam1 fragment cDNA (d); or cotransfected with HA-tagged C1199 Tiam1 cDNA plus GFP-tagged Tiam1 fragment cDNA (c) or vector alone (b). Purified *E. coli*-derived GST-tagged GTPases (e.g., Rac1, Cdc42, or RhoA) were preloaded with GDP. First, 2 pmol ankyrin-associated Tiam1 isolated from various SP1 transfectants was added to the reaction buffer containing 20 mM Tris-HCl, pH 8.0, 100 mM NaCl, 10 mM MgCl<sub>2</sub>, 100  $\mu$ M AMP-PNP, 0.5 mg/ml BSA, and 2.5  $\mu$ M GTP- $\gamma$ - $^{35}$ S (~1,250, Ci/mmol). Subsequently, 2.5 pmol GDP-loaded GST-tagged Rho GTPases (e.g., Rac1, RhoA, Cdc42 or GST alone) were mixed with the reaction buffer containing ankyrin-associated Tiam1 and GTP- $\gamma$ - $^{35}$ S to initiate the exchange reaction at room temperature. At various time points, the reaction of each sample was terminated by adding ice-cold termination buffer as described in Materials and Methods. The termination reactions were filtered immediately through nitrocellulose filters, and the radioactivity associated with the filters were measured by scintillation fluid. The amount of GTP- $\gamma$ - $^{35}$ S bound to Tiam1 or control sample (preimmune serum-conjugated Sepharose beads) in the absence of Rho GTPases (e.g., Rac1, Cdc42, or RhoA) was subtracted from the original values. Data represent an average of triplicates from three to five experiments. SD < 5%.

is specific since no label (Fig. 10 a) is detected in these GFP-Tiam1 fragment-overexpressed cells (Fig. 10 b) using normal mouse IgG (Fig. 10 a). No colocalization (Fig. 10 c) of normal mouse IgG (Fig. 10 a) and GFP-Tiam1 fragment (Fig. 10 b) is observed in these transfectants. Moreover, we have demonstrated that overexpression of the GFP-tagged Tiam1 fragment in SP1 transfectants downregulates ankyrin-associated Tiam1-Rac1 signaling (Fig. 10 d), tumor cell invasion (Table II, A), as well as cell migration (Table II, B).

Finally, cotransfection of SP1 cells with HA-tagged C1199 Tiam1 cDNA and GFP-tagged Tiam1 fragment cDNA was carried out. Using anti-HA or anti GFP-mediated immunoblotting technique, we have detected coexpression of both C1199 Tiam1 (Fig. 9 D, a) and Tiam1 fragment (Fig. 9 D, b) in SP1 transfectants. In controls, no signal was detected in HA-tagged C1199 Tiam1 cDNA-transfected cells or GFP-tagged Tiam1 fragment cDNA-

**Table II. Measurement of Tumor Cell Invasion and Migration**

Cells	Cell invasion* Percent control†	
	DMSO-treated	Cytochalasin D-treated
<b>In vitro cell invasion</b>		
Untransfected cells (control)	100	22
Vector-transfected cells	96	24
Tiam1 fragment	95	20
cDNA-transfected cell		
C1199 Tiam1	155	50
cDNA-transfected cells		
C1199 Tiam1 cDNA and Tiam1 fragment cDNA-cotransfected cells	90	17
<b>In vitro cell migration</b>		
Untransfected cells (control)	100	20
Vector-transfected cells	98	23
Tiam1 fragment	93	22
cDNA-transfected cell		
C1199 Tiam1	158	55
cDNA-transfected cells		
C1199 Tiam1 cDNA and Tiam1 fragment cDNA-cotransfected cells	88	14

\*SP1 cells (~10<sup>4</sup> cells/well in PBS, pH 7.2), in the presence or absence of 20  $\mu$ M/ml cytochalasin D (dissolved in DMSO) or DMSO alone, were placed in the upper chamber of the transwell unit. In some cases, SP1 cells were transfected with either HA-tagged C1199 Tiam1 cDNA or GFP-tagged Tiam1 fragment cDNA or HA-tagged C1199 Tiam1 cDNA plus GFP-tagged Tiam1 fragment cDNA or vector alone. After an 18-h incubation at 37°C in a humidified 95% air/5% CO<sub>2</sub> atmosphere, cells on the upper side of the filter were removed by wiping with a cotton swap. Cell migration processes were determined by measuring the cells that migrate to the lower side of the polycarbonate filters containing serum by standard cell number counting assays as described in Materials and Methods. Each assay was set up in triplicate and repeated at least three times. All data were analyzed statistically by *t* test and statistical significance was set at *P* < 0.01. In these experiments ~30–40% of input cells (~10<sup>4</sup> cells/well) undergo in vitro cell invasion and migration in the control samples.

†The values expressed in this table represent an average of triplicate determinations of three to five experiments with an SD less than  $\pm$  5%.

transfected cells using anti-GFP (Fig. 9 B, b) or anti-HA (Fig. 9 C, a)-mediated immunoblotting, respectively. Furthermore, immunocytochemical staining results show that ankyrin (Fig. 10 d) and the GFP-tagged Tiam1 fragment (Fig. 10 e) are colocalized (Fig. 10 f) in the plasma membranes of SP1 transfectants. In contrast, C1199 Tiam1 (Fig. 10 J) fails to display plasma membrane localization. Consequently, the level of colocalization (Fig. 10 L) between C1199 Tiam1 (Fig. 10 J) and Tiam1 fragment (Fig. 10 K) is greatly reduced. In addition, it is noted that no significant stimulation of long membrane projections was observed in these transfectants (Fig. 10, J–L and d–f). Other tumor-specific behaviors such as Tiam1-Rac1 activation (Fig. 11 c) and cytoskeleton-mediated breast tumor cell invasion (Table II, A) and migration (Table II B) are also greatly inhibited. These findings suggest that the ankyrin-binding domain-containing Tiam1 fragment acts as a dominant negative mutant that effectively competes for ankyrin binding to C1199 Tiam1 in vivo and blocks ankyrin-regulated Tiam1 function associated with tumor-specific phenotypes.

## Discussion

The invasive phenotype of breast tumors, determined by

characteristics such as tumor cell motility and membrane perturbations, is clearly linked to cytoskeletal function. For example, recent studies have shown that certain metastasis-specific molecules (e.g., CD44 $v_{3,8-10}$  isoform [Bourguignon et al., 1998b, 1999] and its associated matrix metalloproteinase, MMP-9 [Bourguignon et al., 1998b; Yu and Stamenkovic, 1999], as well as Rho kinase [Bourguignon et al., 1999]) are closely associated with the cytoskeleton during tumor cell function. To further examine the regulatory mechanism(s) involved in cytoskeleton-mediated oncogenic signaling leading to tumor cell invasion and migration, we have focused on GEFs (the Dbl or DH family), such as Tiam1, which are known to display oncogenic capability and function as upstream activators of Rho-like GTPases (e.g., Rac1 or Cdc42; Woods et al., 1991; Habets et al., 1994; Michiels et al., 1995; Nobes and Hall, 1995; Van Leeuwen et al., 1995). In breast tumor cells, such as SP-1 cells, Tiam1 is detected as a 200-kD protein (Fig. 1), which is similar to the Tiam1 described in other cell types (Woods and Bryant, 1991; Michiels et al., 1995; Nobes and Hall, 1995; Van Leeuwen et al., 1995, 1997; Hordijk et al., 1997; Stam et al., 1997; Bourguignon et al., 2000). Tiam1, isolated from SP-1 cells, is also capable of carrying out GDP/GTP exchange for Rac1 in vitro (Fig. 2). Sequence analysis of Tiam1 suggests that its association with the invasive and metastatic phenotype is mediated via membrane-linked cytoskeletal regulation and/or activation of Rho family GTPases (Habets et al., 1994; Nobes and Hall, 1995).

Rac1 acts downstream of Tiam1 signaling and regulates the function of several cell adhesion molecules such as the laminin receptor,  $\alpha 6 \beta 1$  integrin (Van Leeuwen et al., 1997), E-cadherin (Hordijk et al., 1997), and the hyaluronan receptor, CD44 (Bourguignon et al., 2000). Tiam1-Rac1 activation also has been shown to be stimulated by certain serum-derived growth activators (e.g., S1P and LPA) during T-lymphoma cell invasion (Stam et al., 1998). However, in epithelial MDCK cells, Tiam1-Rac1 signaling plays an invasion/suppressor role in Ras-transformed MDCK cells (Hordijk et al., 1997). Apparently, various responses by Tiam1-catalyzed Rac1 signaling may be controlled by selective upstream activators (e.g., availability of certain cytoskeletal proteins [e.g., ankyrin], cell adhesion receptors [e.g., CD44, integrin or E-cadherin], growth activators [e.g., serum, S1P, or LPA] or extracellular matrix components [hyaluronic acid, collagen, or fibronectin, etc.]). Moreover, Tiam1 is found to be involved in promoting both Rac1- and RhoA-mediated pathways during neurite formation in nerve cells (Van Leeuwen et al., 1997). The balance between Rac1 and RhoA determines a particular cellular morphology and migratory behavior (Sander et al., 1999).

Ankyrin is a family of membrane-associated cytoskeletal proteins expressed in a variety of biological systems including epithelial cells and tissues (Peters and Lux, 1993). Presently, at least three ankyrin genes have been identified: *ankyrin 1* (Ank 1 or *ankyrin R*), *ankyrin 2* (Ank 2 or *ankyrin B*), and *ankyrin 3* (Ank 3 or *ankyrin G*; Lux et al., 1990; Otto et al., 1991; Kordeli et al., 1995; Peters et al., 1995). These molecules belong to a family of related genes that probably arose by duplication and divergence of a common ancestral gene. Ankyrin is known to bind to a

number of plasma membrane-associated proteins including the following: band 3, two other members of the anion exchange gene family (Bennet, 1992), Na<sup>+</sup>/K<sup>+</sup>-ATPase (Nelson and Veshnock, 1987; Zhang et al., 1998), the amiloride-sensitive Na<sup>+</sup> channel (Smith et al., 1991), the voltage-dependent Na<sup>+</sup> channel (Kordeli et al., 1995), Ca<sup>2+</sup> channels (Bourguignon et al., 1993b, 1995a; Bourguignon and Jin, 1995) and the adhesion molecule CD44 (Bourguignon et al., 1986, 1991, 1992, 1993a; Kalomiris and Bourguignon, 1988, 1989; Lokeshwar and Bourguignon, 1991, 1992; Lokeshwar et al., 1994, 1996). It has been suggested that the binding of ankyrin to certain membrane-associated molecules is necessary for signal transduction, cell adhesion, membrane transport, cell growth, migration, and tumor metastasis (Bennet, 1992; Bourguignon et al., 1995b, 1996, 1997, 1998a; De Matteis and Morrow, 1998; Zhu and Bourguignon, 1998, 2000).

In this study, we have presented new evidence showing the interaction between ankyrin and Tiam1. Specifically, we have demonstrated that Tiam1 and ankyrin (e.g., ANK1 and ANK3) are physically linked to each other as a complex in vivo (Figs. 3 and 10) and in vitro (Figs. 5–7), and that ankyrin binding to Tiam1 promotes Rac1 activation (Figs. 8 and 11). Using purified Tiam1 and GST-tagged ankyrin repeat domain (GST-ARD; Fig. 5) to examine the interaction between Tiam1 and ankyrin in vitro, we have found that ARD is directly involved in the binding of Tiam1 (Fig. 5, C and D, and Fig. 6, C–E). In fact, the binding affinity of ARD to Tiam1 is very comparable to that of intact erythrocyte ankyrin binding to Tiam1 (Fig. 5, C and D). These findings support the conclusion that the ARD fragment of ankyrin is directly involved in the recognition of Tiam1. The 24 ankyrin repeats within the ARD are known to form binding sites for at least seven distinct membrane protein families (Michaely and Bennett, 1995). Often, ARD is organized into four folding subdomains: subdomain 1 (S1), subdomain 2 (S2), subdomain 3 (S3), and subdomain 4 (S4). Recently, we have shown that the S2 subdomain, but not the other subdomains, of ARD binds to the adhesion molecule CD44 directly (Zhu and Bourguignon, 2000). Overexpression of subdomain (S2) of ARD promotes CD44-mediated tumor cell migration (Zhu and Bourguignon, 2000). The question of which ARD subdomain fragment(s) is (are) involved in regulating Tiam1 function remains to be determined.

The structural homology between the ankyrin binding domain of Tiam1 (the sequence between amino acids 717 and 727) and CD44 is quite striking (Lokeshwar et al., 1994). The cytoplasmic domain of CD44 (~70 amino acids long) is highly conserved ( $\geq 90\%$ ) in most of the CD44 isoforms; and it is clearly involved in specific ankyrin binding (Lokeshwar et al., 1994; Zhu and Bourguignon, 1998). The ankyrin-binding domain of CD44 has also been mapped using deletion mutation analyses and mammalian expression systems (Lokeshwar et al., 1994; Zhu and Bourguignon, 1998). In particular, the ankyrin-binding domain (e.g., NGGNGTVEDRKPSSEL between amino acids 306 and 320 in the mouse CD44 [Lokeshwar et al., 1994] and NSGNGAVEDRKPSGL amino acids 304 and 318 in human CD44 [Zhu and Bourguignon, 1998]) is required for cell adhesion (Lokeshwar et al., 1994; Zhu and Bourguignon, 1998), the recruitment of Src kinase (Zhu and

Bourguignon, 1998), and the onset of tumor cell transformation (Bourguignon et al., 1998b; Zhu and Bourguignon, 1998). The facts that (1) the recombinant C1199 Tiam1 interacts with ARD fusion protein directly with a stoichiometry of 1:1 (Fig. 6, D and E); (2) a peptide with the sequence <sup>717</sup>GEGTDAVKRS<sup>727</sup>L of Tiam1 binds to ankyrin and ARD but not ankyrin's spectrin binding domain or spectrin (Table I); (3) a Tiam1 peptide (amino acids 717–727) competes with Tiam1 for the binding to ankyrin (Fig. 7 A); (4) the Tiam1 deletion mutant protein (e.g., C1199 Tiam1Δ717–727; Fig. 7 B) fails to bind ankyrin (Fig. 7 D); and (5) ankyrin stimulates Tiam1-catalyzed GDP/GTP exchange activity on Rac1 (Fig. 8) strongly suggest that the sequence (<sup>717</sup>GEGTDAVKRS<sup>727</sup>L) of Tiam1 is an important region for ankyrin binding.

Furthermore, we have shown that transfection of SP-1 cells with HA-tagged NH<sub>2</sub> terminally truncated C1199 Tiam1 cDNA stimulates ankyrin-associated GDP/GTP exchange on Rac1 (Fig. 11) as well as tumor cell invasion (Table II, A) and migration (Table II, B). These Tiam1-activated oncogenic responses are consistent with previous studies indicating that Tiam1-activated Rho-like GTPases may act as downstream effectors of Ras in both tumorigenesis and progression to metastatic diseases (Habets et al., 1994, 1995; van Leeuwen et al., 1995). The amino acids 393–738 Tiam1 fragment (Fig. 6 C) contains not only the putative ankyrin-binding domain (amino acids 717–727), but also the NH<sub>2</sub>-terminal pleckstrin homology (PHn), the coiled-coil region (CC) and an additional adjacent region (Ex) (also designated as PHn-CC-Ex domain; Michiels et al., 1997). This Tiam1 fragment has been shown to be responsible for Tiam1's membrane localization, Rac1-dependent membrane ruffling, and C-Jun NH<sub>2</sub>-terminal kinase activation in fibroblasts and COS cells (Michiels et al., 1997; Stam et al., 1997). In this study, we have found that cotransfection of SP1 cells with Tiam1 fragment cDNA and C1199 Tiam1 cDNA effectively blocks tumor cell-specific behaviors (e.g., C1199 Tiam1 association with ankyrin in the cell membrane [Fig. 10], Rac1 activation [Fig. 11], tumor cell invasion [Table II, A], and migration [Table II B]). These findings further support our conclusion that the ankyrin-binding domain-containing Tiam1 fragment acts as a potent competitive inhibitor, which is capable of interfering with C1199 Tiam1–ankyrin interaction *in vivo*. Recently, we have also demonstrated that the Tiam1 fragment is required for CD44 (the hyaluronan receptor) binding (Bourguignon et al., 2000). Most importantly, Tiam1–CD44 interaction promotes Rac1 activation and hyaluronic acid-mediated breast tumor cell migration (Bourguignon et al., 2000). These observations clearly suggest that the amino acids 393–738 of Tiam1 contains multiple functional domains (e.g., membrane localization site(s) and cytoskeleton binding domains) required for the regulation of Tiam1–Rac1 signaling and cytoskeleton function. Taken together, we believe that ankyrin–Tiam1 interaction plays a pivotal role in regulating Rac1-activated oncogenic signaling and cytoskeleton-mediated metastatic breast tumor cell progression.

We gratefully acknowledge Dr. Gerard J. Bourguignon's assistance in the preparation of this paper. We would also like to thank Dr. Dan Zhu's help in preparing ARD cDNA construct and illustrations as well as reviewing the manuscript.

This work was supported by United States Public Health grants (CA66163 and CA 78633) and DOD grants (DAMD 17-94-J-4121, DAMD 17-97-1-7014, and DAMD 17-99-1-9291) and Sylvester Cancer Center.

Submitted: 5 October 1999

Revised: 31 May 2000

Accepted: 1 June 2000

## References

- Bagrodia, S., and R.A. Cerione. 1999. PAK to the future. *Trends Cell Biol.* 9:350–355.
- Bennett, V. 1992. Ankyrins. *J. Biol. Chem.* 267:8703–8706.
- Bennett, V., and D.M. Gilligan. 1993. The spectrin-based membrane skeleton and micro-scale organization of the plasma membrane. *Annu. Rev. Cell Biol.* 9:27–66.
- Bourguignon, L.Y.W. 1996. Interaction between membrane-cytoskeleton and CD44 during lymphocyte signal transduction and cell adhesion. *Curr. Top. Membr.* 43:293–312.
- Bourguignon, L.Y.W., and H. Jin. 1995. Identification of the ankyrin-binding domain of the mouse T-lymphoma cell inositol 1,4,5-triphosphate (IP<sub>3</sub>) receptor and its role in the regulation of IP<sub>3</sub>-mediated internal Ca<sup>2+</sup> release. *J. Biol. Chem.* 270:7257–7260.
- Bourguignon, L.Y.W., G. Walker, S. Suchard, and K. Balazovich. 1986. A lymphoma plasma membrane-associated protein with ankyrin-like properties. *J. Cell Biol.* 102:2115–2124.
- Bourguignon, L.Y.W., E. Kalomiris, and V.B. Lokeshwar. 1991. Acylation of the lymphoma transmembrane glycoprotein, GP85, may be required for GP85–ankyrin interaction. *J. Biol. Chem.* 266:11761–11765.
- Bourguignon, L.Y.W., V.B. Lokeshwar, J. He, X. Chen, and G.J. Bourguignon. 1992. A CD44-like endothelial cell transmembrane glycoprotein (GP116) interacts with extracellular matrix and ankyrin. *Mol. Cell. Biol.* 12:4464–4471.
- Bourguignon, L.Y.W., V.B. Lokeshwar, X. Chen, and W.G.L. Kerrick. 1993a. Hyaluronic acid-induced lymphocyte signal transduction and HA receptor (GP85/CD44)–cytoskeleton interaction. *J. Immunol.* 151:6634–6644.
- Bourguignon, L.Y.W., H. Jin, N. Iida, N. Brandt, and S.H. Zhang. 1993b. The involvement of ankyrin in the regulation of inositol 1,4,5-triphosphate receptor-mediated internal Ca<sup>2+</sup> release from Ca<sup>2+</sup> storage vesicles in mouse T-lymphoma cells. *J. Biol. Chem.* 268:7290–7297.
- Bourguignon, L.Y.W., A. Chu, H. Jin, and N.R. Brandt. 1995a. Ryanodine receptor–ankyrin interaction regulates internal Ca<sup>2+</sup> release in mouse T-lymphoma cells. *J. Biol. Chem.* 270:17917–17922.
- Bourguignon, L.Y.W., N. Iida, C.F. Welsh, D. Zhu, A. Krongrad, and D. Pasquale. 1995b. Involvement of CD44 and its variant isoforms in membrane-cytoskeleton interaction, cell adhesion and tumor metastasis. *J. Neuro. Oncol.* 26:201–208.
- Bourguignon, L.Y.W., H. Zhu, A. Chu, N. Iida, L. Zhang, and H.C. Hung. 1997. Interaction between the adhesion receptor, CD44 and the oncogene product, p185<sup>HER2</sup>, promotes human ovarian tumor cell activation. *J. Biol. Chem.* 272:27913–27918.
- Bourguignon, L.Y.W., D. Zhu, and H.B. Zhu. 1998a. CD44 isoform–cytoskeleton interaction in oncogenic signaling and tumor progression. *Front. Biosci.* 3:637–649.
- Bourguignon, L.Y.W., Z. Gunja-Smith, N. Iida, H.B. Zhu, L.J.T. Young, W.J. Muller, and R.D. Cardiff. 1998b. CD44<sub>v3.8-10</sub> is involved in cytoskeleton-mediated tumor cell migration and matrix metalloproteinase (MMP-9) association in metastatic breast cancer cells. *J. Cell Physiol.* 176:206–215.
- Bourguignon, L.Y.W., H.B. Zhu, L. Shao, D. Zhu, and Y.W. Chen. 1999. Rho-kinase (ROK) promotes CD44<sub>v3.8-10</sub>–ankyrin interaction and tumor cell migration in metastatic breast cancer cells. *Cell Motil. Cytoskeleton.* 43:269–287.
- Bourguignon, L.Y.W., H. Zhu, L. Shao, and Y.W. Chen. 2000. CD44 interaction with Tiam1 promotes Rac1 signaling and hyaluronic acid (HA)-mediated breast tumor cell migration. *J. Biol. Chem.* 275:1829–1838.
- Davis, L., and V. Bennett. 1990. Mapping the binding sites of human erythrocyte ankyrin of the anion exchanger and spectrin. *J. Biol. Chem.* 265:10589–10596.
- De Matteis, M.A., and J.S. Morrow. 1998. The role of ankyrin and spectrin in membrane transport and domain formation. *Curr. Opin. Cell Biol.* 10:542–549.
- Dickson, R.B., and M.E. Lippman. 1995. The Molecular Basis of Cancer. J. Mendelsohn, P.M. Howlwy, and M.A. Israel, and L.A. Liotta, editors. W.B. Saunders Company, Philadelphia. 359 pp.
- Elliott, B.E., L. Maxwell, M. Arnold, W.Z. Wei, and E.R. Miller. 1988. Expression of epithelial-like markers and class-I major histocompatibility antigens by a murine carcinoma growing in the mammary gland and in metastasis: orthotopic site effects. *Cancer Res.* 48:7237–7245.
- Habets, G.G.M., E.H.M. Scholtes, D. Zuydgeest, R.A. van der Kammen, J.C. Stam, A. Berns, and J.G. Collard. 1994. Identification of an invasion-inducing gene, Tiam-1, that encodes a protein with homology to GDP-GTP exchangers for Rho-like proteins. *Cell.* 77:537–549.
- Habets, G.G.M., R.A. van der Kammen, J.C. Stam, F. Michiels, and J.G. Collard. 1995. Sequence of the human invasion-inducing Tiam-1 gene, its conservation in evolution and its expression in tumor cell lines of different tissue

- origin. *Oncogene*. 10:1371-1376.
- Hall, A. 1998. Rho GTPase and the actin cytoskeleton. *Science*. 279:509-514.
- Hart, M.J., A. Eva, T. Evans, S.A. Aaronson, and R.A. Cerione. 1991. Catalysis of guanine nucleotide exchange on the CDC42Hs protein by the dbl oncogene product. *Nature*. 354:311-314.
- Hart, M.J., A. Eva, D. Zangrilli, S.A. Aaronson, T. Evans, R.A. Cerione, and Y. Zheng. 1994. Cellular transformation and guanine nucleotide exchange activity are catalyzed by a common domain on the dbl oncogene product. *J. Biol. Chem.* 269:62-65.
- Hordijk, P.L., J.P. ten Klooster, R.A. van der Kammen, F. Michiels, L.C. Oomen, and J.G. Collard. 1997. Inhibition of invasion of epithelial cells by Tiam1-Rac signaling. *Science*. 278:1464-1466.
- Jiang, W.G., M.C.A. Puntis, and M.B. Hallett. 1994. Molecular and cellular basis of cancer invasion and metastasis: implications for treatment. *Br. J. Surg.* 81:1576-1590.
- Kalomiris, E.L., and L.Y.W. Bourguignon. 1988. Mouse T-lymphoma cells contain a transmembrane glycoprotein (GP85) which binds ankyrin. *J. Cell Biol.* 106:319-327.
- Kalomiris, E.L., and L.Y.W. Bourguignon. 1989. Lymphoma protein kinase C is associated with the transmembrane glycoprotein, GP85 and may function in GP85-ankyrin binding. *J. Biol. Chem.* 264:8113-8119.
- Knaus, U.G., S. Morris, H. Dong, J. Chernoff, and G.M. Bokoch. 1995. Regulation of human leukocyte p21-activated kinases through G protein-coupled receptors. *Science*. 269:221-223.
- Kordeli, E., S. Lambert, and V. Bennett. 1995. Ankyrin G, a new ankyrin gene with neural-specific isoforms localized at the axonal initial segment and node of Ranvier. *J. Biol. Chem.* 270:2352-2359.
- Lambert, S., H. Yu, J.T. Prchal, J. Lawler, P. Ruff, D. Speicher, and J. Palek. 1990. cDNA sequence for human erythrocyte ankyrin. *Proc. Natl. Acad. Sci. USA*. 87:1730-1734.
- Lauffenburger, D.A., and A.F. Horwitz. 1996. Cell migration: a physically integrated molecular process. *Cell*. 84:359-369.
- Leemans, M.A., K.M. Ferguson, and J. Schlessinger. 1996. PH domains: diverse sequences with a common fold recruit signaling molecules to the cell surface. *Cell*. 85:621-624.
- Lokeshwar, V.B., and L.Y.W. Bourguignon. 1991. Post-translational protein modification and expression of ankyrin-binding site(s) in GP85 (Pgp-1/CD44) and its biosynthetic precursors during T-lymphoma membrane biosynthesis. *J. Biol. Chem.* 266:17983-17989.
- Lokeshwar, V.B., and L.W.B. Bourguignon. 1992. The lymphoma transmembrane glycoprotein GP85(CD44) is a novel guanine nucleotide-binding protein which regulates GP85(CD44)-ankyrin interaction. *J. Biol. Chem.* 267:22073-22078.
- Lokeshwar, V.B., N. Fregien, and L.Y.W. Bourguignon. 1994. Ankyrin-binding domain of CD44(GP85) is required for the expression of hyaluronic acid-mediated adhesion function. *J. Cell Biol.* 126:1099-1109.
- Lokeshwar, V.B., N. Iida, and L.Y.W. Bourguignon. 1996. The cell adhesion molecule, GPIIb is a new CD44 variant (ex14/v10) involved in hyaluronic acid binding and endothelial cell proliferation. *J. Biol. Chem.* 271:23853-23864.
- Lux, S.E., K.M. John, and V. Bennett. 1990. Analysis of cDNA for human erythrocyte ankyrin indicates a repeated structure with homology to tissue-differentiation and cell cycle control proteins. *Nature*. 344:36-43.
- Manser, E., T. Leung, H. Salihuddin, Z. Zhao, and L. Lim. 1994. A brain serine/threonine protein kinase activated by Cdc42 and Rac1. *Nature*. 367:40-46.
- Merzak, A., S. Koochekpour, and G.J. Pilkington. 1994. CD44 mediates human glioma cell adhesion and invasion in vitro. *Cancer Res.* 54:3988-3992.
- Michael, P., and V. Bennett. 1995. Mechanism for binding site diversity on ankyrin. *J. Biol. Chem.* 270:31298-31302.
- Michiels, F., G.G.M. Habets, J.C. Stan, R.A. van der Kammen, and J.G. Collard. 1995. A role for Rac in Tiam1-induced membrane ruffling and invasion. *Nature*. 375:338-340.
- Michiels, F., J.C. Stam, P.L. Hordijk, R.A. van der Kammen, L. Ruuls-Van Stalle, C.A. Feltkamp, and J.G. Collard. 1997. Regulated membrane localization of Tiam1, mediated by the NH<sub>2</sub>-terminal pleckstrin homology domain, is required for Rac-dependent membrane ruffling and c-Jun NH<sub>2</sub>-terminal kinase activation. *J. Cell Biol.* 137:387-398.
- Nelson, W.J., and P.J. Veshnock. 1987. Ankyrin binding to Na<sup>+</sup>/K<sup>+</sup>-ATPase and implications for the organizations of membrane domains in polarized cells. *Nature*. 328:533-536.
- Nobes, C.D., and A. Hall. 1995. Rho, Rac and Cdc42 GTPases regulate the assembly of multi-molecular focal complexes associated with actin stress fibers, lamellipodia and filopodia. *Cell*. 81:53-62.
- Otto, E., M. Kunimoto, T. McLaughlin, and V. Bennett. 1991. Isolation and characterization of cDNA encoding human brain ankyrins reveal a family of alternatively spliced genes. *J. Cell Biol.* 114:241-253.
- Peters, L.L., and S.E. Lux. 1993. Ankyrins: structure and function in normal cells and hereditary spherocytes. *Semin. Hematol.* 30:85-118.
- Peters, L.L., K.M. John, F.M. Lu, E.M. Eicher, A. Higgins, M. Yialamas, L.C. Turtzo, A.J. Otsuka, and S.E. Lux. 1995. Ank3 (epithelial ankyrin), a widely distributed new member of the ankyrin gene family and the major ankyrin in kidney, is expressed in alternatively spliced forms, including forms that lack the repeat domain. *J. Cell Biol.* 130:313-330.
- Platt, O.S., S.E. Lux, and J.F. Falcone. 1993. A highly conserved region of human erythrocyte ankyrin contains the capacity to bind spectrin. *J. Biol. Chem.* 268:24421-24426.
- Pontings, C.P., and C. Phillips. 1995. DHR domains in synaptobrevins, neuronal NO synthases and other intracellular proteins. *Trends Biochem. Sci.* 20:102-103.
- Ridley, A.J., and A. Hall. 1992. The small GTP-binding protein Rho regulate the assembly of focal adhesion and actin fibers in response to growth factors. *Cell*. 70:389-399.
- Sander, E.E., J.P. ten Klooster, S. van Delft, R.A. van der Kammen, and J.G. Collard. 1999. Rac downregulates Rho activity: reciprocal balance between both GTPases determines cellular morphology and migratory behavior. *J. Cell Biol.* 147:1009-1022.
- Smith, P.R., G. Saccomani, E.H. Joe, K.J. Angelides, and D.J. Benos. 1991. Amiloride sensitive sodium channel is linked to the cytoskeleton in renal epithelial cells. *Proc. Natl. Acad. Sci. USA*. 88:6971-6975.
- Stam, J.C., F. Michiels, R.A. van der Kammen, W.H. Moolenaar, and J.G. Collard. 1998. Invasion of T-lymphoma cells: cooperation between Rho family GTPases and lysophospholipid receptor signaling. *EMBO (Eur. Mol. Biol. Organ.) J.* 17:4066-4074.
- Stam, J.C., E.E. Sander, F. Michiels, F.N. van Leeuwen, H.E.T. Kain, R.A. van der Kammen, and J.G. Collard. 1997. Invasion of T-lymphoma cells: cooperation between Rho family GTPases and lysophospholipid receptor signaling. *J. Biol. Chem.* 272:28447-28454.
- Tse, W.T., J.C. Menninger, T.L. Yang-Feng, U. Francke, K.E. Sahr, and B.G. Forget. 1991. Isolation and chromosomal localization of a novel non-erythroid ankyrin gene. *Genomics*. 12:702-704.
- Van Aelst, L., and C. D'Souza-Schoorey. 1997. Rho GTPases and signaling networks. *Genes Dev.* 11:2295-2322.
- Van Leeuwen, F.N., R.A. van der Kammen, G.G.M. Habets, and J.G. Collard. 1995. Oncogenic activity of Tiam1 and Rac1 in NIH3T3 cells. *Oncogene*. 11:2215-2221.
- Van Leeuwen, F.N., H.E. Kain, R.A. Kammen, F. Michiels, O.W. Kranenburg, and J.G. Collard. 1997. The guanine nucleotide exchange factor Tiam1 affects neuronal morphology: opposing roles for the small GTPases Rac and Rho. *J. Cell Biol.* 139:797-807.
- Woods, D.F., and P.J. Bryant. 1991. The discs-large tumor suppressor gene of *Drosophila* encodes a guanylate kinase homolog localized at septate junctions. *Cell*. 66:451-464.
- Yu, Q., and I. Stamenkovic. 1999. Localization of matrix metalloproteinase 9 to the cell surface provides a mechanism for CD44-mediated tumor invasion. *Genes Dev.* 13:35-48.
- Zhang, Y., M.J. Hart, and R.A. Cerione. 1995. Guanine nucleotide exchange catalyzed by dbl oncogene product. In *Methods in Enzymology*. W.E. Balch, C.J. Der, and A. Hall, editors. 256:77-84.
- Zhang, Z., P. Devarajan, A.L. Dorfman, and J.S. Morrow. 1998. Structure of the ankyrin-binding domain of  $\alpha$ -Na, K-ATPase. *J. Biol. Chem.* 273:18681-18684.
- Zhu, D., and L.Y.W. Bourguignon. 1998. The ankyrin-binding domain of CD44s is involved in regulating hyaluronic acid-mediated functions and prostate tumor cell transformation. *Cell Motil. Cytoskelet.* 39:209-222.
- Zhu, D., and L.Y.W. Bourguignon. 2000. Interaction between CD44 and the repeat domain of ankyrin promotes hyaluronic acid-mediated ovarian tumor cell migration. *J. Cell Physiol.* 183:182-195.

## CD44 Interaction with Tiam1 Promotes Rac1 Signaling and Hyaluronic Acid-mediated Breast Tumor Cell Migration\*

(Received for publication, September 3, 1999, and in revised form, October 19, 1999)

Lilly Y. W. Bourguignon‡, Hongbo Zhu, Lijun Shao, and You Wei Chen

From the Department of Cell Biology and Anatomy, School of Medicine, University of Miami, Miami, Florida 33101

In this study we have explored the interaction between CD44 (the hyaluronic acid (HA)-binding receptor) and Tiam1 (a guanine nucleotide exchange factor) in metastatic breast tumor cells (SP1 cell line). Immunoprecipitation and immunoblot analyses indicate that both the CD44v3 isoform and the Tiam1 protein are expressed in SP1 cells and that these two proteins are physically associated as a complex *in vivo*. Using an *Escherichia coli*-derived calmodulin-binding peptide-tagged Tiam1 fragment (*i.e.* the NH<sub>2</sub>-terminal pleckstrin homology (PHn) domain and an adjacent protein interaction domain designated as PHn-CC-Ex, amino acids 393–738 of Tiam1) and an *in vitro* binding assay, we have detected a specific binding interaction between the Tiam1 PHn-CC-Ex domain and CD44. Scatchard plot analysis indicates that there is a single high affinity CD44 binding site in the PHn-CC-Ex domain of Tiam1 with an apparent dissociation constant ( $K_d$ ) of 0.2 nM, which is comparable with CD44 binding ( $K_d = \sim 0.13$  nM) to intact Tiam1. These findings suggest that the PHn-CC-Ex domain is the primary Tiam1-binding region for CD44. Most importantly, the binding of HA to CD44v3 of SP1 cells stimulates Tiam1-catalyzed Rac1 signaling and cytoskeleton-mediated tumor cell migration. Transfection of SP1 cells with Tiam1cDNA promotes Tiam1 association with CD44v3 and up-regulates Rac1 signaling as well as HA/CD44v3-mediated breast tumor cell migration. Co-transfection of SP1 cells with PHn-CC-Ex cDNA and Tiam1 cDNA effectively inhibits Tiam1 association with CD44 and efficiently blocks tumor behaviors. Taken together, we believe that the linkage between CD44v3 isoform and the PHn-CC-EX domain of Tiam1 is required for HA stimulated Rac1 signaling and cytoskeleton-mediated tumor cell migration during breast cancer progression.

The transmembrane glycoprotein CD44 isoforms are all major hyaluronic acid (HA)<sup>1</sup> cell surface receptors that exist on

many cell types, including macrophages, lymphocytes, fibroblasts, and epithelial cells (1–6). Because of their widespread occurrence and their role in signal transduction, CD44 isoforms have been implicated in the regulation of cell growth and activation as well as cell-cell and cell-extracellular matrix interactions (1–7). One of the distinct features of CD44 isoforms is the enormous heterogeneity in the molecular masses of these proteins. It is now known that all CD44 isoforms are encoded by a single gene that contains 19 exons (8). Of the 19 exons, 12 exons can be alternatively spliced (8). Most often, the alternative splicing occurs between exons 5 and 15, leading to an insertion in tandem of one or more variant exons (v1–v10 (exon 6–exon 14) in human cells) within the membrane-proximal region of the extracellular domain (8). The variable primary amino acid sequence of different CD44 isoforms is further modified by extensive *N*- and *O*-glycosylations and glycosaminoglycan additions (9–12). In particular, CD44v3-containing isoforms have a heparin sulfate addition at the membrane-proximal extracellular domain of the molecule that confers the ability to bind heparin sulfate-binding growth factors (9, 10). Cell surface expression of CD44v isoforms changes profoundly during tumor metastasis, particularly during the progression of various carcinomas including breast carcinomas (13–17). In fact, CD44v isoform expression has been used as an indicator of metastasis.

It has been shown that interaction between the cytoskeletal protein, ankyrin, and the cytoplasmic domain of CD44 isoforms plays an important role in CD44 isoform-mediated oncogenic signaling (6, 18, 19). Specifically, the ankyrin-binding domain (*e.g.* NGGNGTVEDRKPSSEL between amino acids 306 and 320 in the mouse CD44 (20) and NSGNGAVEDRKPSGL amino acids 304 and 318 in human CD44 (21)) is required for the recruitment of Src kinase and the onset of tumor cell transformation (21). Furthermore, HA binding to CD44 stimulates a concomitant activation of p185<sup>HER2</sup>-linked tyrosine kinase (linked to CD44s via a disulfide linkage) and results in a direct cross-talk between two different signaling pathways (*e.g.* proliferation *versus* motility/invasion) (22). In tumor cells, the transmembrane linkage between CD44 isoform and the cytoskeleton promotes invasive and metastatic-specific tumor phenotypes (*e.g.* matrix degradation (matrix metalloproteinases) activities (23, 24), “invadopodia” formation (membrane projections), tumor cell invasion, and migration) (23). These findings strongly suggest that the interaction between CD44 isoform and the cytoskeleton plays a pivotal role in the onset of oncogenesis and tumor progression.

The Rho family proteins (*e.g.* Rho, Rac, and Cdc42) are members of the Ras superfamily of GTP-binding proteins structurally related to but functionally distinct from Ras itself (25, 26). They are associated with changes in the membrane-linked cytoskeleton (26). For example, activation of RhoA, Rac1, and Cdc42 have been shown to produce specific structural changes in the plasma membrane-cytoskeleton reorganization leading

\* This work was supported by United States Public Health Grants CA66163 and CA 78633 and Department of Defense Grants DAMD 17-94-J-4121, DAMD 17-97-1-7014, and DAMD 17-99-1-9291. The costs of publication of this article were defrayed in part by the payment of page charges. This article must therefore be hereby marked “advertisement” in accordance with 18 U.S.C. Section 1734 solely to indicate this fact.

‡ To whom reprint request should be addressed: Dept. of Cell Biology and Anatomy, University of Miami Medical School, 1600 N.W. 10th Ave., Miami, FL 33136. Tel.: 305-243-6985; Fax: 305-545-7166; E-mail: Lbourgui@mednet.med.miami.edu.

<sup>1</sup> The abbreviations used are: HA, hyaluronic acid; PHn, pleckstrin homology; PHc, PH domain located at the COOH-terminal region of the molecule; CC, coiled coil region; Ex, extra region; CBP, calmodulin-binding peptide; GFP, green fluorescent protein; GST, glutathione *S*-transferase; PBS, phosphate-buffered saline; PCR, polymerase chain reaction; GTPγS, guanosine 5′-3-*O*-(thio)triphosphate; Rh, rhodamine; FITC, fluorescein isothiocyanate.

to membrane ruffling, lamellipodia, filopodia, and stress fiber formation (26). The coordinated activation of these GTPases is considered to be a possible mechanism underlying cell motility, an obvious prerequisite for metastasis (27–29). In particular, Rac1 activation is known to initiate oncogenic signaling pathways that promote cell shape changes (33, 34), influence actin cytoskeleton organization (33, 34), and stimulate gene expression (35–37). The question of whether Rac1 activation is also involved in CD44v3-related cytoskeleton function that results in the metastatic phenotypes (e.g. tumor cell migration) of breast tumor cells remains to be answered.

Tiam1 (T lymphoma invasion and metastasis 1) has been identified as an oncogene because of its ability to activate Rho-like GTPases during malignant transformation (38, 39). Specifically, Tiam1 is capable of activating Rac1 *in vitro* as a guanine nucleotide exchange factor and inducing membrane cytoskeleton-mediated cell shape changes, cell adhesion, and cell motility (34, 40–42). It also acts as a Rac-specific guanine nucleotide exchange factor *in vivo* and induces an invasive phenotypes in lymphoma cells (40). These findings have prompted several research groups to investigate the mechanisms involved in the regulation of Tiam1. For example, addition of certain serum-derived lipids (e.g. sphingosine-1-phosphate and lysophosphatidic acid) to T-lymphoma cells promotes Tiam1-mediated Rac1 and Cdc42 signaling and T-lymphoma cell invasion (43). Tiam1 has also been found to be phosphorylated by protein kinase C in Swiss 3T3 fibroblasts stimulated by lysophosphatidic acid (44) and platelet-derived growth factor (45). Most recently, Exton and co-workers (46) demonstrate that phosphorylation of Tiam1 by  $\text{Ca}^{2+}$ /calmodulin-dependent protein kinase II (but not protein kinase C) regulates Tiam1-catalyzed GDP/GTP exchange activity *in vitro*. These findings support the notion that posttranslational modifications of Tiam1 by certain serine/threonine kinase(s) during surface receptor-mediated activation may play an important role in Tiam1-Rac1 signaling. Tiam1 transcript has been detected in breast cancer cells (39). However, it is not known at the present time whether there is any structural and functional relationship(s) between Tiam1-Rac1 signaling and CD44v3-mediated invasive and metastatic processes of breast cancer cells.

In this paper, using a variety of biochemical, molecular biological, and immunocytochemical techniques, we have found that the cell adhesion molecule, CD44v<sub>3</sub> isoform, which binds directly to HA, is closely associated with Tiam1 (in particular, the NH<sub>2</sub>-terminal pleckstrin homology (PHn), a putative coiled coil region (CC), and an additional adjacent region (Ex), designated as PHn-CC-Ex domain of Tiam1) in SP1 breast tumor cells. Most importantly, HA binding to CD44v<sub>3</sub> isoform stimulates Tiam1-specific GDP/GTP exchange for Rho-like GTPases such as Rac1 and promotes cytoskeleton-mediated tumor cell migration. These findings suggest that a transmembrane interaction between CD44v3 and Tiam1 plays an important role in promoting oncogenic signaling and tumor cell-specific phenotypes required for HA-mediated breast tumor cell migration.

#### MATERIALS AND METHODS

**Cell Culture**—Mouse breast tumor cells (e.g. SP1 cell line) (provided by Dr. Bruce Elliott, Department of Pathology, and Biochemistry, Queen's University, Kingston, ON, Canada) were used in this study. Specifically, SP1 cell line was derived from a spontaneous intraductal mammary adenocarcinoma that arose in a retired female CBA/J breeder in the Queen's University animal colony. These cells were capable of inducing lung metastases by sequential passage of SP1 cells into mammary gland (47). These cells were cultured in RPMI 1640 medium supplemented with 5–7% fetal calf serum, folic acid (290 mg/liter), and sodium pyruvate (100 mg/liter). COS-7 cells were obtained from American Type Culture Collection and grown routinely in Dulbecco's modified Eagle's medium containing 10% fetal bovine serum, 1% glutamine, 1% penicillin, and 1% streptomycin.

**Antibodies and Reagents**—For the preparation of polyclonal rabbit anti-Tiam1 antibody or rabbit anti-CD44v3 antibody, specific synthetic peptides ( $\approx 15$ –17 amino acids unique for the COOH-terminal sequence of Tiam1 or the CD44v3 sequence) were prepared by the Peptide Laboratories of Department of Biochemistry and Molecular Biology using an Advanced Chemtech automatic synthesizer (model ACT350). These Tiam1-related or CD44v3-related polypeptides were conjugated to polylysine and subsequently injected into rabbits to raise the antibodies, respectively. The anti-Tiam1-specific or anti-CD44v3-specific antibody was collected from each bleed and stored at 4 °C containing 0.1% azide. The anti-Tiam1 IgG or anti-CD44v3 IgG fraction was prepared by conventional DEAE-cellulose chromatography, respectively. Mouse monoclonal anti-HA (hemagglutinin epitope) antibody (clone 12 CA5) was purchased from Roche Molecular Biochemicals. Mouse monoclonal anti-green fluorescent protein (GFP) was purchased from Pharmingen. *Escherichia coli*-derived GST-tagged Rac1 was kindly provided by Dr. Richard A. Cerione (Cornell University, Ithaca, NY).

**Cell Surface Labeling Procedures**—SP1 cells suspended in PBS were surface labeled using the following biotinylation procedure. Briefly, cells ( $10^7$  cells/ml) were incubated with sulfo-succinimidyl-6-(biotinamido)hexanoate (Pierce) (0.1 mg/ml) in labeling buffer (150  $\mu\text{M}$  NaCl, 0.1 M HEPES, pH 8.0) for 30 min at room temperature. Cells were then washed with PBS to remove free biotin. Subsequently, the biotinylated cells were used for anti-CD44v3-mediated immunoprecipitation as described previously (23). These biotinylated materials precipitated by anti-CD44v3 antibody were analyzed by SDS-polyacrylamide gel electrophoresis, transferred to the nitrocellulose filters, and incubated with ExtrAvidin-peroxidase (Sigma). After an addition of peroxidase substrate (Pierce), the blots were developed using ECL chemiluminescence reagent (Amersham Pharmacia Biotech) according to the manufacturer's instructions.

**Immunoprecipitation and Immunoblotting Techniques**—SP1 cells were solubilized in 50 mM Tris-HCl (pH 7.4), 150 mM NaCl, 1% Triton X-100 buffer and immunoprecipitated using rabbit anti-CD44v3 antibody or rabbit anti-Tiam1 antibody followed by goat anti-rabbit IgG, respectively. The immunoprecipitated material was solubilized in SDS sample buffer, electrophoresed, and blotted onto the nitrocellulose. After blocking nonspecific sites with 3% bovine serum albumin, the nitrocellulose filter was incubated with rabbit anti-Tiam1 antibody (5  $\mu\text{g/ml}$ ) or rabbit anti-CD44v3 antibody (5  $\mu\text{g/ml}$ ), respectively, for 1 h at room temperature followed by incubation with horseradish peroxidase-conjugated goat anti-rabbit IgG (1:10,000 dilution) at room temperature for 1 h. The blots were developed using ECL chemiluminescence reagent (Amersham Pharmacia Biotech) according to the manufacturer's instructions.

In some experiments, SP1 cells or COS cells (e.g. untransfected or transfected by various Tiam1 cDNAs including the full-length mouse Tiam1cDNA (FL1591) or HA-tagged NH<sub>2</sub>-terminally truncated C1199 Tiam1cDNA or GFP-tagged PHn-CC-ExcDNA or C1199Tiam1cDNA plus GFP-tagged PHn-CC-ExcDNA (as co-transfection) or vector only) were immunoblotted with mouse anti-HA antibody (5  $\mu\text{g/ml}$ ) or anti-GFP antibody (5  $\mu\text{g/ml}$ ), respectively, for 1 h at room temperature followed by incubation with horseradish peroxidase-conjugated goat anti-mouse IgG or goat anti-mouse IgG (1:10,000 dilution) at room temperature for 1 h. The blots were developed using ECL chemiluminescence reagent (Amersham Pharmacia Biotech) according to the manufacturer's instructions.

**Cloning, Expression, and Purification of CD44 Cytoplasmic Domain (CD44cyt) from *E. coli***—The procedure for preparing the fusion protein of the cytoplasmic domain of CD44 was the same as described previously (48). Specifically, the cytoplasmic domain of human CD44 (CD44cyt) was cloned into pFLAG-AST using the PCR-based cloning strategy. Using human CD44 cDNA as template, one PCR primer pair (left, FLAG-EcoRI; right, FLAG-XbaI) was designed to amplify complete CD44 cytoplasmic domain. The amplified DNA fragments were one-step cloned into a pCR2.1 vector and sequenced. Then the DNA fragments were cut out by double digestion with *EcoRI* and *XbaI* and subcloned into *EcoRI/XbaI* double-digested pFLAG-AST (Eastman Kodak Co., Rochester, NY) to generate FLAG-pCD44cyt construct. The nucleotide sequence of FLAG/CD44cyt junction was confirmed by sequencing. The recombinant plasmids were transformed to BL21-DE3 to produce FLAG-CD44cyt fusion protein. The FLAG-CD44cyt fusion protein was further purified by anti-FLAG M2 affinity gel column (Eastman Kodak Co.). The nucleotide sequence of primers used in this cloning protocol are: FLAG-EcoRI, 5'-GAGAATTGCAACAGTCGAA-GAAGGTGTCTCTTAAGC-3', and FLAG-XbaI, 5'-AGCTCTAGATTACACCCCAATCTTCAT-3'.

**Expression Constructs**—Both the full-length mouse Tiam1cDNA

(FL1591) and the NH<sub>2</sub>-terminally truncated Tiam1cDNA (C1199) were kindly provided by Dr. John G. Collard (The Netherlands Cancer Institute, Amsterdam, The Netherlands). Specifically, the full-length Tiam1 (FL1591) cDNA was cloned into the eukaryotic expression vector, pMT2SM. The NH<sub>2</sub>-terminally truncated C1199 Tiam1 cDNA (carrying a HA epitope tag at the 3' end) was cloned into the eukaryotic expression vector, pUTSV1 (Eurogentec, Belgium). The Tiam1 fragment, PHn-CC-Ex domain was cloned into calmodulin-binding peptide (CBP)-tagged vector (pCAL-n) (Stratagen) using the PCR-based cloning strategy. Using human Tiam1 cDNA as a template, PHn-CC-Ex domain was amplified by PCR with two specific primers (left, 5'-AACTCGAGATGAGTACCACCAACAGTGAG-3', and right, 5'-AAAAAGCTTTCAGC-CATCTGGAACAGTGCATC-3') linked with specific enzyme digestion site (*Xho*I or *Hind*III). PCR product digested with *Xho*I and *Hind*III was purified with QIAquick PCR Purification Kit (Qiagen). The PHn-CC-Ex domain cDNA fragment was cloned into pCAL-n vector digested with *Xho*I and *Hind*III. The inserted PHn-CC-Ex domain sequence was confirmed by nucleotide sequencing analyses. The recombinant plasmids were transformed to BL21-DE3 to produce CBP-tagged PHn-CC-Ex fusion protein. This fusion protein was purified from bacteria lysate by calmodulin affinity resin column (Sigma).

The PHn-CC-Ex domain cDNA fragment was also cloned into pEG-FPN1 vector (CLONTECH) digested with *Xho*I and *Hind*III to create GFP-tagged PHn-CC-Ex cDNA. The inserted PHn-CC-Ex domain sequence was confirmed by nucleotide sequencing analyses. This GFP-tagged PHn-CC-Ex domain cDNA was then used for transient expression in SP1 cells as described below. The molecular mass of the GFP-tagged PHn-CC-Ex is expressed as 68 kDa in SP1 or COS-7 cells by SDS-polyacrylamide gel electrophoresis and immunoblot analyses.

**Cell Transfection**—To establish a transient expression system, SP1 cells (or COS-7 cells) were transfected with various plasmid DNAs (e.g. HA-tagged C1199 Tiam1cDNA, GFP-tagged PHn-CC-ExcDNA, or HA-tagged C1199Tiam1cDNA plus GFP-tagged PHn-CC-ExcDNA (as co-transfection) or vector alone) using electroporation methods according to those procedures described previously (74). Briefly, SP1 cells were plated at a density of  $2 \times 10^6$  cells/100-mm dish and transfected with 25  $\mu$ g/dish plasmid cDNA using electroporation at 230 V and 960 microfaraday with a Gene Pulser (Bio-Rad). Transfected cells were grown in the culture medium for at least 24–48 h. Various transfectants were then analyzed for their protein expression (e.g. Tiam1-related proteins) by immunoblot, GDP/GTP exchange reaction on Rac1, and tumor cell migration assays as described below.

**In Vitro Binding of Tiam1/Tiam1 Fragment to CD44**—Aliquots (0.5–1 ng of protein) of purified FLAG-CD44cyt fusion protein bound to Anti-FLAG M2 antibody immunoaffinity beads were incubated in 0.5 ml of binding buffer (20 mM Tris-HCl (pH 7.4), 150 mM NaCl, 0.1% bovine serum albumin, and 0.05% Triton X-100) containing various concentrations (10–800 ng/ml) of <sup>125</sup>I-labeled intact Tiam1 (purified from SP1 cells) (5000 cpm/ng protein) or <sup>125</sup>I-labeled recombinant Tiam1 fragment (CBP-tagged PHn-CC-Ex) at 4 °C for 4 h. Specifically, equilibrium binding conditions were determined by performing a time course (1–10 h) of <sup>125</sup>I-labeled Tiam1 (or CBP-tagged PHn-CC-Ex) binding to CD44 at 4 °C. The binding equilibrium was found to be established when the *in vitro* Tiam1 (or PHn-CC-Ex)-CD44 binding assay was conducted at 4 °C after 4 h. Following binding, the immunobeads were washed extensively in binding buffer, and the bead-bound radioactivity was counted. Nonspecific binding was determined using a 50–100-fold excess of unlabeled Tiam1 (or PHn-CC-Ex) in the presence of the same concentration of <sup>125</sup>I-labeled Tiam1 or <sup>125</sup>I-labeled CBP-tagged PHn-CC-Ex. Nonspecific binding, which was approximately 20% of the total binding, was always subtracted from the total binding. Our binding data are highly reproducible. The values expressed in Fig. 5 represent an average of triplicate determinations of three to five experiments with a standard deviation less than  $\pm 5\%$ .

In some cases, 0.1  $\mu$ g of surface biotinylated CD44v3 was incubated with various Tiam1-related proteins (e.g. purified intact Tiam1, HA-tagged C1199, CBP-PHn-CC-Ex, or HA/CBP-coated beads) in the presence and absence of 100-fold excess amount of CBP-PHn-CC-Ex at room temperature in the binding buffer (20 mM Tris-HCl (pH 7.4), 150 mM NaCl, 0.1% bovine serum albumin, and 0.05% Triton X-100) for 1 h. After binding, biotinylated CD44v3 bound to the beads was analyzed by SDS-polyacrylamide gel electrophoresis, transferred to the nitrocellulose filters, and incubated with ExtrAvidin-peroxidase (Sigma). After an addition of peroxidase substrate (Pierce), the blots were developed using ECL chemiluminescence reagent (Amersham Pharmacia Biotech) according to the manufacturer's instructions.

**Tiam1-mediated GDP/GTP Exchange for Rac1 Proteins**—Purified *E. coli*-derived GST-tagged Rac1 (20 pmol) was preloaded with GDP (30

$\mu$ M) in 10  $\mu$ l of buffer containing 25 mM Tris-HCl (pH 8.0), 1 mM dithiothreitol, 4.7 mM EDTA, 0.16 mM MgCl<sub>2</sub>, and 200  $\mu$ g/ml bovine serum albumin at 37 °C for 7 min. To terminate preloading procedures, additional MgCl<sub>2</sub> was then added to the solution (reaching a final concentration of 9.16 mM) as described previously (40, 49). Subsequently, 2 pmol of Tiam1 (in anti-Tiam1 (or anti-HA or anti-CD44v3)-Sepharose bead-conjugated forms) isolated from COS-7 cells (transfected with either the full-length Tiam1cDNA or NH<sub>2</sub>-terminally truncated Tiam1cDNA) or SP1 cells (transfected with various plasmid DNAs such as HA-tagged C1199 Tiam1cDNA, GFP-tagged PHn-CC-ExcDNA or HA-tagged C1199Tiam1cDNA plus GFP-tagged PHn-CC-ExcDNA (as co-transfection) or vector alone, grown in the presence or absence of hyaluronic acid (100  $\mu$ g/ml)) or control samples (nonspecific cellular material associated with preimmune serum-conjugated Sepharose beads) was preincubated with 2.5  $\mu$ M [<sup>35</sup>S]GTP $\gamma$ S ( $\approx 1,250$  Ci/mmol) (in the presence or absence of 2.25  $\mu$ M GTP $\gamma$ S for 10 min followed by adding 2.5 pmol of GDP-loaded GST-tagged Rac1GTPase as described previously) (49). The amount of [<sup>35</sup>S]GTP $\gamma$ S bound to Tiam1 (conjugated to anti-Tiam1-Sepharose beads) or control sample (preimmune serum-conjugated Sepharose beads) in the absence of Rac1GTPase was subtracted from the original values. Data represent an average of triplicates from three to five experiments. The standard deviation was less than 5%.

**Double Immunofluorescence Staining**—SP1 cells (transfected with various plasmid DNAs such as HA-tagged C1199 Tiam1cDNA, GFP-tagged PHn-CC-ExcDNA, or HA-tagged C1199Tiam1cDNA plus GFP-tagged PHn-CC-ExcDNA (as co-transfection) or vector alone) were first washed with PBS buffer (0.1 M phosphate buffer (pH 7.5) and 150 mM NaCl) and fixed by 2% paraformaldehyde. Subsequently, SP1 transfectants were stained with rhodamine (Rh)-labeled rabbit anti-CD44v3 antibody. In some cases, Rh-labeled cells were then rendered permeable by ethanol treatment followed by incubating with FITC-conjugated mouse anti-HA IgG. To detect nonspecific antibody binding, Rh-CD44v3-labeled cells were incubated with FITC-conjugated normal mouse IgG. No labeling was observed in such control samples. The fluorescein- and rhodamine-labeled samples were examined with a confocal laser scanning microscope (MultiProbe 2001 Inverted CLSM system, Molecular Dynamics, Sunnyvale, CA).

**Cell Adhesion Assay**—SP1 cells were metabolically labeled with Tran<sup>35</sup>S label (20  $\mu$ Ci/ml) as described above. After labeling, the cells were washed in PBS and incubated in PBS containing 5 mM EDTA at 37 °C to obtain a nonadherent single cell suspension. Labeled cells ( $\approx 9.1 \times 10^5$  cpm/ $10^5$  cells) (in the presence or absence of anti-CD44v3 antibody) were plated on the HA-coated plates at 4 °C for 30 min. Following incubation, the wells were washed three times in PBS, the adherent cells were solubilized in PBS containing 1% SDS, and the well bound radioactivity was determined by liquid scintillation counting. Nonspecific binding was determined by including 300  $\mu$ g/ml soluble HA during the incubation of cells on HA-coated wells. The nonspecific binding was 10–15% of the total well-associated radioactivity and has been subtracted.

**Tumor Cell Migration Assays**—Twenty-four transwell units were used for monitoring *in vitro* cell migration as described previously (23). Specifically, the 5- $\mu$ m porosity polycarbonate filters (CoStar Corp., Cambridge, MA) were used for the cell migration assay. SP1 cells ( $\approx 1 \times 10^4$  cells/well in PBS, pH 7.2) (in the presence or absence of anti-CD44v3 antibody (50  $\mu$ g/ml)) were placed in the upper chamber of the transwell unit. In some cases, cells were transfected with either C1199Tiam1cDNA, PHn-CC-ExcDNA, C1199Tiam1cDNA plus PHn-CC-ExcDNA, or vector alone. The growth medium containing high glucose Dulbecco's modified Eagle's medium supplemented with 200  $\mu$ g/ml hyaluronic acid was placed in the lower chamber of the transwell unit. After 18 h of incubation at 37 °C in a humidified 95% air/5% CO<sub>2</sub> atmosphere, the 3-(4,5-dimethyl thiazol-2-yl)-2,5-diphenyl tetrazolium bromide (Promega) was added at a final concentration of 0.2 mg/ml to both the upper and the lower chambers and incubated for an additional 4 h at 37 °C. Migrative cells at the lower part of the filter were removed by swabbing with small pieces of Whatman filter paper. Both the polycarbonate filter and the Whatman paper were placed in dimethyl sulfoxide to solubilize the crystal. Color intensity was measured in 450 nm. Cell migration processes were determined by measuring the cells that migrate to the lower side of the polycarbonate filters by standard cell number counting methods as described previously (23, 49). The CD44-specific cell migration was determined by subtracting nonspecific cell migration (i.e. cells migrate to the lower chamber in the presence of anti-CD44v3 antibody treatment) from the total migrative cells in the lower chamber. The CD44-specific cell migration in vector-transfected cells (control) is designated as 100%. Each assay was set up in triplicate

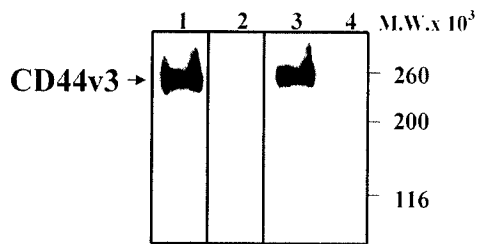


**FIG. 1. Expression of CD44v3 in breast tumor cells.** Breast tumor cells (SP1 cell line) were surface biotinylated (or unlabeled) and solubilized in a buffer containing 50 mM Tris-HCl (pH 7.4), 150 mM NaCl, and 1% Triton X-100. The solubilized materials were then immunoblotted or immunoprecipitated by anti-CD44v3 antibody as described under "Materials and Methods." *Lane 1*, immunoblot of unlabeled SP1 cell lysate using rabbit anti-CD44v3 antibody; *lane 2*, immunoblot of unlabeled SP1 cells with preimmune rabbit serum; *lane 3*, immunoprecipitation of surface biotinylated SP1 cells using rabbit anti-CD44v3 antibody; *lane 4*, immunoprecipitation of surface biotinylated SP1 cells with preimmune rabbit serum.

and repeated at least three times. All data were analyzed statistically using the Student's *t* test, and statistical significance was set at  $p < 0.01$ .

## RESULTS

**Identification of CD44 Variant Isoform(s) as HA Receptor(s) in SP1 Cells**—The expression of CD44 variant isoforms such as CD44v3 is known to be closely correlated with metastatic and proliferative behavior of a variety of tumor cells including various carcinomas such as human breast tumor cells (14–19). Immunoblotting with anti-CD44v3 antibody (recognizing the v3-specific sequence located at the membrane-proximal region of the extracellular domain of CD44) indicates that a single CD44v3 protein (molecular mass = ~260 kDa) is expressed in SP1 cells (Fig. 1, *lane 1*). Furthermore, we have utilized surface biotinylation techniques and anti-CD44v3-mediated immunoprecipitation to characterize this CD44v3 molecule. Our results show that the 260-kDa CD44v3 molecule can be surface-biotinylated and is located on the surface of SP1 cells (Fig. 1, *lane 3*). No CD44v3-containing material is observed in control samples when preimmune rabbit serum is used in either immunoblot (Fig. 1, *lane 2*) or immunoprecipitation experiments (Fig. 1, *lane 4*). Further analyses using reverse transcriptase-PCR, cloning, and nucleotide sequence techniques indicate that this CD44v3 belongs to the CD44v<sub>3,8–10</sub> isoform in SP1 cells (data not shown). This CD44v<sub>3,8–10</sub> variant exon structure was previously identified in human breast carcinoma samples (14–19), and its molecular mass (expressed at the protein level) has been shown to be ~260 kDa (9).

CD44 is the major hyaluronan cell surface receptor (50), and a cellular adhesion molecule in many different cell types (51). Specific HA-binding motifs have been identified and localized in the extracellular domain of all CD44 isoforms (52, 53). To determine whether HA promotes cell adhesion, breast tumor cells (SP1 cell line) were incubated with plastic dishes coated with HA. As shown in Table I, SP1 cells adhere to the HA-coated dishes very well. In addition, because preincubation with anti-CD44v3 antibody blocks the adhesion of SP1 cells to HA-coated dishes, these data clearly indicate that CD44v3 isoform involves a specific binding interaction with the extracellular matrix component such as HA and is a cell surface adhesion molecule in SP1 cells.

**Analysis of a Complex Formed between CD44v3 and Tiam1 in SP1 Cells in Vivo**—Both CD44v isoforms (14–19) and Tiam1 (39) have been detected in a variety of tumor cells. In this study we have addressed the question of whether there is an interaction between CD44v3 isoform and Tiam1 in breast tumor cells (e.g. SP1 cells). First, we have analyzed Tiam1 expression

**TABLE I**  
CD44v<sub>3</sub>-mediated adhesion of metabolically labeled SP1 cells to HA-coated plates

Trans<sup>35</sup>S-labeled SP1 cells were pretreated with or without anti-CD44v<sub>3</sub> antibody treatment. Subsequently, these cells were incubated in tissue culture wells coated with HA as described under "Materials and Methods." The background level of binding was determined by cell adhesion performed in the presence of an excess amount of soluble HA. The results were expressed in terms of HA-specific binding in which the background levels of binding have been subtracted. Data are expressed as mean cpm ± S.E. of triplicate determinations.

Treatments	CD44v <sub>3</sub> -specific adhesion to HA-coated plates	
	cpm	% of control
Untreated cells (control)	5,057 ± 201	100
Anti-CD44v <sub>3</sub> -treated cells	1,091 ± 136	21

(at the protein level) in breast tumor cells such as SP-1 cell line. Immunoblot analysis, utilizing anti-Tiam1 antibody designed to recognize the specific epitope located at the COOH-terminal sequence of Tiam1 reveals a single polypeptide (molecular mass = ~200 kDa) (Fig. 2, *lane 2*). We have demonstrated that Tiam1 detected in SP1 cells revealed by anti-Tiam1-mediated immunoblot is specific because no protein is detected in these cells using preimmune rabbit IgG (Fig. 2, *lane 1*). Furthermore, we have carried out anti-CD44v3-mediated and anti-Tiam1-mediated precipitation followed by anti-Tiam1 immunoblot (Fig. 2, *lane 3*) or anti-anti-CD44v3 immunoblot (Fig. 2, *lane 4*), respectively, using SDS-polyacrylamide gel electrophoresis analyses. Our results clearly indicate that the Tiam1 band is revealed in anti-CD44v3-immunoprecipitated materials (Fig. 2, *lane 3*). The CD44v3 band can also be detected in the anti-Tiam1-immunoprecipitated materials (Fig. 2, *lane 4*). These findings clearly establish the fact that CD44v3 and Tiam1 are closely associated with each other *in vivo* in breast tumor cells.

**In Vitro Binding Between Tiam1 (or PHn-CC-Ex Domain) and CD44**—Previous studies indicate that Tiam1 membrane localization (through its NH<sub>2</sub>-terminal PHn domain and an adjacent protein interaction domain (designated as PHn-CC-Ex, a sequence between amino acids 393–738 of Tiam1)) (Fig. 3, A and C) is required for the activation of Rac1 signaling pathways leading to membrane ruffling and c-Jun NH<sub>2</sub>-terminal kinase activation (37, 54). To test whether CD44 is one of the membrane proteins involved in the direct binding to Tiam1, we have used purified CBP-tagged PHn-CC-Ex fusion protein (Figs. 3C and 4, *lane 1*) and the FLAG-tagged cytoplasmic domain of CD44 (FLAG-CD44cyt) fusion protein (Fig. 4, *lane 2*) to identify the CD44 binding site on the Tiam1 molecule. Specifically, we have tested the binding of FLAG-CD44cyt to <sup>125</sup>I-labeled CBP-PHn-CC-EX (or <sup>125</sup>I-labeled intact Tiam1) under equilibrium binding conditions. Scatchard plot analyses presented in Fig. 5 indicate that PHn-CC-Ex binds to the cytoplasmic domain of CD44 (CD44cyt) at a single site (Fig. 5A) with high affinity (an apparent dissociation constant ( $K_d$ ) of ~0.2 nM). This interaction between PHn-CC-Ex and CD44 is comparable in affinity with CD44 binding ( $K_d$  = ~0.13 nM) to intact Tiam1 (Fig. 5B). These findings clearly indicate that Tiam1 (in particular, PHn-CC-Ex domain) contains the CD44 binding site.

Further analyses using an *in vitro* binding assay show that surface biotinylated CD44v3 (isolated from SP1) specifically binds to Tiam1 (including intact Tiam1 (Fig. 6, *lane 1*), HA-tagged C1199 Tiam1 (Fig. 6, *lane 2*) or Tiam1 fragment (PHn-CC-Ex) (Fig. 6, *lane 3*)-coated beads. In the presence of an excess amount (~100-fold) of recombinant PHn-CC-Ex Tiam1 fragment, the binding interaction between CD44v3 and these Tiam1-related proteins is readily abolished (Fig. 6, *lanes 4–6*). These observations suggest that (i) the breast tumor cell-spe-

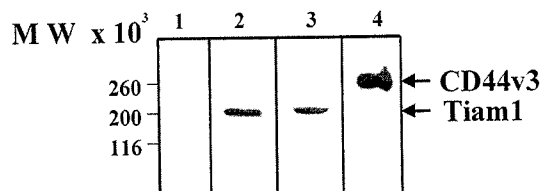


**FIG. 2. Detection of Tiam1 and Tiam1-CD44v3 complex in SP1 cells.** SP1 cells ( $5 \times 10^5$  cells) were solubilized by 1% Nonidet P-40 buffer followed by immunoprecipitation and/or immunoblot by anti-Tiam1 antibody or anti-CD44v3 antibody, respectively, as described under "Materials and Methods." Lane 1, immunoblot of SP1 cells with preimmune rabbit serum; lane 2, detection of Tiam1 with anti-Tiam1-mediated immunoblot of SP1 cells; lane 3, detection of Tiam1 in the complex by anti-CD44v3-immunoprecipitation followed by immunoblotting with anti-Tiam1 antibody; lane 4, detection of CD44v3 in the complex by anti-Tiam1 immunoprecipitation followed by immunoblotting with anti-CD44v3 antibody.

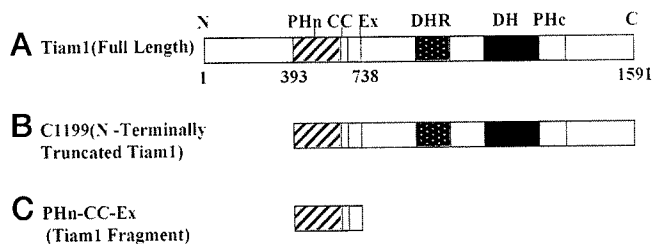


**FIG. 3. Illustration of Tiam1 full-length (A) and deletion mutant cDNA constructs (B and C).** The full-length Tiam1 contains a Dbl homology domain (DH), a Discs large homology region (DHR), two pleckstrin homology (PH) domains (including the NH<sub>2</sub>-terminal PH (PHn) and the COOH-terminal PH (PHc)), a putative coiled coil region (CC), and an additional adjacent region (Ex). The NH<sub>2</sub>-terminally truncated C1199 Tiam1 encodes the COOH-terminal 1199 amino acids (B). PHn-CC-Ex domain of Tiam1 encodes the sequence between amino acids 393 and 738 (C).

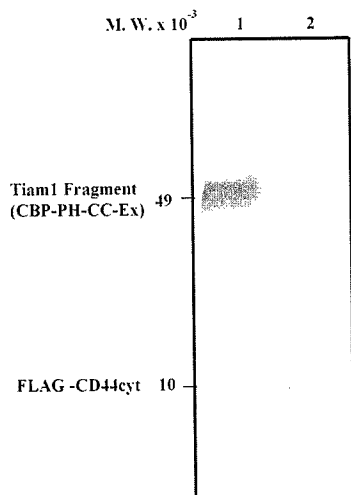


**FIG. 4. Characterization of various recombinant proteins used in the *in vitro* binding assay.** Lane 1, a Coomassie Blue staining of CBP-PH-CC-Ex fusion protein purified by calmodulin affinity resin column chromatography; lane 2, a Coomassie Blue staining of FLAG-CD44cyt fusion protein eluted from affinity column chromatography with FLAG peptide.

cific CD44v3 is also capable of interacting with Tiam1 (e.g. intact Tiam1 (Fig. 6, lane 1), HA-tagged C1199 Tiam1 (Fig. 6, lane 2), or Tiam1 fragment (PHn-CC-Ex) (Fig. 6, lane 3)); and (ii) the Tiam1 fragment such as PHn-CC-Ex acts as a potent competitive inhibitor for Tiam1 binding to CD44v3 *in vitro* (Fig. 6, lanes 4–6).

**Tiam1-catalyzed Rac1 Activation in SP1 Cells**—Rac1 GTPase becomes activated when bound GDP is exchanged for GTP by a

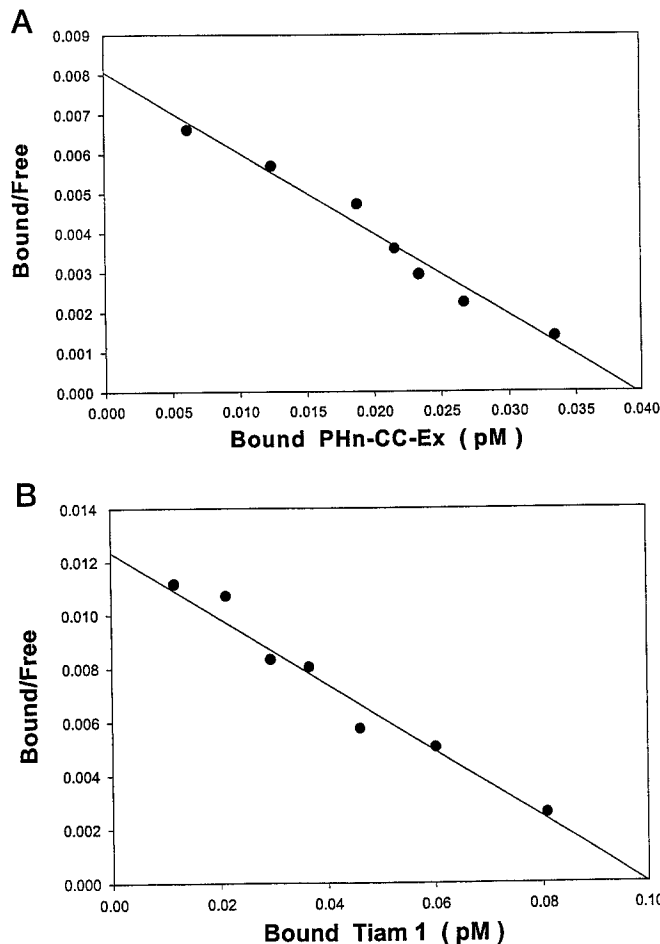


**FIG. 5. Binding of  $^{125}\text{I}$ -labeled PHn-CC-Ex (or Tiam1) to FLAG-CD44cyt.** Various concentrations of  $^{125}\text{I}$ -labeled PHn-CC-Ex (or Tiam1) were incubated with FLAG-CD44cyt-coupled beads at 4 °C for 4 h. Nonspecific binding was determined in the presence of 50-fold excess of unlabeled PHn-CC-Ex (or Tiam1) and subtracted from the total binding. Results represent an average of duplicate determinations from the same experiment. Data presented are the representative of three individual binding experiments. A, Scatchard plot analysis of the equilibrium binding data between  $^{125}\text{I}$ -labeled PHn-CC-Ex and FLAG-CD44cyt. B, Scatchard plot analysis of the equilibrium binding data between  $^{125}\text{I}$ -labeled intact Tiam1 and FLAG-CD44cyt.

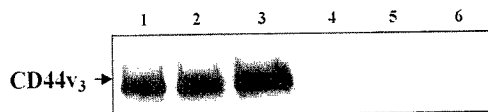


**FIG. 6. *In vitro* binding between CD44v3 and Tiam1-related protein.** CD44v3 was immunoprecipitated from surface biotinylated SP1 cells by anti-CD44v3 antibody as described under "Materials and Methods." Subsequently, purified surface biotinylated CD44v3 was incubated with Tiam1, C1199 Tiam1, or PHn-CC-Ex-coated beads in the binding buffer (20 mM Tris-HCl, pH 7.4, 150 mM NaCl, 0.1% bovine serum albumin, and 0.05% Triton X-100) at room temperature for 1 h. After extensive washing, protein bound on the beads were eluted and analyzed with Extravidin (horseradish peroxidase-conjugated). Lane 1, binding of CD44v3 to Tiam1-conjugated beads; lane 2, binding of CD44v3 to C1199 Tiam1-conjugated beads; lane 3, binding of CD44v3 to PHn-CC-Ex-conjugated beads; lane 4, binding of CD44v3 to Tiam1-conjugated beads in the presence of an excess amount ( $\approx 100$ -fold) of soluble PHn-CC-Ex; lane 5, binding of CD44v3 to C1199 Tiam1-conjugated beads in the presence of an excess amount ( $\approx 100$ -fold) of soluble PHn-CC-Ex; lane 6, binding of CD44v3 to PHn-CC-Ex-conjugated beads in the presence of an excess amount ( $\approx 100$ -fold) of soluble PHn-CC-Ex.

process catalyzed by guanine nucleotide (GDP-GTP) exchange factors or GDP dissociation stimulator proteins (i.e. promoting GTP binding to RhoA by facilitating the release of GDP) (25,

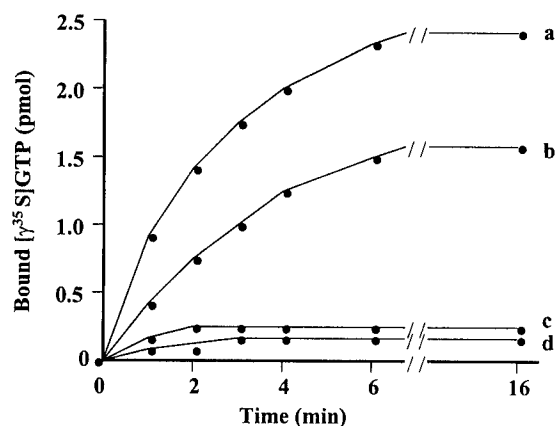


**FIG. 7. Tiam1-mediated GDP/GTP exchange for Rac1 protein.** Tiam1 isolated from SP1 cells (treated with HA or without any treatment) was preincubated for 10 min with  $0.25 \mu\text{M}$  [ $^{35}\text{S}$ ]GTP $\gamma\text{S}$  ( $1,250 \text{ Ci/mmol}$ ) and  $2.25 \mu\text{M}$  GTP $\gamma\text{S}$  (or in the presence of  $1 \text{ mM}$  unlabeled GTP $\gamma\text{S}$ ) followed by adding GDP-loaded GST-Rac1 GTPases (or GST alone). The amount of [ $^{35}\text{S}$ ]GTP $\gamma\text{S}$  bound to samples in the absence of GTPases was subtracted from the original values. Data represent an average of triplicates from three to five experiments. The standard deviation was less than 5%. *Line a*, kinetics of [ $^{35}\text{S}$ ]GTP $\gamma\text{S}$  bound to GDP-loaded GST-Rac1 in the presence of Tiam1 (isolated from SP1 cells treated with HA); *line b*, kinetics of GTP $\gamma\text{S}$  bound to GDP-loaded GST-Rac1 in the presence of Tiam1 (isolated from SP1 cells without any treatment); *line c*, kinetics of [ $^{35}\text{S}$ ]GTP $\gamma\text{S}$  bound to GDP-treated GST in the presence of Tiam1 (isolated from SP1 cells treated with HA); *line d*, kinetics of [ $^{35}\text{S}$ ]GTP $\gamma\text{S}$  bound to GDP treated GST in the presence of Tiam1 (isolated from SP1 cells without any treatment).

26). Tiam1 is known to function as an exchange factor for the Rho-like GTPases such as Rac1 (34, 40–42). To investigate whether Tiam1 complexed with CD44v3 acts as a GDP/GTP exchange factor (or a GDP dissociation stimulator protein) for *E. coli*-derived GST-Rac1, we have isolated Tiam1 complexed with CD44v3 from SP1 cells using anti-Tiam1-conjugated Sepharose beads. Our data show that Tiam1 complexed with CD44v3 from SP1 cells causes the exchange of preloaded GDP for [ $^{35}\text{S}$ ]GTP $\gamma\text{S}$  on GST-Rac1 in a time-dependent manner (Fig. 7, lines *a* and *b*). Most importantly, addition of HA to CD44v3 containing SP1 cells stimulates the total amount of bound [ $^{35}\text{S}$ ]GTP $\gamma\text{S}$  to GST-Rac1 (Fig. 7, line *b*) (at least 1.5-fold increase) as compared with Tiam1 isolated from untreated SP1 cells (Fig. 7, line *b*) or HA-treated SP1 cells in the presence of anti-CD44v3 antibody (data not shown). No [ $^{35}\text{S}$ ]GTP $\gamma\text{S}$ -bound material was detected in these samples containing GST alone under the same GDP/GTP exchange reaction using Tiam1 isolated from SP1 cells (in the presence (Fig. 7, line *c*) or absence (Fig. 7, line *d*) of HA treatment). These findings suggest that the HA interaction with CD44v3 isoform-containing SP1 cells promotes Tiam1 activation of Rac1.

**CD44v3-Tiam1 Interaction in Rac1 Signaling and Cytoskeleton-mediated Tumor Cell Migration**—Previous studies indicate that the invasive phenotype of tumor cells characterized by an invadopodia structure (or membranous projections) (56, 57) and tumor cell migration (28, 29) is closely associated with CD44v<sub>3,8–10</sub>-linked cytoskeleton function (23). In this study we have transiently transfected breast tumor cells (e.g. SP-1 cells) with HA-tagged NH<sub>2</sub>-terminally truncated C1199 Tiam1 cDNA (Fig. 3B). Our results show that the C1199 Tiam1 is expressed as a 150-kDa protein (Fig. 8A, lane 1) detected by anti-HA-mediated immunoblot in CD44v<sub>3</sub>-positive breast tumor cells (SP1 cells). No protein band was detected in vector-transfected SP1 cells by anti-HA-mediated immunoblotting (Fig. 8A, lane 3). Using anti-CD44v3 immunoprecipitation of SP1 cellular protein followed by immunoblotting with anti-HA antibody, we have found that the 150-kDa C1199 Tiam1 is co-precipitated

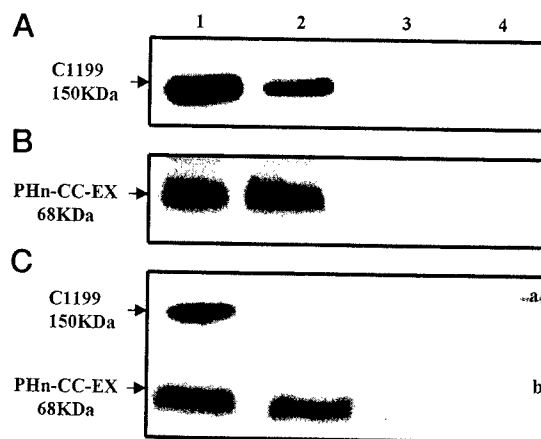


**FIG. 8. Transfection of SP1 cells with HA-tagged C1199Tiam1cDNA (A) or GFP-tagged PHn-CC-ExcDNA (B) or co-transfection of HA-tagged C1199Tiam1cDNA and GFP-tagged PHn-CC-ExcDNA (C).** A, detection of C1199 Tiam1 expression by anti-HA-mediated immunoblot in HA-tagged C1199 Tiam1cDNA transfected cells (lane 1) or in vector-transfected cells (lane 3); immunoblot of anti-CD44v3 immunoprecipitated materials (lane 2) or rabbit preimmune IgG precipitated materials (lane 4) from HA-tagged C1199 Tiam1cDNA transfected cells with anti-HA antibody. B, detection of PHn-CC-Ex expression by anti-GFP-mediated immunoblot in GFP-tagged PHn-CC-Ex cDNA transfected cells (lane 1) or vector-transfected cells (lane 3); immunoblot of anti-CD44v3 immunoprecipitated materials (lane 2) or rabbit preimmune IgG precipitated materials (lane 4) from GFP-tagged PHn-CC-Ex cDNA transfected cells with anti-GFP antibody. C, detection of co-expression of C1199 Tiam1 and PHn-CC-Ex by immunoblotting of cells (co-transfected with HA-tagged C1199 Tiam1cDNA and GFP-tagged PHn-CC-Ex cDNA) with anti-HA antibody (row *a*, lane 1) and anti-GFP antibody (row *b*, lane 1), respectively; immunoblotting of vector-transfected cell lysate with anti-HA antibody (row *a*, lane 3) and anti-GFP antibody (row *b*, lane 3), respectively; immunoblot of anti-CD44v3 immunoprecipitated materials (from HA-tagged C1199 Tiam1cDNA and GFP-tagged PHn-CC-Ex cDNA co-transfected cells) using anti-HA antibody (row *a*, lane 2) and anti-GFP antibody (row *b*, lane 2), respectively. Immunoblot of rabbit preimmune IgG-precipitated materials (from HA-tagged C1199 Tiam1cDNA and GFP-tagged PHn-CC-Ex cDNA co-transfected cells) using anti-HA antibody (row *a*, lane 4) and anti-GFP antibody (row *b*, lane 4), respectively.

with CD44v3 (Fig. 8A, lane 2). In control samples, immunoblotting of rabbit preimmune IgG-precipitated material using anti-HA antibody does not reveal any protein associated with this material (Fig. 8A, lane 4). Double immunofluorescence staining data also confirms the close association between CD44v3 (Fig. 9A) and the C1199 Tiam1 (Fig. 9B) in the plasma membranes and long membrane projections. In contrast, vector-transfected cells expressing CD44v3 on the surface (Fig. 9, inset *a*) (with no detectable C1199 Tiam1 by anti-HA label (Fig. 9, inset *b*)) fail to display long membrane projections. Furthermore, we have demonstrated that transfection of SP1 cells with C1199 Tiam1 cDNA stimulates CD44v3-associated Tiam1-catalyzed GDP/GTP exchange on Rac1 (Table II) and induces a significant amount of increase in CD44v3-specific and HA-mediated breast tumor cell migration (Table II) compared with vector-transfected SP1 transfectants (Table II). These results are consistent with previous findings indicating that transfection of NIH3T3 cells with the NH<sub>2</sub>-terminally truncated C1199 Tiam1 cDNA confers potent oncogenic properties (42). Treatment of SP1 cells (e.g. untransfected cells or transfected cells) with certain agents (e.g. cytochalasin D (a microfilament inhibitor)) causes a remarkable inhibition of CD44v3/HA-specific tumor cell migration (Table II). These observations suggest that CD44v3-associated Tiam1 signaling and cytoskeleton-mediated tumor cell motility are closely coupled.

Moreover, we have found that SP1 cells transfected with GFP-tagged PHn-CC-Ex Tiam1 cDNA express a 68-kDa pro-

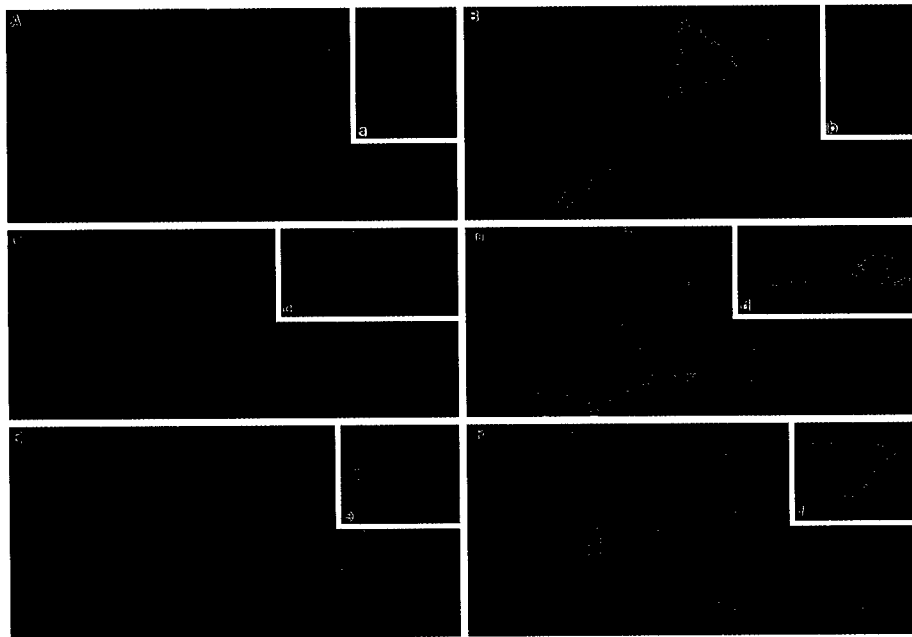


**FIG. 9. Double immunofluorescence staining of CD44v3 and Tiam1 cDNA (e.g. C1199 Tiam1 cDNA or PHn-CC-Ex cDNA)-transfected SP1 cells.** SP1 cells (transfected with HA-tagged C1199 Tiam1 cDNA or GFP-tagged PHn-CC-Ex cDNA or co-transfected with HA-tagged C1199 Tiam1 cDNA plus GFP-tagged PHn-CC-Ex cDNA) were fixed by 2% paraformaldehyde. Subsequently, cells were surface labeled with Rh-labeled rabbit anti-CD44v3 antibody. Some cells were then rendered permeable by ethanol treatment and stained with FITC-labeled mouse anti-HA IgG. **A and B**, Rh-labeled anti-CD44v3 staining (**A**) and FITC-anti-HA-labeled C1199 Tiam1 staining (**B**) in HA-tagged C1199 Tiam1 cDNA transfected SP1 cells. **Insets a and b**, Rh-labeled anti-CD44v3 staining (**a**) and FITC-anti-HA staining (**b**) in vector-transfected SP1 cells. **C and D**, Rh-labeled anti-CD44v3 staining (**C**) and GFP-tagged PHn-CC-Ex domain (**D**) in GFP-tagged PHn-CC-Ex cDNA transfected SP1 cells. **Insets c and d**, Rh-labeled preimmune IgG staining (**c**) and GFP-tagged PHn-CC-Ex domain (**d**) in GFP-tagged PHn-CC-Ex cDNA transfected SP1 cells. **E and F**, Rh-labeled anti-HA staining of C1199 Tiam1 (**E**) and GFP-tagged PHn-CC-Ex domain (**F**) in SP1 cells co-transfected with HA-tagged C1199 cDNA and GFP-tagged PHn-CC-Ex cDNA. **Insets e and f**, Rh-labeled anti-CD44v3 staining (**e**) and GFP-tagged PHn-CC-Ex domain (**f**) in SP1 cells co-transfected with HA-tagged C1199 cDNA and GFP-tagged PHn-CC-Ex cDNA.

tein as detected by anti-GFP antibody (Fig. 8B, lane 1). In vector-transfected SP1 cells, we are not able to detect any protein band by anti-GFP-mediated immunoblotting (Fig. 8B, lane 3). Using anti-CD44v3 immunoprecipitation of SP1 cellular protein followed by immunoblotting with anti-GFP antibody, we have found that the 68-kDa PHn-CC-Ex Tiam1 fragment is co-precipitated with CD44v3 (Fig. 8B, lane 2). No protein band was found when immunoblotting of rabbit preimmune IgG-precipitated materials with anti-GFP antibody was used (Fig. 8B, lane 4). It is also noted that both GFP-tagged PHn-CC-Ex domain (Fig. 9D) and CD44v3 are co-localized in the plasma membranes (Fig. 9C). However, no significant stimulation of long membrane projection was observed in these cells (Fig. 9, C, D, and insets c and d). Furthermore, we have demonstrated that CD44v3 staining detected in these SP1 transfectants revealed by anti-CD44v3-mediated immunostaining is specific because no surface label (Fig. 9, inset c) is detected in these GFP-PHn-CC-Ex overexpressed cells (Fig. 9, inset d) using preimmune rabbit IgG (Fig. 9, inset c). Additionally, we have demonstrated that overexpression of GFP-tagged PHn-CC-Ex domain in SP1 transfectants does not cause any significant changes of breast tumor cell properties (e.g. CD44v3-associated Tiam1-Rac1 signaling or HA-mediated tumor cell migration (Table II))

Finally, we have conducted co-transfection of SP1 cells with HA tagged C1199 Tiam1 cDNA and GFP-tagged PHn-CC-Ex cDNA. Our results indicate that C1199 Tiam1 and PHn-CC-Ex Tiam1 fragment are co-expressed as a 150-kDa protein (Fig. 8C, row a, lane 1) and a 68-kDa protein (Fig. 8C, row b, lane 1), respectively, in SP1 cells. No protein band was revealed in vector-transfected SP1 cells by anti-HA (Fig. 8C, row a, lane 3) or anti-GFP-mediated (Fig. 8C, row b, lane 3) immunoblotting. Using anti-CD44v3 antibody immunoprecipitation of SP1 cell lysate followed by immunoblotting with anti-GFP antibody and

anti-HA, respectively, we have found that the 68-kDa PHn-CC-Ex Tiam1 fragment (Fig. 8C, row b, lane 2) (but not 150-kDa C1199 Tiam1 (Fig. 8C, row a, lane 2)) is co-precipitated with CD44v3. In control samples, immunoblotting of rabbit preimmune IgG-precipitated material using anti-HA antibody (Fig. 8C, row a, lane 4) or anti-GFP antibody (Fig. 8C, row b, lane 4) does not reveal any protein associated with this material. Immunocytochemical staining results confirm that the PHn-CC-Ex Tiam1 fragment (Fig. 9, inset e) is co-localized with CD44v3 (Fig. 9, inset f) in the plasma membranes of SP1 transfectants. In contrast, the C1199 Tiam1 (Fig. 9E) fails to display plasma membrane localization as the PHn-CC-Ex domain does (Fig. 9F). Co-expression of PHn-CC-Ex domain and C1199 Tiam1 also efficiently blocks CD44v3-associated Tiam1-Rac1 activation and CD44v3-dependent and HA-mediated breast tumor cell migration (Table II). These results are consistent with a previous report showing that co-transfection of COS-7 cells with PHn-CC-Ex cDNA and C1199 Tiam1 cDNA results in an inhibition of C1199 Tiam1-induced Rac1 signaling and membrane ruffling (54). These findings suggest that the NH<sub>2</sub>-terminal PHn domain and an adjacent protein interaction domain (PHn-CC-Ex) play an important role in regulating Tiam1 localization to the plasma membrane proteins such as CD44v3 isoforms and for oncogenic signaling during extracellular matrix component (e.g. hyaluronic acid)-regulated breast tumor cell invasion and migration.

#### DISCUSSION

CD44 denotes a family of glycoproteins (e.g. CD44s (standard form), CD44E (epithelial form), and CD44v (variant isoforms)) that are expressed in a variety of cells and tissues (1–6). Clinical studies indicate that a number of CD44v isoforms have been detected at high levels on the surface of tumor cells during tumorigenesis and metastasis (13–17). As the histologic grade

TABLE II  
Measurement of CD44v<sub>3</sub>-associated Tiam1-catalyzed Rac1 activation  
and HA-mediated/cytoskeleton-mediated breast tumor cell migration

	CD44v <sub>3</sub> -associated Tiam1-catalyzed Rac1 activation: Amount of [ $\gamma$ - <sup>35</sup> S]GTP bound to GST-Rac1 <sup>a</sup>	
	pmol	% of control <sup>b</sup>
Untransfected cells (control)	1.50	100
Vector-transfected cells	1.47	98
PHn-CC-ExcDNA-transfected cells	1.42	95
C1199 Tiam1 cDNA-transfected cells	2.28	152
C1199 Tiam1 cDNA and PHn-CC-Ex cDNA co-transfected cells	1.35	90

	<i>In vitro</i> HA-mediated/CD44v <sub>3</sub> - specific cell migration <sup>a</sup>	
	Me <sub>2</sub> SO-treated control	Cytochalasin D-treated
	% of control <sup>b</sup>	
Untransfected cells (control)	100	20
Vector-transfected cells	97	25
PHn-CC-ExcDNA-transfected cells	95	23
C1199 Tiam1 cDNA-transfected cells	155	50
C1199 Tiam1 cDNA and PHn-CC-Ex cDNA co-transfected cells	90	15

<sup>a</sup> SP1 cells ( $\approx 1 \times 10^4$  cells/well in PBS, pH 7.2) (in the presence or absence of 20  $\mu$ g/ml cytochalasin D (dissolved in Me<sub>2</sub>SO) or Me<sub>2</sub>SO alone) were placed in the upper chamber of the transwell unit. In some cases, SP1 cells were transfected with either HA-tagged C1199 Tiam1 cDNA or GFP-tagged PHn-CC-ExcDNA or HA-tagged C1199 Tiam1 cDNA plus GFP-tagged PHn-CC-ExcDNA or vector alone. After 18 h of incubation at 37 °C in a humidified 95% air/5% CO<sub>2</sub> atmosphere, cells on the upper side of the filter were removed by wiping with a cotton swab. Cell migration processes were determined by measuring the cells that migrate to the lower side of the polycarbonate filters containing HA by standard cell number counting assays as described under "Materials and Methods." Procedures for measuring CD44v<sub>3</sub>-associated Tiam1-catalyzed GDP/GTP exchange reaction on GST-Rac1 were described under "Materials and Methods." Each assay was set up in triplicate and repeated at least three times. All data were analyzed statistically by Student's *t* test, and statistical significance was set at *p* < 0.01. In these experiments  $\approx 30$ –40% of input cells ( $\approx 1 \times 10^4$  cells/well) undergo *in vitro* cell invasion and migration in the control samples.

<sup>b</sup> The values expressed in this table represent an average of triplicate determinations of three to five experiments with a standard deviation of less than 5%.

of each of the tumors progresses, the percentage of lesions expressing an associated CD44v isoform increases. In particular, the CD44v<sub>3</sub>-containing isoforms are detected preferentially on highly malignant breast carcinoma tissue samples. In fact, there is a direct correlation between CD44v<sub>3</sub> isoform expression and increased histologic grade of the malignancy (14, 17, 57).

It has been speculated that some of these CD44v<sub>3</sub> isoforms on epithelial cells may act as surface modulators to facilitate unwanted growth factor receptor-growth factor interactions (9, 10) and subsequent tumor formation. The CD44-related glycoproteins are also known to mediate cell adhesion to extracellular matrix components (e.g. HA) and to function as the major hyaluronate receptor (50). In this study we have demonstrated that a 260-kDa CD44v<sub>3</sub> isoform is expressed on the surface of breast tumor cells (SP1 cell line) (Fig. 1) and that it interacts with extracellular matrix HA as an adhesion receptor (Table I). Furthermore, addition of HA to SP1 cells stimulates tumor cell migration in a CD44v<sub>3</sub>-specific and cytoskeleton-dependent manner (Table II). These findings are consistent with previous findings that CD44v isoforms expressed in tumor cells often display enhanced hyaluronic acid binding, which increases cell migration capability (58, 59).

The invasive phenotype of CD44v<sub>3</sub>-mediated breast tumor cells, characterized by invadopodia formation (23), matrix metalloproteinase-9 activation (23, 24), and tumor cell motility (23, 48) has been linked to cytoskeletal function, a process in which

the small GTP-binding proteins such as RhoA and Rac1 are shown to play important roles. Tsukita and co-workers (60) have reported that Rho-like proteins participate in the interaction between the CD44 and the ERM cytoskeletal proteins. Our recent study determined that RhoA is physically linked to CD44v<sub>3</sub> isoform (e.g. CD44v<sub>3, 8–10</sub>) in breast tumor cells (48). Rho-kinase stimulated by activated RhoA (GTP-bound form of RhoA) appears to play a pivotal role in promoting CD44v<sub>3, 8–10</sub>-ankyrin interaction during membrane-cytoskeleton function and metastatic breast tumor cell migration (48). Signaling to the RacGTPase known to regulate actin assembly associated with membrane ruffling, pseudopod extension, cell motility, and cell transformation (33–37) has been shown to be abnormal in breast tumor cells as compared with normal breast epithelial cells (61). The fact that Rac1 induces stress fiber formation in a Rho-dependent manner suggests that cross-talk occurs between the Rho and Rac1 signaling pathways (33). The question of whether the activation of Rac1 signaling is involved in CD44v<sub>3</sub>-cytoskeleton-mediated breast tumor-specific events remains to be answered.

Tiam1, which was identified by retroviral insertional mutagenesis and selected for its invasive cell behavior *in vitro*, has been shown to regulate Rac1 activation (38, 39). This molecule is largely hydrophilic and contains several functional domains including a Dbl homology domain (38, 62, 63), a Discs large homology region (38, 64), and two pleckstrin homology (PH) domains (e.g. PHn (the PH domain located at the NH<sub>2</sub>-terminal region of the molecule; and PHc (the PH domain located at the COOH-terminal region of the molecule)) (Fig. 3) (38). In particular, the Dbl homology domain of Tiam1 exhibits GDP/GTP exchange activity for specific members of the Ras superfamily of GTP-binding proteins (62, 63) and plays an important role in Rac1 signaling and cellular transformation (33–37). In breast tumor cells (e.g. SP1 cells), Tiam1 is detected as a 200-kDa protein (Fig. 2) that is capable of carrying out GDP/GTP exchange for Rac1 (Fig. 7), similar to Tiam1 described in other cell types (34, 40–42, 65, 66). Other functional domains such as Discs large homology region have been implicated in the binding of membrane protein networks (38, 64). The PH domain may mediate association with the submembrane region of the cell via protein-protein or protein-lipid interactions (67). Based on mutational analyses and immunofluorescence staining, Collard and co-workers (37, 54) report that the NH<sub>2</sub>-terminal PHn domain (but not PHc) and an adjacent protein interaction domain (e.g. PHn-CC-Ex domain) (Fig. 3) are required for Tiam1 targeting to the plasma membrane and Rac1 activation in fibroblasts. At the present time, identification of the membrane protein(s) involved in Tiam1 binding has not been established.

In this study we have presented new evidence that a close interaction occurs between Tiam1 and certain plasma membrane proteins such as CD44v<sub>3</sub> isoform. Using two recombinant proteins (CBP-tagged PHn-CC-Ex domain (Fig. 4, lane 1) and FLAG-tagged CD44 cytoplasmic domain (FLAG-CD44cyt) (Fig. 4, lane 2)), we have demonstrated that the PHn-CC-Ex domain of Tiam1 is directly involved in the binding to the cytoplasmic domain of CD44 (Figs. 5 and 6). In fact, the binding affinity of the PHn-CC-Ex domain of Tiam1 to CD44 is comparable with the intact Tiam1 binding to CD44 (Figs. 5 and 6). In the presence of PHn-CC-Ex, the binding between Tiam1 and CD44 (e.g. CD44v<sub>3</sub>) is greatly reduced (Fig. 6). The ability of PHn-CC-Ex to effectively compete for Tiam1 binding to the plasma membrane proteins such as CD44v<sub>3</sub> (Fig. 6) strongly suggests that the PHn-CC-Ex of Tiam1 is responsible for the recognition of CD44 *in vitro*.

In addition, we have detected that Tiam1 and CD44v<sub>3</sub> are physically linked to each other as a complex *in vivo* (Figs. 2, 8,

and 9) and that HA binding to CD44v3 promotes Tiam1-catalyzed Rac1 activation (Fig. 7 and Table II) and tumor cell migration (Table II). Our data also indicate that overexpression of Tiam1 (by transfecting SP1 cells with C1199 Tiam1cDNA) (Figs. 8 and 9) not only promotes C1199 Tiam1 association with CD44v3 (Figs. 8 and 9) but also enhances the metastatic capability of tumor cells (e.g. Rac1 activation and tumor cell migration (Table II)). These results suggest that Tiam1 and CD44v3 are not only structurally linked but also functionally coupled. Previously, it has been shown that Tiam1-activated Rac1 initiates oncogenic signaling cascades that involve activation of c-Jun NH<sub>2</sub>-terminal kinase (37, 54) and a novel family of serine/threonine kinases, Paks (p-21 activated kinases) (68, 69). However, the identification of CD44v3-Tiam1-mediated downstream targets (e.g. c-Jun NH<sub>2</sub>-terminal kinase and/or Paks activities) during HA-mediated breast tumor progression and metastasis remains to be answered.

Furthermore, we have found that co-transfection of SP1 cells with PHn-CC-Ex cDNA and C1199 Tiam1cDNA (Figs. 8 and 9) effectively blocks tumor cell-specific behaviors (e.g. C1199 Tiam1 association with CD44v3 (Figs. 8 and 9), Rac1 signaling (Table II), and tumor cell migration (Table II)). These findings further support our conclusion that PHn-CC-Ex acts as a potent competitive inhibitor that is capable of interfering with C1199 Tiam1-CD44v3 interaction *in vivo*. Recently, we have also identified a unique sequence residing within the PHn-CC-Ex domain as the putative cytoskeletal binding site of Tiam1 (70). Most importantly, interaction between Tiam1 and the cytoskeleton up-regulates the GDP/GTP exchange activity of Rho-like GTPases and stimulates breast tumor cell invasion/migration (70). These observations clearly suggest that the PHn-CC-Ex fragment of Tiam1 is one of the important regulatory domains required for Tiam1 function.

In fibroblasts, Tiam1-induced membrane ruffling is dependent on Rac1 (but not RhoA) activity (71). The fact that Tiam1 is involved in both Rac1- and RhoA-mediated pathways during neurite formation in nerve cells suggests that the balance between two Tiam1-activated Rho-like GTPases (e.g. Rac1 and RhoA) determines a particular biological activity (65). Tiam1-Rac1 signaling is also implicated in promoting integrin-mediated cell-cell and cell-extracellular matrix interaction and lymphoid cell invasion (34, 65). In addition, the laminin receptor,  $\alpha_6\beta_1$  integrin appears to require Rac1 as a downstream of Tiam1 signaling in neuroblastoma cell activation (65). In epithelial Madin-Darby canine kidney cells, fibronectin and/or laminin1-induced Tiam1-Rac1 signaling up-regulates E-cadherin-mediated adhesion and plays an invasion-suppressor role in Ras-transformed Madin-Darby canine kidney cells (66). However, if Madin-Darby canine kidney cells were grown on different collagen substrates, the expression of Tiam1 or constitutively activated Rac1 (V12Rac) in these cells is able to inhibit the appearance of E-cadherin adhesion and promote cell migration (72, 73). Our studies show that approximately 60% ( $63 \pm 4\%$ ,  $n = 5$ ) of the GDP dissociation activity can be detected in the guanine nucleotide exchange assay using Tiam1 isolated from untreated breast tumor cells (Fig. 7 and Table II). We have also observed that approximately 90% ( $92 \pm 5\%$ ,  $n = 5$ ) of Rac1 is exchanging GDP for GTP in the presence of Tiam1 isolated from either HA-treated cells (Fig. 7) or C1199 Tiam1 cDNA-transfected breast tumor cells (Table II). These findings suggest that Tiam1-catalyzed Rac1 activation is tightly regulated by various signals. Apparently, different responses by Tiam1-catalyzed Rho-like GTPases are controlled by specific upstream activators (in particular, cell adhesion receptors (e.g. CD44, integrin, or E-cadherin, etc.) or extracellular matrix components (e.g. HA, collagens, laminin, or fibronectin, etc.)),

which may result in selective Tiam1-activated Rho-like GTPases and distinct biological outcome. In summary, we believe that Tiam1-CD44v3 interaction plays a pivotal role in regulating oncogenic signaling required for RhoGTPase activation and cytoskeleton function during HA-mediated metastatic breast tumor cell progression. This could be one of the critical steps in CD44 variant isoform-mediated breast tumor spread and metastasis.

**Acknowledgments**—We gratefully acknowledge Dr. Gerard J. Bourguignon's assistance in the preparation of this paper. We also thank Dr. Dan Zhu for help in reviewing the manuscript.

## REFERENCES

- Lesley, J., Hyman, R., and Kincade, P. W. (1993) *Adv. Immunol.* **54**, 271–335
- Picker, L. J., Nakache, M., and Butcher, E. C. (1989) *J. Cell Biol.* **109**, 927–937
- Bourguignon, L. Y. W., Lokeshwar, V. B., He, J., Chen, X., and Bourguignon, G. J. (1992) *Mol. Cell. Biol.* **12**, 4464–4471
- Zhu, D., and Bourguignon, L. Y. W. (1996) *Oncogene* **12**, 2309–2314
- Brown, T. A., Bouchard, T., St. John, T., Wayner, E., and Carter, W. G. (1991) *J. Cell Biol.* **113**, 207–221
- Bourguignon, L. Y. W. (1996) *Curr. Topics Membr.* **43**, 293–312
- Stamenkovic, I., Amiot, M., Pesando, J. M., and Seed, B. (1991) *EMBO J.* **10**, 343–347
- Screation, G. R., Bell, M. V., Jackson, D. G., Cornelis, F. B., Gerth, U., and Bell, J. I. (1992) *Proc. Natl. Acad. Sci. U. S. A.* **89**, 12160–12164
- Bennett, K. L., Jackson, D. G., Simon, J. C., Tanczos, E., Peach, R., Modrell, B., Stamenkovic, I., Plowman, G., and Aruffo, A. (1995) *J. Cell Biol.* **128**, 687–698
- Jackson, D. G., Bell, J. I., Dickinson, R., Timans, J., Shields, J., and Whittle, N. (1995) *J. Cell Biol.* **128**, 673–685
- Jalkanen, S. P., and Jalkanen, M. (1992) *J. Cell Biol.* **116**, 817–825
- Lokeshwar, V. B., and Bourguignon, L. Y. W. (1991) *J. Biol. Chem.* **266**, 17983–17989
- Dall, P., Heider, K.-H., Sinn, H.-P., Skroch-Angel, P., Adolf, G., Kaufmann M., Herrlich, P., and Ponta, H. (1995) *Int. J. Cancer* **60**, 471–477
- Iida, N., and Bourguignon, L. Y. W. (1995) *J. Cell. Physiol.* **162**, 127–133
- Kaufmann, M., Meider, K. H., Sinn, H. P., von Minckwitz, G., Ponta, H., and Herrlich, P. (1995) *Lancet* **345**, 615–619
- Rodriguez, C., Monges, G., Rouanet, P., Dutrillaux, B., Lefrancois, D., and Theillet, C. (1995) *Int. J. Cancer* **64**, 347–354
- Kalish, E., Iida, N., Moffat, E. L., and Bourguignon, L. Y. W. (1999) *Front. Biosci.* **4**, 1–8
- Bourguignon, L. Y. W., Zhu, D., and Zhu, H. B. (1998) *Front. Biosci.* **3**, 637–649
- Bourguignon, L. Y. W., Iida, N., Welsh, C. F., Zhu, D., Krongrad, A., and Pasquale, D. (1995) *J. Neuro-Oncol.* **26**, 201–208
- Lokeshwar, V. B., Fregien, N., and Bourguignon, L. Y. W. (1994) *J. Cell Biol.* **126**, 1099–1109
- Zhu, D., and Bourguignon, L. Y. W. (1998) *Cell Motil. Cytoskelet.* **39**, 209–222
- Bourguignon, L. Y. W., Zhu, H., Chu, A., Iida, N., Zhang, L., and Hung, H. C. (1997) *J. Biol. Chem.* **272**, 27913–27918
- Bourguignon, L. Y. W., Gunja-Smith, Z., Iida, N., Zhu, H. B., Young, L. J. T., Muller, W. J., and Cardiff, R. D. (1998) *J. Cell. Physiol.* **176**, 206–215
- Yu, Q., and Stamenkovic, I. (1999) *Genes Dev.* **13**, 35–48
- Ridley, A. J., and Hall, A. (1992) *Cell* **70**, 389–399
- Hall, A. (1998) *Science* **279**, 509–514
- Dickson, R. B., and Lippman, M. E. (1995) *The Molecular Basis of Cancer* (Mendelsohn, J., Howlwy, P. M., and Israel, M. A., and Liotta, L. A., eds) pp. 358–359. W. B. Saunders Company, Philadelphia, PA
- Jiang, W. G., Puntis, M. C. A., and Hallett, M. B. (1994) *Br. J. Surgery* **81**, 1576–1590
- Lauffenburger, D. A., and Horwitz, A. F. (1996) *Cell* **84**, 359–369
- Deleted in proof
- Deleted in proof
- Deleted in proof
- Ridley, A. J., Paterson, C. L., Johnston, C. L., Diekmann, D., and Hall, A. (1992) *Cell* **70**, 401–410
- Nobes, C. D., and Hall, A. (1995) *Cell* **81**, 53–62
- Coso, O. A., Chiariello, M., Yu, J. C., Teramoto, H., Crespo, P., Xu, N. G., Miki, T., and Gutkind, J. S. (1995) *Cell* **81**, 1137–1146
- Minden, A., Lin, A. N., Claret, F. X., Abo, A., and Karin, M. (1995) *Cell* **81**, 1147–1157
- Michiels, F., Stam, J. C., Hordijk, P. L., van der Kammen, R. A., Ruuls-Van Stalle, L., Feltkamp, C. A., and Collard, J. G. (1997) *J. Cell Biol.* **137**, 387–398
- Habets, G. G. M., Scholtes, E. H. M., Zuydgeest, D., van der Kammen, R. A., Stam, J. C., Berns, A., and Collard, J. G. (1994) *Cell* **77**, 537–549
- Habets, G. G. M., van der Kammen, R. A., Stam, J. C., Michiels, F., and Collard, J. G. (1995) *Oncogene* **10**, 1371–1376
- Michiels, F., Habets, G. G. M., Stan, J. C., van der Kammen, R. A., and Collard, J. G. (1995) *Nature* **375**, 338–340
- Woods, D. F., and Bryant, P. J. (1991) *Cell* **66**, 451–464
- Van Leeuwen, F. N., van der Kammen, R. A., Habets, G. G. M., and Collard, J. G. (1995) *Oncogene* **11**, 2215–2221
- Stam, J. C., Michiels, F., van der Kammen, R. A., Moolenaar, W. H., and Collard, J. G. (1998) *EMBO J.* **17**, 4066–4074
- Fleming, I. N., Elliott, C. M., Collard, J. G., and Exton, J. H. (1997) *J. Biol. Chem.* **272**, 33105–33110
- Fleming, I. N., Elliott, C. M., and Exton, J. H. (1998) *FEBS Lett.* **429**, 229–233

46. Fleming, I. N., Elliott, C. M., Bruchanan, F. G., Downes, C. P., and Exton, J. H. (1999) *J. Biol. Chem.* **274**, 12753-12758
47. Elliott, B. E., Maxwell, L., Arnold, M., Wei, W. Z., and Miller, E. R. (1988) *Cancer Res.* **48**, 7237-7245
48. Bourguignon, L. Y. W., Zhu, H. B., Shao, L., Zhu, D., and Chen, Y. W. (1999) *Cell Motil. Cytoskelet.* **43**, 269-287
49. Zhang, Y., Hart, M. J., and Cerione, R. A. (1995) *Methods Enzymol.* **256**, 77-84
50. Underhill, C. B., Green, S. J., Comoglio, P. M., and Tarone, G. (1987) *J. Biol. Chem.* **262**, 13142-13146
51. Lesley, J., Hyman, R., and Kincade, P. (1993) *Adv. Immunol.* **54**, 271-235
52. Peach, R. J., Hollenbaugh, D., Stamenkovic, I., and Aruffo, A. (1993) *J. Cell Biol.* **122**, 257-264
53. Liao, H. X., Lee, D. M., and Haynes, B. F. (1995) *J. Immunol.* **155**, 3938-3945
54. Stam, J. C., Sander, E. E., Michiels, F., van Leeuwen, F. N., Kain, H. E. T., van der Kammen, R. A., and Collard, J. G. (1997) *J. Biol. Chem.* **272**, 28447-28454
55. Deleted in proof
56. Mueller, S. C., and Chen, W. T. (1991) *J. Cell Sci.* **99**, 213-225
57. Sinn, H. P., Heider, K. H., Skroch-Angel, P., von Minckwitz, G., Kaufmann, M., Herrlich, P., and Ponta, H. (1995) *Breast Cancer Res. Treat.* **36**, 307-313
58. Horst, E., Meijer, C. J., Radaszkiewicz, T., Ossekoppele, G. J., Van Krieken, J. H., and Pals, S. T. (1990) *Leukemia* **4**, 595-599
59. Jalkanen, S., Joensuu, H., Oderstr, S., Ko, O., and Kleini, P. (1991) *J. Clin. Invest.* **87**, 1835-1840
60. Hirao, M., Sato, N., Kondo, T., Yonemura, S., Monden, M., Sasaki, T., Takai, Y., Tsukita, S., and Tsukita, S. (1996) *J. Cell Biol.* **135**, 36-51
61. Johnston, C. L., Cox H. C., Gomm, J. J., and Coombes, R. C. (1995) *Biochem. J.* **306**, 609-616
62. Hart, M. J., Eva, A., Evans, T., Aaronson, S. A., and Cerione, R. A. (1991) *Nature* **354**, 311-314
63. Hart, M. J., Eva, A., Zangrilli, D., Aaronson, S. A., Evans, T., Cerione, R. A., and Zheng, Y. (1994) *J. Biol. Chem.* **269**, 62-65
64. Pontings, C. P., and Phillips, C. (1995) *Trends Biochem. Sci.* **20**, 102-103
65. Van Leeuwen, F. N., Kain, H. E., Kammen, R. A., Michiels, F., Kranenburg, O. W., and Collard, J. G. (1997) *J. Cell Biol.* **139**, 797-807
66. Hordijk, P. L., ten Klooster, J. P., van der Kammen, R. A., Michiels, F., Oomen, L. C., and Collard, J. G. (1997) *Science* **278**, 1464-1466
67. Lemmon, M. A., Ferguson, K. M., and Schlessinger, J. (1996) *Cell* **85**, 621-624
68. Manser, E., Leung, T., Salihuddin, H., Zhao, Z., and Lim, L. (1994) *Nature* **367**, 40-46
69. Knaus, U. G., Morris, S., Dong, H., Chernoff, J., and Bokoch, G. M. (1995) *Science* **269**, 221-223
70. Bourguignon, Lilly Y. W., H. Zhu, L. Shao, and Y. W. Chen, (1999) *Proc. Am. Assoc. Cancer Res.* **40**, 196
71. Nishiyama, T., Sasaki, T., Takaishi, K., Kato, M., Yaku, M., Araki, K., Matsuura, Y., and Takai, Y. (1994) *Mol. Cell. Biol.* **14**, 2447-2456
72. Sander, E. E., van delft, S., ten Klooster, J. P., Reid, T., van der kammen, R. A., Michiels, F., and Collard, J. G. (1998) *J. Cell Biol.* **143**, 1385-1398
73. Michiels, F., and Collard, J. G. (1999) *Biochem. Soc. Symp.* **65**, 125-146
74. Chu, G., Hayakawa, H., and Berg, P. (1987) *Nucleic Acids Res.* **15**, 1311-1326

## CD44-Mediated Oncogenic Signaling and Cytoskeleton Activation During Mammary Tumor Progression

Lilly Y. W. Bourguignon<sup>1,2</sup>

CD44, a hyaluronan (HA)<sup>3</sup> receptor, belongs to a family of transmembrane glycoproteins which exists as several isoforms. Cell surface expression of certain CD44 isoforms is closely correlated with the progression and prognosis of breast cancers. A number of angiogenic factors (e.g., VEGF and FGF-2) and matrix degrading enzymes (MMPs) are tightly complexed with CD44 isoforms, suggesting that they are involved in the onset of oncogenic signals required for breast tumor cell invasion and migration. Most importantly, interaction of extracellular matrix components (e.g., HA) with cells triggers the cytoplasmic domain of CD44 isoforms to bind its unique downstream effectors (e.g., the cytoskeletal protein ankyrin or various oncogenic signaling molecules-Tiam1, RhoA-activated ROK, c-Src kinase and p185<sup>HER2</sup>) and to coordinate intracellular signaling pathways (e.g., Rho/Ras signaling and receptor-linked/non-receptor-linked tyrosine kinase pathways), leading to a concomitant onset of multiple cellular functions (e.g., tumor cell growth, migration and invasion) and breast tumor progression.

**KEY WORDS:** CD44; oncogenic signaling; ankyrin; Rho GTPases; breast tumor progression.

### INTRODUCTION

Most breast cancers develop from mammary epithelial tissue. The resulting tumors (carcinomas) are very heterogeneous—ranging from very slow growing to highly aggressive, metastatic forms resistant to chemotherapy (1, 2). Breast carcinomas *in situ* (either ductal or lobular in origin) can progress to infiltrating carcinomas in the breast stroma, and finally metastasize to distant tissues (most often bone, lung, liver or brain) via the extensive breast lymphatic network (1, 2). Diagnosis of whether a lesion is benign or

malignant is often difficult, since definitive breast cancer cellular markers are lacking. Furthermore, the basic cellular and molecular processes underlying breast tumor cell invasion and metastasis are poorly understood. It is quite clear, however, that cell membrane-cytoskeleton interactions are generally involved in tumor cell motility, invasion of surrounding tissue and metastasis (2, 3). In particular, it is known that membrane-associated cytoskeletal proteins and the actomyosin-based contractile machinery are required for tumor cell movement and infiltration of surrounding tissue (2, 3). The details of this process, however, remain to be determined.

A number of studies have been aimed at identifying molecules expressed by breast tumor cells which correlate with metastatic behavior. Among such candidates are the CD44 isoforms, a family of transmembrane glycoproteins that contain a variable extracellular domain, a single 23 amino acid transmembrane domain and a 70 amino acid cytoplasmic domain (4). A distinct feature of CD44 isoforms is the enormous heterogeneity in the molecular masses of these proteins. CD44 isoforms are the major hyaluronan cell surface receptors (5). The extracellular domain of

<sup>1</sup> Department of Cell Biology and Anatomy, University of Miami Medical School, Miami, Florida 33136. e-mail: lbourgui@med.miami.edu

<sup>2</sup> Present address: Department of Medicine, University of California San Francisco, VA Medical Center, San Francisco, California 94121.

<sup>3</sup> Abbreviations: hyaluronic acid (HA); glycosaminoglycan (GAG); fibroblast growth factor-2 (FGF-2); interleukin 8 (IL-8); vascular epithelial growth factor (VEGF); matrix metalloproteinases (MMPs); ankyrin repeat domain (ARD); Rho-Kinase (ROK); guanine nucleotide exchange factors (GEFs); T lymphoma invasion and metastasis1 (Tiam1).

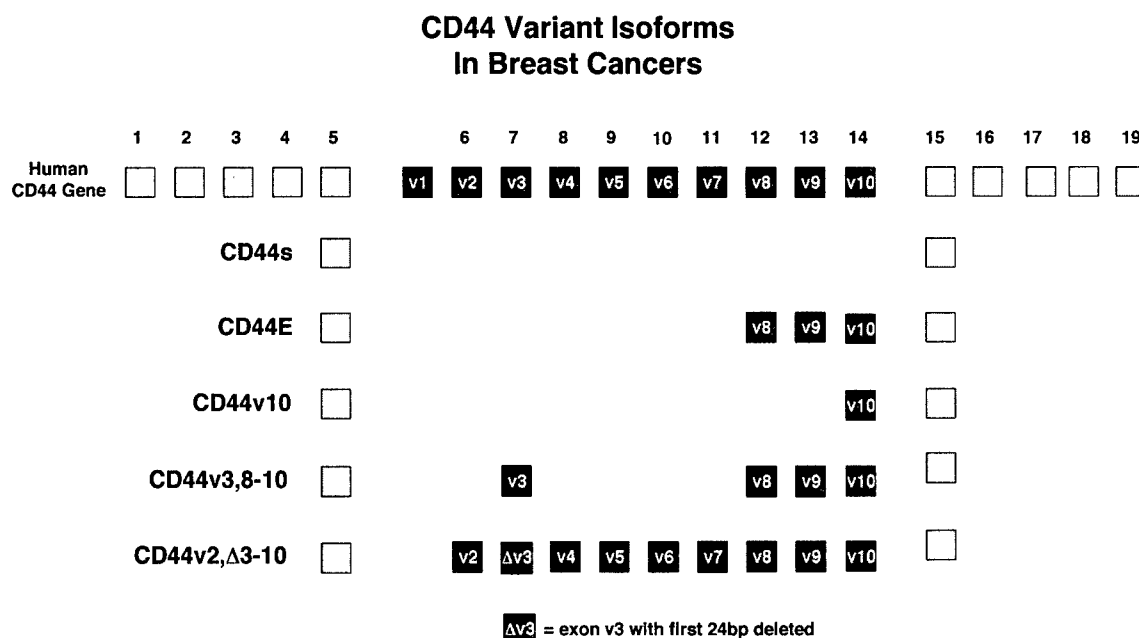


**Fig. 1.** Exon map of CD44 in human and schematic illustration of the CD44 isoforms, CD44s (the standard form), CD44E (the epithelial form), CD44v10, CD44v3,8–10 and CD44v2,Δv3–10 isoform detected in primary breast tumor tissues and axillary lymph nodal metastases.

CD44 isoforms mediate cell adhesion to hyaluronic acid (HA), the major glycosaminoglycan in the extracellular matrix (ECM) of most mammalian tissues (6). Both CD44 and HA are overexpressed at sites of tumor attachment, and are involved in cell aggregation, proliferation, migration and angiogenesis (7–10).

All CD44 isoforms are encoded by a single gene which contains 19 exons (Fig. 1) (11). The most common form, CD44s (CD44 standard form), contains exons 1–4 (N-terminal 150 a.a.), exons 5, 15 and 16 (membrane proximal 85 a.a.), exon 17 (transmembrane domain), and a portion of exons 17 and 19 (cytoplasmic tail, 70 a.a.) (Fig. 1) (11). Out of the 19 exons, 12 exons can be alternatively spliced (Fig. 1) (11). Most often, the alternative splicing occurs between exons 5 and 15, leading to an insertion in tandem of one or more variant exons (exon 6–exon 14; v1–v10 in human cells) within the membrane proximal region of the extracellular domain (Fig. 1) (11). For example, epithelial cells contain additional exons 12–14 which are inserted into the CD44s transcripts (Fig. 1) (11). This isoform has been designated as CD44E (Fig. 1) (11). Various tumor cells and tissues express different CD44 variant (CD44v) isoforms in addition to CD44s and CD44E (Fig. 1) (11). These CD44v isoforms have the same amino acid sequences at the two ends of the molecule but differ in a middle region

which contains a variable number of exon insertions (exons 6–14) within the CD44 membrane proximal region located at the external side of the membrane (Fig. 1) (11). Different CD44 isoforms are further modified by extensive N- and O-glycosylations and glycosaminoglycan (GAG) additions (12–14). Apparently, both post-translational modifications and/or the alternative splicing within the CD44 isoform structure determine the functional attributes of this molecule.

### CD44s (CD44 STANDARD FORM) AND ITS INTERACTION WITH TYROSINE KINASES IN ONCOGENESIS

CD44 isoforms are often up-regulated in breast carcinomas (15–19). In fact, the presence of a high level of CD44 isoform (particularly CD44s) expression is emerging as an important metastatic tumor marker in a number of carcinomas and is also implicated in the unfavorable prognosis of a variety of cancers (15–19). Carcinomas expressing high levels of CD44s are more malignant than those carcinomas with a low level of CD44s expression (16). Cells expressing a high level of CD44s also display enhanced hyaluronic acid (HA) binding, which increases their migration capability (20, 21). It is likely that the binding of extracellular matrix materials (e.g.,

hyaluronic acid) to overexpressed CD44s triggers specific oncogenic signaling pathways leading to metastatic breast tumor cell-specific behaviors.

Specifically, CD44s is tightly coupled with at least two different tyrosine kinase oncogenic regulators, p185<sup>HER2</sup> (22) and c-Src kinase (23, 24), in epithelial tumor cells. Both CD44s and tyrosine kinases (e.g., p185<sup>HER2</sup> and c-Src kinase) are often overexpressed in human tumor cells (15–28). In particular, CD44s and the receptor-linked tyrosine kinase p185<sup>HER2</sup> are shown to be closely associated in a complex involving interchain disulfide bonds in metastatic epithelial tumor cells (22). Based on the predicted sequence obtained from cDNA cloning of the human CD44s gene, 8–9 cysteine residues have been identified: 6–7 cysteine residues in the external domain, one cys(aa 286) in the transmembrane region and one cys(aa 295) in the cytoplasmic domain (11). The functional significance of the cysteine residues in the external domain of CD44s is not clear at the present time. However, point mutation of <sup>286</sup>cys (but not <sup>295</sup>cys) of human CD44s has been reported to cause a reduction (or loss) of hyaluronic acid (HA) binding (29). Two cysteine residues (e.g., <sup>286</sup>cys in the transmembrane domain and/or <sup>295</sup>cys in the cytoplasmic domain) in mouse CD44s have been shown to play an important role in signal transduction and cell adhesion (29). For example, these residues appear to be involved in CD44s fatty acylation required for CD44s and ankyrin interaction (30). It is possible that some of these cysteine residues of CD44s are also involved in the disulfide linkage with one or more cysteine residues in p185<sup>HER2</sup>. Most importantly, the binding of HA to tumor cells stimulates CD44-associated p185<sup>HER2</sup> tyrosine kinase activity (shown to activate Ras signaling), causing an increase in tumor cell growth (22).

Several lines of evidence indicate that phosphorylation of proteins on tyrosine residues by non-receptor-linked protein tyrosine kinases, such as those in the Src family, is involved in the progression of human breast cancer (26). The activity of c-Src kinase appears to be closely correlated with its ability to interact with tyrosine-phosphorylated p185<sup>HER2</sup> (31). The Src kinase family signaling pathway is also closely associated with CD44-mediated cytoskeleton function (23, 24). Recent studies have shown that a specific interaction occurs between the cytoplasmic domain of CD44s and c-Src kinase in epithelial tumor cells (24). The binding of HA to tumor cells promotes c-Src kinase recruitment to CD44s and stimulates c-Src kinase activity which, in turn, increases tyrosine phosphorylation of the cytoskeletal protein, cortactin.

Subsequently, tyrosine phosphorylation of cortactin attenuates its ability to cross-link filamentous actin *in vitro* (24). Furthermore, overexpression of a dominant-active form of c-Src kinase, by transfecting CD44s-positive tumor cells with c-Src (Y527F) cDNA, promotes the activation of CD44s/c-Src kinase-regulated cortactin function and tumor cell migration. Transfection of CD44s-positive tumor cells with a dominant-negative mutant of c-Src kinase (K295R-kinase dead) effectively blocks the tumor cell-specific phenotype. Therefore, CD44 activated c-Src kinase signaling appears to be directly involved in stimulating the cortactin-cytoskeleton interaction and HA-mediated tumor cell migration. In addition, the CD44s/c-Src kinase interaction also initiates epithelial tumor cell growth and transformation (23). An active form of Src tyrosine kinase has been shown to be closely linked to G-protein-coupled receptors during MAP kinase activation in PC-12 cells (32). These results suggest that the preferential binding of the active form of c-Src tyrosine kinase(s) to the cytoplasmic domain of CD44s is required for HA-mediated tumor cell transformation and migration.

#### CD44 VARIANT (CD44v) ISOFORMS IN MAMMARY TUMOR PROGRESSION

Breast cancer cells and tissues have been found to express numerous patterns of CD44 alternative splicing, compared to their normal tissue counterparts, during tumor growth and metastasis (15–19). One such CD44 variant isoform containing v6 (i.e., CD44v6) has been correlated with a poor prognosis in a rat pancreatic carcinoma and non-Hodgkin's lymphoma (33, 34). In the case of breast cancer, it is still controversial whether CD44v6 has prognostic value for survival, since some studies indicated that CD44v6 might serve as a differentiation marker but not a predictor of tumor progression in human mammary carcinoma (35). Among tumor-associated CD44 isoforms several variant CD44 isoforms (CD44v10 and CD44v3) have been detected from the early stage of mammary tumor development to lymph node metastasis (Fig. 1) and appear to play an important role in promoting breast tumor progression.

#### CD44v10 and Mammary Tumor Cell Transformation

Cell surface expression of CD44v10 changes profoundly during tumor metastasis—particularly

during the progression of various carcinomas, including breast carcinomas (15–19). Overexpression of CD44v10 on epithelial tumor cells (HBL100 cell line) alters several important biological properties when compared to the normal epithelial cells (36). Specifically, breast tumor cells overexpressing CD44v10 display a significant reduction in hyaluronic acid (HA)-binding and cell adhesion to HA-coated plates and show an increased migration capability in collagen-matrix gels (36). Furthermore, breast tumor cells expressing a high level of CD44v10 constitutively produce certain angiogenic factors, such as interleukin 8 (IL-8) and fibroblast growth factor-2 (FGF-2), and effectively promote tumorigenesis in athymic nude mice (36). These findings suggest that the overexpression of CD44v10 may play a pivotal role in triggering the onset of cell transformation required for breast cancer development.

CD44v10 is also known to undergo extensive posttranslational modification, including N-/O-linked glycosylation and chondroitin sulfate addition (14). The inclusion of glycosylation and/or chondroitin sulfate in the v10-encoded structure at a membrane proximal region may prevent the dimerization (clustering) of CD44 molecules known to provide high affinity binding to HA (37). The insertion of an additional 68 amino acids in the CD44v10 may cause a conformational change in the HA-binding domains located in the extracellular domains of this molecule, resulting in a loss of HA binding. It is also possible that overexpression of CD44v10 induces heparan sulfate-chondroitin sulfate switching (38), which causes a decrease in cell adhesion. The reduction of HA-mediated binding and cell adhesion in CD44v10-overexpressing breast tumor cells may be one of the earliest changes occurring in mammary epithelial cell transformation. However, the lack of HA-binding and adhesion does not result in a loss of intracellular signaling. In fact, overexpression of the CD44v10 isoform stimulates invasive potential and tumorigenesis, as demonstrated *in vivo* by tumor formation in nude mice and altered secretion of angiogenic factors, such as interleukin 8 (IL-8) and FGF-2 (37). These observations lead to the interesting hypothesis that overexpression of CD44v10 in mammary epithelial cells is sufficient to trigger CD44-mediated intracellular signaling without binding to the HA ligand. The loss of HA-mediated cell adhesion in cells expressing CD44v10 may be one of the earliest events in the onset of breast tumor migration and invasion processes.

### CD44v3 and Mammary Tumor Cell Invasion and Migration

The level of CD44v3 isoform expression often increases as the histologic grade of each of the breast tumors progresses. In fact, there is a direct correlation between CD44v3 isoform expression and increased histologic grade of the malignancy (16, 19). These lines of evidence suggest that expression of certain CD44v3 isoform(s) may be an accurate predictor of eventual survival (e.g., nodal status, tumor size, and grade) during breast cancer progression (17). CD44v3 has a heparin sulfate addition site in the membrane-proximal extracellular domain of the molecule that confers the ability to bind heparin sulfate-binding growth factors (39). In particular, CD44v3 (with heparan sulfate addition) has been found to bind FGF-2 *in vitro* (39). Both CD44v3 and FGF-2 are also colocalized in normal skin and epidermal skin cancers (40). Most importantly, the binding of FGF-2 to CD44v3 stimulates cell proliferation of normal and transformed keratinocytes (40). In breast tumor cells, the external domain of sulfated glycosaminoglycan-containing CD44v3 preferentially binds vascular epithelial growth factor (VEGF), but not FGF-2 (41). VEGF is a specific mitogen for endothelial cells and a potent microvascular permeability factor (42). It plays an integral role in angiogenesis, and thus potentiates solid tumor growth (42). A previous study showed that breast tumor cells containing CD44v3 are capable of inducing a high level of intratumoral microvessel formation (43, 44). Therefore, the attachment of VEGF to the heparin sulfate sites on CD44v3 may be responsible for the onset of breast tumor-associated angiogenesis.

A number of different matrix metalloproteinases (MMPs), including the 72 kDa gelatinase (gelatinase A, type IV collagenase, MMP-2), the 92 kDa gelatinase (gelatinase B, type V collagenase, MMP-9), the stromelysins (MMP-3, MMP-11) and the interstitial fibroblast-type collagenase (MMP-1) are thought to play an important role in degrading extracellular matrix components during tumor invasion and metastases (45). In breast tumor cells, CD44v3 and MMP-9 (gelatinase B) are closely associated in the plasma membrane (44). Furthermore, MMP-9 is present in a proteolytically active form and is preferentially localized at the "invadopodia" of the breast tumor cells (Fig. 2). These findings are consistent with previous findings indicating that certain proteases are localized on "invadopodia" of human malignant melanoma cells (46). Therefore, it is likely that the close interaction between CD44v3 and the

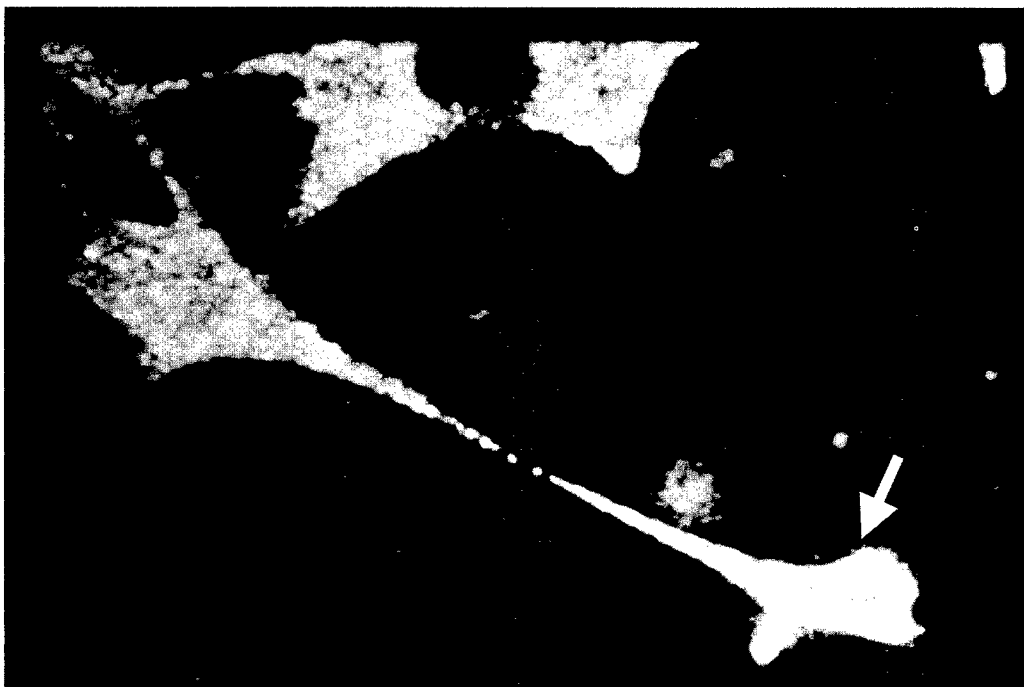


**Fig. 2.** Immunofluorescence staining of membrane-bound MMP-9 using fluorescein-labeled rabbit anti-MMP-9 IgG and confocal analysis of "Invadopodia" structures (indicated by an arrow) in breast tumor cells (Met-1 cell line) expressing CD44v3 isoform.

active form of MMP-9 in the "invadopodia" of breast tumor cells may be required for the degradation of extracellular matrix (ECM) during breast tumor cell invasion and metastasis.

Overexpression of CD44v3 isoforms also promotes breast tumor cell migration (44). CD44v3 is found to be closely linked to the cytoskeleton and actomyosin contractile system required for "invadopodia" formation and tumor cell migration (44). Treatment of breast tumor cells with certain agents, including cytochalasin D (a microfilament inhibitor) and W-7 (a calmodulin antagonist), but not colchicine (a microtubule disrupting agent), effectively inhibits "invadopodia" formation, matrix degradation activities and subsequent tumor cell migration (44). These findings support the notion that CD44v3 interaction with the cytoskeleton plays an important role in breast tumor progression.

#### **CD44 ISOFORM INTERACTION WITH THE CYTOSKELETAL PROTEIN ANKYRIN IN MAMMARY TUMOR PROGRESSION**

CD44 isoforms bind extracellular matrix components (e.g., hyaluronic acid) via their extracellular

domain (23, 47, 48). The cytoplasmic domain of CD44 (approximately 70 a.a. long) is highly conserved in most CD44 isoforms and is clearly involved in a specific binding interaction with certain cytoskeletal proteins, such as ankyrin (23, 48). Deletion mutation analysis indicates that at least two subregions within the cytoplasmic domain of CD44 isoforms constitute the ankyrin binding-region I (the high affinity ankyrin-binding region) and region II (the regulatory region) (48). In particular, the region I of the ankyrin-binding domain plays an important role in HA-mediated functions. Further studies have shown that the ankyrin binding region of CD44 isoforms is also necessary for both oncogenic signaling and tumor cell transformation (23, 48). Therefore, we proposed that the binding of HA to CD44's external region and the linkage of ankyrin to CD44's internal tail region are directly involved in tumor cell adhesion, invasion and metastasis in a variety of human solid neoplasms, particularly those of mammary epithelial origin.

Ankyrin belongs to a family of cytoskeletal proteins that mediate linkage of integral membrane proteins with the spectrin-based skeleton and thereby can regulate a variety of biological activities (49, 50). Presently, at least three ankyrin genes have been identified: ankyrin 1 (ANK 1 or ankyrin R), ankyrin 2

(ANK 2 or ankyrin B) and ankyrin 3 (ANK 3 or ankyrin G) (49, 51). All three ankyrin species are monomers comprised of two highly conserved domains and a variable domain. Both conserved domains are located in the N-terminal region and include a membrane-binding site (molecular mass  $\approx 89$ –95 kDa), also called the ankyrin repeat domain (ARD) (52), and a spectrin binding domain (SBD) (molecular mass  $\approx 62$  kDa) (53). The striking feature shared by all three forms of ankyrins is the repeated 33-amino acid motif present in 24 contiguous copies within the ARD. The ARD of ANK 1, ANK 2 and ANK 3 is highly conserved. A number of tumor cells, including breast tumor cells, express a high level of ankyrin (54, 55). A recent study determined that the ankyrin repeat domain (ARD) is directly involved in the binding of ankyrin to CD44. In fact, subdomain 2 (S2, aa218-aa381) of ankyrin is the only ankyrin repeat domain sequence which binds strongly to CD44.

Other ankyrin subdomains, such as subdomain 1 (S1), subdomain 3 (S3) or subdomain 4 (S4), do not bind to CD44. Overexpression of S2 ankyrin fragment or ARD by microinjection of S2 or ARD fusion proteins into CD44s-positive ovarian tumor cells (e.g., SK-OV-3) induces CD44-ankyrin association in the membrane projections (54). We have also observed that transfection of SK-OV-3 cells with S2cDNA or ARDcDNA promotes HA-mediated tumor cell migration (54). These findings support the notion that interaction between the ankyrin repeat domain and the cytoplasmic region of CD44 is required for hyaluronic acid-regulated CD44 function, including tumor cell migration.

In human mammary epithelial cells, HA or a small fragment of HA (10–15 disaccharide units) stimulates CD44s-specific chemokine (e.g., interleukin-8) expression at both the transcriptional (Fig. 3A) and protein levels (Fig. 3B) (56). Recent data indicate

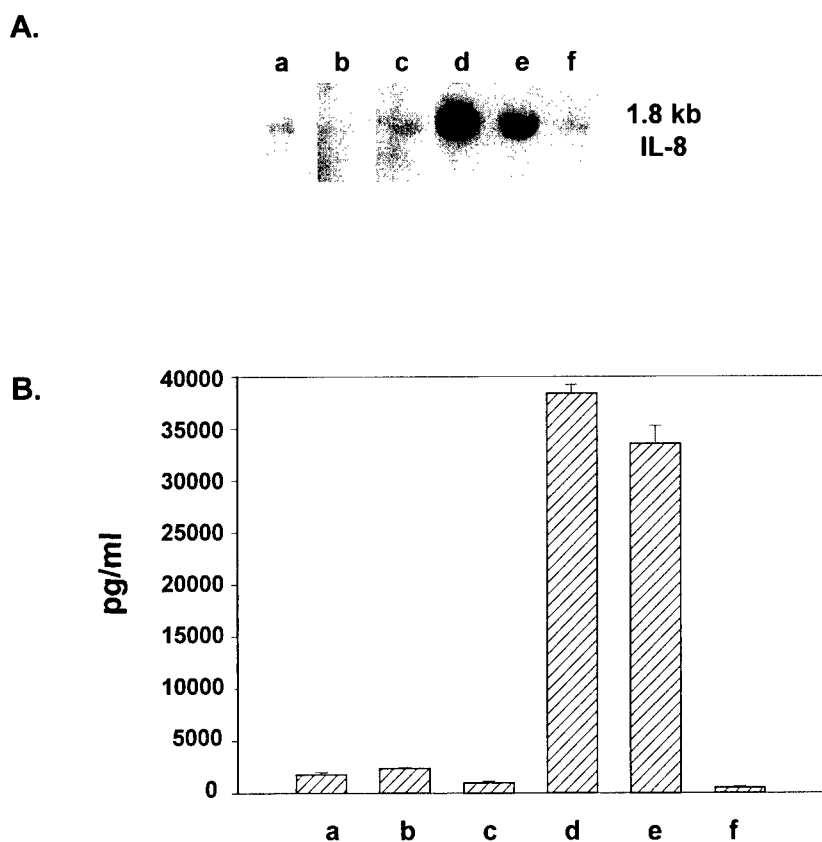


**Fig. 3.** Effects of HA or HA fragments on IL-8 gene expression (A) and protein production (B) in human mammary epithelial tumor cells (HBL100 cell line) treated with no HA (a); or treated with small HA fragments of  $\approx 2$  disaccharide units (b), 2–3 disaccharide units (c), 10–15 disaccharide units (d), intact HA (e), or anti-CD44 antibody plus intact HA (f).

**Table I.** Measurement of HA-Mediated Breast Tumor Cell Adhesion and IL8 Production

Transfectants	(% of control)	
	Cell Adhesion	IL8 Production
Untransfected cells (control)	100	100
Control (neo-transfected)	98	96
CD44s $\Delta$ 304-361cDNA transfected cells	23	20

All numbers represent an average of triplicate determinations of at least three separate experiments with a standard deviation  $<\pm 5\%$ .

that the cytoplasmic deletion mutant CD44s $\Delta$ 304-361 (a mutant cDNA with 58 aa cytoplasmic deletion), which lacks an ankyrin binding site (23), functions as a potent dominant-negative inhibition mutant and effectively down-regulates HA-mediated cell adhesion (Table I) and IL-8 gene expression (56) as well as IL-8 production (Table I). These findings further support the notion that the cytoplasmic domain of CD44s (containing the ankyrin binding site) plays a pivotal role in HA-mediated signaling required for both oncogenic signaling and angiogenic factor (e.g., IL-8) production during human mammary epithelial cell transformation.

#### CD44-MEDIATED Rho SIGNALING IN CYTOSKELETON-REGULATED BREAST TUMOR PROGRESSION

Members of the Rho subclass of the Ras superfamily, small molecular weight GTPases, (e.g., RhoA, Rac1 and Cdc42) are known to transduce signals regulating many cellular processes (57). In particular, activation of RhoA, Rac1 and Cdc42 has been shown to be associated with the membrane-linked cytoskeleton and produce specific structural changes resulting in membrane ruffling, lamellipodia, filopodia, and stress fiber formation (57). The coordinated activation of these RhoGTPases is considered to be a possible mechanism underlying cell motility, an obvious prerequisite for metastasis (2, 3). Our recent study also supports the notion that CD44v isoforms, such as CD44v<sub>3,8-10</sub>, and RhoGTPases are both structurally and functionally coupled in breast tumor cells (58).

#### RhoA-Activated Rho-Kinase (ROK) In CD44 Signaling

Several enzymes have been identified as possible downstream targets for RhoGTPases (e.g., RhoA)

in regulating cytoskeleton-mediated cell motility (59–61). One such enzyme is Rho-Kinase (ROK, also called Rho-binding kinase) which is a serine-threonine kinase (59). ROK interacts with RhoA in a GTP-dependent manner and phosphorylates a number of cellular proteins (58–60). In particular, phosphorylation of myosin light chain (59) and myosin light chain phosphatase (60) by ROK activates myosin adenosine triphosphatase (ATPase), leading to actomyosin-mediated cell movement (59, 60). Structurally, ROK is composed of catalytic (CAT), coiled-coil, Rho-binding (RB) and pleckstrin-homology (PH) domains. Expression of the catalytic (CAT) domain alone by deleting the Rho-binding (RB) domain causes ROK to be constitutively active (61). If the RB domain is overexpressed alone, ROK activity is readily inhibited (61). Therefore, the catalytic (CAT) fragments appears to act as a dominant active form, and the Rho-binding (RB) fragment functions as a dominant negative form of the ROK molecule (61). ROK is overexpressed in breast tumor cells (58) and is capable of phosphorylating the cytoplasmic domain of CD44v<sub>3</sub> (58). Moreover, phosphorylation of the cytoplasmic domain of CD44 by ROK enhances its binding interaction with ankyrin (58). Overexpression of the Rho-binding domain (a dominant-negative form) of ROK by transfecting breast tumor cells with RB cDNA induces reversal of tumor cell-specific phenotypes (58). Therefore, the CD44v<sub>3</sub> and RhoA-mediated signaling appear to be involved in the up-regulation of ROK needed for membrane-cytoskeleton interactions and tumor cell migration during the progression of metastatic breast tumor cells.

#### Tiam1-Catalyzed Rac1 Activation in CD44 Signaling

Signaling to the RacGTPase is known to regulate actin assembly associated with membrane ruffling, pseudopod extension, cell motility and cell transformation (57, 62) and has been shown to be abnormal in transformed cells (63). The fact that Rac1 induces stress fiber formation in a Rho-dependent manner indicates that "cross-talk" occurs between the Rho and Rac1 signaling pathways (62).

Several guanine nucleotide exchange factors (GEFs, the db1 or DH family) have been identified as oncogenes by their ability to upregulate RhoGTPase activity during malignant transformation (57, 63). One of these GEFs is Tiam1 (T lymphoma invasion and metastasis), which was identified by retroviral

insertional mutagenesis and selected for its invasive cell behavior *in vitro* (64). It has been shown to regulate Rac1 activation (64, 65). Tiam1 is a largely hydrophilic molecule that contains several functional domains, including a DbI homology (DH) domain, a Discs-large homology region (DHR), and two pleckstrin homology (PH) domains (PHn, the PH domain located at the NH<sub>2</sub>-terminal region of the molecule; and PHc, the PH domain located at the COOH-terminal region of the molecule) (64). The DH domain of Tiam1 exhibits GDP/GTP exchange

activity for specific members of the Ras superfamily of GTP-binding proteins (64) and plays an important role in Rac1 signaling and cellular transformation (64, 65). In breast tumor cells (e.g., SP1 cells), Tiam1 is detected as a 200 kDa protein that is capable of catalyzing GDP/GTP exchange for Rac1 as described for Tiam1 in other cell types (55, 66). Recently, we have presented new evidence that a close interaction occurs both *in vivo* and *in vitro* between Tiam1 and the CD44v3 isoform. The CD44v<sub>3</sub> isoform is closely associated with Tiam1 aa393-aa738 containing the

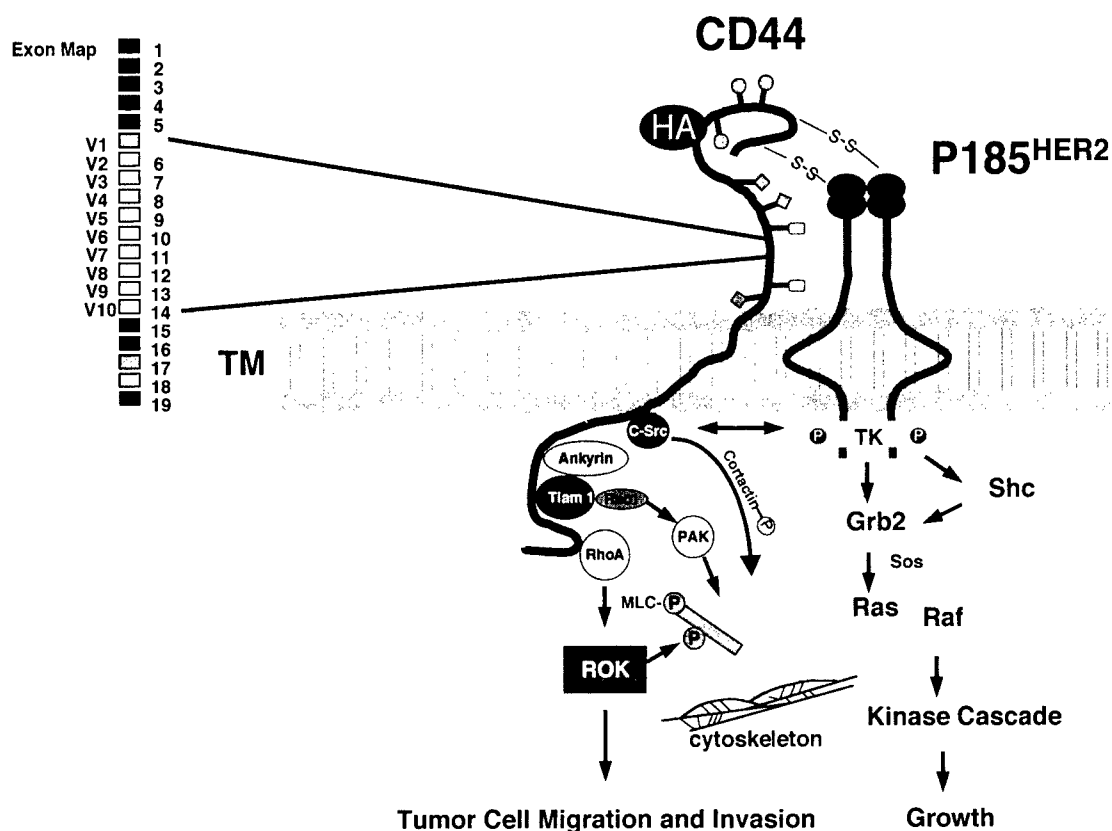


**Fig. 4.** Current model for CD44 isoform-cytoskeleton interaction in oncogenic signaling and breast tumor progression. Specific CD44 signaling events including CD44 (by itself) signaling and CD44 (complexed with p185<sup>HER2</sup>) signaling are described as follows: (I) CD44 (by itself) Signaling: Binding of HA to CD44 isoform (containing variant exon-coded structures) induces CD44 isoform interaction with both ankyrin and Tiam1 which, in turn, activates RhoGTPase (Rac1) signaling leading to PAK (p21 activated kinase)-mediated cytoskeleton activation. The cytoplasmic domain of CD44 isoforms is also tightly coupled with c-Src kinase or RhoA in a complex which up-regulates the activities of c-Src kinase or Rho-Kinase (ROK), respectively. Specifically, CD44-mediated stimulation of c-Src kinase promotes tyrosine phosphorylation of cortactin and cytoskeleton reorganization. ROK activation by CD44-associated RhoA is responsible for myosin light chain phosphorylation (MLC-P) and actomyosin-mediated contractility. All these events lead to breast tumor cell migration and invasion. (II) CD44 (complexed with p185<sup>HER2</sup>) Signaling: HA binding to CD44 isoform-p185<sup>HER2</sup> complex (formed by a disulfide linkage) is also involved in the onset of p185<sup>HER2</sup> tyrosine kinase (TK) activation which triggers Shc/Grb2/Sos & Ras-mediated signaling leading to Raf-related kinase cascade and tumor cell growth.

In conclusion, we believe that the selective interaction of the cytoplasmic domain of CD44 isoforms with its unique downstream effectors plays a pivotal role in coordinating intracellular signaling pathways (e.g., Rho/Ras signaling and receptor-linked/non-receptor-linked tyrosine kinase pathways) to generate a concomitant onset of tumor cell growth, migration and invasion leading to mammary tumor progression.

NH2-terminal pleckstrin homology (PHn), a putative coiled coil region (CC) and an additional adjacent region (Ex) (designated as PHn-CC-Ex domain of Tiam1) in breast tumor cells (66). Most importantly, HA binding to the CD44v<sub>3</sub> isoform stimulates Tiam1-specific GDP/GTP exchange for Rho-like GTPases such as Rac1, and promotes cytoskeleton-mediated tumor cell migration (66). These findings are consistent with a study by Oliferenko *et al.* (67) showing that Rac1 activation can be induced by HA binding to CD44.

A recent study in our laboratory has demonstrated that the PHn-CC-Ex domain of Tiam1 also contains an ankyrin binding site (55). The structural homology between the ankyrin binding domain of Tiam1 (the sequence between aa717 and aa727 within the PHn-CC-Ex domain) and CD44 is quite striking. Most importantly, the Tiam1-ankyrin interaction promotes Rac1 activation and breast tumor cell migration (55). These observations suggest that Tiam1 contains multiple functional domains (e.g., a CD44-specific membrane localization site and a cytoskeleton binding region for ankyrin) required for the regulation of Tiam1-Rac1 signaling and cytoskeleton function. Taken together, these results suggest that the Tiam1 interaction with CD44v<sub>3</sub> and ankyrin plays a pivotal role in regulating Rac1-activated oncogenic signaling and cytoskeleton-mediated metastatic breast tumor progression.

## CONCLUSION

As summarized in Fig. 4, the binding of HA to CD44 isoforms (e.g., CD44s and/or CD44v isoforms), which are physically linked to p185<sup>HER2</sup> tyrosine kinase (via a disulfide linkage) and c-Src kinase, triggers direct "cross-talk" between two different tyrosine kinase-linked signaling pathways (cell growth vs cortactin-mediated cell migration). In addition, certain angiogenic factors (e.g., VEGF or FGF-2) and matrix-degradating enzymes (MMPs) are also tightly complexed with CD44v isoforms, suggesting that they play a synergistic role in the generation of oncogenic signals leading to tumor-specific behaviors (e.g., invasion and motility/migration) in a cytoskeleton-dependent manner. Most importantly, the cytoplasmic domain of CD44 isoforms binds unique downstream effectors (e.g., cytoskeletal proteins, ankyrin or various oncogenic signaling molecules, Tiam1 and RhoA-activated ROK) and coordinates intracellular signaling pathways (e.g., Rho/Ras signaling and

receptor-linked/non-receptor-linked tyrosine kinase pathways) to generate a concomitant onset of multiple cellular functions (e.g., tumor cell growth, migration and invasion) leading to mammary tumor progression.

## ACKNOWLEDGMENTS

I gratefully acknowledge Dr. Gerard J. Bourguignon's assistance in the preparation of this paper. This work was supported by United States Public Health grants (CA66163 and CA 78633) and DOD grants [DAMD 17-97-1-7014 and DAMD 17-99-1-9291].

## REFERENCES

1. R. B. Dickson and M. E. Lippman (1996). New approaches in the therapy of breast cancer. *Breast Cancer Res. & Treatment* **38**:1-2.
2. W. G. Jiang, M. C. A. Puntis, and M. B. Hallett (1994). Molecular and cellular basis of cancer invasion and metastasis: Implications for treatment. *British J. Surgery* **81**:1576-1590.
3. D. A. Lauffenburger and A. F. Horwitz (1996). Cell migration: A physically integrated molecular process. *Cell* **84**:359-369.
4. L. A. Goldstein, D. F. H. Zhou, L. J. Picker, C. N. Minty, R. F. Bargatze, J. F. Ding, and E. C. Butcher (1989). A human lymphocyte homing receptor, the hermes antigen, is related to cartilage proteoglycan core and link proteins. *Cell* **56**:1063-1072.
5. C. B. Underhill, S. J. Green, P. M. Comoglio, and G. Tarone (1987). The hyaluronate receptor is identical to a glycoprotein of 85,000 Mr. (gp85) as shown by a monoclonal antibody that interferes with binding activity. *J. Biol. Chem.* **262**:13142-13146.
6. T. C. Laurent and J. R. Fraser (1992). Hyaluronan. *FASEB J.* **6**:2397-2404.
7. S. J. Green, G. Tarone, and C. B. Underhill (1988). Aggregation of macrophages and fibroblasts is inhibited by a monoclonal antibody to the hyaluronate receptor. *Exp. Cell. Res.* **178**:224-232.
8. D. C. West and S. Kumar (1989). The effect of hyaluronate and its oligosaccharides on endothelial cell proliferation and monolayer integrity. *Exp. Cell. Res.* **183**:179-196.
9. E. A. Turley, L. Austen, K. Vandelligt, and C. Clary (1991). Hyaluronan and a cell-associated hyaluronan binding protein regulate the locomotion of ras-transformed cells. *J. Cell. Biol.* **112**:1041-1047.
10. P. Rooney, S. Kumar, and M. Wang (1995). The role of hyaluronan in tumor neovascularization. *Int J Cancer* **60**:632-636.
11. G. R. Screaton, M. V. Bell, D. G. Jackson, F. B. Cornelis, U. Gerth, and J. I. Bell (1992). Genomic structure of DNA coding the lymphocyte homing receptor CD44 reveals 12 alternatively spliced exons. *Proc. Natl. Acad. Sci. U. S. A.* **89**:12160-12164.
12. V. B. Lokeshwar and L. Y. W. Bourguignon (1991). Post-translational protein modification and expression of ankyrin binding site(s) in GP85(Pgp-1/CD44) and its biosynthetic

- precursors during T-lymphoma membrane biosynthesis. *J. Biol. Chem.* **266**:17983–17989.
13. L. Y. W. Bourguignon, V. B. Lokeshwar, J. He, X. Chen, and G. J. Bourguignon (1992). A CD44-like endothelial transmembrane glycoprotein (GP116) Interacts with extracellular matrix and ankyrin. *Mol. Cell. Biol.* **12**:4464–4471.
  14. V. B. Lokeshwar, N. Iida, and L. Y. W. Bourguignon (1996). The cell adhesion molecule, GP116 is a new CD44 variant (ex14/v10) involved in hyaluronic acid binding and endothelial cell proliferation. *J. Biol. Chem.* **271**:23853–23864.
  15. P. Dall, K.-H. Heider, H.-P. Sinn, P. Skroch-Angel, G. Adolf, M. Kaufmann, P. Herrlich, and H. Ponta (1995). Comparison of immunohistochemistry and RT-PCR for detection of CD44v-expression, a new prognostic factor in human breast cancer. *Int. J. Cancer.* **60**:471–477.
  16. N. Iida and L. Y. W. Bourguignon (1995). New CD44 splice variants associated with human breast cancers. *J. Cell. Physiol.* **162**:127–133.
  17. M. Kaufmann, K. H. Heider, H. P. Sinn, G. von Minckwitz, H. Ponta, and P. Herrlich (1995). CD44 variant exon epitopes in primary breast cancer and length of survival. *Lancet* **345**:615–619.
  18. M. S. Sy, H. Mori, and D. Liu (1997). CD44 as a marker in human cancers. *Curr. Opin. Oncol.* **9**:108–112.
  19. E. Kalish, N. Iida, F. L. Moffat, and L. Y. W. Bourguignon (1999). A new CD44v3-containing isoform is involved in tumor cell migration and human breast cancer progression. *Front Biosci.* **4**:1–8.
  20. E. Horst, C. J. Meijer, T. Radaszkiewicz, G. J. Ossekoppele, J. H. Van Krieken, and S. T. Pals (1990). Adhesion molecules in the prognosis of diffuse large-cell lymphoma: Expression of a lymphocyte homing receptor (CD44), LFA (CD11a/18), and ICAM-1 (CD54). *Leukemia* **4**:595–599.
  21. S. Jalkanen, H. Joensuu, K. O. Soderstrom, and P. Klemi (1991). Lymphocyte homing and clinical behavior of non-Hodgkin's lymphoma. *J. Clin. Invest.* **87**:1835–1840.
  22. L. Y. W. Bourguignon, H. B. Zhu, A. Chu, L. Zhang, and Mien-Chie Hung (1997). Interaction between the adhesion receptor, CD44 and the oncogene product, p185<sup>HER2</sup>, promotes human ovarian tumor cell activation. *J. Biol. Chem.* **272**:27913–27918.
  23. D. Zhu and L. Y. W. Bourguignon (1998). The ankyrin-binding domain of CD44s is involved in regulating hyaluronic acid-mediated function and prostate tumor cell transformation. *Cell Motil. Cytoskel.* **39**:209–222.
  24. L. Y. W. Bourguignon, H. Zhu, L. Shao, and Y. W. Chen (2001). CD44 interaction with c-Src kinase promotes cortactin-mediated cytoskeleton function and hyaluronic acid (HA)-dependent ovarian tumor cell migration. *J. Biol. Chem.* **276**:7327–7336.
  25. D. J. Slamon, G. Williams, L. A. Jones, J. A. Holt, S. G. Wong, D. E. Keith, W. J. Levin, S. G. Stuart, J. Udove, A. Ullrich, and M. F. Press (1989). Studies of the HER-2/*neu* proto-oncogene in human breast and ovarian cancer. *Science* **244**:707–710.
  26. D. K. Luttrell, A. Lee, T. J. Lansing, R. M. Crosby, K. D. Jung, D. Willard, M. Luther, M. Rodriguez, J. Berman, and T. M. Gilmer (1994). Involvement of pp60c-Src with two major signaling pathways in human breast cancer. *Proc. Natl. Acad. Sci. U.S.A.* **91**:83–87.
  27. N. Rahimi, W. Hung, E. Tremblay, R. Saulnier, and B. Elliott (1998). c-Src kinase activity is required for hepatocyte growth factor-induced motility and anchorage-independent growth of mammary carcinoma cells. *J. Biol. Chem.* **273**:33714–33721.
  28. D. Naor, R. V. Sionov, and D. Ish-Shalom (1997). CD44: structure, function, and association with the malignant process. *Adv. Cancer. Res.* **71**:241–319.
  29. D. Liu and M. S. Sy (1996). A cysteine residue located in the transmembrane domain of CD44 is important in binding of CD44 to hyaluronic acid. *J. Exp. Med.* **183**:1987–1994.
  30. L. Y. W. Bourguignon, E. L. Kalomiris, and V. B. Lokeshwar (1991). Acylation of the lymphoma transmembrane glycoprotein, GP85, may be required for GP85-ankyrin interaction. *J. Biol. Chem.* **266**:11761–11765.
  31. R. Karni, R. Jove, and A. Levitzki (1999). Inhibition of pp60c-Src reduces Bel-XL expression and reverses the transformed phenotype of cells overexpressing EGF and HER-2 receptors. *Oncogene* **18**:4654–4662.
  32. I. Dikic, G. Tokiwa, S. Lev, S. A. Courtneidge, and J. Schlessinger (1996). A role for Pyk2 and Src in linking G-protein-coupled receptors with MAP kinase activation. *Nature* **383**:547–550.
  33. G. Koopman, K. H. Heider, E. Horst, G. R. Adolf, F. van den Berg, H. Ponta, and P. Herrlich (1993). Activated human lymphocytes and aggressive non-Hodgkin's lymphomas express a homologue of the rat metastasis-associated variant of CD44. *J. Exp. Med.* **177**:897–904.
  34. U. Gunthert, M. Hofmann, M. Rudy, S. Reber, M. Zoller, I. Haussmann, and S. Matzku (1991). A new variant of glycoprotein CD44 confers metastatic potential to rat carcinoma cells. *Cell* **65**:13–24.
  35. K. Friedrichs, F. Franke, B.-W. Lisboa, G. Kugler, I. Gille, H.-J. Terpe, F. Holzel, H. Maass, and U. Gunthert (1995). CD44 isoforms correlate with cellular differentiation but not with prognosis in human breast cancer. *Cancer Res.* **55**:5424–5433.
  36. N. Iida and L. Y. W. Bourguignon (1997). Coexpression of CD44 Variant (v10/ex 14) and CD44s in human mammary epithelial cells promotes tumorigenesis. *J. Cell. Physiol.* **171**:152–160.
  37. I. Stamenkovic, M. Amiot, J. M. Pesando, and B. Seed (1991). The hemopoietic and epithelial forms of CD44 are distinct polypeptides with different adhesion potentials for hyaluronan-bearing cells. *EMBO J.* **10**:343–347.
  38. M. Bernfield, M. Gotte, P. W. Park, O. Reizes, M. L. Fitzgerald, J. Lincecum, and M. Zako (1999) Functions of cell surface heparan sulfate proteoglycans. *Annu. Rev. Biochem.* **68**:729–777.
  39. K. Bennett, D. G. Jackson, J. C. Simon, E. Tanczos, R. Peach, B. Modrell, I. Stamenkovic, G. Plowman, and A. Aruffo (1995). CD44 isoforms containing exon v3 are responsible for the presentation of heparin-binding growth factor. *J. Cell. Biol.* **128**:687–698.
  40. H. U. Grimme, C. C. Termeer, K. L. Bennett, J. M. Weiss, E. Schopf, A. Aruffo, and J. C. Simon (1999). Colocalization of basic fibroblast growth factor and CD44 isoforms containing the variable spliced exon v3 (CD44v3) in normal skin and in epidermal skin cancers. *British J. Dermatol.* **141**:824–832.
  41. L. Y. W. Bourguignon, D. Zhu, and H. Zhu (1998). CD44 isoform-cytoskeleton interaction in oncogenic signaling and tumor progression. *Front Biosci.* **3**:637–649.
  42. H. F. Dvorak, L. F. Brown, M. Detmar, and A. M. Dvorak (1995). Review: Vascular permeability factor/vascular endothelial growth factor, microvascular hyperpermeability, and angiogenesis. *Am. J. Pathol.* **146**:1029–1039.
  43. A. T. W. Cheung, L. J. T. Young, P. C. Y. Chen, C. Y. Chao, A. Ndoye, P. A. Barry, W. J. Muller, and R. D. Cardiff (1997).

- Microcirculation and metastasis in a new mammary tumor model system. *Int. J. Oncol.* **11**:69–77.
44. L. Y. W. Bourguignon, Z. Gunja-Smith, N. Iida, H. B. Zhu, L. J. T. Young, W. Muller, and R. D. Cardiff (1998) CD44<sup>v3,8–10</sup>-cytoskeleton interaction is involved in matrix metalloproteinase (MMP-9) function and tumor cell migration and invasion in metastatic breast tumor cells. *J. Cell. Physiol.* **176**: 206–215.
45. L. A. Liotta (1984). Tumor invasion and metastasis: Role of the basement membrane. *Am. J. Pathol.* **117**:339–348.
46. W. T. Chen (1996). Proteases associated with invadopodia, and their role in degradation of extracellular matrix. *Enzyme & Protein* **49**:59–71.
47. L. Y. W. Bourguignon (1996). Interaction between membrane-cytoskeleton and CD44 during lymphocyte signal transduction and cell adhesion. In W. J. Nelson (ed.), *Current Topics in Membranes* **43**:293–312.
48. V. B. Lokeshwar, N. Fregien, and L. Y. W. Bourguignon (1994). Ankyrin binding domain of CD44(GP85) is required for the expression of hyaluronic acid-mediated adhesion function. *J. Cell. Biol.* **126**:1099–1109.
49. V. Bennet (1992). Ankyrins. *J. Biol. Chem.* **267**:8703–8706.
50. M. A. De Matteis and J. S. Morrow (1998). The role of ankyrin and spectrin in membrane transport and domain formation. *Curr. Opin. Cell. Biol.* **10**:542–549.
51. L. L. Peters, K. M. John, F. M. Lu, E. M. Eicher, A. Higgins, M. Yialamas, L. C. Turtzo, A. J. Otsuka, and S. E. Lux (1995). Ank3 (epithelial ankyrin), a widely distributed new member of the ankyrin gene family and the major ankyrin in kidney, is expressed in alternatively spliced forms, including forms that lack the repeat domain. *J. Cell. Biol.* **130**:313–330.
52. L. Davis and V. Bennett (1990). Mapping the binding sites of human erythrocyte ankyrin of the anion exchanger and spectrin. *J. Biol. Chem.* **265**:10589–10596.
53. O. S. Platt, S. E. Lux, and J. F. Falcone (1993). A highly conserved region of human erythrocyte ankyrin contains the capacity to bind spectrin. *J. Biol. Chem.* **268**:24421–24426.
54. D. Zhu and L. Y. W. Bourguignon (2000). Interaction between CD44 and the repeat domain of ankyrin promotes hyaluronic acid (HA)-mediated ovarian tumor cell migration. *J. Cell. Physiol.* **183**:182–195.
55. L. Y. W. Bourguignon, H. Zhu, L. Shao, and Y. W. Chen (2000). Ankyrin-Tiam1 interaction promotes Rac1 signaling and metastatic breast tumor cell invasion and migration. *J. Cell. Biol.* **150**:177–191.
56. L. Y. W. Bourguignon, H. B. Zhu, N. Iida, and L. Shao (1998). The cytoplasmic deletion (dominant-negative) mutant of CD44s down-regulates hyaluronan-mediated Tiam1-Rac1 signaling and IL-8 gene activation in human mammary epithelial cells. *Mol. Biol. Cell.* **9**:301a.
57. A. Hall (1998). Rho GTPase and the actin cytoskeleton. *Science* **279**:509–514.
58. L. Y. W. Bourguignon, H. Zhu, L. Shao, D. Zhu, and Y. W. Chen (1999). Rho-Kinase (ROK) promotes CD44<sup>v3,8–10</sup>-Ankyrin interaction and tumor cell migration in metastatic breast cancer cells. *Cell. Motil. Cytoskel.* **43**:269–287.
59. M. Amano, M. Ito, K. Kimura, Y. Fukata, K. Chihara, T. Nakano, Y. Matsuura, and K. Kaibuchi (1996). Phosphorylation and activation of myosin by Rho-associated kinase (Rho-kinase). *J. Biol. Chem.* **271**:20246–20249.
60. N. Kimura, M. Ito, M. Amano, K. Chihara, Y. Fukata, M. Nakafuku, B. Yamamori, J. Feng, T. Nakano, K. Okawa, K. Iwamatsu, and K. Kaibuchi (1996). Regulation of myosin phosphatase by Rho and Rho-associated kinase (Rho-kinase). *Science* **273**:245–248.
61. M. Amano, K. Chihara, K. Kimura, Y. Fukata, N. Nakamura, Y. Matsuura, and K. Kaibuchi (1997). Formation of actin stress fibers and focal adhesions enhanced by Rho-kinase. *Science* **275**:1308–1311.
62. A. J. Ridley, H. F. Paterson, C. L. Johnston, D. Diekmann, and A. Hall (1992). The small GTP-binding protein rac regulates growth factor-induced membrane ruffling. *Cell* **70**:401–410.
63. F. Michiels, G. G. M. Habets, J. C. Stam, R. A. van der Kammen, and J. G. Collard (1995). A role for Rac in Tiam1-induced membrane ruffling and invasion. *Nature* **375**:338–340.
64. G. G. M. Habets, E. H. M. Scholtes, D. Zuydgeest, R. A. van der Kammen, J. C. Stam, A. Berns, and J. G. Collard (1994). Identification of an invasion-inducing gene, Tiam-1, that encodes a protein with homology to GDP-GTP exchangers for Rho-like proteins. *Cell* **77**:537–549.
65. G. G. M. Habets, R. A. van der Kammen, J. C. Stam, F. Michiels, and J. G. Collard (1995). Sequence of the human invasion-inducing Tiam-1 gene, its conservation in evolution and its expression in tumor cell lines of different tissue origin. *Oncogene* **10**:1371–1376.
66. L. Y. W. Bourguignon, H. Zhu, L. Shao, and Y. W. Chen (2000). CD44 interaction with Tiam1 promotes Rac1 signaling and hyaluronic acid (HA)-mediated breast tumor cell migration. *J. Biol. Chem.* **275**:1829–1838.
67. S. Oliferenko, I. Kaverina, J. V. Small, and L. A. Huber (2000). Hyaluronic acid (HA) binding to CD44 activates Rac1 and induces lamellipodia outgrowth. *J. Cell. Biol.* **148**:1159–1164.

# Hyaluronan Promotes Signaling Interaction between CD44 and the Transforming Growth Factor $\beta$ Receptor I in Metastatic Breast Tumor Cells\*

Received for publication, May 2, 2002, and in revised form, June 13, 2002  
Published, JBC Papers in Press, July 26, 2002, DOI 10.1074/jbc.M204320200

Lilly Y. W. Bourguignon<sup>‡</sup>, Patrick A. Singleton<sup>§</sup>, Hongbo Zhu, and Bo Zhou

From the Department of Medicine, University of California, San Francisco, and the Endocrine Unit, Veterans Affairs Medical Center, San Francisco, California 94121

In this study we have examined the interaction between CD44 (a hyaluronan (HA) receptor) and the transforming growth factor  $\beta$  (TGF- $\beta$ ) receptors (a family of serine/threonine kinase membrane receptors) in human metastatic breast tumor cells (MDA-MB-231 cell line). Immunological data indicate that both CD44 and TGF- $\beta$  receptors are expressed in MDA-MB-231 cells and that CD44 is physically linked to the TGF- $\beta$  receptor I (TGF- $\beta$ RI) (and to a lesser extent to the TGF- $\beta$  receptor II (TGF- $\beta$ RII)) as a complex *in vivo*. Scatchard plot analyses and *in vitro* binding experiments show that the cytoplasmic domain of CD44 binds to TGF- $\beta$ RI at a single site with high affinity (an apparent dissociation constant ( $K_d$ ) of  $\sim 1.78$  nM). These findings indicate that TGF- $\beta$ RI contains a CD44-binding site. Furthermore, we have found that the binding of HA to CD44 in MDA-MB-231 cells stimulates TGF- $\beta$ RI serine/threonine kinase activity which, in turn, increases Smad2/Smad3 phosphorylation and parathyroid hormone-related protein (PTHrP) production (well known downstream effector functions of TGF- $\beta$  signaling). Most importantly, TGF- $\beta$ RI kinase activated by HA phosphorylates CD44, which enhances its binding interaction with the cytoskeletal protein, ankyrin, leading to HA-mediated breast tumor cell migration. Overexpression of TGF- $\beta$ RI by transfection of MDA-MB-231 cells with TGF- $\beta$ RIcDNA stimulates formation of the CD44-TGF- $\beta$ RI complex, the association of ankyrin with membranes, and HA-dependent/CD44-specific breast tumor migration. Taken together, these findings strongly suggest that CD44 interaction with the TGF- $\beta$ RI kinase promotes activation of multiple signaling pathways required for ankyrin-membrane interaction, tumor cell migration, and important oncogenic events (e.g. Smad2/Smad3 phosphorylation and PTHrP production) during HA and TGF- $\beta$ -mediated metastatic breast tumor progression.

transmembrane glycoproteins that exist as several isoforms (2). Cell surface expression of certain CD44 isoforms is closely correlated with breast tumor development and metastasis (3–8). Most often, CD44 isoforms are up-regulated in breast carcinomas (3–8). In fact, the presence of a high level of various CD44 isoform (particularly CD44s (the standard form), CD44v3, and CD44v10) expression is emerging as an important metastatic tumor marker in a number of carcinomas and is also implicated in the unfavorable prognosis for a variety of cancers (7). Carcinomas expressing high levels of CD44 isoforms are more malignant than those carcinomas with a low level of CD44 isoform expression (3–8). Cells expressing a high level of CD44 isoforms also display enhanced HA binding that increases their migration capability (9–12). Recently, a number of studies indicate that interaction of certain extracellular matrix components (e.g. HA) with cells triggers the cytoplasmic domain of various CD44 isoforms to bind unique downstream oncogenic signaling molecules: Tiam1 (9), Vav2 (10), RhoA-activated ROK (11), c-Src kinase (12), and p185<sup>HER2</sup> (13) and to coordinate intracellular signaling pathways (e.g. Rho/Ras signaling and receptor-linked/non-receptor-linked tyrosine kinase pathways) leading to the onset of multiple cellular functions (e.g. tumor cell growth, migration, and invasion) and breast tumor progression.

CD44 isoforms are also directly involved in the binding of cytoskeletal proteins such as ankyrin (14, 15). Deletion mutation analyses indicate that at least two sub-regions within the CD44 cytoplasmic domain contribute to the ankyrin binding: region I (e.g. the high affinity ankyrin-binding region) and region II (e.g. the regulatory region). In particular, the region I ankyrin-binding domain (e.g. NGGNGTVEDRKPSSEL between amino acids 306 and 320 in the mouse CD44 (14) and NSGN-GAVEDRKPSGL between amino acids 304 and 318 in the human CD44 (15)) is required for hyaluronan-mediated binding and cell adhesion (14, 15). An ankyrin-binding domain of CD44 isoforms has also been shown as necessary for oncogenic signaling and tumor cell transformation (15, 16). Moreover, certain ankyrin fragments (e.g. the ankyrin repeat domain (ARD) and/or the subdomain 2 (S2) of ARD) have been identified as an ankyrin-binding region for both CD44 (16) and Tiam1 (17). Overexpression of these ankyrin fragments promotes hyaluronan-dependent and CD44-specific tumor cell migration (16). These observations support the notion that CD44-ankyrin interaction is not only very important for presenting CD44 properly for hyaluronan binding but is also required for

CD44, a hyaluronan (HA)<sup>1</sup> receptor (1), belongs to a family of

\* This work was supported in part by United States Public Health Service Grants CA66163 and CA78633 and Department of Defense Grant DAMD 17-99-1-9291. The costs of publication of this article were defrayed in part by the payment of page charges. This article must therefore be hereby marked "advertisement" in accordance with 18 U.S.C. Section 1734 solely to indicate this fact.

<sup>‡</sup> To whom correspondence and reprint requests should be addressed: Endocrine Unit (111N), Dept. of Medicine, University of California, San Francisco, and Veterans Affairs Medical Center, 4150 Clement St., San Francisco, CA 94121. Tel.: 415-221-4810 (Ext. 3321); Fax: 415-383-1638; E-mail: lillyb@itsa.ucsf.edu.

<sup>§</sup> Supported by an American Heart Association predoctoral fellowship.

<sup>1</sup> The abbreviations used are: HA, hyaluronan; TGF- $\beta$ , transforming

growth factor  $\beta$ ; PTH, parathyroid hormone; PTHrP, parathyroid hormone-related protein; DMEM, Dulbecco's modified Eagle's medium; SF, serum-free; CHAPS, 3-[(3-cholamidopropyl)dimethylammonio]-1-propanesulfonic acid; MMP, metalloproteinase; ARD, ankyrin repeat domain.

cytoskeleton activation during hyaluronan signaling.

Cytokines, such as the transforming growth factor  $\beta$  (TGF- $\beta$ ) superfamily (18, 19), are multifunctional peptides that are known to regulate a diverse set of cellular processes by binding to their specific surface receptors (18, 19). Three mammalian TGF- $\beta$  isoforms (TGF- $\beta$ 1, TGF- $\beta$ 2, and TGF- $\beta$ 3), coded by different genes, have been identified (20). TGF- $\beta$  interacts with three surface receptors known as type I (TGF- $\beta$ RI), type II (TGF- $\beta$ RII), and type III (TGF- $\beta$ RIII) receptors (18, 19). TGF- $\beta$ 1 mediates its activity by high affinity binding to the type II (TGF- $\beta$ RII) receptor, which has been identified as a 70–80-kDa transmembrane protein with a cytoplasmic serine/threonine kinase domain (18–22). For cellular signaling, the TGF- $\beta$ RII requires both its kinase activity and association with members of a series of related 55-kDa TGF- $\beta$ RIIs (designated as activin receptor-like kinase-ALK (1–6 different subtypes)). Of these, only ALK5 has been shown to represent a functional TGF- $\beta$ RI (18–23). Subsequently, the TGF- $\beta$  signal is propagated from the plasma membranes (via TGF- $\beta$ RII/TGF- $\beta$ RI kinases) by phosphorylation of the Smad proteins that belong to a class of intracellular mediators known to regulate transcriptional responses and gene expression in the nucleus (24–26). The type III receptor (TGF- $\beta$ RIII) also binds TGF- $\beta$  and may function in capturing TGF- $\beta$  for presentation to the signaling receptors (27, 28). In cancers, the TGF- $\beta$  receptors on tumor cells are often mutated or functionally defective (29). For example, defective ligand binding to the cell surface caused by the absence of TGF- $\beta$ RII, or expression of a truncated form or splice variant of TGF- $\beta$ RII, may account for the resistance to activated TGF- $\beta$  in cancer cells (30–32). Some studies also indicate that decreased expression of TGF- $\beta$ RII may contribute to breast cancer progression and is related to a more aggressive phenotype in both *in situ* and invasive carcinomas (33–36).

TGF- $\beta$  is known to increase parathyroid hormone-related protein (PTH-rP) production by cancer cells (37). PTH-rP shares many, but not all, properties of parathyroid hormone (PTH). Both of these hormones share homology in 8 of the first 13 amino acids and bind to the type 1 PTH receptor (38–40). PTH-rP, like PTH, is a potent activator of bone resorption but unlike PTH does not appear to stimulate bone formation (38–40). This makes PTH-rP a particularly potent osteolytic agent (38–40). Thus, cells expressing PTH-rP in bone are likely to gain a foothold thereby stimulating the removal of the calcified matrix (38–40). However, buried within the matrix of bone are high concentrations of certain cytokines (e.g. TGF- $\beta$ ) that can feed back on the metastases to promote their tumor growth (33–36). Mice inoculated with breast tumor cells (e.g. MDA-MB-231 cells) engineered to express a dominant-negative form of the TGF- $\beta$  receptor had fewer and smaller osteolytic metastases (35, 36, 41). The net result in this situation is that PTH-rP production by breast cancers increases metastasis of breast cancer to bone. Because both CD44 and TGF- $\beta$ -mediated signaling events are important in breast tumor progression, the question of whether the interaction between CD44 and TGF- $\beta$  receptor(s) plays a significant role in regulating metastatic breast tumor cell-specific behaviors (e.g. Smad activation, PTH-rP production, membrane-cytoskeleton interaction, and tumor cell migration) is the primary focus of this study.

#### MATERIALS AND METHODS

**Cell Culture**—The breast tumor cell line (MDA-MB-231 cells) was obtained from the American Type Culture Collection (ATCC) and grown in Eagle's minimum essential medium supplemented with Earle's salt solution, essential and non-essential amino acids, vitamins, and 10% fetal bovine serum.

**Antibodies and Reagents**—Monoclonal rat anti-human CD44 antibody (Clone, 020; isotype, IgG<sub>2b</sub>; obtained from CMB-TECH, Inc., San Francisco) used in this study recognizes a common determinant of the

CD44 class of glycoproteins. For the preparation of polyclonal rabbit anti-CD44v3 antibody, specific synthetic peptides (~15–17 amino acids unique for the v3 sequence of CD44) were prepared, respectively, by the Peptide Laboratories using an Advanced Chemtech automatic synthesizer (model ACT350). All CD44 antibodies were prepared using conventional DEAE-cellulose chromatography and tested to be monospecific (by immunoblot assays). Mouse monoclonal anti-ankyrin was prepared as described previously (42). Monoclonal mouse anti-HA1 (hemagglutinin epitope) antibody (clone 12 CA5) and rabbit anti-phospho-Smad2 (Ser-465/467)/Smad3 IgG were obtained from Roche Molecular Biochemicals and Upstate Biotechnology, Inc., respectively. Both rabbit anti-TGF- $\beta$ RI IgG (specific for the ALK-5 form of TGF- $\beta$ RI p55) and rabbit anti-TGF- $\beta$ RII IgG (specific for TGF- $\beta$ RII p70) were purchased from Santa Cruz Biotechnology. Rabbit anti-phosphothreonine antibody and rabbit anti-phosphoserine antibody were purchased from Zymed Laboratories Inc..

**Cloning, Expression, and Purification of CD44 Cytoplasmic Domain (CD44cyt) from *Escherichia coli***—The cytoplasmic domain of human CD44 (CD44cyt) was cloned into pFLAG-AST using the PCR-based cloning strategy. By using human CD44 cDNA as template, one PCR primer pair (left, FLAG-EcoRI; right, FLAG-XbaI) was designed to amplify complete CD44 cytoplasmic domain. The amplified DNA fragments were one-step cloned into a pCR2.1 vector and sequenced. Then the DNA fragments were cut out by double digestion with EcoRI and XbaI and subcloned into EcoRI/XbaI double-digested pFLAG-AST (Eastman Kodak Co.) to generate FLAG-pCD44cyt construct. The nucleotide sequence of FLAG/CD44cyt junction was confirmed by sequencing. The recombinant plasmids were transformed to BL21-DE3 to produce FLAG-CD44cyt fusion protein. The FLAG-CD44cyt fusion protein was further purified by anti-FLAG M2 affinity gel column (Kodak). The nucleotide sequence of primers used in this cloning protocol is as follows: FLAG-EcoRI, 5'-GAGAATTCCGAACAGTCGAAGAAGGTGTCTCTTAAGC-3'; FLAG-XbaI, 5'-AGCTCTAGATTACACCCCAATCTTCAT-3'.

**Cell Transfection**—The cDNA encoding human TGF- $\beta$ RI (full-length) (43) is driven by the cytomegalovirus promoter and preceded by the hemagglutinin epitope (HA1) tag in the expression vector pCGN-Bam, which contains the hygromycin-resistant gene as a selection marker. To establish a transient expression system, cultured cells (e.g. MDA-MB-231 cells or COS-7 cells) were transfected with two plasmid DNAs (e.g. HA1-tagged TGF- $\beta$ RIcDNA or vector alone) using LipofectAMINE 2000. These transfectants were then analyzed for their protein expression (e.g. TGF- $\beta$ RI-related proteins) by immunoprecipitation/immunoblot, TGF- $\beta$ RI kinase activity, TGF- $\beta$ RI interaction with CD44 and ankyrin, as well as breast tumor cell migration assays as described below.

**Immunoblotting and Immunoprecipitation Techniques**—Unlabeled MDA-MB-231 cells (or surface-biotinylated) were solubilized in 50 mM HEPES (pH 7.5), 150 mM NaCl, 20 mM MgCl<sub>2</sub>, 1.0% Nonidet P-40, 0.2 mM Na<sub>2</sub>VO<sub>4</sub>, 0.2 mM phenylmethylsulfonyl fluoride, 10  $\mu$ g/ml leupeptin, and 5  $\mu$ g/ml aprotinin. The sample was then centrifuged at 14,927  $\times$  g for 15 min, and the supernatant was analyzed by SDS-PAGE in a 5 or 7.5% polyacrylamide gel. Separated polypeptides were then transferred onto nitrocellulose filters. After blocking nonspecific sites with 2% bovine serum albumin, the nitrocellulose filters were incubated with each of the specific immuno-reagents (e.g. rat anti-CD44 IgG (5  $\mu$ g/ml), rabbit anti-CD44v3 IgG (5  $\mu$ g/ml), rabbit anti-TGF- $\beta$ RI IgG (5  $\mu$ g/ml), and rabbit anti-TGF- $\beta$ RII IgG (5  $\mu$ g/ml)) followed by incubating with horseradish peroxidase-labeled goat anti-rat IgG, horseradish peroxidase-labeled goat anti-mouse IgG or ExtrAvidin peroxidase (to detect surface-biotinylated proteins). The blots were then developed by the ECL system (Amersham Biosciences). For analyzing the complex formation between endogenous TGF- $\beta$ RI, TGF- $\beta$ RII, or ankyrin into CD44v3 complex, MDA-MB-231 cells treated with various reagents (e.g. HA (50  $\mu$ g/ml; Sigma) or TGF- $\beta$ 1 (50 ng/ml; R & D Systems) or pre-treated with anti-CD44 antibody followed by HA (50  $\mu$ g/ml) or TGF- $\beta$ 1 (50 ng/ml) treatment or without any treatment) were solubilized by 1.0% Nonidet P-40 and immunoprecipitated with rat anti-CD44 antibody followed by anti-TGF- $\beta$ RI (or anti-TGF- $\beta$ RII or anti-ankyrin)-mediated immunoblot, or anti-phosphoserine/anti-phosphothreonine-mediated immunoblot, or immunoprecipitated with anti-TGF- $\beta$ RI antibody followed by anti-CD44-mediated immunoblot or anti-phosphoserine/anti-phosphothreonine-mediated immunoblot, respectively. In some experiments, MDA-MB-231 cells (e.g. untransfected or transfected with HA1-tagged TGF- $\beta$ RIcDNA or vector only) (either treated with HA (50  $\mu$ g/ml) or TGF- $\beta$ 1 (50 ng/ml) or without any treatment) were immunoprecipitated with rabbit anti-CD44v3 IgG followed by immunoblotting with rat

anti-CD44 (or mouse anti-HA1 (hemagglutinin epitope) IgG or mouse anti-ankyrin IgG) for 1 h at room temperature followed by incubation with horseradish peroxidase-conjugated goat anti-rabbit IgG (or goat anti-mouse IgG) (1:10,000 dilution) at room temperature for 1 h.

In some experiments, Nonidet P-40-solubilized cell lysate (isolated from cells treated with HA (50  $\mu$ g/ml) or TGF- $\beta$ 1 (50 ng/ml) or pretreated with anti-CD44 antibody followed by HA (50  $\mu$ g/ml) or TGF- $\beta$ 1 (50 ng/ml) treatment or without any treatment) was analyzed by SDS-PAGE followed by immunoblotting with rabbit anti-phospho-Smad2 (50  $\mu$ g/ml) or immunoprecipitated with anti-Smad3 followed by anti-phosphothreonine, anti-phosphoserine, and anti-Smad3-mediated immunoblot, respectively. These blots were then treated with peroxidase-conjugated goat anti-rabbit IgG and ECL chemiluminescence reagent.

**In Vitro Binding of CD44cyt to the TGF- $\beta$ RI**—Aliquots (0.5–1 ng of protein) of HA1-tagged TGF- $\beta$ RI (isolated from COS-7 or MDA-MB-231 cells)-conjugated Sepharose beads were incubated in 0.5 ml of binding buffer (20 mM Tris-HCl (pH 7.4), 150 mM NaCl, 0.1% bovine serum albumin, and 0.05% Triton X-100) containing various concentrations (10–800 ng/ml) of  $^{125}$ I-labeled cytoplasmic domain of CD44 (CD44cyt) fusion protein (5,000 cpm/ng protein) at 4 °C for 4 h. Specifically, equilibrium-binding conditions were determined by performing a time course (1–10 h) of  $^{125}$ I-labeled CD44cyt binding to TGF- $\beta$ RI at 4 °C. The binding equilibrium was found to be established when the *in vitro* CD44-TGF- $\beta$ RI binding assay was conducted at 4 °C after 4 h. Following binding, the CD44-TGF- $\beta$ RI-conjugated beads were washed extensively in binding buffer, and the beads-bound radioactivity was counted. Nonspecific binding was determined using a 50–100-fold excess of unlabeled CD44cyt in the presence of the same concentration of  $^{125}$ I-labeled CD44cyt. Nonspecific binding, which represented ~20% of the total binding, was always subtracted from the total binding. Our binding data are highly reproducible. The values expressed under "Results" represent an average of triplicate determinations of 3–5 experiments with an S.D. less than  $\pm 5\%$ .

**Protein Phosphorylation Assay in Vitro**—The kinase reaction was carried out in 50  $\mu$ l of the reaction mixture containing 40 mM Tris-HCl (pH 7.5), 2 mM EDTA, 1 mM dithiothreitol, 7 mM MgCl<sub>2</sub>, 0.1% CHAPS, 0.1  $\mu$ M calyculin A, 100  $\mu$ M [ $\gamma$ - $^{32}$ P]ATP (15–600 mCi/mmol), purified enzymes (e.g. 100 ng of TGF- $\beta$ RI kinase isolated from MDA-MB-231 cells either treated with HA (50  $\mu$ g/ml) or TGF- $\beta$ 1 (50 ng/ml) or without any treatment), and 1  $\mu$ g of cellular proteins (e.g. myelin basic protein and purified CD44v3). After incubating at 30 °C for 2 h, the reaction mixtures were boiled in SDS-sample buffer and subjected to SDS-PAGE. The protein bands were revealed by silver stain, and the radio-labeled bands were visualized by fluorography or analyzed by liquid scintillation counting.

**Binding of  $^{125}$ I-Labeled Ankyrin to CD44v3**—Purified  $^{125}$ I-labeled ankyrin (0.35 nM protein,  $1.5 \times 10^4$  cpm/ng) was incubated with purified CD44v3 (bound to anti-CD44v3-conjugated beads) (0.80  $\mu$ g of protein in TGF- $\beta$ RI phosphorylated or unphosphorylated form, prepared according to the methods described above) in 0.5 ml of the binding buffer (20 mM Tris-HCl (pH 7.4), 150 mM NaCl, 0.1% (w/v) bovine serum albumin, and 0.05% Triton X-100). Binding was carried out at 4 °C for 5 h under equilibrium conditions. Equilibrium conditions were determined by performing a time course (e.g. 1–10 h) of the binding reaction. Following binding, the beads were washed in the binding buffer, and the bead-bound radioactivity was determined. Nonspecific binding was determined in the presence of either a 100-fold excess of unlabeled ankyrin or using bovine serum albumin-conjugated Sepharose beads. Nonspecific binding was ~20–30% of the total binding and was subtracted from the total binding.

**Measurement of PTH-rP Production**—Breast tumor cells (MDA-MB-231 cells) were washed three times with serum-free (SF)-DMEM and incubated in 3 ml of SF-DMEM containing various reagents (e.g. HA (50  $\mu$ g/ml) or TGF- $\beta$ 1 (50 ng/ml) or anti-CD44 antibody plus HA (50  $\mu$ g/ml) or TGF- $\beta$ 1 (50 ng/ml) treatment or without any treatment) for 24 h at 37 °C in a 5% CO<sub>2</sub> humidified chamber. Subsequently, PTH-rP concentrations in the conditioned medium and cells were determined using a two-site immunoradiometric assay (Nichols Institute Diagnostics, San Juan Capistrano, CA) that detects concentrations as low as 0.3 pM PTH-rP (35, 36). Statistical analysis was done using the Student's *t* test. All data were expressed as the mean  $\pm$  S.D.

**Cell Migration Assay**—Twenty four transwell units were used for monitoring *in vitro* cell migration as described previously (9–12). Specifically, the 8- $\mu$ m porosity polycarbonate filters were used for the cell migration assay (9–12). MDA-MB-231 cells ( $\sim 1 \times 10^4$  cells/well in phosphate-buffered saline, pH 7.2) (in the presence or absence of HA (50  $\mu$ g/ml) or TGF- $\beta$ 1 (50 ng/ml) rat anti-CD44 antibody (50  $\mu$ g/ml) or cytochalasin D (20  $\mu$ g/ml)) were placed in the upper chamber of the

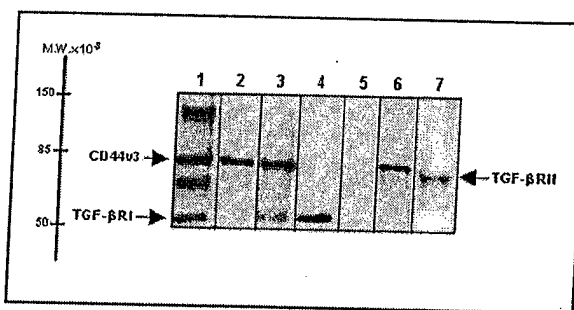


**FIG. 1. Analysis of CD44v3-TGF- $\beta$  receptor complex in human breast tumor cells (MDA-MB-231 cells).** Unlabeled MDA-MB-231 cells (or surface-biotinylated) were solubilized in 50 mM HEPES (pH 7.5), 150 mM NaCl, 20 mM MgCl<sub>2</sub>, and 1% Nonidet P-40 buffer followed by SDS-PAGE analyses and immunoblot and/or immunoprecipitation by various immuno-reagents (e.g. rabbit anti-CD44v3 and/or anti-TGF- $\beta$ RI and -RII antibodies) as described under "Materials and Methods." **Lane 1**, immunoprecipitation of surface-biotinylated MDA-MB-231 cells using monoclonal rat anti-CD44 antibody (recognizing a common determinant of the CD44 class of glycoproteins, including variant isoforms). **Lane 2**, immunoblot of rat anti-CD44-immunoprecipitated materials with rabbit anti-CD44v3 antibody. **Lane 3**, immunoprecipitation of surface-biotinylated MDA-MB-231 cells using rabbit anti-CD44v3 antibody (note that a 55-kDa polypeptide is in the complex with CD44v3). **Lane 4**, detection of TGF- $\beta$ RI in the CD44v3 complex by anti-CD44v3-mediated immunoprecipitation followed by immunoblotting with anti-TGF- $\beta$ RI-specific antibody (note that the TGF- $\beta$ RI is detected in the complex with CD44v3). **Lane 5**, detection of TGF- $\beta$ RII in the CD44v3 complex by anti-CD44v3-mediated immunoprecipitation followed by immunoblotting with anti-TGF- $\beta$ RII-specific antibody (note that the TGF- $\beta$ RII is not detected in the complex with CD44v3). **Lane 6**, detection of CD44v3 in the TGF- $\beta$ RI complex by anti-TGF- $\beta$ RI-mediated immunoprecipitation followed by immunoblotting with anti-CD44v3-specific antibody. **Lane 7**, immunoblot of MDA-MB-231 cell lysate with anti-TGF- $\beta$ RII antibody.

transwell unit. In some cases, MDA-MB-231 cells were transfected with either HA1-tagged TGF- $\beta$ RI cDNA or vector alone. The medium containing high glucose DMEM supplemented with 50  $\mu$ g/ml hyaluronan was placed in the lower chamber of the transwell unit. After 18 h of incubation at 37 °C in a humidified 95% air, 5% CO<sub>2</sub> atmosphere, vital stain 3-(4,5-dimethylthiazol-2-yl)-2,5-diphenyltetrazolium bromide (Sigma) was added at a final concentration of 0.2 mg/ml to both the upper and the lower chambers and incubated for an additional 4 h at 37 °C. Migratory cells at the lower part of the filter were removed by swabbing with small pieces of Whatman filter paper. Both the polycarbonate filter and the Whatman paper were placed in dimethyl sulfoxide to solubilize the crystal. Color intensity was measured in 570 nm. Cell migration was determined by measuring the percent of total cells that migrated to the lower side of the polycarbonate filters by standard cell number counting methods as described previously (9–12). The CD44-specific cell migration was determined by subtracting nonspecific cell migration (i.e. cells migrate to the lower chamber in the presence of rat anti-CD44 antibody treatment) from the total migratory cells in the lower chamber. Each assay was set up in triplicate and repeated at least 3 times. All data were analyzed statistically using the Student's *t* test, and statistical significance was set at *p* < 0.01.

## RESULTS

**Characterization of CD44 and TGF- $\beta$  Receptor Expression in Breast Tumor Cells**—Breast cancer cells overexpress several variant isoforms of the transmembrane protein, CD44 (3–8). These different CD44 variant (CD44v) isoforms appear to confer on breast cancer cells the malignant properties of increased invasion, migration, and proliferation (46).

To examine CD44 expression on the surface of breast tumor cells (MDA-MB-231 cells), we have utilized surface biotinylation techniques and a specific monoclonal rat anti-CD44 antibody (recognizing a common determinant of the CD44 class of glycoproteins, including various variant isoforms)-mediated immunoprecipitation (Fig. 1, lane 1). Our results indicate that multiple surface-biotinylated polypeptides (~125, 85, 70, and

AQ: G

55 kDa) are selectively immunoprecipitated with the monoclonal rat anti-CD44 antibody (Fig. 1, lane 1). In order to further identify the presence of particular CD44 isoform(s) in MDA-MB-231 cells, we immunoblotted these rat anti-CD44-precipitated surface proteins with a specific rabbit antibody against CD44v3. Our data show that a single band of the CD44v3 protein is expressed in MDA-MB-231 cells (Fig. 1, lane 2) which corresponds to the surface-labeled 85-kDa polypeptide (Fig. 1, lane 1). No CD44-containing material is observed in control samples when normal rat IgG or pre-immune rabbit IgG is used in these experiments (data not shown).

Cytokines, such as TGF- $\beta$ , are known to regulate cellular processes by binding to their specific surface receptors (18, 19). Previous studies (47) have shown that both TGF- $\beta$  receptor I (RI, ~55-kDa polypeptide) and TGF- $\beta$  receptor II (RII, ~70–80-kDa polypeptide) are expressed in breast tumor cells such as MDA-MB-231 cells. In this study, using surface biotinylation techniques and specific anti-CD44v3 immunoprecipitation, we have determined that the 85-kDa surface CD44v3 and a 55-kDa surface protein are closely associated in a complex in MDA-MB-231 cells (Fig. 1, lane 3). We have also analyzed these anti-CD44v3-precipitated immunocomplexes by immunoblotting with either anti-TGF- $\beta$ RI (Fig. 1, lane 4) or TGF- $\beta$ RII antibody (Fig. 1, lane 5). Our results reveal the presence of the TGF- $\beta$ RI protein (~55-kDa polypeptide) (Fig. 1, lane 4) but not the TGF- $\beta$ RII protein (Fig. 1, lane 5) in the anti-CD44v3-immunoprecipitated materials. Furthermore, we have carried out anti-TGF- $\beta$ RI-mediated immunoprecipitation followed by anti-CD44v3 immunoblot (Fig. 1, lane 6). The results of this procedure indicate that the 85-kDa CD44v3 band is also present in anti-TGF- $\beta$ RI-immunoprecipitated materials (Fig. 1, lane 6). In order to confirm that the failure of the TGF- $\beta$ RII association with CD44v3 is not due to the lack of TGF- $\beta$ RII expression in MDA-MB-231 cells, we have conducted an immunoblot analysis of MDA-MB-231 cell lysate using anti-TGF- $\beta$ RII antibody. Our results clearly indicate that the 70–80-kDa TGF- $\beta$ RII is expressed in MDA-MB-231 cells (Fig. 1, lane 7). These findings clearly establish the fact that CD44v3 is physically linked to the TGF- $\beta$ RI *in vivo* in the breast tumor cells (MDA-MB-231 cells). The fact that CD44v3 forms a complex with TGF- $\beta$ RI (but not TGF- $\beta$ RII) suggests that a specific interaction occurs between CD44v3 and TGF- $\beta$ RI.

To further test whether TGF- $\beta$  receptors such as TGF- $\beta$ RI are involved in the direct binding to CD44 *in vitro*, we have used purified recombinant TGF- $\beta$ RI and the FLAG-tagged cytoplasmic domain of CD44 (FLAG-CD44cyt) fusion protein to identify the TGF- $\beta$ RI-binding site on the CD44 molecule. Specifically, we have tested the binding of TGF- $\beta$ RI to  $^{125}$ I-labeled FLAG-CD44cyt under equilibrium binding conditions. The results of a Scatchard plot analysis presented in Fig. 2 demonstrate that the cytoplasmic domain of CD44 (CD44cyt) binds to TGF- $\beta$ RI at a single site with high affinity with an apparent dissociation constant ( $K_d$ ) of ~1.78 nM. These findings further support the notion that a strong binding interaction occurs between CD44 and TGF- $\beta$ RI.

**HA-activated CD44/TGF- $\beta$ RI Kinase and Signaling Events**—HA is known to be involved in certain pathophysiological processes. For example, high levels of HA in solid tumors (e.g. breast tumors) appear to be closely associated with tumor progression and metastasis (48, 49). In this study, we have determined that CD44v3-associated TGF- $\beta$ RI serine/threonine kinase is significantly up-regulated by HA treatment as detected by anti-phosphoserine immunoblot (Fig. 3A, lane 2) or anti-phosphothreonine immunoblotting, respectively (Fig. 3B, lane 2). The level of TGF- $\beta$ RI serine/threonine phosphorylation is relatively low in untreated cells (Fig. 3, A, lane 1, and B, lane

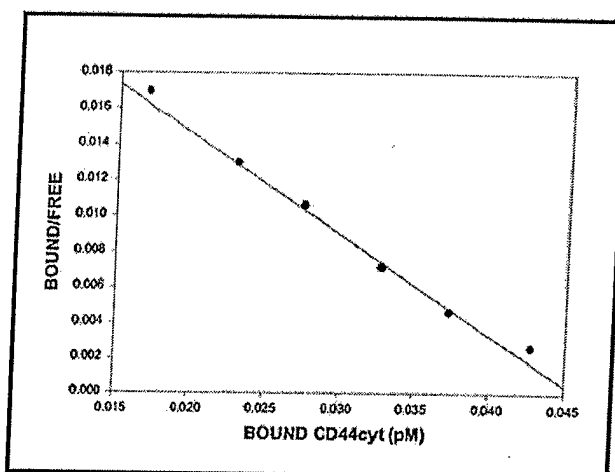


Fig. 2. Scatchard plot analysis of the binding interaction between  $^{125}$ I-labeled FLAG-CD44cyt and TGF- $\beta$ RI. Various concentrations of  $^{125}$ I-labeled FLAG-CD44cyt were incubated with the TGF- $\beta$ RI-coupled beads at 4 °C for 4 h. Following binding, beads were washed extensively in binding buffer, and the bead-bound radioactivity was counted. As a control,  $^{125}$ I-labeled FLAG-CD44cyt was also incubated with uncoated beads to determine the binding observed due to the nonspecific binding of the ligand. Nonspecific binding, which represented ~20% of the total binding, was always subtracted from the total binding. Our binding data are highly reproducible. The values expressed under "Results" represent an average of triplicate determinations of 3–5 experiments with an S.D. less than  $\pm 5\%$ .

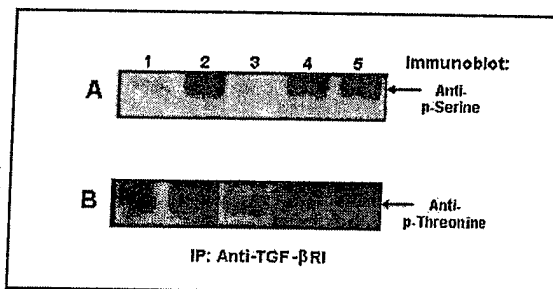
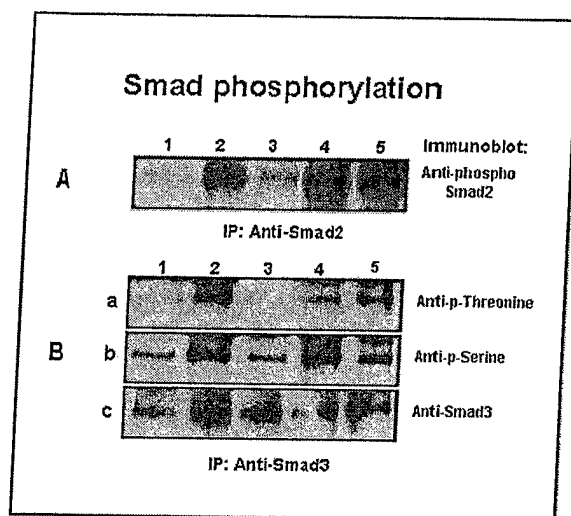


Fig. 3. Detection of TGF- $\beta$ RI phosphorylation. MDA-MB-231 cells treated with various reagents (e.g. HA (50  $\mu$ g/ml) or TGF- $\beta$ 1 (50 ng/ml) or pre-treated with anti-CD44 antibody followed by HA (50  $\mu$ g/ml) or TGF- $\beta$  (50 ng/ml) treatment or without any treatment) were solubilized by 1.0% Nonidet P-40 and immunoprecipitated (IP) with anti-TGF- $\beta$ RI antibody followed by anti-phosphoserine (A) and anti-phosphothreonine (B)-mediated immunoblot as described under "Materials and Methods." Lane 1, untreated cells; lane 2, cells treated with HA (50  $\mu$ g/ml); lane 3, cells pre-treated with anti-CD44 antibody followed by HA (50  $\mu$ g/ml); lane 4, cells treated with TGF- $\beta$ 1 (50 ng/ml); lane 5, cells pre-treated with anti-CD44 antibody followed by TGF- $\beta$ 1 (50 ng/ml) treatment.

1) or those cells pre-treated with anti-CD44 followed by HA treatment (Fig. 3, A, lane 3, and B, lane 3). As a positive control, we have confirmed that TGF- $\beta$  activates TGF- $\beta$ RI serine and threonine kinases (Fig. 3, A, lane 4, and B, lane 4). No significant inhibition of serine/threonine phosphorylation on TGF- $\beta$ RI is observed in cells treated with anti-CD44 followed by TGF- $\beta$  treatment (Fig. 3, A, lane 5, and B, lane 5). These observations strongly support the conclusion that HA-mediated TGF- $\beta$ RI kinase activity is CD44-dependent, whereas TGF- $\beta$ -stimulated TGF- $\beta$ RI kinase activity does not involve CD44. Of course, we cannot preclude the possibility that HA is also capable of interacting with other binding protein(s) which is(are) linked to TGF- $\beta$ -regulated signaling pathways.

Both Smad2/Smad3 phosphorylation (24–26, 37) and PTH-rP production (35–37, 41) are known to be closely associ-



**FIG. 4. Detection of Smad protein phosphorylation.** MDA-MB-231 cells treated with various reagents (e.g. HA (50  $\mu$ g/ml) or TGF- $\beta$ 1 (50 ng/ml) or pre-treated with anti-CD44 antibody followed by HA (50  $\mu$ g/ml) or TGF- $\beta$ 1 (50 ng/ml) treatment or without any treatment) were immunoblotted with anti-phospho-Smad2 (A) or solubilized by 1.0% Nonidet P-40 and immunoprecipitated (IP) with anti-Smad3 (B) followed by anti-phosphothreonine (a), anti-phosphoserine (b), and anti-Smad3 (c)-mediated immunoblot as described under "Materials and Methods." Lane 1, untreated cells; lane 2, cells treated with HA (50  $\mu$ g/ml); lane 3, cells pre-treated with anti-CD44 antibody followed by HA (50  $\mu$ g/ml); lane 4, cells treated with TGF- $\beta$ 1 (50 ng/ml); lane 5, cells pre-treated with anti-CD44 antibody followed by TGF- $\beta$ 1 (50 ng/ml) treatment.

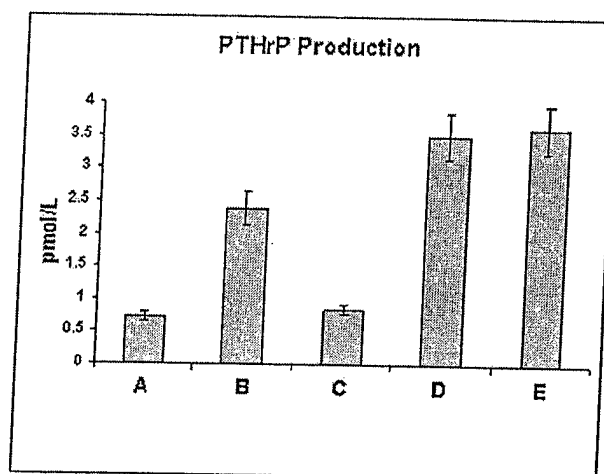


**FIG. 5. Measurement of PTH-rP production.** Breast tumor cells (MDA-MB-231 cells) were washed three times with SF-DMEM and incubated in 3 ml of SF-DMEM containing various reagents (e.g. HA (50  $\mu$ g/ml) or TGF- $\beta$ 1 (50 ng/ml) or anti-CD44 antibody plus HA (50  $\mu$ g/ml) or TGF- $\beta$ 1 (50 ng/ml) treatment or without any treatment) for 24 h at 37  $^{\circ}$ C in a 5% CO<sub>2</sub> humidified chamber. Subsequently, both cells and the conditioned medium will be collected and analyzed for the production of PTH-rP using <sup>125</sup>I-labeled anti-PTH-rP antibodies and radioimmunoassay according to the procedures described under "Materials and Methods." Statistical analysis was done using the Student's *t* test. All data are expressed as the mean  $\pm$  S.D. A, untreated cells; B, cells treated with HA (50  $\mu$ g/ml); C, cells pre-treated with anti-CD44 antibody followed by HA (50  $\mu$ g/ml); D, cells treated with TGF- $\beta$ 1 (50 ng/ml); E, cells pre-treated with anti-CD44 antibody followed by TGF- $\beta$ 1 (50 ng/ml) treatment.

ated with TGF- $\beta$  signaling. In this study, we have observed that both Smad2/Smad3 phosphorylation (Fig. 4, A, lane 2, and B, lane 2) and PTH-rP production (Fig. 5B) occur during HA activation of TGF- $\beta$ RI serine/threonine kinases (Fig. 3, A, lane 2, and B, lane 2). As a positive control, we have confirmed that activation of TGF- $\beta$ RI serine/threonine kinases by TGF- $\beta$  also promotes Smad2/Smad3 phosphorylation (Fig. 4, A, lane 4, and B, lane 4) and PTH-rP production (Fig. 5D) in MDA-MB-231 cells. We believe that HA-mediated TGF- $\beta$ RI kinase activation (Fig. 3, A, lane 2, and B, lane 2) leading to Smad2/Smad3 phosphorylation and PTH-rP production is CD44-specific because control samples (either without HA treatment (Fig. 4, A, lane 1, and B, lane 1, and Fig. 5A) or pre-treatment with anti-CD44 followed by HA addition (Fig. 4, A, lane 3, and B, lane 3, and Fig. 5C)) display very low levels of CD44-associated TGF- $\beta$ RI kinase activity (Fig. 3, A, lane 2 and B, lane 2). Consequently, no significant amount of Smad2/Smad3 phosphorylation (Fig. 4, A, lanes 1 and 3, and B, lanes 1 and 3) and PTH-rP (Fig. 5, A and C) is detected under these conditions. It is also noted that no significant reduction of Smad2/Smad3 phosphorylation (Fig. 4, A, lane 5, and B, lane 5) or PTH-rP production (Fig. 5E) occurs in cells pre-treated with anti-CD44 followed by TGF- $\beta$  treatment. Therefore, we believe that these results provide strong evidence that the physiological ligand for CD44v3, HA, plays an important role in activating CD44v3-associated TGF- $\beta$ RI kinase activity required for the onset of Smad2 (or Smad3)-mediated nuclear activities and PTH-rP production during the progression of breast cancers.

**Effects of TGF- $\beta$  Receptor Kinase-mediated CD44 Phosphorylation on Ankyrin Binding and Tumor Cell Migration**—A number of serine/threonine kinases have been shown to be involved in the regulation of CD44 phosphorylation during HA signaling (11, 50–52). In MDA-MB-231 cells, the level of CD44v3 phosphorylation in the absence of HA treatment is very low (Fig. 6, A, lane 1, and B, lane 1), whereas the amount

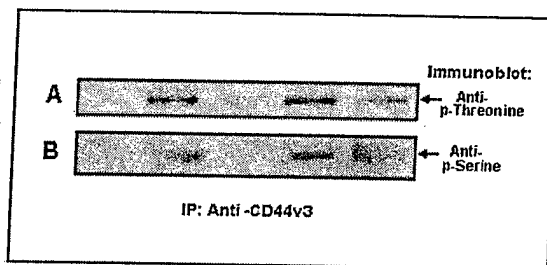


**FIG. 6. Detection of CD44 phosphorylation.** MDA-MB-231 cells treated with various reagents (e.g. HA (50  $\mu$ g/ml) or TGF- $\beta$ 1 (50 ng/ml) or pre-treated with anti-CD44 antibody followed by HA (50  $\mu$ g/ml) or TGF- $\beta$ 1 (50 ng/ml) treatment or without any treatment) were solubilized by 1.0% Nonidet P-40 and immunoprecipitated (IP) with anti-CD44v3 followed by anti-phosphothreonine (A) or anti-phosphoserine (B) as described under "Materials and Methods." Lane 1, untreated cells; lane 2, cells treated with HA (50  $\mu$ g/ml); lane 3, cells pre-treated with anti-CD44 antibody followed by HA (50  $\mu$ g/ml); lane 4, cells treated with TGF- $\beta$ 1 (50 ng/ml); lane 5, cells pre-treated with anti-CD44 antibody followed by TGF- $\beta$ 1 (50 ng/ml) treatment.

of CD44v3 phosphorylation increases significantly during HA treatment (Fig. 6, A, lane 2, and B, lane 2) as detected by anti-threonine and anti-serine antibody, respectively. To test whether CD44 functions as a possible cellular substrate(s) of TGF- $\beta$ RI kinases in MDA-MB-231 cells during HA signaling, we have examined the ability of TGF- $\beta$ RI kinase to phosphorylate CD44v3. Specifically, we have analyzed the stoichiometry of CD44 phosphorylation by TGF- $\beta$ RI kinase, along with myelin basic protein (MBP) phosphorylation as a positive control (Table I). Our results indicate that approximately  $\sim$ 1.2 mol of phosphate becomes maximally incorporated into 1 mol of CD44v3 using TGF- $\beta$ RI kinase isolated from MDA-MB-231 cells treated with HA (Table I). We have also found that  $\sim$ 1 mol of phosphate becomes maximally incorporated into 1 mol of

T1

TABLE I  
Stoichiometry analysis of CD44v3 phosphorylation by TGF- $\beta$ RI kinase

The kinase reaction used in these experiments was the same as described under "Materials and Methods." The amount of [ $\gamma$ - $^{32}$ P]ATP incorporated into CD44v3 and myelin basic protein (MBP) by TGF- $\beta$ RI kinase (isolated from HA-treated or -untreated cells) was measured as described under "Materials and Methods."

Samples	mol $^{32}$ P-incorporated/mol CD44v3	mol $^{32}$ P-incorporated/mol MBP
TGF- $\beta$ RI kinase isolated from untreated cells	$0.1 \pm 0.013$	$0.15 \pm 0.005$
TGF- $\beta$ RI kinase isolated from HA-treated cells	$1.2 \pm 0.06$	$1.0 \pm 0.04$

MBP by HA-activated TGF- $\beta$ RI kinase (Table I). In contrast, phosphorylation of CD44v3 and MBP appears to be minimal (at most  $\sim 0.1$  mol of phosphate incorporated into per mol of CD44v3 or  $\sim 0.15$  mol of phosphate incorporated into per mol of MBP) using TGF- $\beta$ RI kinase isolated from MDA-MB-231 cells without any HA treatment (Table I). Because the stoichiometry of CD44 phosphorylation by HA-activated TGF- $\beta$ RI is comparable with that of MBP phosphorylation (by HA-activated TGF- $\beta$ RI), we conclude that CD44v3 is a good cellular substrate for TGF- $\beta$ RI.

Phosphorylation of the cytoplasmic domain of CD44 has been shown to be important for its interaction with certain cytoskeletal proteins such as ankyrin (11, 14, 15, 50, 53–55). In this study we have examined the effect of TGF- $\beta$ RI kinase-mediated CD44 phosphorylation on ankyrin binding. Specifically, the highly phosphorylated form of CD44v3 (by TGF- $\beta$ RI kinase isolated from HA-activated MDA-MB-231 cells) (as shown in Table I) was incubated with  $^{125}$ I-labeled ankyrin. Our results indicate that the total amount of  $^{125}$ I-ankyrin binding to the TGF- $\beta$ RI kinase-phosphorylated form of CD44v3 (Fig. 7A) is significantly higher than that unphosphorylated form of CD44v3 (Fig. 7B). These results clearly support the notion that phosphorylation of the cytoplasmic domain of CD44v3 by activated TGF- $\beta$ RI kinase enhances its binding interaction with ankyrin. It is likely that this interaction is required for the activation of membrane-associated cytoskeleton function.

We have also demonstrated that in the absence of HA a low amount of ankyrin is associated with CD44v3 as analyzed by anti-CD44v3-mediated immunoprecipitation followed by anti-ankyrin immunoblot in MDA-MB-231 cells (Fig. 8, lane 1). HA treatment of cells recruits a significant amount of ankyrin (Fig. 8, lane 2) into a complex with CD44v3 (Fig. 8, lane 2). When cells were pre-treated with anti-CD44 antibody followed by HA treatment, the recruitment of ankyrin into CD44v3 is greatly reduced (Fig. 8, lane 3). These results are consistent with previous findings showing HA is capable of inducing the accumulation of ankyrin into CD44 complexes (42). Interestingly, TGF- $\beta$  is also causing ankyrin recruitment into CD44v3 (Fig. 8, lane 4). No obvious reduction of CD44v3-ankyrin complex formation is observed in MDA-MB-231 cells pre-treated with anti-CD44 antibody followed by TGF- $\beta$  treatment (Fig. 8, lane 5). These results strongly suggest that the TGF- $\beta$  receptor (in particular, TGF- $\beta$ RI) is not only physically complexed with CD44v3 but also functionally coupled to CD44v3-ankyrin-based cytoskeleton functions.

**Effects of TGF- $\beta$ RI Overexpression on CD44-Ankyrin Interaction and HA-mediated Breast Tumor Migration**—In order to correlate CD44-TGF- $\beta$ RI kinase signaling with breast tumor cell-specific behaviors (e.g. membrane-cytoskeleton interaction and tumor cell migration), we have transiently transfected the breast tumor cells (MDA-MB-231 cells) with a HA1-tagged TGF- $\beta$ RIcDNA (Fig. 9A) and vector alone (Fig. 9B). By using anti-CD44v3-mediated immunoprecipitation of MDA-MB-231 cells transfected with HA1-tagged TGF- $\beta$ RIcDNA followed by immunoblotting with various antibodies (e.g. anti-CD44, anti-HA1, or anti-ankyrin antibody), we have determined that CD44v3 is expressed at comparable levels in these two trans-

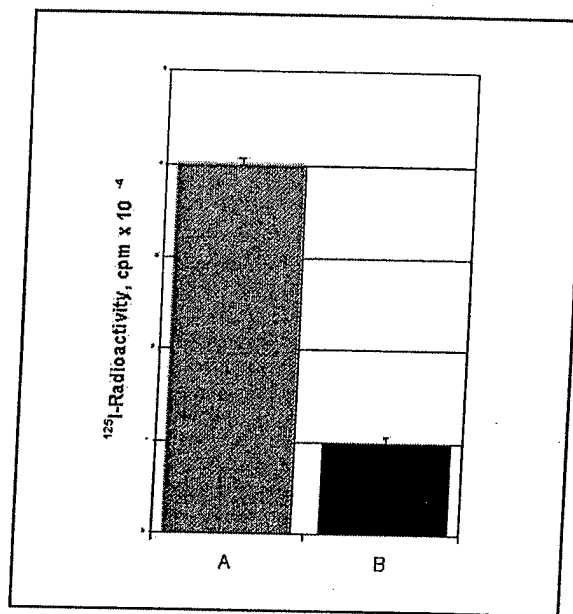


Fig. 7.  $^{125}$ I-Ankyrin binding to TGF- $\beta$ RI-phosphorylated CD44v3: Purified  $^{125}$ I-labeled ankyrin ( $\sim 0.35$  nm protein,  $1.5 \times 10^4$  cpm/ng) was incubated with CD44v3 (bound to anti-CD44v3-conjugated beads) ( $\sim 0.80$   $\mu$ g of protein in TGF- $\beta$ RI-phosphorylated or unphosphorylated form) in 0.5 ml of the binding buffer (20 mM Tris-HCl (pH 7.4), 150 mM NaCl, 0.1% (w/v) bovine serum albumin, and 0.05% Triton X-100) as described under "Materials and Methods." Following binding, the beads were washed in the binding buffer, and the bead-bound radioactivity was determined. Nonspecific binding was determined in the presence of a 100-fold excess of unlabeled ankyrin. A, the amount of  $^{125}$ I-ankyrin binding to highly phosphorylated CD44v3 (by TGF- $\beta$ RI kinase); B, the amount of  $^{125}$ I-ankyrin binding to minimally phosphorylated CD44v3 (in the absence of TGF- $\beta$ RI kinase).

fectants (Fig. 9, A, lane a, and B, lane a) and that only HA1-tagged TGF- $\beta$ RI (Fig. 9B, lane b), but not the vector control sample (Fig. 9A, lane b), is co-precipitated with CD44v3 (Fig. 9B, lane b). By using the same anti-CD44v3-mediated immunoprecipitation procedures, only a low level of ankyrin (Fig. 9A, lane c) was detected in the CD44v3 immunocomplex isolated from cells transfected with vector alone. Overexpression of TGF- $\beta$ RI by transfecting MDA-MB-231 cells with TGF- $\beta$ RIcDNA promotes a significant increase in ankyrin recruitment into CD44v3-TGF- $\beta$ RI complex. These findings suggest that TGF- $\beta$ RI overexpression mimics HA and/or TGF- $\beta$  signaling in the induction of CD44v3-ankyrin complex formation.

Furthermore, by using *in vitro* migration assays, we have demonstrated that incubation of untransfected MDA-MB-231 cells with either HA or TGF- $\beta$  stimulates active tumor cell migration (Table II). However, transfection of MDA-MB-231 cells with TGF- $\beta$ RIcDNA also significantly stimulates CD44 cytoskeleton-dependent breast tumor cell migration (Table II) as compared with vector-transfected cells (Table II). Furthermore, treatment of MDA-MB-231 cells with the microfilament

AQ: H

T2

HA Promotes CD44 and TGF- $\beta$ RI Signaling in Breast Tumor Cells

7

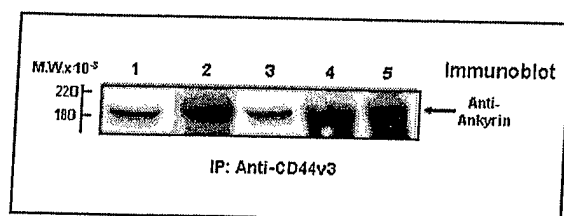


**Fig. 8. Analysis of CD44v3-ankyrin complex in human breast tumor cells (MDA-MB-231 cells).** Unlabeled MDA-MB-231 cells treated with various reagents (e.g. HA (50 µg/ml) or TGF- $\beta$ 1 (50 ng/ml) or pre-treated with anti-CD44 antibody followed by HA (50 µg/ml) or TGF- $\beta$ 1 (50 ng/ml) treatment or without any treatment) were solubilized by 1.0% Nonidet P-40 and immunoprecipitated with anti-CD44v3 followed by anti-ankyrin as described under "Materials and Methods." Lane 1, untreated cells; lane 2, cells treated with HA (50 µg/ml); lane 3, cells pre-treated with anti-CD44 antibody followed by HA (50 µg/ml); lane 4, cells treated with TGF- $\beta$ 1 (50 ng/ml); lane 5, cells pre-treated with anti-CD44 antibody followed by TGF- $\beta$ 1 (50 ng/ml) treatment.

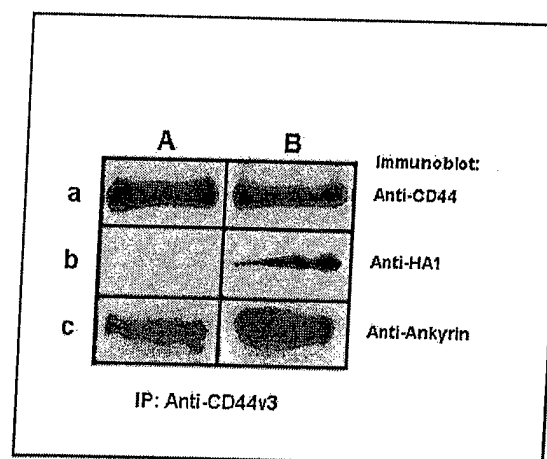


**Fig. 9. Analysis of the signaling complex formation in MDA-MB-231 cells transfected with TGF- $\beta$ RIcDNA.** MDA-MB-231 cells transfected with vector alone (A) or HA1-tagged TGF- $\beta$ RIcDNA (B) were solubilized by Nonidet P-40 (as described above) and immunoprecipitated (IP) with anti-CD44v3 antibody followed by immunoblotting with various immuno-reagents (e.g. anti-CD44 (lane a), anti-HA1 (lane b), or anti-ankyrin (lane c), respectively).

inhibitor, cytochalasin D, causes a significant inhibition of HA- and TGF- $\beta$ -mediated as well as TGF- $\beta$ RIcDNA-transfected breast tumor cell migration (Table II). Taken together, these findings strongly suggest that both HA and TGF- $\beta$  promote CD44-ankyrin-linked cytoskeleton activation required for metastatic breast tumor cell migration.

## DISCUSSION

CD44 contains a variable extracellular domain, a single spanning 23-amino acid transmembrane domain, and a 70-amino acid cytoplasmic domain (56). Nucleotide sequence analyses reveal that many CD44 isoforms (derived from alternative splicing mechanisms) are variants of the standard form, CD44s (2). CD44 isoforms have been detected on highly metastatic breast tumor cell lines, and transfection of these molecules confers metastatic properties to otherwise non-metastatic cells (9–13, 15, 16, 46). By using CD44-specific antibodies, we have found that metastatic breast tumor cells (e.g. MDA-MB-231 cell line) express several CD44 isoforms including CD44v3 (Fig. 1). The level of CD44v3 isoform expression often increases as the histologic grade of each of the breast tumors progresses. In fact, there is a direct correlation between CD44v3 isoform expression and increased histologic grade of the malignancy (5, 8). These lines of evidence suggest that expression of certain CD44v3 isoform(s) may be an accurate predictor of eventual survival (e.g. nodal status, tumor size, and grade) during breast cancer progression (6). CD44v3 has a heparin sulfate addition site in the membrane-proximal extracellular domain of the molecule that confers the ability to bind heparin sulfate-binding growth factors (58). The attachment of growth factor(s) to the heparin sulfate sites on CD44v3 may be responsible for the onset of breast tumor-associated angiogenesis. In breast tumor cells, CD44v3 is also closely associated with metalloproteinases, MMP-9 (gelatinase B), in the plasma membrane (59). Furthermore, MMP-9 is present in a proteolytically active form and is preferentially localized at the "invadopodia" of the breast tumor cells (59). Therefore, it is likely that the close interaction between CD44v3 and the active form of MMP-9 in the invadopodia structure of breast tumor cells may be required for the degradation of extracellular matrix during breast tumor cell invasion and metastasis.

HA is one of the major components of the extracellular matrix glycosaminoglycan. All CD44 isoforms contain a link module HA-binding site in their extracellular domain (60). Thus, CD44 is considered to be one of the major HA receptors (60). Both CD44 and HA are overexpressed at sites of tumor attachment (48, 49). The binding of HA to CD44 is implicated in the stimulation of a variety of cellular functions including tumor

progression (9–13). It is known that CD44 has intricate links to signal transduction processes. In particular, the intracellular domain of CD44 binds to certain cytoskeletal proteins such as ankyrin (11, 14, 15, 50, 53–55) and ERM proteins (ezrin, radixin, and moesin) (61). The transmembrane interaction between CD44 isoforms and ankyrin/ERM provides a direct link between the extracellular matrix and the cytoskeleton. In addition, CD44 couples with tyrosine kinases (e.g. c-Src kinase and p185<sup>HER2</sup> kinase) (12, 13) and serine/threonine kinase (e.g. protein kinase C and Rho-binding kinase) (11, 50). In cancers, the selective interaction between CD44 and its binding partners has been shown to promote a number of downstream effector functions leading to HA-mediated tumor cell-specific behaviors (1).

TGF- $\beta$  signaling plays a central role in regulating a variety of cellular responses and acts as a growth stimulator or inhibitor, depending on the cellular context (18, 19). It is now generally accepted that TGF- $\beta$  is one of the important regulators in the pathogenesis of human cancers, including breast cancers (63–66, 62, 63). Many late stage or invasive/metastatic breast tumors overexpress TGF- $\beta$  which, perhaps due to autocrine and paracrine effects of TGF- $\beta$ , influences tumor cell growth, invasion, and metastasis (19, 62, 63). Three types of TGF- $\beta$  receptors (e.g. RI, RII, and RIII) belonging to the family of serine/threonine kinase membrane receptors have been identified (18–23, 27, 28). TGF- $\beta$  signaling often involves TGF- $\beta$  binding to TGF- $\beta$ RII which recruits and phosphorylates TGF- $\beta$ RI leading to a series of biological events including phosphorylation of Smad family of proteins (18–26). TGF- $\beta$ RIII, which has no known signaling motif, appears to bind and present TGF- $\beta$  to TGF- $\beta$ RII (27, 28). Alterations of TGF- $\beta$  signaling are generally thought to contribute to the development and progression of human breast cancer (29–32). It has been reported that many TGF- $\beta$ s are secreted in a latent form and are converted to an active form. CD44-associated MMP-9 has been found to be involved in the cleavage of TGF- $\beta$  from a latent form into an active form (64). Therefore, it is clear that a close relationship exists between CD44-associated MMPs and the production of an active form of TGF- $\beta$ . However, the question of whether there is a direct interaction between CD44 and TGF- $\beta$  receptor(s) during breast cancer progression has not been addressed previously.

HA Promotes CD44 and TGF- $\beta$ RI Signaling in Breast Tumor CellsTABLE II  
Analysis of breast tumor cell migration

Cells	Tumor cell migration (% control) <sup>a</sup>					
	No treatment	Cytochalasin D	HA	HA and cytochalasin D	TGF- $\beta$	TGF- $\beta$ and cytochalasin D
Untransfected cells (control)	100	<5	156	14	150	15
Vector-transfected cells	97	<5	148	12	153	16
TGF- $\beta$ -RIcDNA-transfected cells	155	15	245	20	250	22

<sup>a</sup> Procedures for measuring tumor cell migration in MDA-MB-231 cells transfected with either TGF- $\beta$ RIcDNA or vector alone were described under "Materials and Methods." Briefly, untransfected MDA-MB-231 cells ( $\approx 1 \times 10^4$  cells/well in phosphate-buffered saline, pH 7.2) were placed in the upper chamber of the transwell unit. In some cases, MDA-MB-231 cells were transfected with either TGF- $\beta$ RIcDNA or vector alone. All cells either pretreated with HA or TGF- $\beta$  or without any treatment (in the presence or the absence of cytochalasin D (20  $\mu$ g/ml)) were incubated at 37 °C for 18 h in a humidified 95% air, 5% CO<sub>2</sub> atmosphere. Cells on the upper side of the filter were removed by wiping with a cotton swap. Cell migration processes were determined by measuring the cells that migrate to the lower side of the polycarbonate filters containing HA (or no HA) by standard cell number counting assays as described under "Materials and Methods." The CD44-specific cell migration was determined by subtracting non-specific cell migration (i.e. cells migrate to the lower chamber in the presence of anti-CD44 antibody treatment) from the total migrative cells in the lower chamber. The CD44-specific cell migration in untransfected cells (control) is designated as 100%. Each assay was set up in triplicate and repeated at least 3 times. All data were analyzed statistically using the Student's *t* test, and statistical significance was set at *p* < 0.01. The values expressed in this table represent an average of triplicate determinations of 3–5 experiments with an S.D. less than  $\pm 5\%$ .

In this study we have found that both the TGF- $\beta$  type I and II receptors (RI and RII) are expressed in MDA-MB-231 cells (Fig. 1). However, only TGF- $\beta$  type I receptor (RI) (but not type II (RII)) is closely associated with CD44 in metastatic breast tumor cells (MDA-MB-231 cells) (Fig. 1). An *in vitro* binding assay using two proteins (TGF- $\beta$  type I receptor (TGF- $\beta$ RI) and FLAG-tagged CD44 cytoplasmic domain (FLAG-CD44cyt)) confirms that the TGF- $\beta$ RI is directly involved in the interaction with the cytoplasmic domain of CD44 (Fig. 2). Moreover, HA activates TGF- $\beta$ RI kinase activity (Fig. 3) leading to Smad protein phosphorylation (Fig. 4) in a CD44-dependent manner, whereas TGF- $\beta$ -stimulated TGF- $\beta$  kinase activity (Fig. 3) and Smad protein phosphorylation (Fig. 4) do not appear to involve CD44. Thus, HA and TGF- $\beta$  bind to their own specific receptors (e.g. CD44 or TGF- $\beta$  receptors), but their respective downstream signaling pathway(s) appear to be tightly linked in MDA-MB-231 cells. Phosphorylated forms of Smad2 (or Smad3), which often form a complex with Smad4 in the cytosol, have been shown to be translocated into the nucleus for transcriptional activation of many genes (24–26). A recent study (65) demonstrated that human breast carcinoma cells examined by tissue microarrays frequently contain the phosphorylated form of Smad proteins. Therefore, HA and TGF- $\beta$ -activated Smad protein phosphorylation may contribute one of the important factors required for the onset of breast cancer progression.

In patients with advanced breast cancers, the malignant cells often metastasize to the bone (66–69). It is now known that TGF- $\beta$  receptor-mediated signaling plays an integral role in stimulating osteolytic bone metastasis by inducing the production of PTH-rP by the tumor cells (66). PTH-rP was originally isolated and cloned from tumors removed from patients with the common paraneoplastic syndrome called humoral hypercalcemia of malignancy (66–69). We have now determined that TGF- $\beta$  receptor-mediated signaling leads to an increase in PTH-rP production by the breast cancer cells (in the MDA-MB-231 cell line) (Fig. 5). The fact that HA activates PTH-rP production in a CD44-specific manner (Fig. 5) suggests that HA-CD44 signaling is also involved in breast tumor-specific hormone production required for breast cancer progression. Other studies have shown that stimulation of PTH-rP by TGF- $\beta$  is regulated through mRNA stabilization (37) or is controlled by a novel Smad3/Ets1 synergism on the P3 promoter of the PTH-rP (70). The question of which mechanism(s) (i.e. mRNA stabilization and/or Smad3-Ets1 interaction) is(are) involved in HA-CD44-mediated PTH-rP expression in the MDA-MB-231 cell awaits future investigation.

In addition, our results indicate that both HA and TGF- $\beta$  are capable of inducing CD44 phosphorylation *in vivo* (Fig. 6).

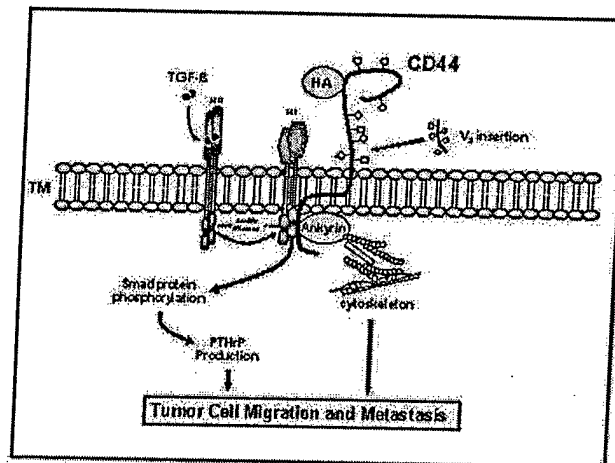


Fig. 10. A proposed model for the interaction between CD44v3 and TGF- $\beta$  receptor I (RI) during oncogenic signaling and breast tumor progression. CD44v3 (containing the v3 exon-encoded structure) is tightly complexed with TGF- $\beta$ RI. This CD44v3-associated TGF- $\beta$ RI kinase can be activated by HA and/or TGF- $\beta$  leading to phosphorylation of Smad proteins (Smad2 and Smad3) and PTH-rP production which is known to cause metastasis (e.g. osteolytic bone metastasis). Moreover, HA- and/or TGF- $\beta$ -activated CD44v3-TGF- $\beta$ RI kinase is also capable of phosphorylating CD44v3. Most importantly, CD44v3 phosphorylation enhances its binding to the cytoskeletal protein ankyrin which, in turn, interacts with the cytoskeleton and induces tumor cell migration. In conclusion, we believe that CD44v3-TGF- $\beta$ RI interaction plays a pivotal role in the activation of multiple signaling pathways required for ankyrin-membrane interaction, tumor cell migration, and important oncogenic events (e.g. Smad2/Smad3 phosphorylation and PTH-rP production) during HA- and TGF- $\beta$ -mediated breast tumor progression.

Moreover, TGF- $\beta$ RI kinase isolated from MDA-MB-231 cells can directly phosphorylate CD44 *in vitro* (Table I). Biochemical analyses indicate that the stoichiometry of CD44 phosphorylation by TGF- $\beta$ RI isolated from HA-activated MDA-MB-231 cells is comparable with that of MBP phosphorylation (by HA-activated TGF- $\beta$ RI) (Table I). Therefore, we conclude that CD44 may function as one of the cellular substrates for the TGF- $\beta$ RI kinase. Our findings are consistent with previous studies (11, 50–52) showing CD44 can be phosphorylated by several serine-threonine kinases. It is likely that TGF- $\beta$ RI kinase is phosphorylating certain CD44 site(s) such as threonine (amino acids 341, 347, or 351) and serine (amino acids 318, 325, 327, 339, or 356). The identification of the specific phosphorylation site(s) is currently undergoing investigation.

HA Promotes CD44 and TGF- $\beta$ RI Signaling in Breast Tumor Cells

9

Isacke and co-workers (51, 52) have reported that serine (amino acid 325) is the principal CD44 phosphorylation site(s) by serine-threonine kinases and that mutation of this residue blocks CD44-mediated cell migration but not HA binding (51, 52). Thus, the interaction between phosphorylated CD44 and specific intracellular component(s) (e.g. cytoskeletal protein(s)) may be required for cell migration.

Several lines of evidence indicate that the transmembrane interaction between the cytoplasmic domain of CD44 and cytoskeletal proteins (e.g. ankyrin) plays an important role in CD44-mediated oncogenic signaling (15, 16). In particular, the S2 subdomain (but not other subdomains) of the ARD binds to CD44 directly (16); overexpression of the S2 subdomain of ARD promotes CD44-mediated tumor cell migration (16). Ankyrin is also involved in the up-regulation of a Rac1-specific guanine nucleotide (GDP/GTP) exchange factor, Tiam1 (T lymphoma invasion and metastasis), in metastatic breast tumor cell migration (17). In this study we have observed that CD44 phosphorylation by HA-activated TGF- $\beta$ RI kinase stimulates its binding to the cytoskeletal protein ankyrin both *in vitro* (Fig. 7) and *in vivo* (Fig. 8). To elucidate further TGF- $\beta$ RI interaction with CD44 and ankyrin *in vivo*, we have transfected MDA-MB-231 cells with HA1-tagged TGF- $\beta$ RIcDNA (Fig. 9). Our data also confirm that overexpression of the HA1-tagged TGF- $\beta$ RI promotes its association with CD44v3 (Fig. 9) and stimulates recruitment of ankyrin into the CD44v3-TGF- $\beta$ RI complex (Fig. 9) leading to breast tumor cell migration (Table II). Finally, we have found that treatment of MDA-MB-231 cells with cytochalasin D (Table II) induces a reversal of tumor cell-specific phenotypes such as tumor cell migration (Table II). This finding suggests that some actin polymerization or microfilamentous cytoskeleton is required in this event. It is quite possible that the recruitment of ankyrin into CD44v3 induced by either HA/TGF- $\beta$  signaling (Fig. 8) or TGF- $\beta$ RI overexpression (Fig. 9) could contribute to cytoskeleton-mediated breast tumor cell migration (Table II). A previous study (57) has shown that HA is able to bind TGF- $\beta$ 1 directly. Therefore, it is possible that the HA-TGF- $\beta$ 1 complex in the extracellular matrix also plays a role in stimulating oncogenic signaling and cytoskeletal activation during breast tumor progression

As summarized in Fig. 10, we propose that CD44v3 is tightly complexed with TGF- $\beta$ RI. This CD44v3-associated TGF- $\beta$ RI kinase can be activated by HA and/or TGF- $\beta$  leading to phosphorylation of Smad proteins (Smad2 and Smad 3) and PTH-rP production which is known to cause breast tumor metastasis (in particular, osteolytic bone metastasis). Moreover, HA and/or TGF- $\beta$ -activated CD44v3-TGF- $\beta$ RI kinase is also capable of phosphorylating CD44v3. Most importantly, CD44v3 phosphorylation enhances its binding to the cytoskeletal protein ankyrin which, in turn, interacts with the cytoskeleton and induces tumor cell migration. Therefore, we believe that CD44v3-TGF- $\beta$ RI interaction promotes activation of multiple signaling pathways required for ankyrin-membrane interaction, tumor cell migration, and important oncogenic events (e.g. Smad2/Smad3 phosphorylation and PTH-rP production) during HA- and TGF- $\beta$ -mediated breast tumor progression.

**Acknowledgments**—We gratefully acknowledge Dr. Gerard J. Bourguignon for assistance in the preparation of this paper. We also thank Dr. Falko Diedrich for help in data preparation.

## REFERENCES

- Turley, E. A., Nobel, P. W., and Bourguignon, L. Y. W. (2002) *J. Biol. Chem.* 277, 4589–4592
- Screation, G. R., Bell, M. V., Jackson, D. G., Cornelis, F. B., Gerth, U., and Bell, J. I. (1992) *Proc. Natl. Acad. Sci. U. S. A.* 89, 12160–12164
- Bourguignon, L. Y. W. (2000) *J. Mammary Gland Biol. & Neoplasia* 6, 287–297
- Dall, P., Heider, K.-H., Sinn, H.-P., Skroch-Angel, P., Adolf, G., Kaufmann, M., Herrlich, P., and Ponta, H. (1995) *Int. J. Cancer* 60, 471–477
- Iida, N., and Bourguignon, L. Y. W. (1995) *J. Cell. Physiol.* 162, 127–133
- Kaufmann, M., Heider, K. H., Sinn, H. P., von Minckwitz, G., Ponta, H., and Herrlich, P. (1995) *Lancet* 345, 615–619
- Sy, M. S., Mori, H., and Liu, D. (1997) *Curr. Opin. Oncol.* 9, 108–112
- Kalish, E., Iida, N., Moffat, F. L., and Bourguignon, L. Y. W. (1999) *Front. Biosci.* 4, 1–8
- Bourguignon, L. Y. W., Zhu, H., Shao, L., and Chen, Y. W. (2000) *J. Biol. Chem.* 275, 1829–1838
- Bourguignon, L. Y. W., Zhu, H., Zhou, B., Diedrich, F., Singleton, P. A., and Hung, M. C. (2000) *J. Biol. Chem.* 276, 48679–48692
- Bourguignon, L. Y. W., Zhu, H., Shao, L., Zhu, D., and Chen, Y. W. (1999) *Cell Motil. Cytoskeleton* 43, 269–287
- Bourguignon, L. Y. W., Zhu, H., Shao, L., and Chen, Y. W. (2001) *J. Biol. Chem.* 276, 7327–7336
- Bourguignon, L. Y. W., Zhu, H., Chu, A., Iida, N., Zhang, L., and Hung, M. C. (1997) *J. Biol. Chem.* 272, 27913–27918
- Lokeshwar, V. B., Fregien, N., and Bourguignon, L. Y. W. (1994) *J. Cell Biol.* 126, 1099–1109
- Zhu, D., and Bourguignon, L. Y. W. (1998) *Cell Motil. Cytoskeleton* 39, 209–222
- Zhu, D., and Bourguignon, L. Y. W. (2000) *J. Cell. Physiol.* 183, 182–195
- Bourguignon, L. Y. W., Zhu, H., Shao, L., and Chen, Y. W. (2000) *J. Cell Biol.* 150, 177–191
- Massague, J. (1998) *Annu. Rev. Biochem.* 67, 753–791
- Blobe, G. C., Schiemann, W. P., and Lodish, H. F. (2000) *N. Engl. J. Med.* 342, 1350–1358
- Massague, J., Cheifetz, S., Laiho, M., Ralph, D. A., Weis, F. M. B., and Zentella, A. (1992) *Cancer Surv.* 12, 81–103
- Wrana, J. L., Attisano, L., Carcamo, J., Zentella, A., Doody, J., Laiho, M., Wang, X.-F., and Massague, J. (1992) *Cell* 71, 1003–1014
- Wrana, J. L., Attisano, L., Wieser, R., Ventura, F., and Massague, J. (1994) *Nature* 370, 341–347
- Chen, X., Weisberg, E., Fridmacher, V., Watanabe, M., Naco, G., and Whitman, M. (1997) *Nature* 389, 85–89
- Heldin, C.-H., Miyazono, K., and ten Dijke, P. (1997) *Nature* 390, 465–471
- Massague, J., and Wotton, D. (2000) *EMBO J.* 19, 1745–1754
- Shi, Y. (2001) *Bioessays* 23, 223–232
- Lopez-Casilla, F., Cheifetz, S., Doody, J., Andres, J. L., Lane, W. S., and Massague, J. (1991) *Cell* 67, 758–795
- Wang, X.-F., Lin, H. Y., Ng-Eaton, E., Downward, J., Lodish, H. F., and Weinberg, R. A. (1991) *Cell* 67, 797–805
- Carcamo, J., Zentella, A., and Massague, J. (1995) *Mol. Cell. Biol.* 15, 1573–1581
- Kalkhoven, E., Roelen, B. A. J., de Winter, J. P., Mummery, C. L., van den Eijnden-van Raaij, A. J. M., van der Saag, P. T., and van der Burg, B. (1995) *Cell Growth Differ.* 6, 1151–1161
- Kadin, M. E., Cavaille-Coll, M. W., Gertz, R., Massague, J., Cheifetz, S., and George, D. (1994) *Proc. Natl. Acad. Sci. U. S. A.* 91, 6002–6006
- Park, K., Kim, S.-J., Ban, Y.-J., Park, J.-G., Kim, N. K., Roberts, B. A., and Sporn, M. B. (1994) *Proc. Natl. Acad. Sci. U. S. A.* 91, 8772–8776
- Oft, M., Heider, K.-H., and Beug, H. (1998) *Curr. Biol.* 8, 1243–1252
- Wu, G., Fan, R. S., Li, W., Srinivas, V., and Brattain, M. G. (1998) *J. Biol. Chem.* 273, 7749–7756
- Yin, J. J., Selander, K., Chirgwin, J. M., Dallas, M., Grubbs, B. G., Wieser, R., Massague, J., Mundy, G. R., and Guise, T. A. (1999) *J. Clin. Invest.* 103, 197–206
- Yoneda, T., Williams, P. J., Hiraga, T., Niewolna, M., and Nishimura, R. (2001) *J. Bone Miner. Res.* 16, 1486–1495
- Merryman, J. I., DeWille, J. W., Werkmeister, J. R., Capen, C. C., and Rosol, T. J. (1994) *Endocrinology* 134, 2424–2430
- Goltzman, D., and Henderson, J. E. (1996) in *Principles of Bone Biology* (Bilezikian, J. P., Raisz, L. G., and Rodan, G. A., eds) pp. 809–826, Academic Press, New York
- Kal, H. Y., and Stewart, A. F. (1996) in *Principles of Bone Biology* (Bilezikian, J. P., Raisz, L. G., and Rodan, G. A., eds) pp. 347–362, Academic Press, New York
- Segre, G. V. (1996) in *Principles of Bone Biology* (Bilezikian, J. P., Raisz, L. G., and Rodan, G. A., eds) pp. 377–403, Academic Press, New York
- Yin, J. J., Taylor, S. D., Dallas, M., Massague, J., Mundy, G. R., and Guise, T. A. (1996) *J. Bone Miner. Res.* 11, 1994–2004
- Bourguignon, L. Y. W., Lokeshwar, V. B., Chen, X., and Kerrick, W. G. L. (1993) *J. Immunol.* 151, 6634–6644
- Franzen, P., ten Dijke, P., Ichijo, H., Yamashita, H., Schulz, P., Heldin, C. H., and Miyazono, K. (1993) *Cell* 75, 681–692
- Budayr, A. A., Nissenson, R. A., Klein, R. F., Pun, K. K., Clark, O. H., Diep, D., Arnaud, C. D., and Strewler, G. J. (1989) *Ann. Intern. Med.* 111, 807–812
- Hawker, C. D. (1983) in *Assay of Calcium-regulating Hormones* (Bikle, D. D., ed) pp. 218–218, Springer-Verlag, New York
- Iida, N., and Bourguignon, L. Y. W. (1997) *J. Cell. Physiol.* 171, 152–160
- Koli, K. M., and Arteaga, C. L. (1997) *Cancer Res.* 57, 970–977
- Smith, H. S., Stern, R., Liu, E., and Benz, C. (1991) *Basic Life Sci.* 57, 329–337
- Yeo, T. K., Nagy, J. A., Yeo, K. T., Dvorak, H. F., and Toole, B. P. (1996) *Am. J. Pathol.* 148, 1733–1740
- Kalomiris, E. L., and Bourguignon, L. Y. W. (1989) *J. Biol. Chem.* 264, 8113–8119
- Lewis, C. A., Townsend, P. A., and Isacke, C. M. (2001) *Biochem. J.* 357, 834–850
- Peck, D., and Isacke, C. M. (1998) *J. Cell Sci.* 111, 1595–1601
- Bourguignon, L. Y. W., Lokeshwar, V. B., He, J., Chen, X., and Bourguignon, G. J. (1992) *Mol. Cell. Biol.* 12, 4464–4471
- Bourguignon, L. Y. W. (2000) *Curr. Top. Membr.* 43, 293–312
- Bourguignon, L. Y. W., Zhu, D., and Zhu, H. (1998) *Front. Biosci.* 3, 637–649
- Goldstein, L. A., Zhou, D. F. H., Picker, L. J., Minty, C. N., Bargatze, R. F., Ding, J. F., and Butcher, E. C. (1989) *Cell* 56, 1063–1072
- Locci, P., Marinucci, L., Lilli, C., Martinese, D., and Bechetti, E. (1995) *Cell*

AQ: J

AQ: K

F10

AQ: M

AQ: N

(c) 1999

AQ: O

AQ: P

AQ: L

AQ: Q

- Tissue Res.* 281, 317-324
58. Bennett, K., Jackson, D. G., Simon, J. C., Tanczos, E., Peach, R., Modrell, B., Stamenkovic, I., Plowman, G., and Aruffo, A. (1995) *J. Cell Biol.* 128, 687-698
59. Bourguignon, L. Y. W., Gunja-Smith, Z., Iida, N., Zhu, H. B., Young, L. J. T., Muller, W., and Cardiff, R. D. (1998) *J. Cell. Physiol.* 176, 206-215
60. Banerji, S. N. I. J., Wang, S. X., Clasper, S., Su, J., Tammi, R., Jones, M., and Jackson, D. G. (1999) *J. Cell Biol.* 144, 789-801
61. Tsukita, S., Oishi, K., Sato, N., Sagara, I., Kawai, A., and Tsukita, S. (1994) *J. Cell Biol.* 126, 391-401
62. Chirgwin, J. M., and Guise, T. A. (2000) *Crit. Rev. Eukaryotic Gene Expr.* 10, 159-178
63. Tobin, S. W., Douville, K., Benbow, U., Brinckerhoff, C. E., Memoli, V. A., and Arrick, B. A. (2002) *Oncogene* 21, 108-118
64. Yu, Q., and Stamenkovic, I. (2000) *Gene Dev.* 14, 163-176
65. Xie, W., Mertens, J. C., Reiss, D. J., Rimm, D. L., Camp, R. L., Haffty, B. G., and Reiss, M. (2002) *Cancer Res.* 62, 497-505
66. Guise, T. A., and Mundy, G. R. (1998) *Endocr. Rev.* 19, 18-54
67. Aaron, A. D. (1994) *J. Am. Med. Assoc.* 272, 1206-1209
68. Powell, G. J., Southy, J., Danks, J. A., Stillwell, R. G., Hayman, J. A., Henderson, M. A., Bennett, R. C., and Martin, T. J. (1991) *Cancer Res.* 51, 3059-3061
69. Hortobagyi, G. N., Theriault, R. L., Porter, L., Blayney, D., Lipton, A., Sinoff, C., Wheeler, H., Simeone, J. F., Seaman, J., and Knight, R. D. (1996) *N. Engl. J. Med.* 335, 1785-1791
70. Lindemann, R. K., Ballschmieter, P., Nordheim, A., and Dittmer, J. (2001) *J. Biol. Chem.* 276, 46661-46670

